

University of Southampton

**Structural basis of acute intermittent porphyria
and the relationship between mutations in
human porphobilinogen deaminase and enzyme
activity**

Abeer M. Al-Dbass

Thesis submitted for the degree of Doctor of Philosophy

**FACULTY OF SCIENCE
DIVISION OF BIOCHEMISTRY AND MOLECULAR BIOLOGY**

November 2001

UNIVERSITY OF SOUTHAMPTON

ABSTRACT

FACULTY OF SCIENCE

DIVISION OF BIOCHEMISTRY AND MOLECULAR BIOLOGY

Doctor of Philosophy

Structural basis of acute intermittent porphyria and the relationship between mutations in human porphobilinogen deaminase and enzyme activity

By: Abeer M. Al-Dbass

The autosomal dominant human disease, acute intermittent porphyria, is caused by mutations in the gene specifying porphobilinogen deaminase, the third enzyme of the haem biosynthesis pathway. The disease is characterized by acute attacks exhibiting a range of clinical symptoms, elevated urinary levels of 5-aminolaevulinic acid and porphobilinogen and levels of porphobilinogen deaminase approximately 50% of normal activity. Over a hundred mutations are known from over forty families, many of which involve a single amino acid. The study of such naturally occurring mutations provides valuable insight into the role of the mutated residue in the structure and functioning of the enzyme. This thesis deals with several human mutations that involve conserved arginine residues. Using molecular biology techniques, several recombinant human ubiquitous mutant porphobilinogen deaminases have been generated from cDNA specifying the enzyme and the recombinant mutant proteins have been overexpressed in *E. coli*.

Three arginine mutants, Arg 149 Gln, Arg 167 Gln and Arg 173 Gln were generated using PCR mutagenesis. Arg 149 Gln exhibits a CRIM-ve phenotype whereas Arg 167 Gln and Arg 173 Gln are examples of CRIM+ve mutations. The mutant deaminases have been investigated with respect to their specific activity, thermal stability and the presence of the dipyrromethane cofactor. Arg 167 Gln exhibits weak enzyme activity but is particularly interesting because it accumulates stable, partially assembled enzyme intermediate complexes. Both Arg 149 Gln and Arg 173 Gln mutants are essentially inactive, contain no dipyrromethane cofactor and exist as heat labile apo-enzymes.

Two other mutants, Arg 167 Trp and Trp 198 Ter, have also been investigated. The Arg 167 Trp mutant exhibits similar properties to the Arg 167 Gln mutant, showing weak enzyme activity and forming stable enzyme intermediate complexes. In contrast, the Trp 198 Ter mutant, the most common cause of AIP in Sweden, is an insoluble and completely inactive truncated protein.

Finally, studies have been initiated to crystallize and to determine the 3-dimensional structure of the Arg 167 Gln ubiquitous human deaminase mutant. A preliminary X-ray structure at a resolution of 2.65 Å, in collaboration with Mohammed Fiyaz (Fiyaz, PhD Thesis, 2001), was obtained that shows only small differences from the *E. coli* enzyme, except for a large insertion in domain 3 that is partially resolved. Some insight into substrate binding is obtained from the structure.

ACKNOWLEDGMENTS

I would like to extend my sincere gratitude to Professor P. M. Shoolingin-Jordan not only for supervising this research, but also for providing fine opportunities for my development. I extend my gratitude to Dr. Muhammad Sarwar for his scientific advice and support, especially in molecular biology and for preparation of the mutants studied in this thesis.

My thanks to all members of the academic and non-academic staff in the Department of the Biochemistry, especially Professor Steve Wood and Dr. Raj Gill for invaluable discussions and advice. In the same vein, I would also like to thank Professor M. Akhtar and Dr. J. Cooper for their support, Will Rees-Blanchard and Neville Wright for their technical assistance, and Fiyaz Mohammed for providing the crystallographic figures.

Many thanks to all my fellow laboratory colleagues, especially Ipsita, Jack and Julie who made difficult times pass easier. Special thanks to Sooad Al-Daihan, a close friend and a colleague, for her encouragement when my spirits were lowest and for Danica Butler whose contribution to this thesis is invaluable and who become a dear friend.

I am forever indebted to my parents to whom I owe much more than words can express. I am very much indebted to my husband Dr. Abdulhakim Al-Babtain for all his love, and without whose endurance, encouragement, motivation and patience the mission would not have been accomplished. I would, also, like to express my deep gratitude to my father in-law and my mother in-law for their love and support.

Finally, I cannot forget my dear children Hadeel, Abdulmohsin, and Aljohara, and I dedicate this thesis to them and my husband for their patience and tolerance throughout my study.

Lastly I would like to thank my brothers and sister Abdullah, Saad and Sammer for their support.

This research was supported by a grant from the government of the Kingdom of Saudi Arabia through my employer King Saud University.

Contents

1	Introduction	1
1.1	Biosynthesis of tetrapyrroles	1
1.1.1	5-Aminolaevulinic acid synthase	7
1.1.2	5-Aminolaevulinic acid dehydratase	8
1.1.3	Porphobilinogen deaminase	9
1.1.4	Uroporphyrinogen III synthase	10
1.1.5	Uroporphyrinogen III decarboxylase	10
1.1.6	Coproporphyrinogen III oxidase	12
1.1.7	Protoporphyrinogen IX oxidase	12
1.1.8	Ferrochelatase	12
1.2	Porphyrias	13
1.2.1	Acute porphyrias	14
1.2.2	Non-acute porphyrias	17
1.2.3	Acute intermittent porphyria (AIP)	20
1.3	Porphobilinogen deaminase (PBGD)	22

1.3.1	The structure of porphobilinogen deaminase	24
1.3.2	The dipyrromethane cofactor	30
1.3.3	Intermediate complexes of porphobilinogen deaminase	34
1.3.4	Substrates and inhibitors of porphobilinogen deaminase	35
1.3.5	The mechanism of action of porphobilinogen deaminase	36
1.3.6	Studies using site-directed mutagenesis in <i>E. coli</i> PBGD	39
1.3.7	The molecular biology of human PBGD	41
1.4	Aims of this project	42
2	Materials and Methods	45
2.1	Materials	45
2.1.1	Bacterial strains and plasmids	46
2.1.2	Bacterial media	49
2.1.3	Buffers and solutions	49
2.2	Molecular biology methods	54
2.2.1	Agarose gel electrophoresis	54
2.2.2	Recovery of DNA from an agarose gel, Geneclean TM	54
2.2.3	Site directed mutagenesis by PCR	55
2.2.4	DNA digestion	58
2.2.5	DNA ligation	59
2.2.6	Isolation of DNA (small scale)	59
2.2.7	Photography of agarose gels	60

2.2.8 Transformation of competent cells	61
2.3 Recombinant ubiquitous human porphobilinogen deaminase isolation and characterisation methods	62
2.3.1 Properties of recombinant ubiquitous human porphobilinogen deaminase	62
2.3.2 Purification of recombinant human ubiquitous porphobilinogen deaminase	66
2.3.3 Crystallization of recombinant human ubiquitous porphobilinogen deaminase Arg 167 Gln mutant	69
2.3.4 Electrospray mass spectrometry (ESMS)	70
2.3.5 High resolution ion-exchange chromatography	70
2.3.6 Preparation of <i>E. coli</i> porphobilinogen deaminase holo-enzyme	70
2.3.7 Purification of human recombinant ubiquitous porphobilinogen deaminase Arg 149 Gln mutant	72
2.3.8 Purification of recombinant human ubiquitous porphobilinogen deaminase Trp 198 Ter mutant	73
2.3.9 Detection of the dipyrromethane cofactor in the recombinant ubiquitous human porphobilinogen deaminase	74
2.3.10 Attempts to reconstitute human ubiquitous porphobilinogen deaminase holo-enzyme from the apo-enzyme using preuroporphyrinogen	76
2.3.11 Quantitative estimation of PBG	79
2.3.12 Porphobilinogen synthesis	80
3 Studies on recombinant human ubiquitous porphobilinogen deaminase arginine mutants Arg 167 Gln and Arg 167 Trp	82
3.1 Introduction	82

3.2 Results	84
3.2.1 PCR and cloning of cDNA specifying recombinant human ubiquitous porphobilinogen deaminase native enzyme into the expression vector pT7-7	84
3.2.2 Theoretical primer optimisation	85
3.2.3 Site directed mutagenesis of cDNA specifying human ubiquitous porphobilinogen deaminase by PCR	85
3.2.4 Digestion of cDNA fragments specifying the human ubiquitous porphobilinogen deaminase Arg 167 Gln mutant and ligation into the pT7-7 plasmid	88
3.2.5 Transformation of cDNA specifying the human ubiquitous porphobilinogen deaminase Arg 167 Gln mutant into <i>E. coli</i> strain DH5 α and screening for positive clones	88
3.2.6 Expression and purification of recombinant human ubiquitous porphobilinogen deaminase Arg 167 Gln and Arg 167 Trp mutants	91
3.2.7 Attempts to separate and characterize the double bands of the native recombinant human ubiquitous porphobilinogen deaminase observed in native gels	105
3.2.8 Assay for the determination of K_m and V_{max} for recombinant human ubiquitous porphobilinogen deaminase Arg 167 Gln and Arg 167 Trp mutants	116
3.2.9 Electrospray mass spectrometry (ESMS) of recombinant human ubiquitous porphobilinogen deaminase Arg 167 Gln and Arg 167 Trp mutants	122
3.2.10 Reaction with modified Ehrlich's reagent to check the presence of the dipyrromethane cofactor and the porphyrin products of the recombinant human ubiquitous porphobilinogen deaminase Arg 167 Gln mutant, compared to the native enzyme	122
3.2.11 Determination of the isoelectric point of ubiquitous human porphobilinogen deaminase by isoelectric focussing (IEF)	130

3.2.12	Determination of pH optimum of human ubiquitous porphobilinogen deaminase Arg 167 Gln and Arg 167 Trp mutants	133
3.2.13	Thermal stability of the recombinant human ubiquitous porphobilinogen deaminase Arg 167 Gln mutant	138
3.2.14	Studies on the stability of ES complexes of recombinant human ubiquitous porphobilinogen deaminase Arg 167 Gln and Arg 167 Trp mutants using non-denaturing PAGE	138
3.3	Discussion and conclusions	146
4	Studies on the recombinant human ubiquitous porphobilinogen deaminase Arg 173 Gln, Arg 149 Gln and Trp 198 Ter mutants	153
4.1	Introduction	153
4.2	Results	156
4.2.1	Site directed mutagenesis of cDNA specifying human ubiquitous porphobilinogen deaminase by PCR	156
4.2.2	Digestion of the mutagenic DNA fragments and ligation into the pT7-7 plasmid	156
4.2.3	Transformation of cDNA specifying human ubiquitous porphobilinogen deaminase Arg 173 Gln and Arg 149 Gln mutants into <i>Escherichia coli</i> strain DH5 α and screening for positive mutants	160
4.2.4	Expression and purification of recombinant human ubiquitous porphobilinogen deaminase Arg 173 Gln mutant	160
4.2.5	Expression and purification of recombinant human ubiquitous porphobilinogen deaminase Arg 149 Gln mutant	163
4.2.6	Reaction of recombinant human ubiquitous porphobilinogen deaminase Arg 173 Gln and Arg 149 Gln mutants with modified Ehrlich's reagent to check the presence of the dipyrromethane cofactor	166

4.2.7	Attempts to reconstitute recombinant human ubiquitous porphobilinogen deaminase Arg 173 Gln and Arg 149 Gln mutant holo-enzymes from the apo-enzymes, using preuroporphyrinogen 167	167
4.2.8	Electrospray mass spectrometry (ESMS) of recombinant human ubiquitous porphobilinogen deaminase Arg 173 Gln and Arg 149 Gln mutants	171
4.2.9	Expression and purification of recombinant human ubiquitous porphobilinogen deaminase Trp 198 Ter mutant	174
4.2.10	Discussion and conclusions	181
5	Crystallization and X-ray structure of the recombinant ubiquitous human porphobilinogen deaminase Arg 167 Gln mutant	185
5.1	Introduction	185
5.2	Preparation of Arg 167 Gln for crystallization	187
5.3	Crystallisation of Arg 167 Gln by the vapour diffusion method	187
5.4	X-Ray crystallography	188
5.5	The X-ray structure of the recombinant human ubiquitous porphobilinogen deaminase Arg 167 Gln mutant	194
5.6	The structure of the active site and the dipyrro-methane cofactor and implications for the properties of Arg 149, Arg 167 and Arg 173 mutations	194
5.7	Comparison between the human ubiquitous de-aminase and the <i>E. coli</i> enzyme	200
References		203
Appendix		212

Abbreviations and nomenclature

Abbreviations

5-ALA	5-Aminolaevulinic acid
Å	Ångström
Abs	Absorbtion
AIP	Acute intermittent porphyria
ALAD	Aminolaevulinic acid dehydratase
amu	Atomic mass unit
CoA	Coenzyme A
CRIM	Cross reacting immunoreactive material
ε_m	Molar extinction coefficient
DEAE	Diethylaminoethyl
DNA	Deoxyribonucleic acid
dNTPs	Deoxyribonucleoside triphosphates
DTT	Dithiothreitol
EDTA	Ethylenediaminetetra-acetic acid
f.p.l.c.	Fast protein liquid chromatography
GABA	γ -Aminobutyric acid
huPBGD	Human ubiquitous porphobilinogen deaminase
IEF	Isoelectric focusing
IPTG	Isopropyl-thiogalactoside
K_m	Dissociation constant
kb	Kilobase pair
M_r	Relative molecular mass
mRNA	Messenger ribonucleic acid
PBG	Porphobilinogen
PBGD	Porphobilinogen deaminase
PCR	Polymerase chain reaction
pI	Isoelectric point
PLP	Pyridoxal 5'-phosphate
SDS	Sodium dodecylsulphate
TEMED	N,N,N',N'-Tetramethylenediamine
Ter	Stop codon
Tris	Tris(hydroxymethyl)aminomethane
UPBGD	Ubiquitous porphobilinogen deaminase
u.v.	Ultraviolet

Amino acids and their abbreviations

Amino acid	Three letter abbreviation	Single letter abbreviation
Alanine	Ala	A
Arginine	Arg	R
Asparagine	Asn	N
Aspartate	Asp	D
Cysteine	Cys	C
Glutamate	Glu	E
Glutamine	Gln	Q
Glycine	Gly	G
Histidine	His	H
Isoleucine	Ile	I
Leucine	Leu	L
Lysine	Lys	K
Methionine	Met	M
Phenylalanine	Phe	F
Proline	Pro	P
Serine	Ser	S
Threonine	Thr	T
Tryptophan	Trp	W
Tyrosine	Tyr	Y
Valine	Val	V

Nomenclature

The side chains of the pyrrole rings have been abbreviated to single letters as follows:

A	Acetate	$-\text{CH}_2\text{COOH}$
P	Propionate	$-\text{CH}_2\text{CH}_2\text{COOH}$
M	Methyl	$-\text{CH}_3$
V	Vinyl	$-\text{CH}=\text{CH}_2$

The first ring of the dipyrrromethane cofactor is C1 and the second ring is C2. Enzyme intermediate complexes are abbreviated to:

- ES Enzyme with one substrate molecule bound.
- ES_2 Enzyme with two substrate molecules bound.
- ES_3 Enzyme with three substrate molecules bound.
- ES_4 Enzyme with four substrate molecules bound.

Chapter 1

Introduction

1.1 Biosynthesis of tetrapyrroles

In most organisms tetrapyrrole biosynthesis produces the macrocyclic ring system in the form of haem as an essential component for life. Haem is an essential prosthetic group for a wide range of haem-containing proteins including haemoglobin and myoglobin for oxygen binding and transport; respiratory cytochromes as components of the mitochondrial electron-transport chain; catalases and peroxidases for decomposition of hydrogen peroxide; microsomal P450s required for steroid hormone synthesis and the oxidative metabolism of lipophilic compounds; tryptophan pyrrolase, that degrades tryptophan (May, *et al.*, 1995, and Kappas, *et al.*, 1989).

The biosynthesis of haem in mammalian cells, occurs through a series of eight enzyme-catalyzed reactions, the basic details of which were elucidated more than 30 years ago (for a historical review see Jordan 1991). The first and last three steps occur in mitochondria and the remaining steps in the cytosol. The eight enzymes are encoded by nuclear DNA, synthesized in the cytosol and finally four of them are imported into the mitochondria. Chemically, haem consists of a porphyrin, known

as protoporphyrin IX and an atom of ferrous ion that is chelated in the centre of the porphyrin ring system (figure 1.1). The central iron of haem plays a vital role in hemoproteins. Iron normally exists in its two main redox states, ferrous and the ferric, although higher oxidation states are used in the cytochrome P450 enzymes. The ferrous state has a high affinity for oxygen and can be reversibly oxidised to the ferric state by transferring an electron. As a result, the prosthetic group is able to function as a single-electron carrier to serve as a catalyst for redox reactions involving oxygen, and to function as an oxygen carrier (May *et al.*, 1995).

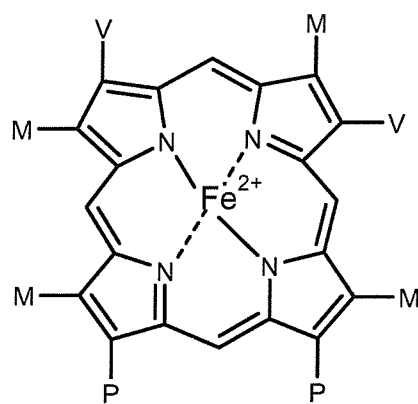


Figure 1.1: **The structure of the haem macrocycle.** M = $-\text{CH}_3$; V = $-\text{CH}=\text{CH}_2$; P = $-\text{CH}_2\text{CH}_2\text{COOH}$

The first committed intermediate of haem synthesis is the highly reactive 2-aminoketone, 5-aminolaevulinic acid, which is synthesized by two distinct routes, the C5 pathway and the glycine pathway. In the former, the utilization of the carbon skeleton of glutamate is the distinctive feature. This pathway uses three enzymes, glutamyl-tRNA synthase, glutamyl-tRNA reductase and glutamate 1-semi aldehyde aminotransferase. The C5 pathway is present in many anaerobic bacteria and plants. The glycine pathway, often called the Shemin pathway, involves the condensation between glycine and succinyl-CoA and is catalysed by 5-aminolaevulinic acid synthase. Although occurring in some bacteria, this pathway is restricted mainly to animals and other eukaryotes, see figure 1.2.

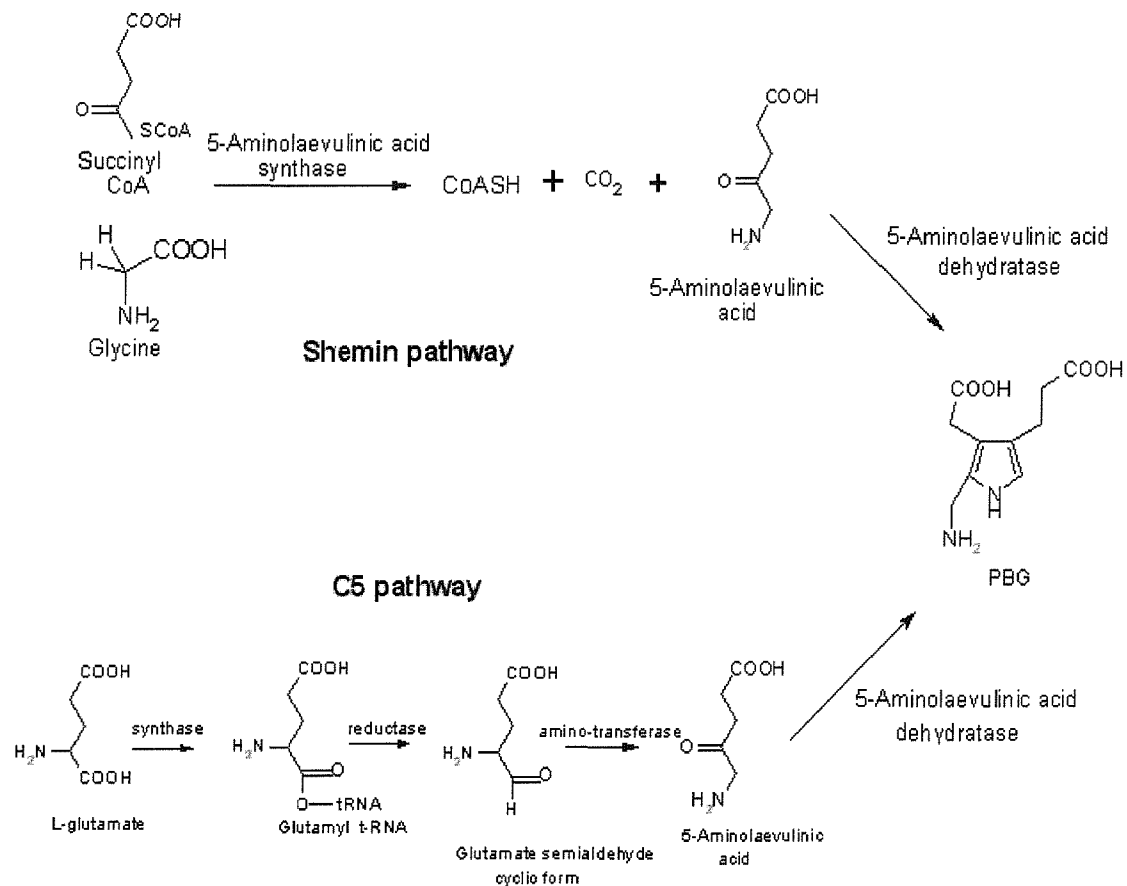


Figure 1.2: **5-Aminolaevulinic acid is synthesized by two distinct routes.** The C5 pathway, in which the utilization of the carbon skeleton of glutamate is the distinctive feature. This pathway is present in many anaerobic bacteria and in plants. Secondly, the Shemin pathway, in which the condensation between glycine and succinyl-CoA occurs in the presence of 5-aminolaevulinic acid synthase, located in the matrix side of mitochondria. Although occurring in some bacteria, this pathway is restricted mainly to animals and other eukaryotes.

After leaving the mitochondrion, 5-aminolaevulinic acid is transformed into the tetrapyrrole macrocycle in three enzymic reactions in the cytosol (see figure 1.3). In the first of these reactions, two molecules of 5-aminolaevulinic acid condense with one another, catalyzed by 5-aminolaevulinic acid dehydratase, to form the basic pyrrole building block, porphobilinogen. In the next reaction, porphobilinogen deaminase catalyses the polymerization of four molecules of porphobilinogen in a chain to generate a highly unstable 1-hydroxymethylbilane called preuroporphyrinogen. In the third reaction, preuroporphyrinogen is transformed into uroporphyrinogen III by uroporphyrinogen III synthase in a reaction involving dehydration, rearrangement of ring D and cyclization. In the absence of this enzyme, preuroporphyrinogen cyclises non-enzymatically to form the uroporphyrinogen I isomer that has no biological function. The remaining cytosolic enzyme, uroporphyrinogen III decarboxylase, catalyses the decarboxylation of the carboxyl groups from the acetic acid side chains on all four of the pyrrole rings of uroporphyrinogen III to form coproporphyrinogen III. Coproporphyrinogen III is now imported into the mitochondria for the remaining reactions of the pathway (May *et al.*, 1995).

In the intermembrane space of the mitochondria, coproporphyrinogen III oxidase converts coproporphyrinogen III to protoporphyrinogen IX. This product is then oxidized to protoporphyrin IX by protoporphyrinogen IX oxidase which is located in the inner mitochondrial membrane. Finally, the ferrous iron is inserted into protoporphyrin IX to give haem in a reaction catalyzed by ferrochelatase, that is located in the inner mitochondrial membrane (figure 1.3). It has been suggested that the terminal 3 enzymes of haem biosynthesis exist in some form of complex (figure 1.4). The haem thus synthesised is utilized for mitochondrial respiratory cytochromes, or transported from the mitochondrion to the cytosol to be used by other proteins (May *et al.*, 1995). Although dietary sources contain some haem and a small portion of this is actually absorbed in the small intestine, the majority of the haem used in the body is derived from endogenous synthesis.

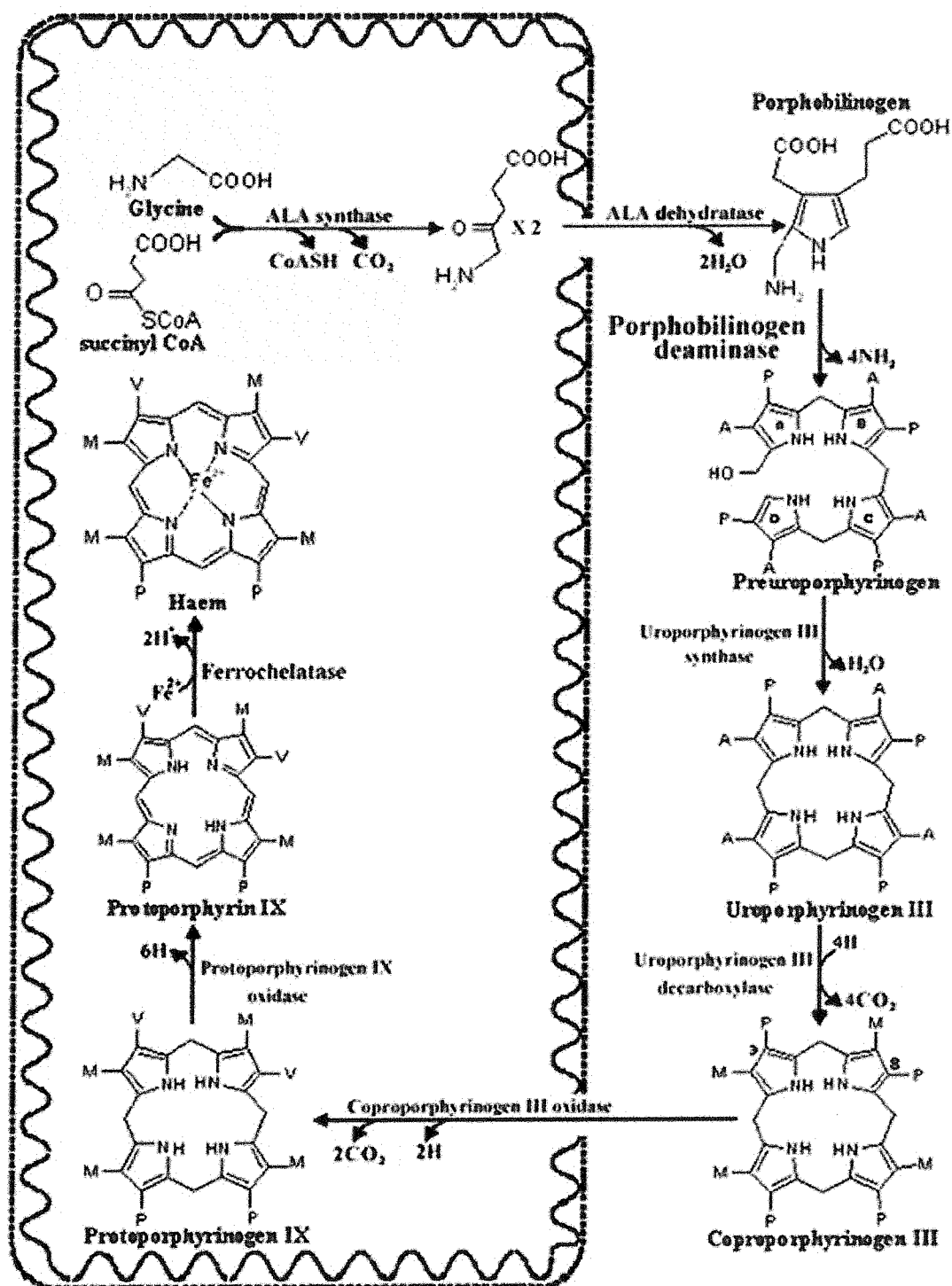


Figure 1.3: The biosynthesis of haem in mammalian cells, occurs through a series of eight enzyme-catalyzed reactions. $\text{A} = -\text{CH}_2\text{COOH}$; $\text{P} = -\text{CH}_2\text{CH}_2\text{COOH}$; $\text{V} = -\text{CH}=\text{CH}_2$ and $\text{M} = -\text{CH}_3$.

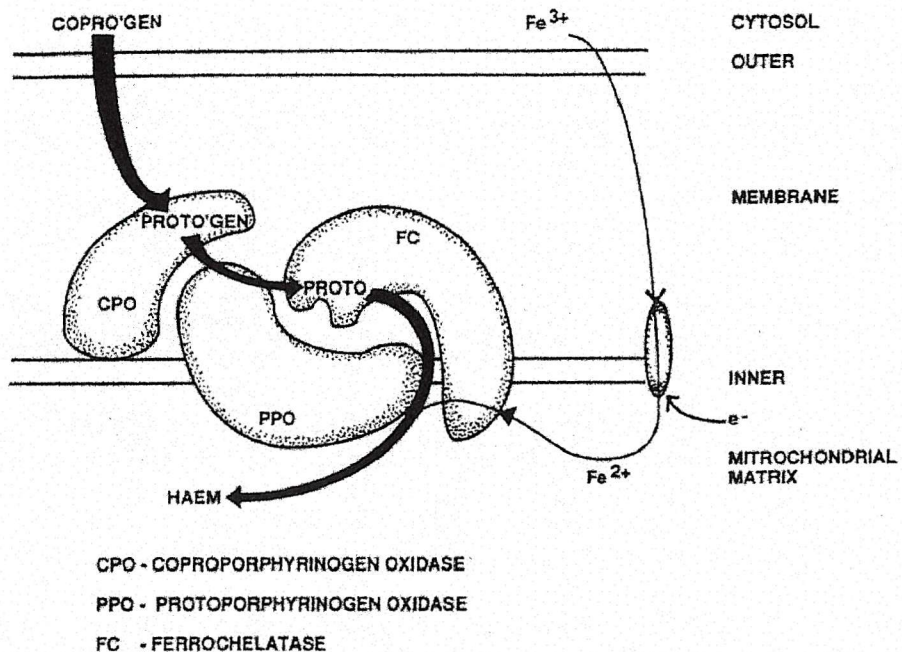


Figure 1.4: The diagram shows a designed multi-enzyme complex synthesizing haem in the latter mitochondrial stages of haem biosynthesis. The last three enzymes of haem synthesis, coproporphyrinogen oxidase, protoporphyrinogen oxidase and ferrochelatase straddle the inner mitochondrial membrane. A hypothesized picture of their inter-relationships is shown here. Each enzyme is linked to the next permitting the staged oxidation and translocation of coproporphyrinogen to protoporphyrin with the final insertion of ferrous iron by ferrochelatase. The oxidation could be driven by the concurrent translocation and reduction of extramitochondrial ferric iron to ferrous iron in the mitochondrion. In this model it is designed that these three enzymes span the inner mitochondrial membrane and provide a channel which permits the oxidative entry of coproporphyrinogen to the mitochondrion as protoporphyrin into which ferrous iron can be inserted to form haem (Moore, 1993).

Although this thesis focuses on the third enzyme of haem biosynthesis, porphobilinogen deaminase (PBGD) a short description of all eight enzymes of haem biosynthesis is given below followed by a brief summary of the naturally occurring types of porphyria caused by genetic defects in the genes specifying these enzymes. PBGD will then be discussed from three standpoints: firstly, the different types mutations of that occur in PBGD causing different defects that result in acute intermittent porphyria (AIP) in humans; secondly, a brief description of the disease AIP that arises as a result of the genetic defects in PBGD leading normally to 50% of the normal activity; thirdly, the structure of the enzyme, the enzyme cofactor, the intermediate complexes, substrate and inhibitors and finally the mechanism.

1.1.1 5-Aminolaevulinic acid synthase

5-Aminolaevulinic acid synthase, is the first enzyme in the tetrapyrrole synthesis pathway; it catalyzes the formation of 5-aminolaevulinic acid by the condensation of succinyl-CoA and glycine. ALAS-catalyzed reaction is the rate limiting step of haem synthesis in the liver and is controlled by a negative feedback mechanism involving the end product, free or non-protein-bound haem. ALAS requires the cofactor, pyridoxal 5'-phosphate, which forms a Schiff base with the amino group of glycine during the reaction. ALAS is located in the matrix side of the inner mitochondrial membrane. The enzyme has been purified from several different sources and consists of two identical subunits having M_r values ranging from 40,000 to 70,000 (Kappas *et al.*, 1989; Ferreira and Gong, 1995).

In mammalian, two isozymes for ALAS are encoded by two separate genes; a house-keeping isozyme, the hepatic form of ALAS, which is encoded by the ubiquitous gene (ALA-H or ALAS1) on chromosome 3 and is induced by certain drugs in the liver; an erythroid-specific isozyme, which is encoded by the erythroid gene (ALAS-E or ALAS2) on the X-chromosome and expressed only in erythroid tissues, (Cotter *et al.*,

1995; Ferreira and Gong, 1995). ALAS2 is induced by erythropoietin during erythroid differentiation. The two isozymes have different functions with house-keeping isozyme used for haem synthesis for P450s and other hemoproteins in the newborn and adult liver, while erythroid-specific isozyme supplies haem for haemoglobin. Genetic defects in the ALAS2 gene are responsible for X-linked sideroblastic anemias, (Bottomley *et al.*, 1995).

1.1.2 5-Aminolaevulinic acid dehydratase

5-Aminolaevulinic acid dehydratase, ALAD, is classified into two main groups according to its metal requirements, activation by thiols, sensitivity to inhibition with EDTA and pH optimum. These eukaryotic ALADs are cytosolic octameric enzymes with M_r values around 280,000 consisting of eight identical subunits, each with M_r values of about 35,000. On the other hand, enzymes from plants and some bacteria require Mg^{2+} and are not activated by thiols. The bacterial enzyme isolated from *R. sphaeroides* has a pH optimum range from 8 to 8.5 and has an additional requirement for potassium ions. ALAD catalyses the assymetric condensation of two molecules of ALA to form the monopyrrole intermediate, porphobilinogen, with the elimination of two molecules of water. ALAD from yeast has been expressed in *E. coli* and its X-ray structure has been determined (Erskine *et al.*, 1997). 5-Aminolaevulinic acid dehydratases purified from mammalian liver and erythrocytes require sulphhydryl compounds such as β -mercaptoethanol or dithiothreitol (DTT) and Zn^{2+} ion for maximal activity. Human ALAD is very sensitive to inhibition by some heavy metals, such as lead, that accounts for the anaemia found in lead poisoning where the level of ALA, but not PBG, increases. The human ALAD gene contains two promoter regions that express two isozymes, housekeeping and erythroid-specific (Sassa and Kappas, 2000). Genetic defects affecting the ALAD gene lead to a marked decrease in its activity and in the rare homozygous form cause Doss porphyria, where the patient suffers from severe neurological symptoms without cutaneous photosensitivity

(Kappas *et al.*, 1989).

1.1.3 Porphobilinogen deaminase

Porphobilinogen deaminase (PBGD), formerly uroporphyrinogen I synthase, and also known as hydroxymethylbilane synthase, is the third enzyme in the haem biosynthesis pathway. PBGD requires a cofactor, the dipyrromethane cofactor, for its activity and stability. The dipyrromethane is bound covalently to the enzyme through a thiol ether linkage via Cys 261 (Cys 242 in *E. coli* PBGD). PBGDs catalyze the polymerization of four molecules of porphobilinogen, to form the unstable intermediate, preuroporphyrinogen, a hydroxymethylbilane. In the absence of the fourth enzyme in the haem biosynthesis, uroporphyrinogen III synthase (UROS), preuroporphyrinogen is converted nonenzymatically into uroporphyrinogen I. However, in the presence of UROS, preuroporphyrinogen is converted directly to uroporphyrinogen III, the main precursor for all tetrapyrroles.

PBGDs have been isolated from many different sources and characterized as monomers with M_r values ranging from 34,000 to 44,000. From the X-ray structure of *E. coli* PBGD, it has been found that the enzyme consists of three domains linked to one another by flexible strands with the cofactor situated between domains 1 and 2 attached covalently to domain 3 (Louie *et al.*, 1992). Human deaminase exists as two isozymes, a ubiquitous form and an erythroid specific form, both transcribed from the same gene but controlled by different promoters. Genetic defects in the deaminase gene lead typically to 50% enzyme activity and cause the autosomal dominant disorder, acute intermittent porphyria.

1.1.4 Uroporphyrinogen III synthase

Uroporphyrinogen III synthase, is the fourth enzyme in haem biosynthesis pathway, where preuroporphyrinogen is cyclized by connecting ring A with ring D, after rearrangement of ring D, to form uroporphyrinogen III, see figure 1.5.

Uroporphyrinogen III is the universal cyclic tetrapyrrole from which all haems, bacteriochlorophylls, chlorophylls, corrins, factor F430 and all other cyclic and linear tetrapyrroles are biosynthesized (Jordan, 1994b). Uroporphyrinogen III synthases are monomeric proteins with M_r values range from 26,000 to 31,000 and are highly thermolabile enzymes (Shoolingin-Jordan and Cheung, 1999; Shoolingin-Jordan, 1995). Mutations in the human gene for uroporphyrinogen III synthase lead to decreased activity of the enzyme. Mutations in both alleles cause the disease congenital erythropoietic porphyria (CEP), which is expressed in infancy and results in cutaneous photosensitivity (Kappas *et al.*, 1989).

1.1.5 Uroporphyrinogen III decarboxylase

Uroporphyrinogen III decarboxylase is the fifth enzyme of haem biosynthesis which catalyses the conversion of uroporphyrinogen III to coproporphyrinogen III by decarboxylation of all four acetic acid side chains. Uroporphyrinogen III decarboxylases have been isolated from a variety of sources and all have M_r values of around 42,000 and appear to exist as dimers. No metal or coenzyme is required and appears to arise from a single gene on the short arm of chromosome 1 in humans. Heterozygous and homozygous deficiency of cytosolic enzyme uroporphyrinogen III decarboxylase lead to the disease porphyria cutanea tarda and hepatoerythropoietic porphyria, respectively (Elder and Roberts, 1995; Shoolingin-Jordan and Cheung, 1999). The X-ray structure of human uroporphyrinogen decarboxylase has been determined (Whitby *et al.*, 1998).

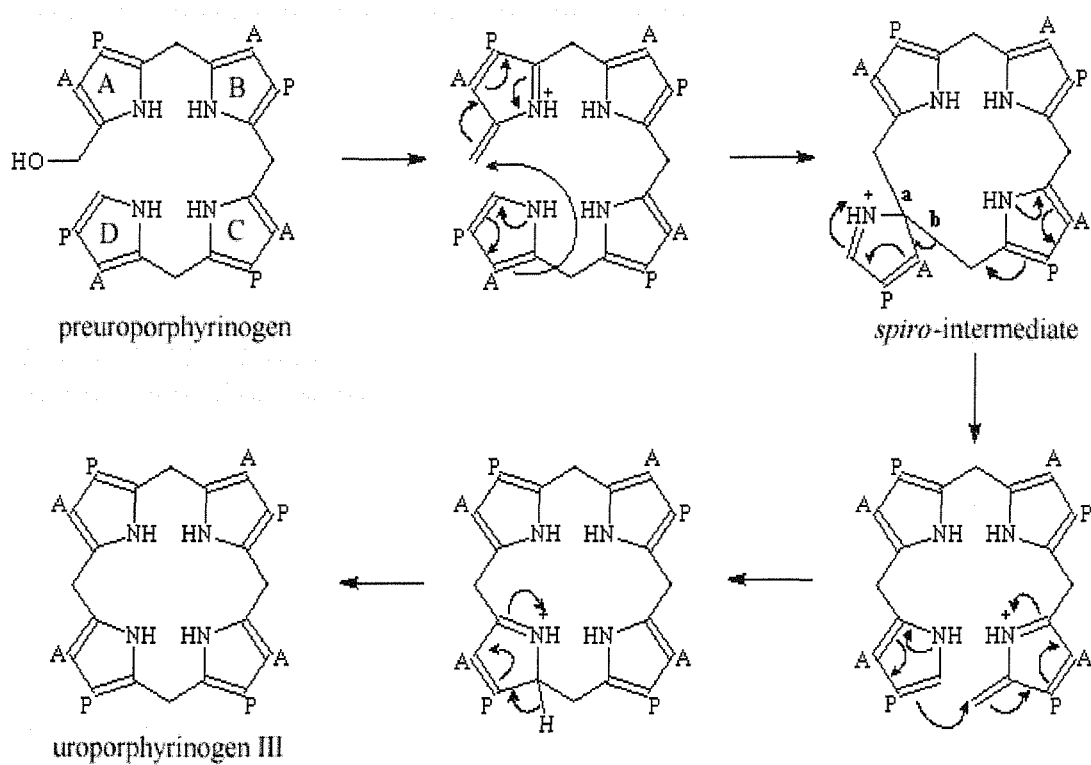


Figure 1.5: The mechanism for the biosynthesis of uroporphyrinogen III from preuroporphyrinogen, suggested originally by Mathewson and Corwin in 1961. In this mechanism, the key feature is the reaction of the substituted α -position of ring D (C-16) to form a methylene bridge (bond a) with the ring A. As a result, the attractive compound, spiro-pyrrolidine (or spiro-intermediate), is formed. In the next step, the bond between ring D and C-15 (bond b) in the spiro-pyrrolidine is cleaved to generate an azafulvene and finally the cyclization process occurs to produce uroporphyrinogen III (Shoolingin-Jordan and Cheung, 1999; Jordan, 1991).

1.1.6 Coproporphyrinogen III oxidase

Mammalian coproporphyrinogen III oxidase (CPO) is a mitochondrial enzyme that catalyses the conversion of two propionate groups at positions 3 and 8 of coproporphyrinogen III to vinyl groups to form protoporphyrinogen IX (Ferreira, 1995; Shoolingin-Jordan and Cheung, 1999). Purified CPO, from bovine liver, is a dimer with M_r of 72,000 as measured by gel filtration. It has been found that oxygen is essential for the enzymatic function (Sassa and Kappas, 2000). A dominant disease associated with a deficiency of this enzyme leads to a form of hereditary hepatic porphyria, known as hereditary coproporphyria.

1.1.7 Protoporphyrinogen IX oxidase

Protoporphyrinogen IX oxidase (PPO) is a mitochondrial enzyme that catalyses the oxidation of protoporphyrinogen IX to form the very water-insoluble haem precursor, protoporphyrin IX. In this reaction, six hydrogen atoms are removed from the porphyrinogen nucleus which perfectly positions the four pyrrole nitrogen atoms of protoporphyrin to chelate ferrous iron. In bovine and murine species, PPO is a monomer with M_r of around 65,000. PPO is an oxygen dependent enzyme, that acts specifically on protoporphyrinogen. The M_r of human PPO is approximately 50,800 (Sassa and Kappas, 2000). A deficiency in the protoporphyrinogen oxidase activity causes a dominant disease called variegate porphyria.

1.1.8 Ferrochelatase

Ferrochelatase, is last enzyme in haem biosynthesis which catalyses the insertion of ferrous iron into protoporphyrin IX to form protoheme (Ferreira, 1995). This enzyme is mitochondrial but is synthesized in the cytosol in a larger precursor form

and imported into mitochondria. Human ferrochelatase has a M_r of 47,833 as a precursor protein, with a leader. The mature enzyme has a M_r of only 42,168 (Sassa and Kappas, 2000). The enzyme is made up from two topologically related domains held together by two protein strands with a deep cleft between the domains that is considered to represent the catalytic site (Al-Karadaghi *et al.*, 1997). Ferrochelatase requires reducing substances for its activity and a partial deficiency in this activity leads to erythropoietic protoporphyria.

1.2 Porphyrias

The original root of porphyria is derived from the Greek word, porphurose, which means a purple colour (Warren *et al.*, 1996). The porphyrias are a fascinating and varied group of disorders caused by deficiencies in the enzymes involved in haem biosynthesis. Defects in all enzymes in the haem biosynthetic pathway, apart from 5-aminolaevulinic acid synthase, can cause different types of porphyria (May *et al.*, 1995). Thus, in each porphyria there is a specific pattern of accumulation and excretion of porphyrins or their precursors, 5-aminolaevulinic acid and porphobilinogen. Porphyrias have been classified as either hepatic or erythropoietic depending on the main site of expression of the defective enzyme (Kappas *et al.*, 1989). Alternatively, porphyrias are classified clinically into three classes, acute porphyrias that are accompanied by neurological abnormalities; non-acute porphyrias characterized by cutaneous photosensitivity; porphyrias that exhibit both neurological and cutaneous abnormalities (Thadani *et al.*, 2000; May *et al.*, 1995), see table 1.1. Each symptom has a specific biochemical cause, for instance, the neurological defects in patients with acute porphyrias are thought to result either from the effects of the early intermediates 5-aminolaevulinic acid and porphobilinogen in blood, urine and cerebrospinal fluid or the deficiency of the end product, haem, in neural tissue. Photosensitization is caused by the accumulation of porphyrins in tissues which can interact with molecular oxygen and light to produce damaging free-radical species (Warren *et al.*, 1996).

Patients with acute porphyrias suffer from severe attacks of abdominal pain, constipation, vomiting, paralysis and psychiatric disorders; while non-acute porphyrias cause burning pain, itching, pigmentation and skin fragility with blisters and scarring.

Within the acute porphyrias, there are four main types; acute intermittent porphyria (AIP), ALAD deficiency porphyria (Doss-porphyria), hereditary coproporphyria (HC) and variegate porphyria (VP). The first two types are predominantly neuropsychiatric, while the last two types of acute porphyria show both neurological and cutaneous abnormalities. The non-acute porphyrias comprise; congenital erythropoietic porphyria, porphyria cutanea tarda and erythropoietic protoporphyrina, all of which lead to predominantly cutaneous manifestations.

Porphyrias are generally inherited as Mendelian autosomal dominant traits excluding the rare congenital erythropoietic porphyria (CEP) and ALAD deficiency porphyria that are inherited as autosomal recessive traits (Moore, 1993). A more severe homozygous form of PCT, hepatoerythropoietic porphyria, has also been described. Patients with porphyrias need to be advised to avoid factors that precipitate attacks, for instance, certain drugs and dietary regimes. The 8 different types of porphyria will be described briefly below.

1.2.1 Acute porphyrias

Some enzymes of the haem biosynthesis pathway; porphobilinogen deaminase, coproporphyrinogen oxidase, and protoporphyrinogen oxidase have low relative activities compared with other enzymes in the liver (May *et al.*, 1995). Reduction of levels of these three enzymes to 50% of normal are responsible for the three autosomal dominant types of acute hepatic porphyrias. Clinical manifestations are often in the form of acute attacks of neurological dysfunction and may be life threatening (Thunell *et al.*, 2000; Elder *et al.*, 1997). These disorders are usually latent and most patients do not show symptoms. The attack can be precipitated by a diversity of

	Classification	Deficient enzyme	Inheritance	Principal-Symptomatology
Acute	Acute intermittent porphyria (hepatic)	PBG deaminase	Autosomal dominant	Neurovisceral
	ALA-dehydratase deficiency porphyria (hepatic)	ALA dehydratase	Autosomal recessive	Neurovisceral
	Hereditary coproporphyria (hepatic)	Coproporphyrinogen oxidase	Autosomal dominant	Neurovisceral ± Photosensitivity
	Variegate porphyria (hepatic)	Protoporphyrinogen oxidase	Autosomal dominant	Neurovisceral ± Photosensitivity
Non-acute	Congenital erythropoietic porphyria (erythropoietic)	Uroporphyrinogen III synthase	Autosomal recessive	Photosensitivity
	Porphyria cutanea tarda (hepatic)	Uroporphyrinogen decarboxylase	Variable	Photosensitivity
	Hepato erythropoietic porphyria (hepatic)	Uroporphyrinogen decarboxylase	Autosomal recessive	Photosensitivity ± Neurovisceral
	Erythropoietic protoporphyrria (erythropoietic)	Ferrochelatase	Autosomal dominant	Photosensitivity

Table 1.1: Classification of the major human porphyrias.

exogenous and endogenous precipitating factors; these include pharmaceutical drugs (such as sulfonamides, barbiturates, phenytoin), alcohol, fasting, steroid hormones, etc. These diseases are therefore also called inducible porphyrias. There are four types of acute porphyria, acute intermittent porphyria (AIP), ALA-dehydratase deficiency porphyria, hereditary coproporphyria (HC) and variegate porphyria (VP).

Acute intermittent porphyria (AIP)

The most common autosomal dominant form of the acute hepatic porphyrias is AIP, which is caused by 50% deficiency of porphobilinogen deaminase. Despite this, AIP has low penetrance with roughly 90% of patients who inherit the deaminase deficiency remaining clinically unaffected throughout their lives unless exposed to exogenous or endogenous precipitating factors. Some drugs, hormonal and nutritional factors may provoke the disease, normally by inducing hepatic 5-aminolaevulinic acid synthase (ALAS). AIP appears to be latent before puberty and is more frequent in females than in males. Patients with AIP suffer from neurological symptoms but lack cutaneous photosensitivity. Treatment consists of intravenous haem-arginate or glucose, careful regulation of the diet and avoidance of exposure to harmful drugs (Kappas *et al.*, 1989; Sassa and Kappas, 2000)

ALA-dehydratase deficiency porphyria (ALADP)

5-Aminolaevulinic acid dehydratase deficiency porphyria (ALADP), or Doss-porphyria, is an autosomal recessive hepatic porphyria. It is a very rare form of porphyria as levels of ALAD below 50% are sufficient for normal function. Only a few cases have been reported (Sassa and Kappas, 2000), caused by a homozygous deficiency in ALA dehydratase (ALAD) activity. The clinical symptoms and management are similar to that in AIP patients.

Hereditary coproporphyria (HC)

Hereditary coproporphyria is an autosomal dominant hepatic porphyria caused by mutation of the gene encoding the enzyme coproporphyrinogen oxidase (COPRO oxidase) that leads to 50% of the normal enzyme activity. The neurological features and the management of HC are generally identical to acute intermittent porphyria, although it is milder, with only slightly raised amounts of ALA and PBG (Sassa and Kappas, 2000). The management of the disease is generally similar to that used for AIP. In addition to the AIP-like symptoms, HC may cause skin photosensitivity as a result of the accumulation of coproporphyrin in the skin, which can be minimized by β -carotene and avoidance of sunlight (Kappas *et al.*, 1989).

Variegate porphyria (VP)

Variegate porphyria is also an autosomal dominant hepatic porphyria and most common in South African families. VP is due to a mutation resulting in a 50% deficiency of protoporphyrinogen oxidase (PROTO oxidase) activity. The clinical symptoms and the disease management are identical to AIP. In addition, there is photosensitivity due to the accumulation of porphyrins in the skin and this is more common in VP than in HC. Photosensitivity can be minimized as mentioned for HC (Sassa and Kappas, 2000; Kappas *et al.*, 1989).

1.2.2 Non-acute porphyrias

Unlike the acute porphyrias, non-acute porphyrias do not cause neurological symptoms. Patients with non-acute porphyrias suffer mainly from cutaneous photosensitivity. It has been found that in all cutaneous porphyrias, porphyrins (which are photosensitizing) are deposited in the upper epidermal layer of the skin and that these are responsible for the characteristic skin lesions. Porphyrins become pho-

toexcited by the action of sunlight in the skin and promote the formation of singlet oxygen (a reactive form of molecular oxygen) that causes cellular damage (Sassa and Kappas, 2000). The four types of non-acute porphyrias are listed as, congenital erythropoietic porphyria (CEP), porphyria cutanea tarda (PCT), hepatoerythropoietic porphyria (HEP) and erythropoietic protoporphyrphyria (EPP).

Congenital erythropoietic porphyria (CEP)

Congenital erythropoietic porphyria is an autosomal recessive erythropoietic porphyria. This porphyria is caused by a genetic defect that leads to a deficiency of uroporphyrinogen III cosynthase (URO cosynthase) that is usually apparent at birth. CEP is characterized by marked skin photosensitivity as a result of over production of porphyrins in tissues due to the defect in URO cosynthase, especially under the skin. Red blood cells show intense fluorescence due to the accumulation of uroporphyrin I. Haemolysis, which also increases the level of porphyrin in the bone marrow, is another symptom of CEP. Congenital erythropoietic porphyria can be treated by protecting patients from sunlight and haemolysis may improve after splenectomy (Kappas *et al.*, 1989).

Porphyria cutanea tarda (PCT) and hepatoerythropoietic porphyria (HEP)

Porphyria cutanea tarda (PCT) and hepatoerythropoietic porphyria (HEP) are the heterozygous and homozygous deficiency, respectively, of the cytosolic enzyme, uroporphyrinogen decarboxylase (UROD). The most common autosomal dominant form of non-acute hepatic porphyria is porphyria cutanea tarda which appears usually in middle or later adult life. PCT may be inherited (familial, or type II), about 25%, or, acquired (sporadic, or type I), 75% (Elder and Roberts, 1995; Kappas *et al.*, 1989). PCT, like some of the acute hepatic porphyrias, is latent until the patient has been exposed to exogenous or endogenous precipitating factors. These include, alcohol, estrogen ingestion, sufficient iron overload or liver disease where the level

of uroporphyrin that accumulates is sufficient to produce the symptoms. However, unlike the acute hepatic porphyrias, the neurological symptoms are not apparent in PCT and neither 5-aminolaevulinic acid nor porphobilinogen accumulate. The clinical symptoms of PCT are characterized by marked skin photosensitivity, as a result of the overproduction of porphyrins in tissues, especially under the skin, due to the defective UROD. Porphyria cutanea tarda can be treated by avoiding precipitating factors and, in some cases, by phlebotomy that reduces the over accumulation of iron (Kappas *et al.*, 1989).

HEP is a rare homozygous form of porphyria cutanea tarda. Clinical symptoms of HEP, like those of CEP, are characterized by childhood onset of severe photosensitivity and skin fragility. HEP can be treated by avoidance of the sunlight and the use of topical sunscreens (Kappas *et al.*, 1989).

Erythropoietic protoporphyrinia (EPP)

Erythropoietic protoporphyrinia is an autosomal dominant porphyria causing a 50% decrease in the activity of ferrochelatase. The disease is characterized by mild to moderate cutaneous photosensitivity due to a massive accumulation of protoporphyrin in erythrocytes, plasma and stools (Kappas *et al.*, 1989). Since the protoporphyrin is insoluble in water, it is not excreted in the urine. The clinical symptoms of EPP are apparent at infancy as temporary skin redness with swelling occurring immediately after exposure to sunlight. Erythropoietic protoporphyrinia can be treated by avoiding sunlight and taking oral administration of β -carotene (Sassa and Kappas, 2000). Fatal liver disease may occur in a proportion of patients and liver transplantation has been used in preventing the progression of the disease (Moore, 1993).

1.2.3 Acute intermittent porphyria (AIP)

Mutations in the human PBGD gene lead in many cases to a 50% reduction in enzyme activity that causes the disease acute intermittent porphyria (AIP), see figure 1.6. AIP is inherited as an autosomal dominant trait with low penetrance and approximately 90% of individuals who inherit PBGD deficiency remain clinically unaffected. In AIP, the early haem pathway intermediates, 5-aminolaevulinic acid and porphobilinogen, are excreted in the urine at high levels, as indicated by biochemical analysis (Grandchamp *et al.*, 1989c). Since haem regulates its own biosynthesis pathway, any fall in its level leads to the induction of the mRNA encoding the first enzyme in the pathway, 5-aminolaevulinic acid synthase. The increase in the production of 5-aminolaevulinic acid synthase leads to an increase in the flux of 5-aminolaevulinic acid (ALA) into porphobilinogen (PBG), however, the lower level of porphobilinogen deaminase, as a result of the genetic lesion, cannot deal with the higher levels of PBG and, consequently, the level of the intermediates, PBG and ALA, become elevated in the blood and urine (Strand *et al.*, 1970). It has been suggested for many years that 5-aminolaevulinic acid, because of its structural similarity to the inhibitory neurotransmitter γ -aminobutyric acid (GABA), may be toxic to the peripheral and central nervous systems, although there is little direct evidence to support this. It has been found that deficiency of haem impairs the catabolism of L-tryptophan by the haem-dependent hepatic tryptophan pyrolase enzyme and this could result in enhanced levels of tryptophan and serotonin (5-hydroxytryptamine) to neurotoxic levels (Shoolingin-Jordan and Wood, 1998). The current evidence supports the view that AIP is a haem deficiency disease and that the neurological effects of the mutation arise as a result of insufficient haem synthesis in neuronal tissues (Lindberg *et al.*, 1999).

Acute intermittent porphyria is latent before puberty and symptoms are more frequently found in females than in males. The acute attacks are often precipitated by exposure to exogenous and endogenous factors; these include pharmaceutical drugs

such as barbiturates, phenytoin, sulfonamides; alcohol; fasting; stress and steroid hormones. The acute attack of this disease is characterized by clinical symptoms including severe colicky abdominal pain that may be accompanied by neurological and psychiatric symptoms; hypertension; nausea; diarrhoea; constipation; vomiting; muscular weakness and, occasionally, sensory loss can occur (Grandchamp, 1998; Kappas *et al.*, 1989; Moore, 1993). Moreover the patient can suffer from a diverse range of mental symptoms and from pain in the limbs, head, neck or chest. The urine is frequently dark red in colour due to the presence of an oxidation product of porphobilinogen (Sassa and Kappas, 2000). A survey of mutations causing AIP is given in the website "<http://archive.uwcm.ac.uk/uwcm/mg/search/120528.html>", see appendix.

Management of the acute attack

It has been found that extended acute attacks of porphyria carry a high risk of mortality, but with early diagnosis, removal of precipitating factors and the provision of intensive supportive therapy, the risk of mortality decreases. A reference booklet indicating which drugs are safe and which are unsafe is given to patients with AIP (Gorchein, 1997). AIP can be treated directly with exogenous haem, in the form of haem-arginate or haematin, through intravenous injection, since this deregulates the production of ALAS and therefore the concentration of ALA and PBG are lowered to normal levels (Mustajoki and Nordmann, 1993; Kappas *et al.*, 1989). High carbohydrate intake can be used as a therapy for AIP, since the depletion on haem affects the gluconeogenesis process. The effect of haem deficiency on this process, may be explained by the specific requirement for haem by tryptophan pyrolase which is needed to catabolise tryptophan. As a result, the level of tryptophan in the liver increases which inhibits phosphoenolpyruvate carboxykinase and, consequentially, the gluconeogenesis process is disturbed. Recently, a new treatment has been discovered using tin-protoporphyrin, that inhibits hepatic haem oxygenase and, as a result, reduces the rate of hepatic haem degradation (Moore, 1993).

Structural basis of AIP

In patients with AIP, PBGD arginine mutants are the most common and are found typically at positions 26,116,149,167,173 and 201 in humans, equivalent to positions 11,101,131,149,155 and 183 in *E. coli*. Arginines-116 and 201 can form salt-bridges that stabilize the protein structure, whereas arginines 26,149,167 and 173 interact with the cofactor or substrate, or both. Mutations can be divided into two classes, CRIM-ve and CRIM+ve, depending on the ratio of cross-reacting immunological material (CRIM) to enzymatic activity. In CRIM-ve phenotypes there is a correlation between the depressed enzyme activity and the reduced protein, while in CRIM+ve phenotypes normal or even enhanced levels of protein are associated with depressed enzyme activity (Desnick *et al.*, 1985; Wood *et al.*, 1995). The absence of detectable protein can be due to a variety of reasons; for example, transcriptional or translational disturbances, or the formation of an unstable protein that is rapidly degraded (Brownlie *et al.*, 1994). The mutations that involve substrate binding groups are generally CRIM+ve, like the mutant Arg 167 Gln where no apparent structural change occurs to the protein. However, mutations involving key cofactor binding groups such as Arg 149 Gln are unstable and lead to CRIM-ve phenotypes. These mutations form part of the research described in the later part of this thesis.

1.3 Porphobilinogen deaminase (PBGD)

Porphobilinogen deaminase, catalyzes the third step of haem biosynthesis in which four molecules of porphobilinogen polymerize to form a 1-hydroxymethylbilane called preuroporphyrinogen, see figure 1.3. This product is extremely unstable with a short half-life, $t_{1/2} = 4.5$ minutes at pH 8. In living systems preuroporphyrinogen is transformed into uroporphyrinogen III by the enzyme uroporphyrinogen III synthase (Jordan, 1994a). PBGD and uroporphyrinogen III synthase work sequentially but must be together to form uroporphyrinogen III. If the uroporphyrinogen III synthase

Exon	Mutation	Environment	Effect	Reference
1	Splice	Hydrophobic core adjacent L81, L85, and H80	Ubiquitous enzyme only deleted	Grandchamp et al., 1989b
1	Splice	Intron 1	Ubiquitous enzyme only deleted	Grandchamp et al., 1989c
3	Splice -		Truncated protein	Llewellyn et al., 1992a
3	R26H +	Salt bridge with propionate side chain of cofactor ring C2 at putative substrate site	Loss of interactions to substrate	Elder et al., unpubl.
4	A31T +	Packed against R11, insufficient space beyond C β	Steric disruption	Grandchamp et al., unpubl.
4	Q34K	Base of active site cleft, H bonds to S96 and R193	H bonding break, +ve charges close	Mgone et al., 1992
5	AS55 +	Protein surface	Unknown	Grandchamp et al., unpubl.
5	Deletion -	Frameshift (at residue 58)	Truncated protein	Grandchamp et al., unpubl.
5	Insertion -	Frameshift (at residue 61)	Truncated protein	Grandchamp et al., unpubl.
5	Splice -	Intron 5	Truncated protein	Grandchamp et al., unpubl.
7	V93F	Hydrophobic core adjacent L81, L85, and H80	Steric disruption	Chen et al., 1992
7	Q111R	Protein surface	Unknown	Grandchamp et al., unpubl.
8	R116T\			Mgone et al., 1992
8	R116W -	Interdomain salt bridge to E250, H bond to 198CO	Loss of stabilizing interactions	Chen et al., 1992
8	R116Q/			Lee et al., 1990
8	A122G	Hydrophobic core	Destabilizing cavity	Gu et al., 1992
8	Deletion	704 bases missing	Truncated protein	Mgone et al., unpubl.
9	R149L\ -	Salt bridge interaction with cofactor ring	Cofactor binding interactions disrupted	Grandchamp et al., unpubl.
9	R149Q/ -	C1 acetate side chain	Truncated protein	Delfau et al., 1991
9	Q155Stop -		Substrate binding interactions disrupted	Scobie et al., 1990
10	Splice		Truncated protein	Lundin et al., 1993
10	R167W\ +	Salt bridge interaction with cofactor ring C2 acetate side group in putative substrate site		Llewellyn et al., 1992b
10	R167Q/ +			Delfau et al., 1990
10	R173W\ +	Salt bridge interactions to propionate of cofactor ring C1 and acetate of C2 in putative substrate site	Loss of binding interactions to substrate and cofactor	Gu et al., 1992;
10	R173Q/ +			Delfau et al., 1990
10	L177R	Hydrophobic core	Destabilizing buried charge	Mgone et al., 1992
10	W198Stop -		Truncated protein	Lee and Anvret, 1991
10	R201W	Salt bridge to D178	Loss of stabilizing interaction	Chen et al., 1992
10	Q204Stop		Truncated protein	Mgone et al., 1994
10	E209K -	Protein surface	Unknown	Grandchamp et al., unpubl.
10	Splice -	Cryptic splice site activated	Deletes residues 203-205	Delfau et al., 1991
11	E223K -	Salt bridge with H95 at base of active site cleft	Disruption due to close +ve charges	Grandchamp et al., unpubl.
12	Splice -	Intron 11	Truncated protein	Llewellyn et al., 1992a
12	T244STOP		Truncated protein	Mgone et al., 1992
12	Deletion -	Frameshift (R244) generating stop	Truncated protein	Grandchamp et al., unpubl.
12	Insertion -	Frameshift (R248) generating stop	Truncated protein	Grandchamp et al., unpubl.
12	C247F\	Buried in the hydrophobic core	Steric disruption	Chen et al., 1992
12	C247R\			Mgone et al., 1993
12	L245R -	Protein surface	Unknown	Delfau et al., 1991
12	E250K -	Buried interdomain salt bridge to R116	Disruption due to close +ve charges	Grandchamp et al., unpubl.
12	A252T\	Packed at interface of helices $\alpha 1_3$ & $\alpha 2_3$	Steric disruption	Mgone et al., 1993
12	A252V\			Mgone et al., 1993
12	L254P	Near end of $\alpha 1_3$ and cofactor linkage site	Conformation disrupted near cofactor	Mgone et al., unpubl.
12	H256N -	$\alpha 1_3$ helix cap and H bonds N340	Loss of stabilizing interactions	Mgone et al., 1992
12	C261Y	Cofactor linkage site	Cofactor bonding?	Mgone et al., unpubl.
12	Splice +		Exon 12 only deleted	Grandchamp et al., 1989a
13	T269I	Hydrophobic core	Steric disruption	Mgone et al., 1994
13	G274R	Loop $\beta 1_3/\beta 2_3$, positive phi	Folding defect?	Mgone et al., 1994
13	Splice -	Intron 13	Truncated protein	Llewellyn et al., 1992a
14	Deletion -	Frameshift (His 305) generating stop	Truncated protein	Delfau et al., 1991
14	W283stop			Mgone et al., 1994
14	Splice -	Intron 14	Truncated protein	Llewellyn et al., unpubl.

Figure 1.6: AIP associated mutations in the human PBGD gene^a (Brownlie et al., 1994).

^a Where known, the CRIM type is shown as + or -. Deletion and insertion refer to bases in the DNA. "Splice" indicates that the mutation has occurred in the consensus sequence for RNA processing; when such mutations occur within the intron, they are grouped with the adjacent exon.

is absent, preuroporphyrinogen will cyclize non-enzymatically to the physiologically unimportant uroporphyrinogen I isomer, as shown in figure 1.7.

PBGD has been isolated from many different sources, including human erythrocytes and recombinant strains of *Escherichia coli*. It has been found that the amino acid sequences of PBGDs from all species show over 45% similarity (figure 1.8) indicating they are likely to share the same three dimensional structure and mechanism of activity (Louie *et al.*, 1996).

Comparison of the amino acid sequences of PBGDs from different species identified highly conserved arginine residues that were predicted to interact with the carboxylate groups of the porphobilinogen units during the polymerization reaction. This similarity (60% similarity between human and *E. coli* deaminases) has assisted modelling the structure of the human enzyme from the bacterial structure (Jordan, 1994a and Jordan, 1994b). PBGDs have M_r values ranging from 34,000 to 44,000 depending on the species and all appear to exist as monomeric enzymes. PBGDs are stable at 60°C with optimum pHs ranging from 8-8.5, with isoelectric points between pH 4 and 5, K_m values for porphobilinogen of 10 - 50 μM and turnover numbers of about 0.5 sec^{-1} (Shoolingin-Jordan, 1995).

1.3.1 The structure of porphobilinogen deaminase

X-Ray analysis of *E. coli* porphobilinogen deaminase indicates that it has three domains (1, 2 and 3) each of approximately 100 amino acids, linked together by flexible hinge regions (figure 1.9). Insertions in the bacterial sequence found in other deaminases, such as the human enzyme, locate at surface loops that are at structurally reasonable positions. For example, the 29 extra residues in the higher eukaryotic sequences relative to the bacterial sequences could occur in the loop either preceding or following strand $\beta 3_3$ in domain 3, where it is positioned quite distant from the active-site cleft of the molecule (Louie *et al.*, 1992 and 1996)(figure 1.10). Domains

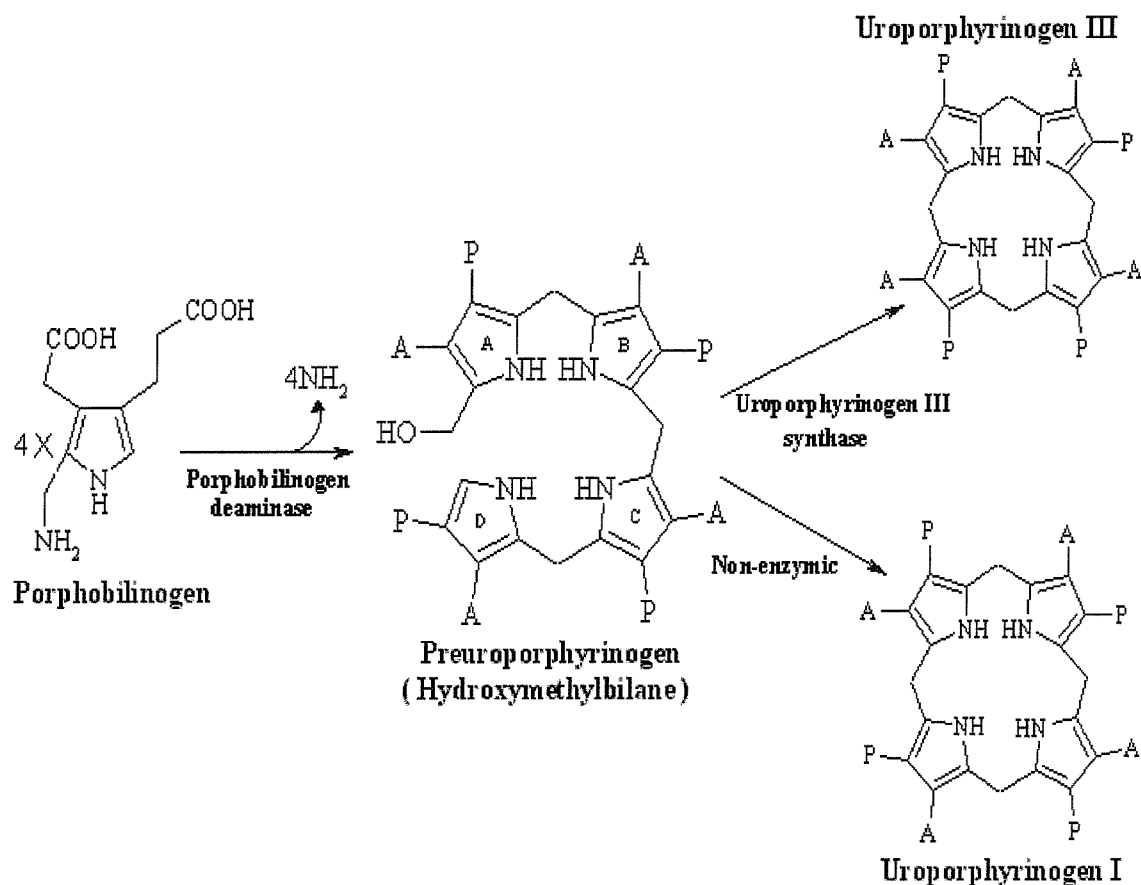


Figure 1.7: Transformation of porphobilinogen to preuroporphyrinogen then to uroporphyrinogen III or uroporphyrinogen I. The cytosolic porphobilinogen deaminase catalyses the polymerization of four molecules of porphobilinogen in a chain to generate a highly unstable 1-hydroxymethylbilane called preuroporphyrinogen. In the next reaction, preuroporphyrinogen is transformed into uroporphyrinogen III by cytosolic uroporphyrinogen III synthase. In the absence of this enzyme, preuroporphyrinogen cyclized nonenzymatically to form the isomer uroporphyrinogen I which has no biological function (Jordan, 1994).

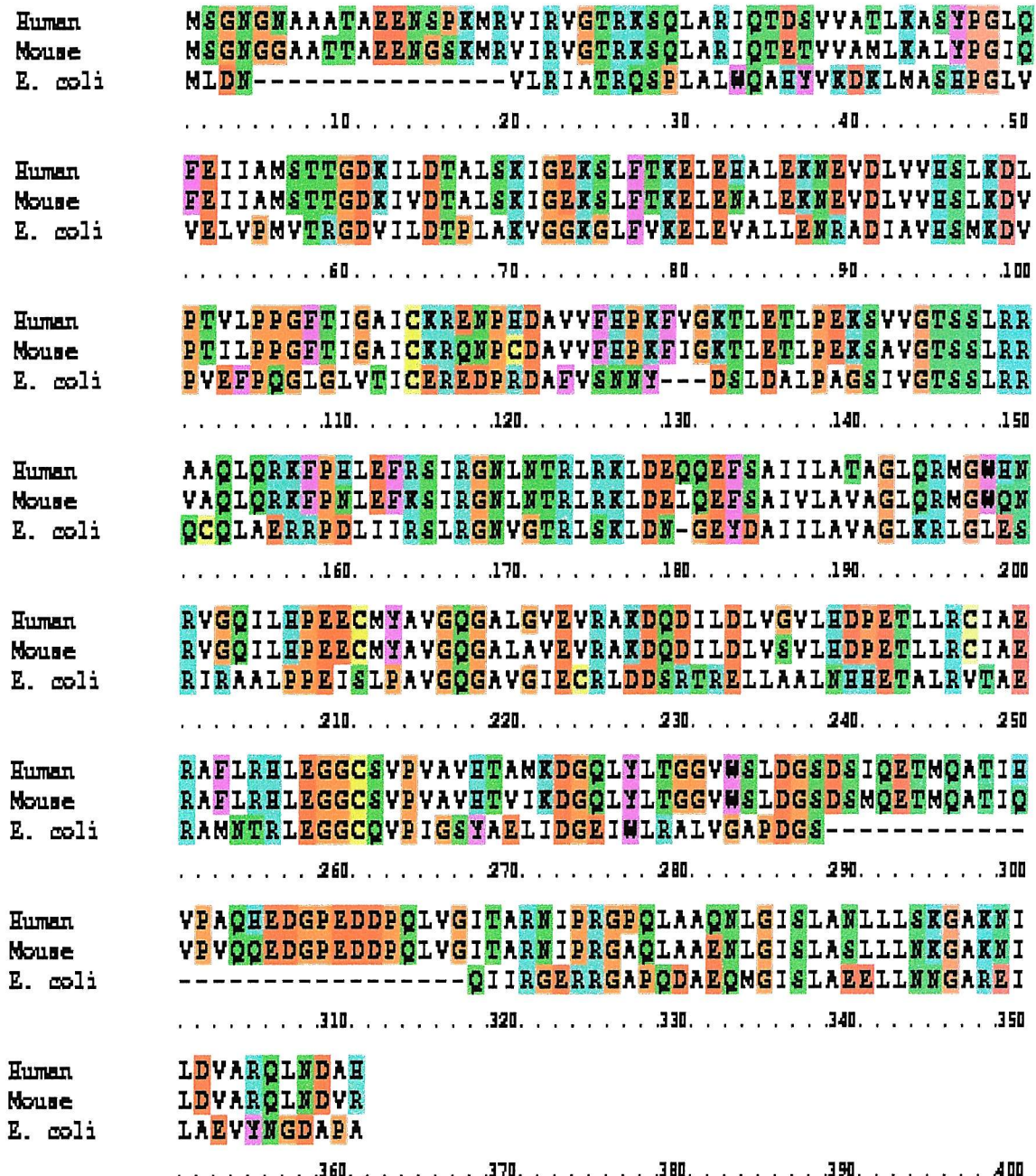


Figure 1.8: Primary sequence alignments of porphobilinogen deaminase (PBGD) from human, mouse and *E. coli* (CINEMA 2.1; Attwood *et al.*, 1997). The alignment was performed using MALIGN (Johnson, 1990). The colour key for residue types is the following: polar positive (blue), polar negative (red), polar neutral (green), nonpolar aliphatic (white), non-polar aromatic (purple), glycine and proline (brown) and cysteine (yellow).

1 and 2 have a similar five-stranded β -sheet arrangement with α -helices flanking each of the β -sheets and running approximately parallel with them. In addition domains 1 and 2, show a remarkable topological similarity to the transferrins and periplasmic ion-binding proteins (Jordan, 1994b). On the other hand, domain 3 is an open-faced three-stranded sheet with three helices packed on one face. Domains 1 and 2 have few interaction between them, and both of them form a complex array of ion pairs and hydrogen bonds with the dipyrromethane cofactor that lies in the cleft between domains 1 and 2. This cleft is large enough to contain the cofactor and the growing polypyrrole chain.

The cofactor is covalently attached by a single thioether bond to cysteine-242 of domain 3, by means of a loop that forms few contacts with domains 1 and 2 and could initiate cofactor movement (Jordan *et al.*, 1988b; Lambert *et al.*, 1994; Louie *et al.*, 1996). The acidic side groups of the cofactor interact very strongly with the basic side chains of several arginine residues, that surround the cofactor cavity (Lambert *et al.*, 1994). The cofactor thus participates in two essential functions; forming the initiation primer for the catalytic reaction and contributing to the three dimensional structure of the enzyme by forming an extensive network of interactions that cross-link the three domains and the cofactor. In fulfilling the latter role the cofactor partially neutralizes the considerable electropositivity within the active-site cleft contributing to a more stable and compact tertiary holo-enzyme structure compared to the apo-enzyme (Louie *et al.*, 1996). The native enzyme has three pyrrole binding sites, two of them are the native binding site for the C1 and C2 rings of the cofactor and the third forms the binding site for the substrate porphobilinogen. The substrate binding site recruits arginines 11, 149 and 155, aspartate 84 and phenylalanine 62 (Louie *et al.*, 1992; Lambert *et al.*, 1994). The cofactor binding site contains lysine 83, and arginines 131, 132, 149 and 155. The deaminase appears to contain only one catalytic site that is used for all reactions with porphobilinogen in the catalytic cycle (Warren and Jordan, 1988)..

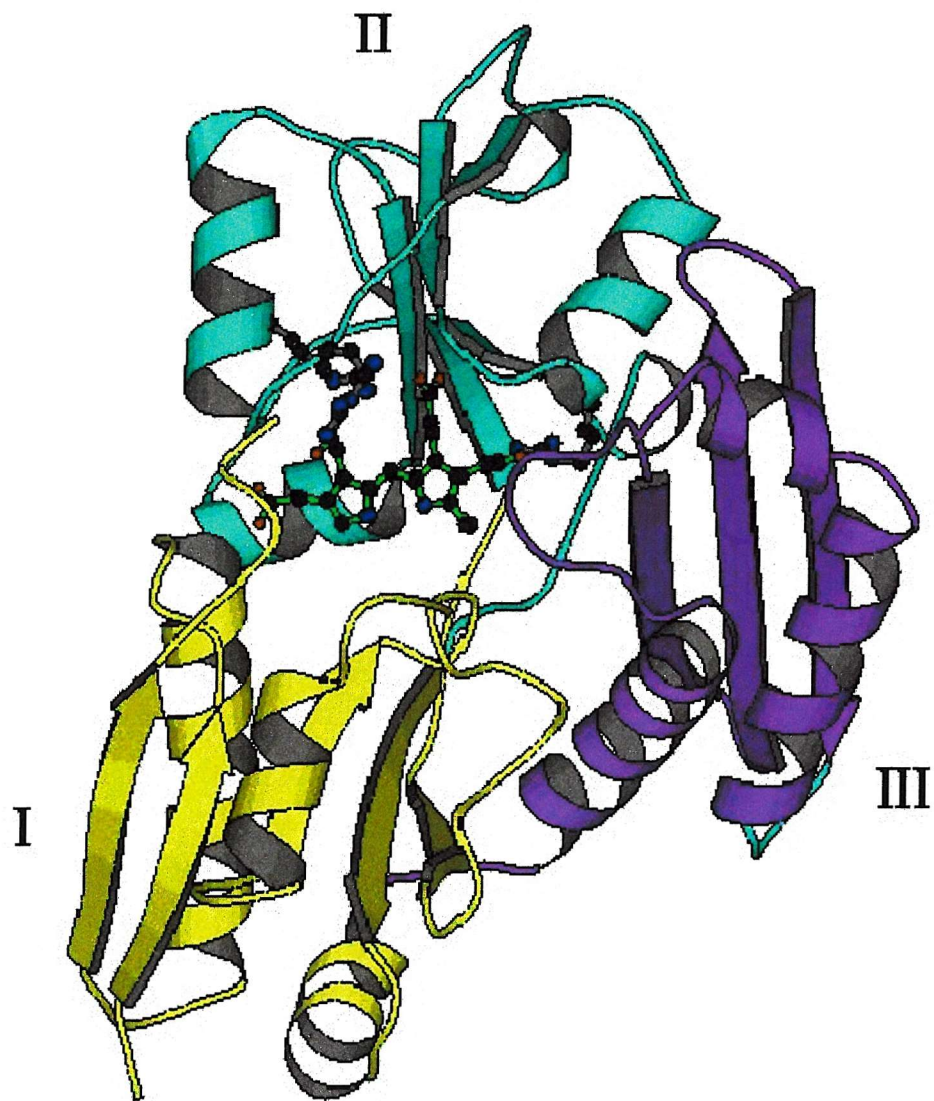


Figure 1.9: Three-dimensional structure of *E. coli* porphobilinogen deaminases that consists of three domains (1, 2 and 3), which have relatively equal size and are linked together by flexible hinge regions where domain I is in yellow, domain II is in blue and domain III is in purple. Domain 1 and 2 have a similar five-stranded β -sheet arrangement with α -helices flanking each of the β -sheet and running approximately parallel with them. On the other hand, domain 3 is an open-faced three-stranded sheet with three helices packed on one face. The cofactor, is covalently attached by a single thioether bond to cysteine-242 of domain 3 through a loop that forms few contacts with domain 1 and 2. β -Strands are represented as broad arrows, α -helices as ribbons, coil regions as thin rope and the cofactor as skeletal form (Wood *et al.*, 1995).

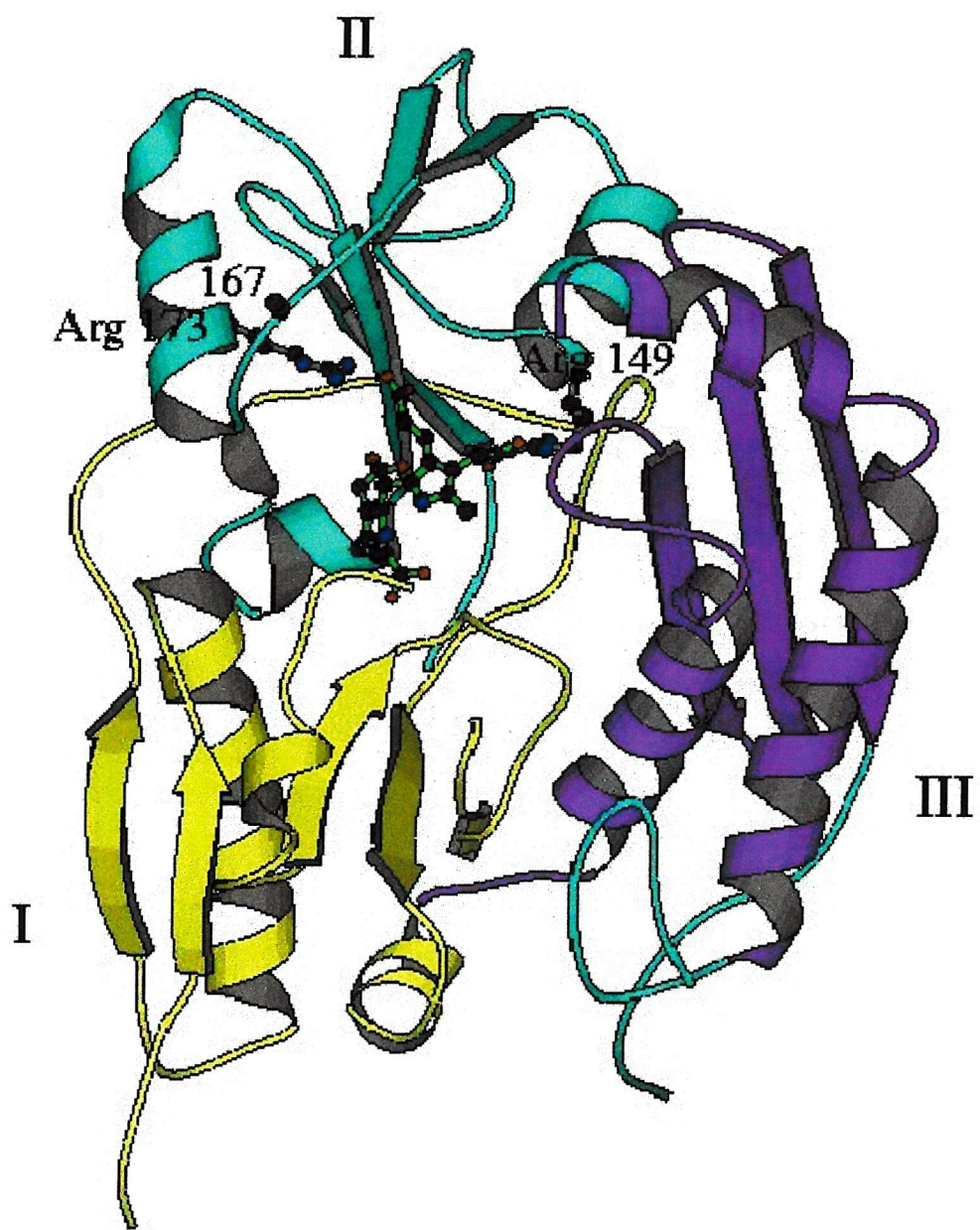


Figure 1.10: **Three-dimensional structure of human porphobilinogen deaminase.** This has approximately the same structure of *E. coli* deaminase except that it has an extra loop, 29 residue in domain III. The location of the three arginine mutants, Arg 149 Gln, Arg 167 Gln and Arg 173 Gln, are shown around the cofactor (Mohammed, 2001).

1.3.2 The dipyrromethane cofactor

The dipyrromethane cofactor consists of two molecules of porphobilinogen attached to the porphobilinogen deaminase through a single thioether bond to cysteine 242, as mentioned previously. The acetate and the propionate side groups of the cofactor rings form salt bridges and hydrogen bonds with the basic side chains of the protein, such as arginines 131, 132, 149, 155 and lysine 83. The two pyrrole nitrogens of the cofactor are hydrogen-bonded to the carboxyl side chain of the aspartate 84 (Brownlie *et al.*, 1994). The C2 ring of the cofactor is stacked against the phenyl ring of phenylalanine 62 (Louie *et al.*, 1992). The acetic acid side chain of the C2 cofactor ring interacts with arginine 149 only when this cofactor pyrrole ring occupies the putative substrate binding site (Shoolingin-Jordan, 1998 and 1995; Brownlie *et al.*, 1994; Lambert *et al.*, 1994), see figure 1.11.

Two conformational structures exist for the dipyrromethane cofactor depending on its oxidation, (figure 1.11). These two conformations contrast in the size of the dihedral angles, since these angles in the reduced form are less obtuse than in the oxidised form and thus the two pyrrole rings have a larger interplanar angle than those of the oxidised form, making a distinct elbow at the methylene group, see figure 1.12.

In the reduced and functional form of the enzyme the cofactor adopts a conformation in which the second pyrrole ring (C2) occupies an internal position in the active site cleft. On the other hand, in the oxidized form of the enzyme, the cofactor adopts a conformation where the C2 ring of the cofactor adopts a more external position which may correspond to the site of substrate binding and polypyrrole chain elongation (Louie *et al.*, 1996).

The assembly of the cofactor starts by the binding of preuroporphyrinogen to the porphobilinogen deaminase apo-enzyme followed by reaction with cysteine 242 to form a “nascent” holo-enzyme, ES_2 , in the form of a tetrapyrrole or bilane. This

“nascent” holo-enzyme is able to complete the normal catalytic cycle by reacting with two further porphobilinogen units to complete the catalytic cycle. Release of preuroporphyrinogen by hydrolysis of the enzyme-bound “hexapyrrole” generates the holo-enzyme with the dipyrromethane cofactor.

The “nascent” holoenzyme can also be converted into the holoenzyme by heat treatment (Shoolingin-Jordan *et al.*, 1996) by the loss of two pyrrole units. The cofactor is not subject to catalytic turnover, as has been established by [¹⁴C] labelling experiments. In these experiments, the deaminase was overexpressed in a *hemA* *E. coli* strain in medium containing 5-amino[5-¹⁴C]laevulinic acid. The enzyme containing the labelled cofactor was then isolated and incubated with non-labelled porphobilinogen. The final product of this incubation had no labelled compounds, which indicated that the dipyrromethane cofactor was not subject to turnover during the catalytic reaction cycle (Jordan and Warren, 1987).

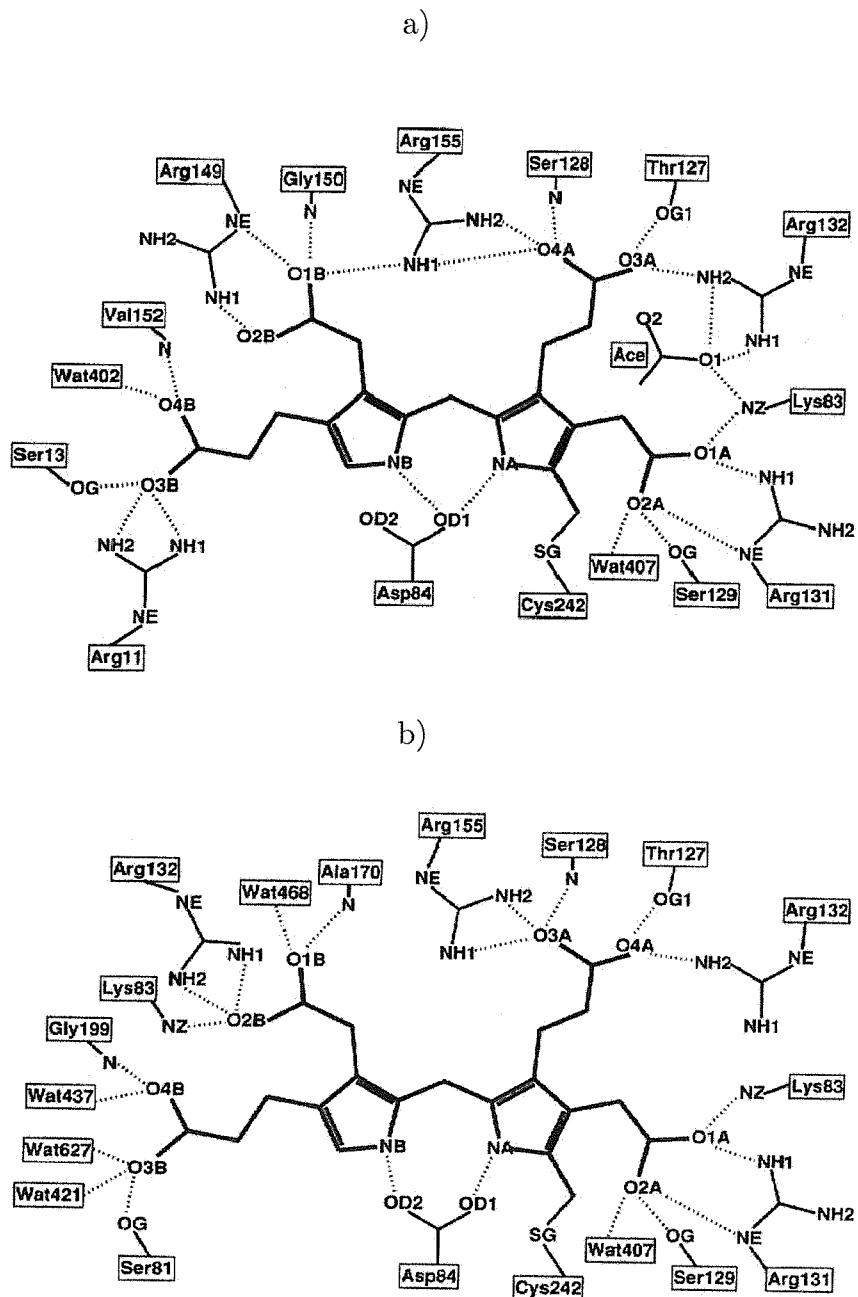


Figure 1.11: The structure of the dipyrromethane cofactor (in *E. coli* PBGD) and the hydrogen-bonding network around the dipyrromethane cofactor dipyrrole in its (a) oxidized and (b) reduced forms (Louie *et al.*, 1996).

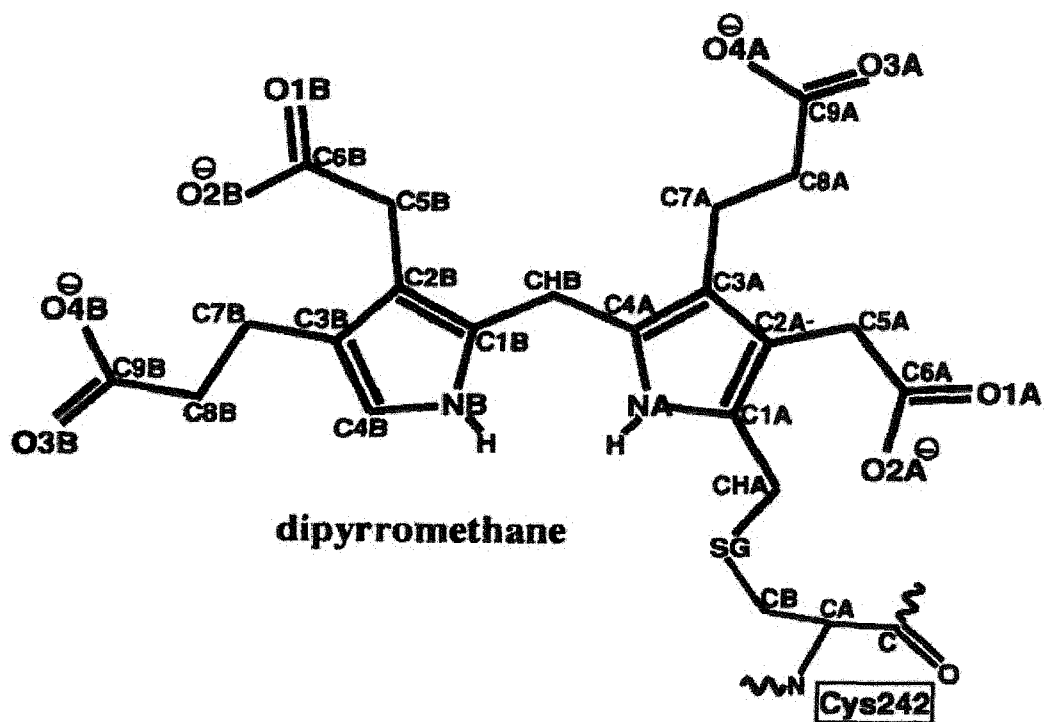


Figure 1.12: Nomenclature for atoms of the dipyrromethane cofactor, to show the two dihedral angles ($C3A-C4A-CHB-C1B-C2B$) and the bridging methylene group. The reduced dipyrromethane cofactor and the oxidized dipyrrole differ in the conformation about the bridging meso-carbon (Louie *et al.*, 1996).

1.3.3 Intermediate complexes of porphobilinogen deaminase

The PBGD reaction proceeds through enzyme intermediate complexes ES , ES_2 , ES_3 and ES_4 to form preuroporphyrinogen, see figure 1.13. In this reaction, four molecules of porphobilinogen are added to the enzyme in a stepwise fashion (A, B, C, then D) as shown by studies by Jordan and Seehra (1979, 1980). Enzyme intermediate complexes of porphobilinogen deaminase were first demonstrated by incubating human erythroid deaminase with $[^3H]$ -porphobilinogen when four labelled enzyme species were produced with one, two, three and four pyrrole units respectively bound to the enzyme as ES , ES_2 , ES_3 and ES_4 (Anderson and Desnick, 1980). These complexes were more negatively charged than the original enzyme and could be separated by ion-exchange chromatography or electrophoresis. The sequential nature of the reaction was also highlighted by the use of the substrate analogue, α -bromoporphobilinogen.

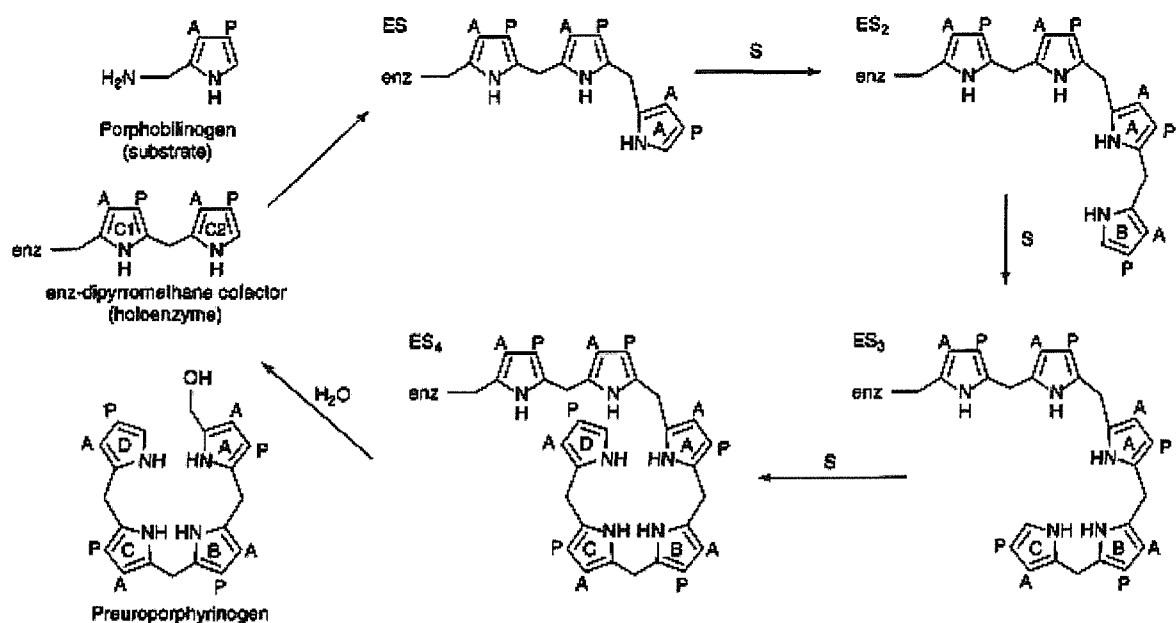


Figure 1.13: Mechanism of porphobilinogen deaminase showing the dipyromethane cofactor and its role in substrate binding and pyrrole chain extension (polymerization), (Jordan, 1991).

In these studies, α -bromoporphobilinogen functioned as a chain terminator and suicide substrate in the polymerization reaction. Since it inactivated the enzyme and inhibited the Ehrlich's reaction, it demonstrated that the inhibitor had bonded covalently with the dipyrromethane cofactor. Other experiments showed that this inhibitor, α -bromoporphobilinogen, reacted with PBGD intermediate complexes, E, ES, ES₂, ES₃ to form EB, ESB, ES₂B, ES₃B (Warren and Jordan, 1988) as shown in figure 1.14.

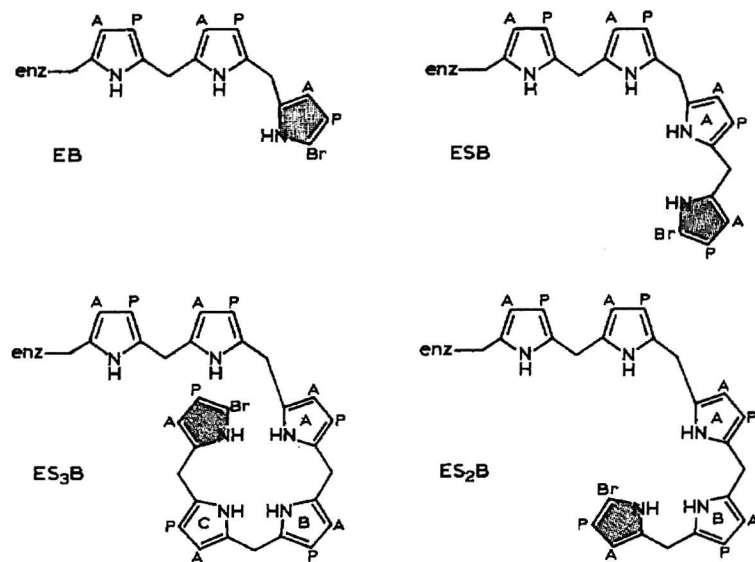


Figure 1.14: Structure of termination complexes of PBGD with α -bromoporphobilinogen added to E, ES, ES₂ and ES₃ complexes, (Jordan, 1991).

1.3.4 Substrates and inhibitors of porphobilinogen deaminase

Porphobilinogen deaminase has two substrates, the physiological substrate, porphobilinogen and the non-physiological hydroxy-analogue. The enzyme can only assemble the tetrapyrrole from a monomeric pyrrole precursor and di- and tripyrroles

cannot act as substrates. Inhibitors include opsopyrrole dicarboxylic acid, porphobilinogen lacking the aminomethyl group, α -bromoporphobilinogen which inactivates PBGD by acting as suicide inhibitor (Warren and Jordan, 1988), the α -fluoro analogue of hydroxyporphobilinogen that, like α -bromoporphobilinogen, acts as a chain terminator. Pyridoxal 5'-phosphate (PLP) and NaBH₄ reacts with the amino groups of lysine residues 55 and 59 which are located close to the active site. Protection from PLP can be achieved with porphobilinogen (Hart *et al.*, 1984). From these and other studies that used PBGD analogues and inhibitors such as NH₃, NH₂OH and NHOCH₃, the deaminase has been shown to be able to catalyze deamination and dehydration as well as the reverse of these reactions, amination and hydration, see figure 1.15. The hydration reaction is fundamental for the final release of the product from the ES₄ complex.

1.3.5 The mechanism of action of porphobilinogen deaminase

PBGD is an exceptional protein since it is able to count accurately and terminate the reaction of repetitive condensations with porphobilinogen units. The apoenzyme has also the ability to assemble its own dipyrrromethane cofactor to form the holoenzyme. During the formation of holoenzyme from the apoenzyme there is a conformational change in the structure that creates a highly stable enzyme. The negative charges of the acetic and propionic acid side chains of cofactor, substrate and intermediate complexes interact with the positive charges of arginine residues in the catalytic cleft (Jordan, 1994a).

The PBGD reaction commences with the binding of one molecule of PBG that is deaminated to produce an azafulvene. This species is subjected to nucleophilic attack by the α -position of the C2 ring of the cofactor (or the α -position of an ES complex) resulting in the formation of a new carbon-carbon bond. The reaction is completed by deprotonation, probably by either aspartate 84 or the propionic acid

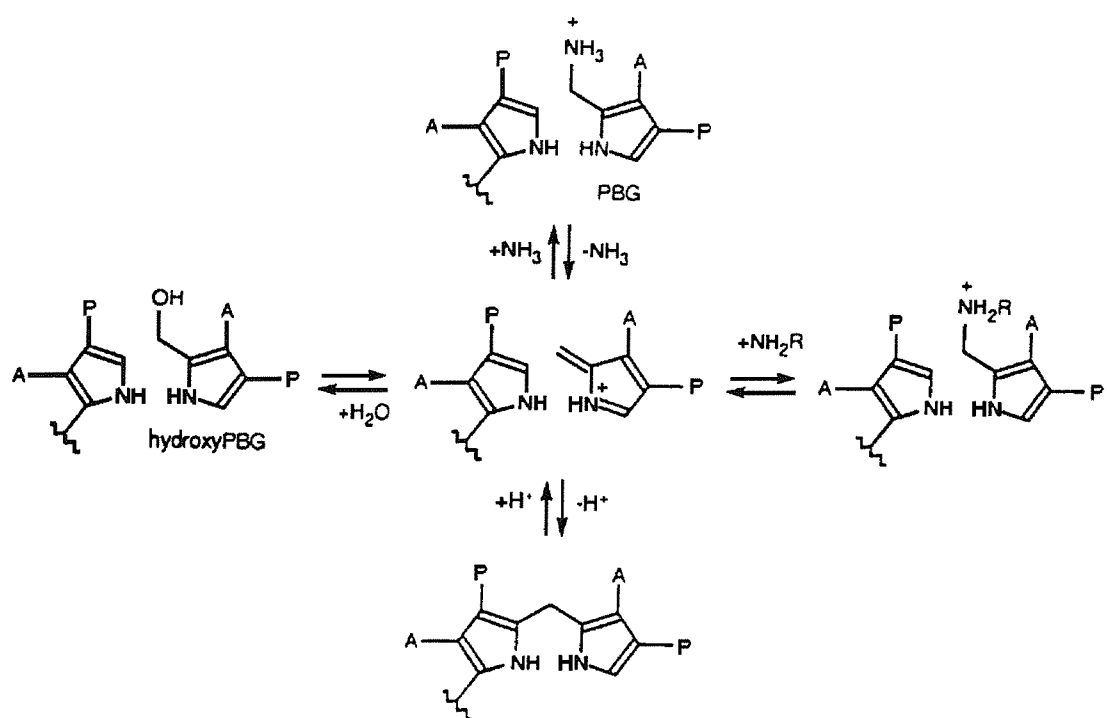


Figure 1.15: Reactions catalyzed by porphobilinogen deaminase through a putative aza-fulvene intermediate (Shoolingin-Jordan, 1995).

moiety of PBG itself. The remaining three PBG molecules are added sequentially in a similar stepwise fashion resulting in the hexapyrrole intermediate (ES_4). The release of preuroporphyrinogen from ES_4 occurs by the reverse reaction in which protonation of the carbon at the α -position of the cofactor ring C2 then cleavage of the C-C bond between the C2 ring and ring A of the tetrapyrrolic methylene pyrrolenine. Finally, reaction of the methylene pyrrolenine with H_2O yields preuroporphyrinogen and regenerates the dipyrromethane cofactor attached to the deaminase, see figure 1.16. The cofactor can be released only if the enzyme is denatured by treatment with acid (Warren and Jordan, 1988; Warren *et al.*, 1995; Lambert *et al.*, 1994).

Many features of the PBGD structure enable it to catalyse its reaction in tetrapyrrole synthesis. Of most importance is the key catalytic group, aspartate 84, that is likely to play a multiple role in the protonation of the leaving group, ammonia, stabilization of the developing charges on the pyrrole rings during the condensation and final deprotonation of the α -proton of the pyrrole ring (Woodcock and Jordan, 1994).

Evidence for conformational changes to the enzyme structure during the catalytic cycle comes from studies with the thiophilic reagent *N*-ethylmaleimide (Warren and Jordan, 1988; Warren *et al.*, 1995). This reagent reacts with the enzyme more rapidly when substrate is bound, suggesting that a thiol group becomes exposed during the catalytic cycle (Warren and Jordan, 1988). The thiol has been identified as cysteine 134 that is located on domain 2 at the interface with domain 3, and clearly becomes accessible suggesting the movement of domains 2 and 3 with respect to one another during the catalytic cycle. PBGD terminates the polymerization after the addition of four molecules, presumably because the size of catalytic cleft is only sufficient to accept four pyrrole units (Louie *et al.*, 1992).

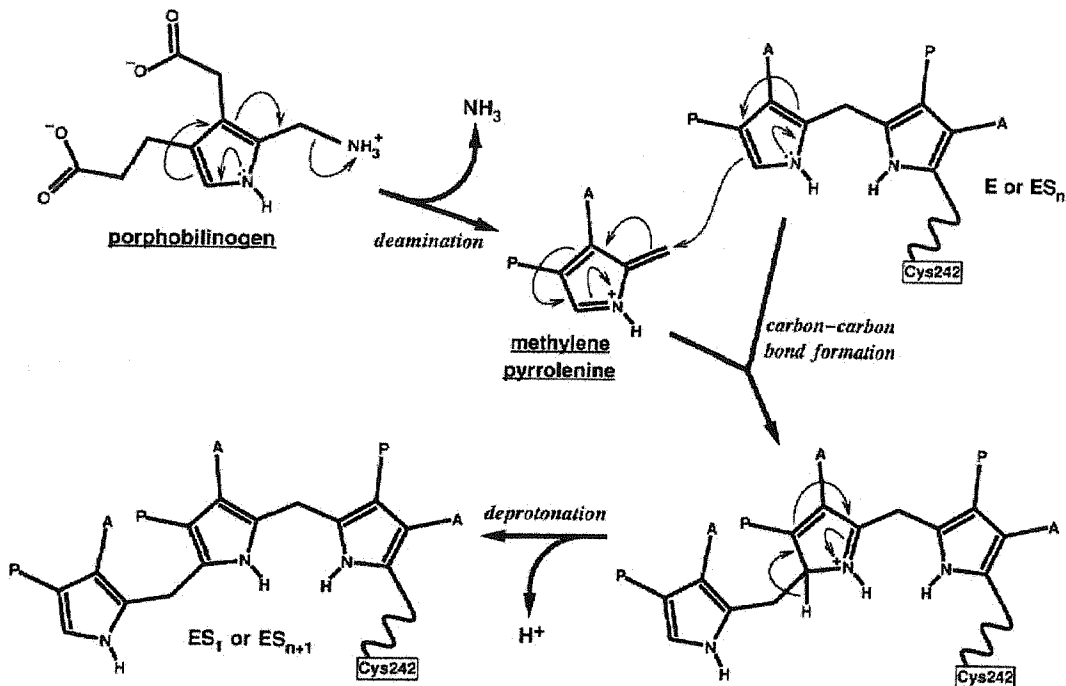


Figure 1.16: The chemistry of a porphobilinogen ring-coupling reaction. Carbon-carbon bond formation proceeds through (1) deamination of the substrate porphobilinogen (PBG) to produce the methylene pyrrolinene (azafulvene); (2) nucleophilic attack by the methylene carbon atom at the free α -position of the terminal, enzyme-bound ring; and (3) deprotonation at this same carbon atom. The acetate and propionate side-groups of the porphobilinogen moieties are denoted by -A and -P, respectively (Louie *et al.*, 1996).

1.3.6 Studies using site-directed mutagenesis in *E. coli* PBGD

Site-directed mutagenesis was used initially to generate a number of mutants in the *E. coli* *hemC* gene which provided important information about the assembly of the PBGD cofactor, substrate binding and catalysis (Jordan and Woodcock, 1991; Lander *et al.*, 1991; Woodcock and Jordan, 1994). Mutagenesis may lead to a loss of activity by affecting the catalytic site or the structure and stability of the enzyme. For example, mutation of arginine 232 in the *E. coli* enzyme, involves a residue far from the active site, affecting an interdomain ion pair that is important for conformational changes to the enzyme that occur during chain elongation. Arginine 176 has no direct interaction with the cofactor but makes a water-mediated hydrogen bond with the C2

ring of the cofactor causing disturbances in the later stages of the extension reaction and inhibits the formation of ES_3 from ES_2 . The substitution of arginine 149 which forms interactions at the putative substrate-binding site, affects the polymerization mechanism, reducing the catalytic activity and leading to the accumulation of the enzyme intermediate complex (ES) in the elongation reaction and a 5-fold rise in K_m (Jordan and Woodcock, 1991). Mutagenesis of arginines 131 and 132 in the *E. coli* PBGD to histidine or leucine prevent cofactor assembly and result in apo-deaminases completely lacking catalytic activity (Jordan and Woodcock, 1991; Lander *et al.*, 1991; Louie *et al.*, 1992). However, mutation of arginines 11 and 155 produced mutants containing the cofactor, but with inability to bind the substrate and almost total loss of enzyme activity. Mutagenesis of other residues that have direct contact with the cofactor, like the cysteine 242, affect the assembly of the dipyrromethane cofactor (Warren and Jordan, 1988). The substitution of the key catalytic group, aspartate 84 to glutamate leads to an enzyme with 1% activity, as the slightly longer glutamate side chain is unable to hydrogen bond correctly with the pyrrole nitrogen of the cofactor ring C2 and at the substrate binding site. In the project described in this thesis, three mutations were generated in the human ubiquitous deaminase cDNA at codons specifying arginines 149, 167 and 173 (131, 149 and 155 in *E. coli* PBGD). Mutations of these arginines cause the most common porphyria, AIP and cover the CRIM-ve and CRIM+ve classes mentioned above.

Arginine 149 (131 in *E. coli*), located in exon 9, is involved in ion pair interactions with the carboxylate of the acetate side group of cofactor ring C1 and forms part of a $\beta\alpha\beta$ segment of domain 2. The Arg 149 Gln mutation is likely to destabilize ion pair interaction between the enzyme and the carboxylate from the acetate side group of cofactor ring C1. With this mutation, the reduced activity of porphobilinogen deaminase correlates with a reduced amount of enzyme (CRIM-ve). Mutation at the equivalent site in the *E. coli* enzyme led to an enzyme that failed to assemble the dipyrromethane cofactor and had essentially no activity.

Arginine 167 (149 in *E. coli*), located in exon 10, forms part of the $\beta\alpha\beta$ segment of domain 2 and is engaged in an ion-pair with the carboxylate of the cofactor ring C2 acetate side chain where the substrate binds. Arginine 173 (155 in *E. coli*), also located in exon 10, contributes to part of the $\beta\alpha\beta$ segment of domain 2, but also forms ion pairs with the propionate carboxyl of cofactor ring C1 and the acetate carboxyl of the cofactor ring C2. Mutations Arg 167 Gln and Arg 173 Gln cause decreased enzyme activity but normal, or even enhanced, levels of protein, (measured immunologically CRIM +ve). It has been found, that in *E. coli*, the Arg 167 mutation affects mainly substrate binding, however the Arg 173 mutation affects a number of steps in the reaction, leading to an enhanced build up of ES, ES₂ and ES₃ intermediates in a different pattern from that observed for the native enzyme (Wood *et al.*, 1995).

In this thesis two further mutations have been analysed, Arg 167 Trp and Trp 198 Ter, both of which are common in Sweden (Andersson *et al.*, 2000). Both arginine 167 and tryptophan 198 are located in exon 10 of ubiquitous human PBGD. The Arg 167 Trp mutation is similar to Arg 167 Gln, while Trp 198 Ter is classified as a CRIM-ve phenotype that forms an unstable, inactive truncated protein (Lee and Anvret, 1991).

1.3.7 The molecular biology of human PBGD

The gene encoding human PBGD is located on the long arm of chromosome 11. The coding sequence of 15 exons extends over 10 kb of DNA specifying the two PBGD isozymes, a ubiquitous housekeeping enzyme, the main subject of this study, and an erythroid-specific enzyme, figure 1.17.

The ubiquitous isozyme, consisting of 361 amino acids, is expressed in all cells, figure 1.18. The erythroid isozyme has a smaller M_r, since it lacks an *N*-terminal extension of 17 amino acids encoded by exon 1 and consists of 344 amino acids. The erythroid enzyme is expressed only in erythroid cells (Grandchamp *et al.*, 1987).

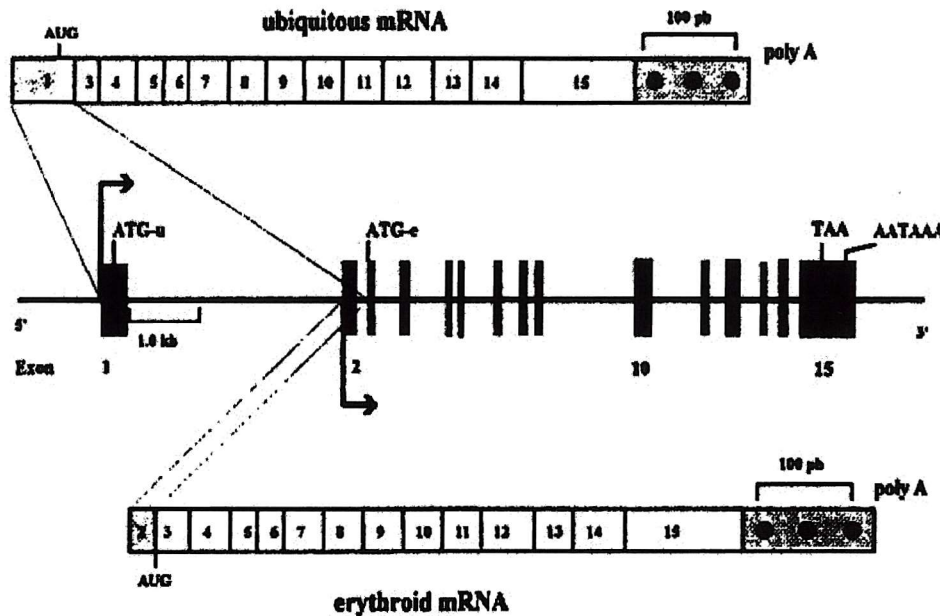


Figure 1.17: Genomic organization of the human PBGD gene and alternative splicing of the housekeeping and erythroid specific transcripts (Deybach and Puy, 1995).

PBGD has a primary protein structure in which 34 amino acids are invariant throughout all species. Of particular note, are the several highly conserved and invariant arginines at positions 26, 149, 150, 167, 173 and 195 (11, 131, 132, 149, 155 and 176 in *E. coli*), which interact with the propionic and the acetic acid side chains of the dipyrrromethane cofactor, substrate, and intermediate complexes (Brownlie, *et al.*, 1994; Shoolingin-Jordan, 1995). In addition, cysteine 261, lysine 98 and its neighbour, the catalytic aspartate 99, are also invariant (Cys 242, Lys 83 and Asp 84 in *E. coli*).

1.4 Aims of this project

Mutations in the human porphobilinogen deaminase gene lead in most cases, to an enzyme with 50% activity that can cause the hereditary disease acute intermittent

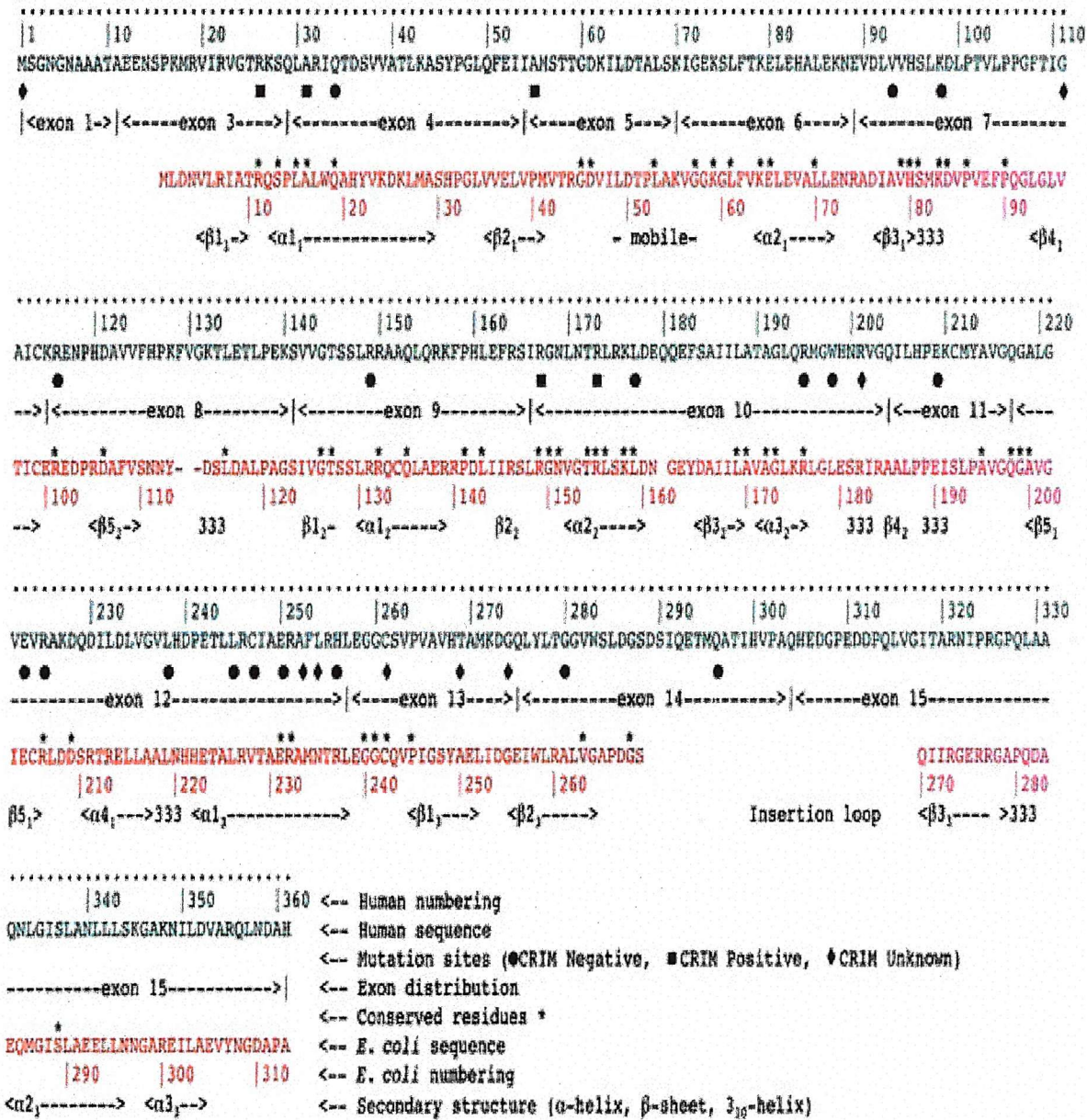


Figure 1.18: The amino acid sequences for human and *E. coli* porphobilinogen deaminase are arranged in an alignment order with each other and with the corresponding exons of the human gene and the secondary structure elements of the three-dimensional structure. Sites of point mutation that cause a change in amino acid sequence are indicated, together with the distribution of locations that have been absolutely conserved in evolution (Wood *et al.*, 1995).

porphyria. The study of the naturally occurring mutations of the enzyme can provide some insight into the role of the mutated residues in the structure and function of the enzyme. Therefore, with the help of molecular biology techniques, several mutations have been generated in the human cDNA and the mutated recombinant proteins have been expressed in *E. coli*.

The thesis commences with detailed studies characterising the two protein species found during expression of human recombinant ubiquitous porphobilinogen deaminase by using the technique of non-denaturing gel electrophoresis. Three arginine mutants, Arg 149 Gln, Arg 167 Gln and Arg 173 Gln were generated using PCR to represent a CRIM-ve (Arg 149 Gln) and CRIM+ve (Arg 167 Gln and Arg 173 Gln) classes of deaminase mutants. Two other mutations, which are the most common in the Swedish population (Arg 167 Trp and Trp 198 Ter), have also been investigated. The effect of each mutated residue on the enzyme activity is reported and the possible role of each residue is discussed.

Finally, crystallography studies have been initiated with the Arg 167 Gln mutant. Crystals have been obtained and a 2.65Å model of the first 3-dimensional structure of a human deaminase has been constructed. This latter work has been in collaboration with Mohammed Fiyaz (Mohammed, 2001).

Chapter 2

Materials and Methods

2.1 Materials

DTT, IPTG and ampicillin were purchased by Melford Laboratories Ltd, England. Tris was from ICN Biomedicals Inc, USA. 4-Dimethylaminobenzaldehyde was from BDH, Poole, UK. Growth media were from Difco, Detroit, USA. Sodium chloride, sodium hydroxide, potassium chloride and potassium hydroxide were supplied by Fisher Scientific UK Limited, Loughborough, UK. All other chemicals were supplied from Sigma Chemical Company, Poole, UK. Wizard[®] Plus SV Minipreps DNA Purification System was purchased from Promega, USA. DNA purification kits (Gene clean II) was from Bio101, Inc, Anachem Ltd. Anachem House, UK. Mimetic Orange 1 was from Affiniti Chromatography Ltd., Isle of Man. Columns for chromatography were purchased from Amersham-Pharmacia Biotech. Ltd., St. Albans, UK. Ultrafiltration cells were from Amicon, Ltd., Upper Mill, Stonehouse, England. Membrane filters (0.2 μ m) and syringe filters (0.2 μ m) were purchased from Sartorius, Göttingen, Germany and gel electrophoresis equipment was supplied by Bio-rad.

Plasmids	Relevant properties	Plasmids size (kb)	Source
pT7-7	T7 promotor system	2.473	Tabor, 1990
pUHD1	pT7-7 carrying <i>hemC</i> (1.14 Kb fragment of a human deaminase gene).	3.613	Dr. Sarwar (This study)
pUHD2	pUHD1 where arginine 167 was mutated to glutamine	3.613	
pUHD3	pUHD1 where arginine 173 was mutated to glutamine	3.613	
pUHD4	pUHD1 where arginine 149 was mutated to glutamine	3.613	
pUHD5	pUHD1 where arginine 167 was mutated to Trp	3.613	
pUHD6	pUHD1 where tryptophan 198 was mutated to stop codon.	3.000	

Table 2.1: Vector and recombinant plasmids.

2.1.1 Bacterial strains and plasmids

In this work, two strains were used, DH5 α F' and BL21(DE3), for DNA manipulation and protein expression , respectively. Both strains were stored in 20% glycerol at -70°C then plated out onto agar plates when required and stored at 4°C for up to two weeks. Single colonies from each plate were picked and grown in 10ml of liquid medium. The pT7-7 vector was used for protein expression. This contains the T7 promoter and is shown in figure 2.1. The plasmids and the strains used in this thesis are listed in tables 2.1 and 2.2.

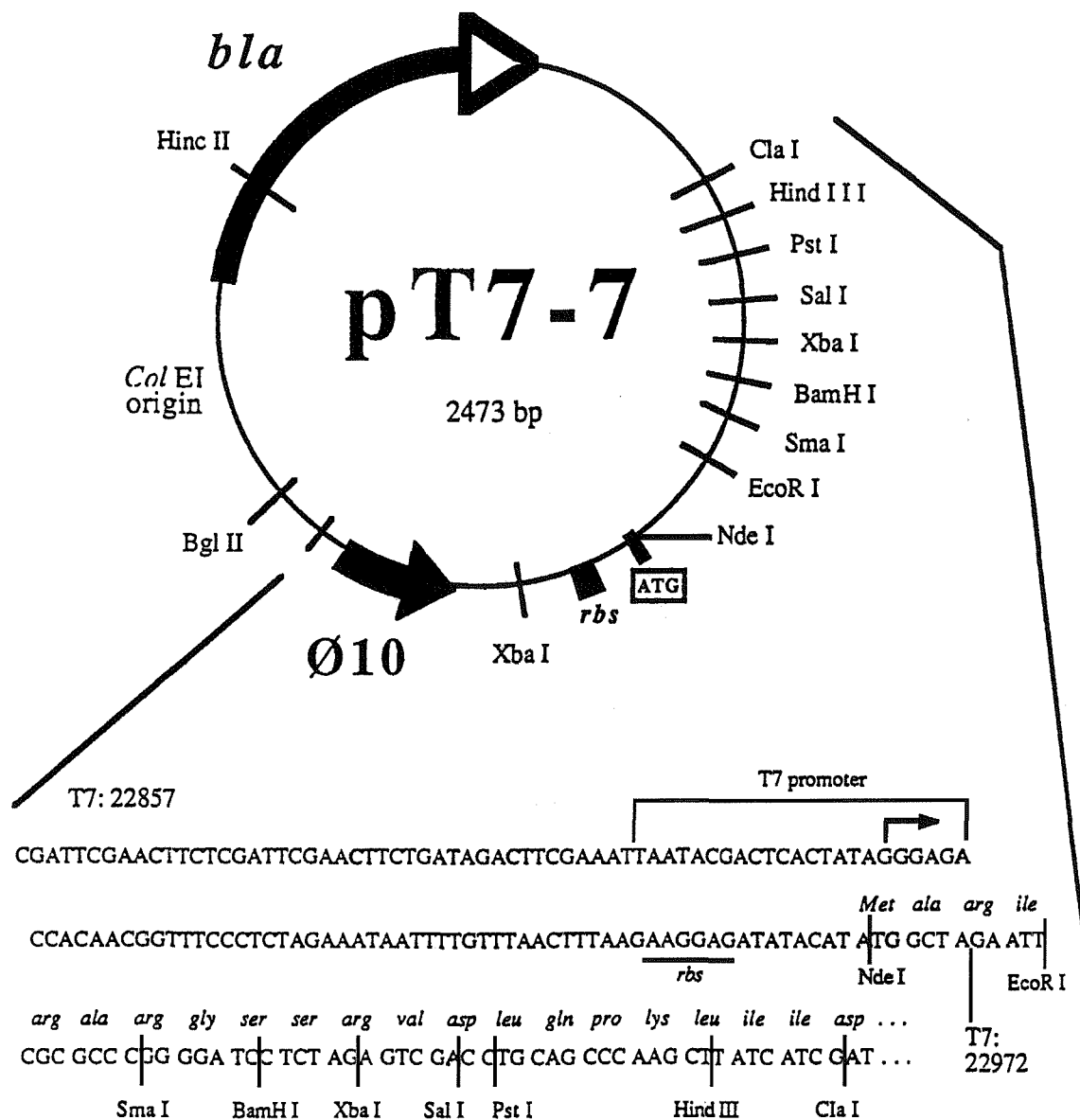


Figure 2.1: The vector pT7-7, which contains the T7 RNA polymerase promoter $\emptyset 10$. The 1.14kb fragment of ubiquitous human porphobilinogen deaminase, cDNA, was inserted into the pT7-7 vector by replacing the fragment *NdeI/BamHI*.

Strains	Genotype or phenotype
BL21(DE3)	F^- <i>ompT gal [dcm] [lon] hsdS_B (r_B⁻m_B⁻ ; an <i>E. coli</i> B strain) With DE3, a λ prophage carrying the T7 RNA polymerase gene.</i>
DH5 α F'	$F'/ endA1 hsdR17(r_K^-m_K^+) supE44 thi-1$ <i>recA1 gyrA(Nal^r) relA1 Δ(lacZYA-argF)</i> <i>U169deoR (φ80dlacΔ(lacZ)M15).</i>
UHDB1	<i>E. coli</i> BL21(DE3) harbouring plasmid pUHD1.
UHDD1	<i>E. coli</i> DH5 α F' harbouring plasmid pUHD1.
UHDB2	<i>E. coli</i> BL21(DE3) harbouring Arg 167 Gln mutant plasmid pUHD2.
UHDD2	<i>E. coli</i> DH5 α F' harbouring Arg 167 Gln mutant plasmid pUHD2.
UHDB3	<i>E. coli</i> BL21(DE3) harbouring Arg 173 Gln mutant plasmid pUHD3.
UHDD3	<i>E. coli</i> DH5 α F' harbouring Arg 173 Gln mutant plasmid pUHD3.
UHDB4	<i>E. coli</i> BL21(DE3) harboring Arg 149 Gln mutant plasmid pUHD4.
UHDD4	<i>E. coli</i> DH5 α F' harbouring Arg 149 Gln mutant plasmid pUHD4.
UHDB5	<i>E. coli</i> BL21(DE3) harbouring Arg 167 Trp mutant plasmid pUHD5.
UHDD5	<i>E. coli</i> DH5 α F' harbouring Arg 167 Trp mutant plasmid pUHD5.
UHDB6	<i>E. coli</i> BL21(DE3) harbouring Trp 198 Ter mutant plasmid pUHD6.
UHDD6	<i>E. coli</i> DH5 α F' harbouring Trp 198 Ter mutant plasmid pUHD6.

Table 2.2: Bacterial strains.

2.1.2 Bacterial media

Luria Broth (LB) contained:

Bactotryptone 10g.
 Bactoyeast extract 5g.
 Sodium chloride 5g.

Dissolved in distilled water, adjusted to a volume of one litre and then autoclaved.

LB plates:

Plates were made by adding 15g bacto agar to one liter of above medium before autoclaving. The plates were stored at 4°C inverted and allowed to dry for 15 minutes just before use.

2.1.3 Buffers and solutions

Agarose gel electrophoresis

TE buffer

10mM Tris/HCl (pH 8.0)
 1mM EDTA pH (8.0)

The mixture of 50ml was autoclaved and stored at room temperature until required.

50×TAE buffer: This buffer was made by dissolving 242g Trizma base and 37.2g Na₂ EDTA with 57ml glacial acetic acid. Finally the volume was made up to one liter with distilled water after adjusting the pH to 8.0.

λ DNA/ <i>EcoRI</i> + <i>Hind III</i>	ϕ X174DNA / <i>Hae III</i>
21,226	1353
5148	1078
4973	827
4268	603
3530	310
2027	281
1904	271
1584	234
1375	194
947	118
831	72
564	
125	

Table 2.3: Molecular weight markers for DNA agarose gels. The first marker λ DNA/*EcoRI* +*HindIII* was used to check the size of the DNA after the mini-prep. However the second marker ϕ X174DNA/*HaeIII* was used to check the DNA fragment after the PCR1. Both markers with their content of different DNA sizes were shown clearly in this table.

DNA loading buffer: To make this buffer, 0.25g of bromophenol blue, 0.25g xylene cyanol and 30ml of glycerol were dissolved in distilled water up to 100ml. Finally, the mixture was autoclaved.

Polyacrylamide gel electrophoresis

Acrylamide stock:

29g Acrylamide
1g N,N-Methylenebisacrylamide

These two components were dissolved in distilled water and the volume was adjusted to 100ml with water. The solution was stirred gently for 30 minutes and finally filtered through a sintered funnel.

Proteins	Proteins Approx. M _r
Bovine serum albumin	66,000
Egg albumin	45,000
Glyceraldehyde-3-P-dehydrogenase	36,000
Bovine carbonic anhydrase	29,000
Bovine pancreas trypsinogen	24,000
Soybean trypsin inhibitor	20,100
α -Lactalbumin	14,200

Table 2.4: The proteins in the Dalton VII-L marker (used for SDS gel electrophoresis) and their molecular weights, from Sigma Chemical Company.

Main Gel	Stacking Gel
2.8ml Distilled H ₂ O	3ml Distilled H ₂ O
3.2ml Acrylamide (30%)	1ml Acrylamide (30%)
2ml 1.5M Tris/HCl buffer, pH 8.8	1ml 0.5 M Tris/HCl buffer, pH 6.8
80 μ l 10%SDS (20gram/200ml distilled H ₂ O)	80 μ l 10%SDS (20gram/200ml distilled H ₂ O)
100 μ l 10%APS (0.1g ammonium persulphate/1ml distilled H ₂ O - fresh)	100 μ l 10%APS (0.1g ammonium persulphate/1ml distilled H ₂ O - fresh)
20 μ l TEMED (final addition)	20 μ l TEMED (final addition)

Table 2.5: Composition of solutions for SDS-PAGE gels (12% acrylamide). The SDS polyacrylamide denaturing gel was prepared in two parts, the main gel and the stacking gel as listed in this table.

Main Gel	Stacking Gel
3ml Distilled H ₂ O	2ml Distilled H ₂ O
3ml Acrylamide (30%)	1ml Acrylamide (30%)
2.8ml 1.5M Tris/HCl buffer, pH 8.8	2ml 0.5 M Tris/HCl buffer, pH 6.8
100 μ l 10%APS (0.1g ammonium persulphate/1ml distilled H ₂ O - fresh)	100 μ l 10%APS (0.1g ammonium persulphate/1ml distilled H ₂ O - fresh)
10 μ l TEMED (final addition)	10 μ l TEMED (final addition)

Table 2.6: Composition of solutions for 10% PAGE gels. The polyacrylamide non-denaturing gel was prepared in two parts, the main gel and the stacking gel as listed in this table.

SDS running buffer (5×) To make this stock buffer, 72g of glycine, 15g of Trizma base and 5g of SDS (sodium dodecylsulphate) were dissolved in distilled water then adjusted to pH 8.3 using concentrated HCl. Finally the volume was made up to 1000ml with distilled water. In the case of non-denaturing PAGE, the sodium dodecyl sulphate was omitted.

Disruption buffer (2×) This buffer was prepared by mixing 2ml of 10% sodium dodecyl sulphate, 1.25ml of 0.5M Tris/HCl buffer, pH 6.8, 1ml glycerol 0.5ml β -mercaptoethanol and 0.25ml distilled water. Finally, 0.01g bromophenol blue was added to the mixture. To make the non-denaturing PAGE sample buffer, SDS was omitted.

Staining solution Staining solution was prepared from, 2.5g Coomassie brilliant blue dissolved in 400ml methanol and 70ml glacial acetic acid, adjusted to a volume 1000ml using distilled water.

Destaining solution The solution was prepared by mixing 400ml of methanol with 70ml of glacial acetic acid then adding distilled water to give a final volume of 1000ml.

Modified Ehrlich's reagent

Modified Ehrlich's reagent was prepared by dissolving 1g of *p*-dimethylaminobenzaldehyde in 42ml of glacial acetic acid and 8ml of perchloric acid (70%). The mixture should be stored in the absence of light at 4°C, in a dark bottle, and used within one week.

Isoelectric focusing (IEF) gel

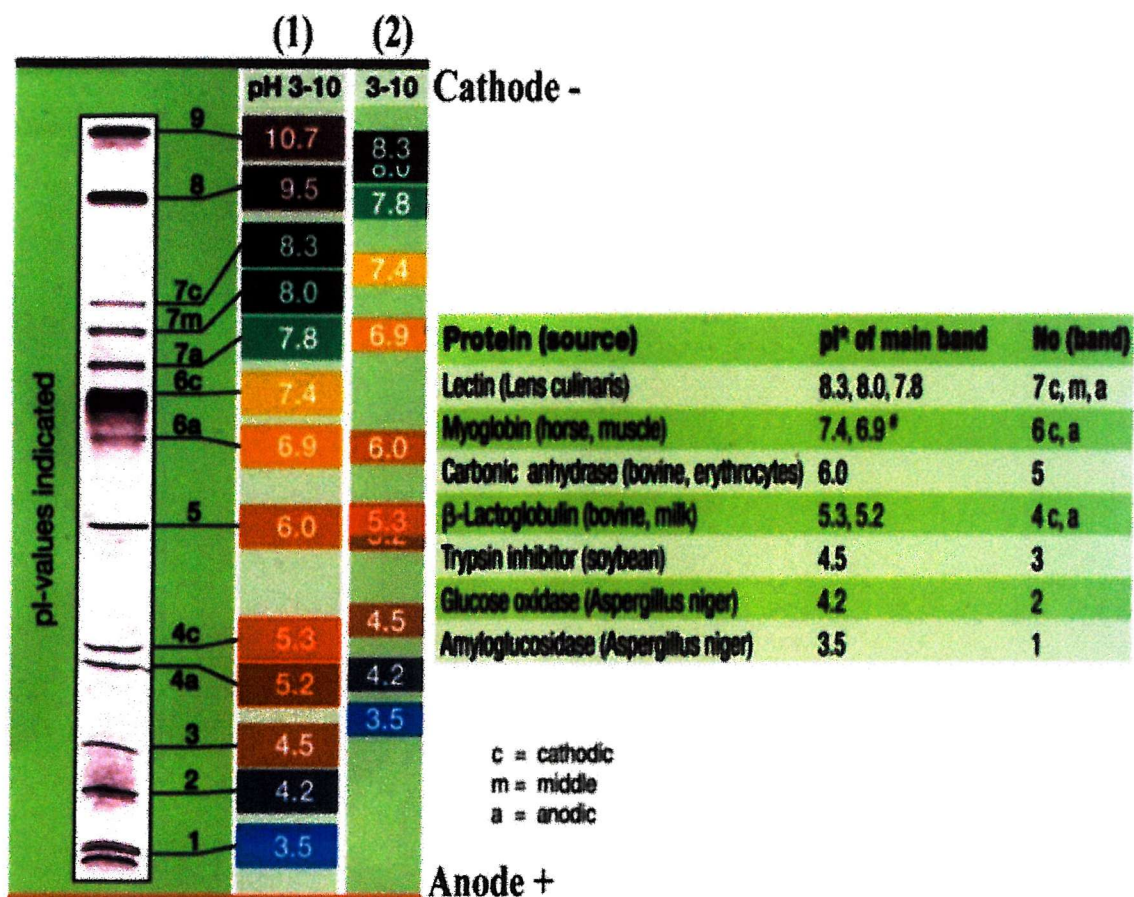


Figure 2.2: The proteins content of IEF Marker 3-10 from Novex and their pI for isoelectric focusing gels, vertical/horizontal, at pH range from 3-10. Track 1, represents the markers using the horizontal gel, track 2, represents the markers using the vertical gel.

Cathode buffer for IEF gels:

Arginine (free base) 3.5g
 Lysine (free base) 2.9g
 Distilled water To 100ml

Anode buffer for IEF gels:

Phosphoric acid (85%) 4.7g
 Distilled water To 100ml

The reader is recommended to refer to Molecular Cloning, book III by Fritsch and Maniatis, 1989.

2.2 Molecular biology methods

2.2.1 Agarose gel electrophoresis

Electrophoresis was used for DNA fragment isolation, identification and purification using Tris/acetate/EDTA buffer. A 1% agarose gel was prepared by melting the agarose in 40ml water containing 0.8ml TAE buffer using a microwave oven. After melting, $1\mu\text{l}$ ethidium bromide (10mg/ml) was added to the mixture which was allowed to cool to 60°C before pouring into the gel casting tray. A comb was added. Once the gel had set, the comb was removed and the gel was submerged in the electrophoresis tank, filled with $1 \times$ TAE buffer. The samples and required markers, see table 2.3, were mixed 1:6 with DNA loading buffer before loading onto the gel. Electrophoresis was carried out at 100V for 45min. - 1 hour.

2.2.2 Recovery of DNA from an agarose gel, GenecleanTM

The DNA, after PCR and digestion, was electrophoresed using 1% agarose gel. The required band was excised from ethidium bromide stained agarose gels with a razor blade, under the UV light, and transferred to a sterile microcentrifuge tube. Three volumes of NaI solution were added and the tube was placed in a 50°C water bath incubator for 5min. until the agarose had melted. If the agarose did not melt, the tube was vortexed and incubated again for 2 min. Then $15\mu\text{l}$ of GlassmilkTM (silica matrix) was added to the solution, which was mixed gently to form a suspension. The resuspended mixture was incubated on ice for 30min. with mixing every 1-2min.

to ensure that the GlassmilkTM remained suspended.

The silica matrix with the bound DNA was centrifuged by microcentrifugation for 5sec. The supernatant was then carefully removed and discarded. The tube was re-centrifuged for 5sec. and any remaining drops of NaI solution were removed using a fine pipette. Pellets were washed three times with ten volumes of ice cold New WashTM (600 μ l), resuspended in the New WashTM and then centrifuged for 5sec. After washing the pellets, they were resuspended in 65 μ l sterile water and incubated at 50°C for 3min. The resuspended mixture was then centrifuged for 1 minute and the supernatant containing the DNA was gently transferred to a fresh sterile microcentrifuge tube. The elution of the DNA from the GlassmilkTM pellets was carried out twice with 65 μ l sterile water. Finally, the DNA was dried using a vacuum centrifuge and stored at -20°C.

2.2.3 Site directed mutagenesis by PCR

DNA amplification to generate PBGD mutations was carried out by Dr. Sarwar (this laboratory) using the polymerase chain reaction (PCR). Two reactions were used to complete the PCR mutation, PCR1 and PCR2 as in figure 2.3.

The mutagenic primers were synthesized by Oswel (Southampton). Mutagenic primers containing *Nde*I, *Bam*HI sites were diluted to a concentration of (100ng/18mer). The template DNA was diluted to a concentration of 100ng/ μ l.

1st PCR reaction

For each mutant, in two sterile 0.5ml Eppendorfs, the DNA template (100ng/18mer) was mixed with 0.5 μ l of 9mM dNTPs and 4 μ l Vent buffer supplied with the Vent enzyme (10 \times conc.). In one tube, the sense primer for pT7-7 (*Nde*I) (T5960) and the

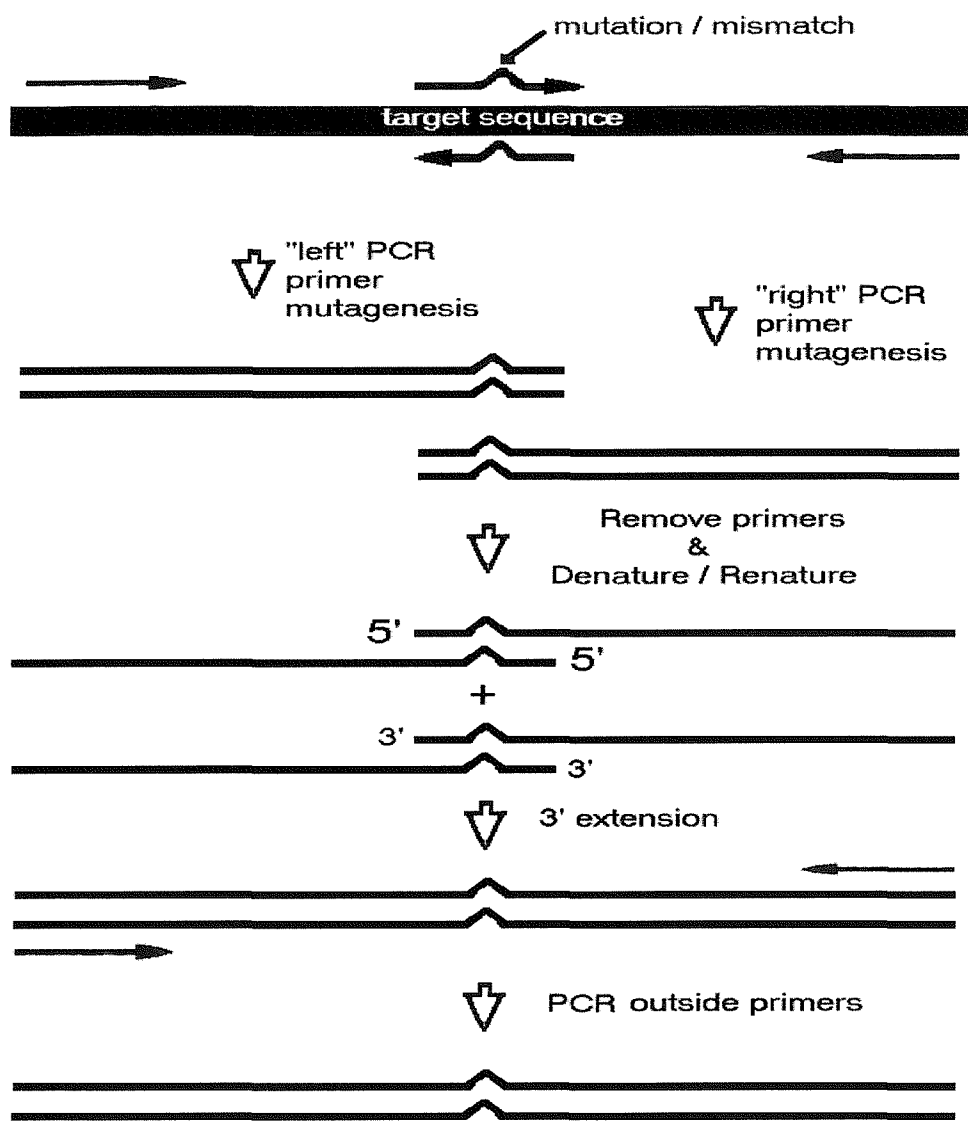


Figure 2.3: **PCR Mutagenesis.** Combining two separate PCR products with overlapping sequence into one longer product. The two overlapping primers ("inside" primers) are shown containing a mismatched base to the target sequence (Innis *et. al.*, 1990).

antisense mutagenic primer were added. In the second tube, the antisense primer for pT7-7 (*Bam*HI) (T5957) and the sense mutagenic primer were added. The volume was made up to 39.5 μ l with sterile water before heating to 95°C for 5min. in a heated PCR block. The Vent polymerase enzyme (0.5 μ l of 2U/ μ l) was then added to each tube and the contents mixed thoroughly prior to 25 cycles of:

- 1) Denaturation of the DNA template at 94°C for 1 minute.
- 2) Annealing of the primers at 60°C for 1 minute.
- 3) Extension of the primers at 72°C for 40 seconds.

The PCR1 products were purified for use in PCR2. The purification was carried out by electrophoresis of the samples in 1% agarose gel, see section 2.2.1 and excising the required bands under the UV light, by comparing their size to the marker ϕ X174 DNA/ *Hae*III, see table 2.3. Finally, the DNA samples were recovered by using the GenecleanTM protocol, see section 2.2.2, and dried using the vacuum centrifuge.

2nd PCR reaction

In PCR2, the products of PCR1 were mixed to synthesize the mutant cDNA. The reaction components of PCR2 were the same as above, except that PCR1 products were used instead of template DNA and both pT7-7 primers, *Nde*I and *Bam*HI were used (100ng/18mer).

The mixture was heated to 95°C for 5 minutes on a heated PCR block before the addition of Vent polymerase. The addition of Vent polymerase (0.5 μ l) of 2U/1 μ l was followed by 5 cycles of:

- a) Denaturation of the DNA template at 95°C for 1 minute.

b) Annealing at 48°C for 1 minute.

c) Extension at 65°C for 1 minute.

After 5 cycles, a further 25 cycles were performed, consisting of:

a) Denaturation at 94°C for 1 minute.

b) Annealing at 60°C for 1 minute.

c) Extension at 72°C for 1 minute.

Again, the DNA products were purified and recovered using both electrophoresis and Geneclean™ protocols, respectively. Finally, the DNA was dried by using the vacuum centrifuge, ready for digestion and ligation.

2.2.4 DNA digestion

PCR2 products were digested to allow ligation into the vector pT7-7, prior to transformation. The dried DNA product of PCR2 was dissolved in 20 μ l sterile H₂O. To the DNA solution, 6 μ l "All for One" buffer (2 \times) (20mM Tris/acetate, pH 7.5, 20mM magnesium acetate and 100mM potassium acetate), 1 μ l *Nde*I restriction enzyme (10 unites) and 1ml sterile H₂O were added. The mixture was incubated for 1 $\frac{1}{2}$ hour at 37°C. After 1 $\frac{1}{2}$ hour, 1 μ l *Bam*HI restriction enzyme was added and the mixture was incubated again for 1 $\frac{1}{2}$ hour at 37°C. Finally, the products were purified and recovered using the electrophoresis and the Geneclean™ protocols respectively, see section 2.2.1 and 2.2.2.

2.2.5 DNA ligation

The final steps in construction of a recombinant plasmid is the ligation of the cDNA into the vector. In the ligation reaction, a mixture of $10\mu\text{l}$ containing $1.5\mu\text{l}$ of digested PCR2 products, from digestion with *Nde*I and *Bam*HI restriction enzymes, $1\mu\text{l}$ of pT7-7 vector (which has been restricted with *Nde*I and *Bam*HI and purified), $1\mu\text{l}$ DNA ligase buffer, $1\mu\text{l}$ ATP (10mM) and $0.5\mu\text{l}$ T4 DNA ligase. The volume was made up to $10\mu\text{l}$ with sterile water and the ligation mixture was centrifuged for 10sec. before incubation at 10°C in a beaker for 4-5 hours. The temperature of the beaker was then increased to 16°C and it was placed in the cold room (4°C) overnight. Finally, the ligation mixture was transformed into the bacterial strain (DH5 α). Colonies were picked and grown overnight in 10ml LB medium containing ampicillin (100 $\mu\text{g}/\text{ml}$). DNA was isolated from the bacteria using small-scale isolation of DNA method described below.

2.2.6 Isolation of DNA (small scale)

DNA was isolated from the *E. coli* strains DH5 α harbouring the required plasmid, see tables 2.1 and 2.2. The small-scale isolation of DNA was rapidly carried out by using a Wizard[®] Plus V Miniprep DNA Purification System.

In the protocol, 10ml of LB medium containing ampicillin (100 $\mu\text{g}/\text{ml}$) was inoculated with the *E. coli* strain DH5 α harbouring the required plasmid, and incubated overnight with shaking at 37°C for 16 hours. The overnight culture was centrifuged at $1900 \times g$ (3000 rpm) for 10 minutes at 4°C by using a Sigma centrifuge (4K-15) fitted with Nr-11150 rotor. The supernatant was discarded completely, the pellets were resuspended with $250\mu\text{l}$ of cell resuspension solution and transferred to sterile microcentrifuge tubes. To the latter suspension, $250\mu\text{l}$ of cell lysis solution was added, gently mixed by inverting the tube and then incubated for 5 min. at room

temperature. Then $10\mu\text{l}$ of alkaline protease was added to the lysate, that was then incubated for 5min. at room temperature. Finally, $350\mu\text{l}$ of neutralization solution was added to the mixture and the tubes were mixed gently by inverting them.

The resulting mixture was then centrifuged at $(14,000 \times g)$ in a microcentrifuge for 10 minutes, the cleared lysate was transferred to a prepared spin column (from the kit) avoiding any white precipitate and centrifuged again at $(14,000 \times g)$ for 1min. The flow-through from the collection tube was discarded and the spin column was reinserted into the collection tubes. To the spin column, $750\mu\text{l}$ of wash solution (previously diluted with 95% ethanol, by adding 7ml of 95% ethanol to 4ml of the wash buffer) was added and centrifugation was carried out $(14,000 \times g)$ for 1 minute. The flow-through from the collection tube was discarded and the spin column was reinserted. A further $250\mu\text{l}$ of wash solution was added and the same procedure was repeated, but for 2 minutes. Finally, the spin column was inserted into a clean sterile microcentrifuge tube, $100\mu\text{l}$ of nuclease-free water was added and the tube was re-centrifuged to elute the plasmid DNA. The DNA was stored as a frozen solution at -20°C , or dried by using a vacuum centrifuge.

2.2.7 Photography of agarose gels

The bands of DNA fragments were visualized by placing the stained gel on an UV transilluminator (Ultraviolet Products Inc., California, USA) and photographed using a Polaroid MP-4 LAND camera. The camera was fitted with a Kodak Wratten 22A filter and Polaroid type 667 film. The film was exposed for 0.5-1sec. at f 5.6 and then processed according to the manufacturer's instruction.

2.2.8 Transformation of competent cells

Two bacterial strains were used for transformation, DH5 α F' and BL21(DE3). DH5 α F' was used for DNA manipulation and BL21(DE3) for protein expression. The required DNA was transformed into the competent cells as described below. Single colony of the required strain, from a plate, was inoculated into 10ml LB medium and the culture was incubated at 37°C overnight. The following morning, 15-20ml LB medium was inoculated with 200 μ l of the overnight culture with shaking, until the O.D₆₀₀ at 600nm had reached 0.3 (about two hours). The culture was centrifuged at 1900 \times g (3000 rpm) for 10 minutes at 4°C by using a Sigma centrifuge (4K-15) fitted with a Nr-11150 rotor. The supernatant was drained and the pellets were suspended in 10ml of 50mM cold CaCl₂. The suspension solution was incubated in ice (4°C) for one hour then centrifuged for 10 min. at room temperature. The pellets were suspended again with 1-2ml of cold 50mM CaCl₂ and left in ice for up to 24 hours.

The competent cells thus obtained could be used immediately, or stored for 24 hours at 0°C until required. The transformation of the competent cells was carried out as follows:

An aliquot (200 μ l) of competent cells was added to 1 μ l of required plasmid DNA (100 ng), or ligation mixture, in a sterile Eppendorf tube and incubated in ice for 25 minutes. The mixture was then heat-shocked for 2 minutes at 42°C and incubated on ice for 5min. After the incubation, 800 μ l of LB medium was added to the DNA mixture and the tube was incubated for 1 hour at 37°C without shaking. Finally, 50-100 μ l of transformed cells were spread onto LB agar containing ampicillin (100 μ g/ml) and incubated, inverted, at 37°C overnight. Only 250 μ l of LB medium was added to the ligation mixture that was spread on LB agar containing ampicillin (100 μ g/ml).

2.3 Recombinant ubiquitous human porphobilinogen deaminase isolation and characterisation methods

2.3.1 Properties of recombinant ubiquitous human porphobilinogen deaminase

Polyacrylamide gel electrophoresis

To prepare both denaturing and non-denaturing gels, all the components in table 2.5 and 2.6, respectively, were mixed except the 10%APS and the TEMED. When the gel plates were assembled, the APS and the TEMED were added to the mixture of the main gel and the mix was poured into the gel plates. The plates were incubated at room temperature until the main gel had set, approximately 15min. The APS and the TEMED were then added to the mixture of stacking gel components, the mix was cast into the gel plate and the comb was inserted to form the sample wells. After approximately 10min. this stacking gel had set. The comb was then removed and the gel was placed in the tank, that was then filled with running buffer.

The protein samples could be prepared before or after the gel preparation. For the 12% denaturing SDS-PAGE gels, 0.5 volume of 1.5 \times SDS disruption buffer was added to each sample and the tubes were placed in boiling water (for 10min. for samples of the bacterial lysate or 2-5min. for other samples). The samples and the Dalton Marker VII-L, see table 2.4, were subjected to electrophoresis at 80V for 20min. then at 180V for 40min. at room temperature. Finally, the gel was stained with Coomassie brilliant blue and destained.

For 10% non-denaturing PAGE, 0.5 volume of 1.5 \times non-denaturing PAGE disruption buffer was added to the samples and they were then loaded directly onto

the gel, without boiling. Electrophoresis was carried out at 4°C, to avoid heating of the gel that may denature the protein samples. The non-denaturing gel was electrophoresed at 80V for 40min., then at 150V for 70min. The gel was stained for PBG deaminase activity using porphobilinogen and porphyrins were visualised under UV light. Alternatively the gel was stained with Coomassie brilliant blue and then destained, see section 2.1.3.

Isoelectric focusing (IEF) gels

For the determination of protein pI values, NOVEX IEF gels (precast vertical gels) from Invitrogen company, were used. NOVEX IEF gels are 5% polyacrylamide non-denaturing gels containing no urea. The pH 3-10 gels which have been used in this project have a pI performance range from 3.5-8.5, see figure 2.2. The samples were prepared by adding one part sample to one part NOVEX IEF Sample Buffer (2×) with thorough mixing. Typically, a 10-20mM salt concentration is optimum for isoelectric focusing. Two buffers were used to run the IEF gel, the cathode buffer and the anode buffer.

The cathode buffer which fills the upper buffer chamber, should be diluted (10×) and degassed for 10min. under vacuum just before use, to reduce the possibility of bubbles from dissolved carbon dioxide forming during the gel run. The anode buffer which fills the lower buffer chamber, should be diluted (50×) before use. When the chamber that contains the IEF gel had been filled with the appropriate amount of buffers, samples were loaded into wells that had been filled with NOVEX IEF cathode buffer.

The gels were run at 100V for 2.5 hours, then the voltage was increased to 200V for 1 hour and finally to 300V for 1.5 hours. When the run was completed, the gel was incubated with a fixer solution for 30min. to fix the protein and to remove the ampholytes. In the last stage, the gel was stained with Coomassie brilliant blue for

5min. and destained with 1× solution of destain. All fixing, staining and destaining should be done with gentle shaking.

Enzyme assays

Assays were carried out on all samples at different stages of purification to measure the enzyme activity as follows:

Materials

50 μ l (4mg/ml) Enzyme solution.

350 μ l 20mM Tris/HCl buffer, pH 8.2, containing 5mM DTT.

50 μ l 2mM Porphobilinogen (0.5mg/1ml in distilled H₂O).

The total volume was 450 μ l. Two blanks were used one containing assay buffer in place of PBG and another containing buffer in place of the enzyme.

Method

1. All sample tubes were preincubated at 37°C for 5 min., before the addition of PBG.
2. Incubation was carried out for 5min for the native enzyme and one hour for low activity mutants.
3. After the incubation, the reaction was stopped by adding 125 μ l 5M HCl followed by 50 μ l benzoquinone (0.1% w/v in methanol).
4. The tubes were covered with aluminum foil and kept in the dark for 20 min. at 0°C to allow oxidation of uroporphyrinogen I to uroporphyrin I, as illustrated in figure 2.4.

5. The tubes were centrifuged for one minute to remove any precipitated protein and $100\mu\text{l}$ of the supernatant was diluted with $900\mu\text{l}$ of 1M HCl (38.9ml conc. HCl made up to 5 liters with distilled H_2O). Finally, the O.D. was measured at 405.5nm. The specific activity was calculated as $\mu\text{moles uroporphyrin produced/mg enzyme/hour}$ using the molar extinction co-efficient for uroporphyrin at 405.5nm of $5.48 \times 10^5 \text{M}^{-1}\text{cm}^{-1}$.

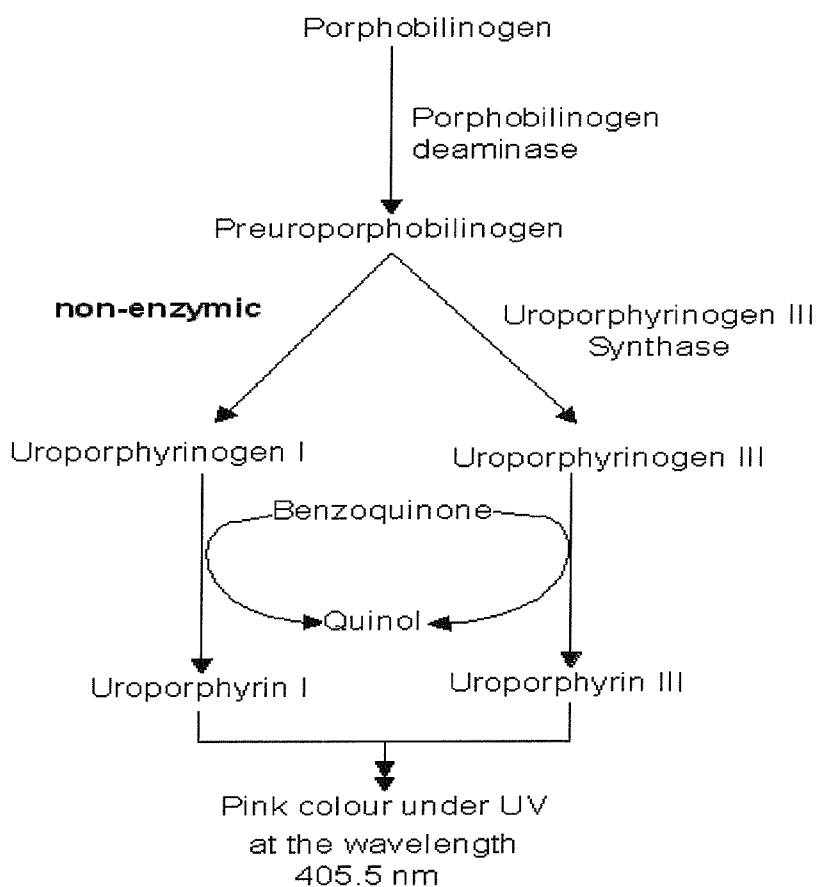


Figure 2.4: The oxidation of uroporphyrinogen I using benzoquinone to determine porphobilinogen deaminase activity.

Bio-Rad protein assay

This reaction was carried out on all samples from different stages of purification to measure the protein concentration as follows:

10 μ l Protein solution.
 790 μ l Distilled H₂O.
 200 μ l Bio-RAD reagent.

The mixture, of final volume 1ml, was incubated at room temperature for 5 min. to develop the colour. The absorbance was then measured at 595nm and the concentration was calculated using the conversion 0.1 O.D = 1.95 μ g protein.

2.3.2 Purification of recombinant human ubiquitous porphobilinogen deaminase

Inoculation

Colonies of the strain BL21(DE3), freshly transformed with the required plasmid, see table 2.1, were grown up overnight in universals containing 10ml LB containing ampicillin (100 μ g/ml) at 37°C with shaking (160 rpm).

The overnight cultures were inoculated into 6 \times 800ml LB medium in 2L baffled flasks containing ampicillin (100 μ g/ml) and grown at 37°C for 3-4 hours until the O.D.₆₀₀ had reached 1.0. To each flask, 800 μ l of IPTG (2.38 g/10 ml distilled H₂O) was added and incubation was continued for a further 3 hours. The cultures were then centrifuged at 4,650 \times g (5000 rpm) for 25min at 4°C using a Beckman instrument (J2-21) fitted with JLA-10.500 rotor. The supernatant was discarded and the pellets were washed with 0.9M NaCl. Finally, the mixture was centrifuged, the supernatant was discarded, and the pellets were stored at - 20°C until required.

Sonication

The bacterial pellets from 6 flasks were resuspended in 80ml of 20mM Tris/HCl buffer, pH 8.2, containing 5mM DTT. To the suspension, PMSF was added immediately before sonication to a final concentration of 200 μ M, to act as a protease inhibitor. The suspension was sonicated for 20 cycles of 30sec. bursts, with 90sec. cooling time between bursts, using a MSE Soniprep 150.

Heat treatment

The extract from the sonication (not the extract from the Arg 173 Gln mutant) was placed in a three necked round flask filled with N₂ gas, heated rapidly to 60°C in a water bath set at 72°C, whilst being constantly stirred, and was maintained at 60°C for 10 minutes. The solution was then rapidly cooled to 4°C by immersion in an ice/water mixture, with stirring. The heat treatment inactivated uroporphyrinogen III synthase and removed a great deal of unwanted protein (Jordan *et al.*, 1988a).

Ultracentrifugation

The heat-treated crude extract (or the extract from the sonicated Arg 173 Gln mutant) was ultracentrifuged using a Beckman instrument at 40,000 rpm (approximately 193,750 \times g) for 1.15hr at 4°C using a Beckman instrument (L7-65) fitted with TFT-45.94 rotor. The pellets were discarded and the supernatant was loaded onto a DEAE-Sephadex column as described below.

Ion exchange chromatography using DEAE-Sephacel

The supernatant from the heat-treated and ultracentrifuged solution, or the cell free supernatant from the Arg 173 Gln mutant, was loaded onto a column of DEAE-Sephacel (Pharmacia column 50K/30) using 120-150ml of DEAE-Sephacel resin, which had been previously pre-equilibrated with 20mM Tris/HCl buffer, pH 8.2, containing 5mM DTT and 100 μ M PMSF. The column was washed with 10 times the volume of the gel, using the same buffer, to remove unbound contaminating proteins. The unwanted proteins were eluted from the column by the application of a linear KCl gradient (0-70mM KCl; 450mls total volume) in the same buffer at a flow rate of 0.35ml/min and then the deaminase was eluted with the same buffer containing 70mM KCl. The deaminase protein started to elute isocratically after approximately 100ml. Elution was continued for a further 1400ml at the same flow rate to recover all the enzyme. Finally, after assaying for PBGD, the active fractions were pooled and concentrated in an Amicon ultrafiltration cell fitted with a PM-10 membrane to approximately 10ml. The protein obtained from this method was homogeneous, as judged by SDS gel electrophoresis in 12% acrylamide, see section 2.3.1.

Gel filtration using a Superdex G-75 preparation grade column

The Arg 167 Gln mutant was subjected to an additional purification step, prior to crystallization. The concentrated sample from the DEAE-Sephacel chromatography (10ml) was further concentrated to 1ml by using a Centricon-10 concentrator tube. The sample was then loaded onto a HiloadTM 16/60 Superdex G-75 preparation grade column (particle size 34 \pm 10mm; column size 120 \times 1.6cm) that was developed with 100mM Tris/HCl buffer, pH 8.2, containing 5mM DTT and 100 μ M PMSF. Fractions (67ml) were collected at a flow rate of 0.5ml/minute. The most active fractions, where a protein peak was evident, were pooled and concentrated to 1ml using a Centricon-10 concentrator tube.

Finally, concentrated protein was diluted in a Centricon-10 tube using 6ml of distilled H₂O, to give a concentration of 20mM Tris instead of 100mM Tris and concentrated again to 1ml. Protein concentration was determined by measuring O.D.₂₈₀ divided by the ε_M (0.2) of the human PBGD, which has three tyrosine and two tryptophan residues, using the following equation.

$$\varepsilon_M = \frac{1100\text{Tyrosine} + 2300\text{Tryptophan}}{39,334.7(M_r)}$$

The concentrated sample was then desalted using a PD-10 column into AnalaR water, freeze-dried and then stored under nitrogen at -20°C.

2.3.3 Crystallization of recombinant human ubiquitous porphobilinogen deaminase Arg 167 Gln mutant

At the last stage of the protein purification, the buffer of the sample was changed to the required buffer, 20mM Tris/HCl buffer, pH 8.2, containing 5mM DTT. Screening for optimal crystallization conditions was achieved using the hanging drop method (Rhodes, 1993). The buffers required were made up using AnalaR water, filtered and sparged with helium just before use. The cover slips that were used to form the hanging drops were prepared by washing them in methanol, dipping in silane solution, then washing in methanol again and oven drying. Crystallization solution (1ml) was added to each of the 24 wells of a Linbro tissue culture plate. The hanging drop was formed by mixing 4 μ l of crystallization solution from the appropriate well with 4 μ l protein solution on the middle of the cover-slip before the cover slip was inverted over the well. The edges of each well had been previously coated with a ring of high vacuum grease. The wells were filled with nitrogen gas before the cover-slips were finally put in place. Finally, the tray was wrapped in foil and left in a dark cupboard at room temperature to allow the crystals to form.

2.3.4 Electrospray mass spectrometry (ESMS)

Samples of protein were prepared by diluting the enzyme to approximately 100 μ g/ml in 50:50 acetonitrile : water + 1%(v/v) formic acid, where 10 μ l (1000ng) from this stock were used in each run. All spectra were run on a Micromass VG Quattro II spectrometer, fitted with a Hewlett Packard Series 1050 pump. Capillary voltage was 3.4kV, HV lens was 0.2kV and cone voltages were between 32V and 34V. The range of the charge/mass was estimated to start from 600 to 2100/e. Data were analyzed using the MassLynx package.

2.3.5 High resolution ion-exchange chromatography

The freeze dried enzyme was dissolved in 20mM Tris/HCl buffer, pH 8.2, containing 5mM DTT, then applied to a high resolution anion exchange Mono Q HR5/5 column, attached to a Pharmacia f.p.l.c. system, that had been pre-equilibrated with 6 volumes of the same buffer. The enzyme was eluted using a linear gradient of sodium chloride (0-160mM; 30ml total volume) at a flow rate of 1ml/minute. The absorbance was monitored at 280nm and the peaks were collected and assayed for porphobilinogen deaminase activity. The recombinant deaminase protein separated into two distinct enzyme peaks. The protein from each peak was pooled separately, after checking by SDS gel electrophoresis in 12% acrylamide, and stored at 4°C under N₂ gas for further studies.

2.3.6 Preparation of *E. coli* porphobilinogen deaminase holo-enzyme

In this purification (Shoolingin-Jordan *et al.*, 1997), the bacterial strain that contains the plasmid harbouring the *E. coli* porphobilinogen deaminase gene, *hemC*,

was grown aerobically in 2L baffled flasks in 800ml of LB, containing ampicillin (100 μ g/ml), overnight at 37°C with continuous shaking of the flasks at 180 rpm.

After 16-18 hours the cells were harvested at 4650 \times g for 25min at 4°C using a Beckman instrument (J2-21) fitted with a JLA-10.500 rotor. The supernatant was discarded and the pellets were washed with 0.9M NaCl. Finally, the mixture was centrifuged, the supernatants were discarded and the pellets were stored at - 20°C until required.

Sonication

The bacterial pellets from the previous stage (2 flasks) were resuspended in a 20ml of 0.1M potassium phosphate buffer, pH 8.0, containing 2mM benzamidine, 1mM EDTA and 14mM β -mercaptoethanol. To the suspension, 0.2M PMSF was added, immediately before sonication, to give a concentration of 200 μ M, to act as a protease inhibitor. The suspension was sonicated on ice for 4 cycles of 45 sec. bursts with 60 sec. cooling time between bursts.

Heat treatment

The extract from the sonication was heat-treated as described in section 2.3.2. The extract was centrifuged at 7740 \times g (8000 rpm) for 20 minutes at 4°C in a Beckman J2-21 centrifuge fitted with a JA20 rotor.

Ammonium sulphate fractionation

To the supernatant from the heat treatment, solid ammonium sulphate was added slowly, with stirring, to give 35% saturation at 4°C. The mixture was left to equilibrate for 30 minutes and then centrifuged at 7740 \times g for 20min. at 4°C in a Beckman

J2-21 fitted with a JA20 rotor. The precipitate was discarded and the supernatant was collected. To the 35% ammonium sulphate supernatant, which contained the porphobilinogen deaminase, further solid ammonium sulphate (200g) was added to give 65% saturation with stirring at 4°C. The mixture was again left to equilibrate for 30min. then centrifuged at 7740 × g for 20 min. at 4°C. After this stage, the deaminase, present in the 35-65% precipitate, was dissolved in a minimal amount (2ml) of 0.1M potassium phosphate buffer, pH 8.0, containing 14mM β -mercaptoethanol and dialysed against 2L of the same buffer at 4°C for at least 5 hours.

Ion exchange chromatography using DEAE-Sephacel

The dialysed sample (4ml) was loaded onto a DEAE-Sephacel anion exchange column (20cm × 2.5cm), that had been pre-equilibrated with 6 volumes of 0.1M potassium phosphate buffer, pH 8.0, containing 14mM β -mercaptoethanol. The enzyme was then eluted isocratically in the same buffer at a flow rate of 3ml/min, collecting 7ml fractions. After the fractions had been assayed for deaminase activity and analysed by SDS-PAGE, appropriate fractions were pooled and concentrated in an Amicon ultrafiltration cell fitted with a PM-10 membrane. The concentrated sample was desalted using a PD-10 column into AnalaR water, freeze-dried and then stored under nitrogen at -20°C.

2.3.7 Purification of human recombinant ubiquitous porphobilinogen deaminase Arg 149 Gln mutant

In this purification the bacterial strain expressing the Arg 149 Gln mutant was grown as described in section 2.3.2. The harvested bacteria were sonicated, as before, but were not heat treated since it was anticipated that the mutant protein may become denatured. After ultracentrifugation, the supernatant (20ml) was loaded immediately

onto a Mimetic Orange 1 dye affinity column (10cm × 2.5cm) A6XL which had been washed with distilled water and pre-equilibrated with six volumes of 20mM Tris/HCl, pH 7.5, containing 5mM DTT in the cold room. The protein was then eluted using 15ml portions of increasing concentrations of NaCl (100mM, 250mM, 500mM and 1000mM). The eluate from each portion was examined immediately by SDS-PAGE to detect the presence of Arg 149 Gln. Additional information is given in section 2.3.1.

For a large scale preparation of this mutant, supernatant (80ml) was loaded immediately onto a Mimetic Orange 1 dye affinity column (45cm × 4.5cm) A6XL which had been washed with distilled water and pre-equilibrated with six volumes of 20mM Tris/HCl, pH 7.5, containing 5mM DTT, in the cold room. The protein was then eluted by a gradient from 100mM to 1000mM NaCl. The fractions were examined immediately by SDS-PAGE to detect the presence of the apo-PBGD Arg 149 Gln mutant. Once the apoenzyme had been detected by SDS-PAGE, the protein eluting between 250mM and 500mM NaCl (30ml total) (the first 25 tubes in the large scale preparation) were pooled and concentrated to 2.5ml in an Amicon ultrafiltration cell fitted with a PM-10 membrane. The concentrated sample was desalted into distilled water by gel filtration through a PD-10 column that had been previously washed with dist. H₂O. Finally the sample was freeze dried using a vacuum dryer and stored at -20°C.

2.3.8 Purification of recombinant human ubiquitous porphobilinogen deaminase Trp 198 Ter mutant

In this purification, the bacterial strain expressing the Trp 198 Ter mutant was grown as described in section 2.3.2. The harvested bacteria expressed a large amount of Trp 198 Ter, as judged by the analysis of complete cell lysates, however, the ultracentrifuged sonicated cell free extract showed a lack of the Trp 198 Ter protein.

The truncated Trp 198 Ter mutant therefore appeared to be insoluble, existing as coaggregates with the bacterial membrane fraction, see chapter 4 (section 4.2.9). Two procedures were used to solubilise this insoluble mutant (Frankel *et al*, 1991) by using different concentrations of the detergent, Sarkosyl.

Firstly, the formation of coaggregates could be prevented by adding Sarkosyl to the harvested bacteria before sonication. The bacterial pellets were first resuspended in 20mM Tris/HCl buffer, pH 8.2, containing 5mM DTT, 100 μ M PMSF and 0.2% Sarkosyl. The suspension was then sonicated and ultracentrifuged as described in section 2.3.2. The supernatant was retained for analysis and the pellet was re-suspended in 1% Sarkosyl and re-sonicated. This sonicated mixture was ultracentrifuged, the pellet was discarded and the supernatant was retained.

Secondly, coaggregates formed during sonication without Sarkosyl were solubilised by the addition of Sarkosyl to the pellets following centrifugation of the sonicated extract. The supernatant was saved to check its content by SDS-PAGE and the pellets were re-suspended either in buffer containing 0.5% Sarkosyl or buffer containing 1.5% Sarkosyl. Both mixtures were sonicated and ultracentrifuged and the supernatants containing the solubilised mutant were retained.

Finally, the protein obtained from each step of the two procedures was analysed by SDS-PAGE.

2.3.9 Detection of the dipyrromethane cofactor in the recombinant ubiquitous human porphobilinogen deaminase

Modified Ehrlich's reagent (500 μ l), see section 2.1.3, was mixed with an equal volume of a solution of the pure enzyme (400 μ g) or of a crude cell extract. If the cofactor was present in the solution, a pink colour developed immediately with $\lambda_{\text{max}} = 595\text{nm}$ that, after 15 minutes, changed to an orange colour, $\lambda_{\text{max}} = 495\text{nm}$., see

figure 2.5. For each test, a scan was taken between 380nm and 600nm at zero time and after 15min. These spectroscopic changes confirm the presence of the cofactor. Samples of apoenzyme would not be expected to show such a reaction.

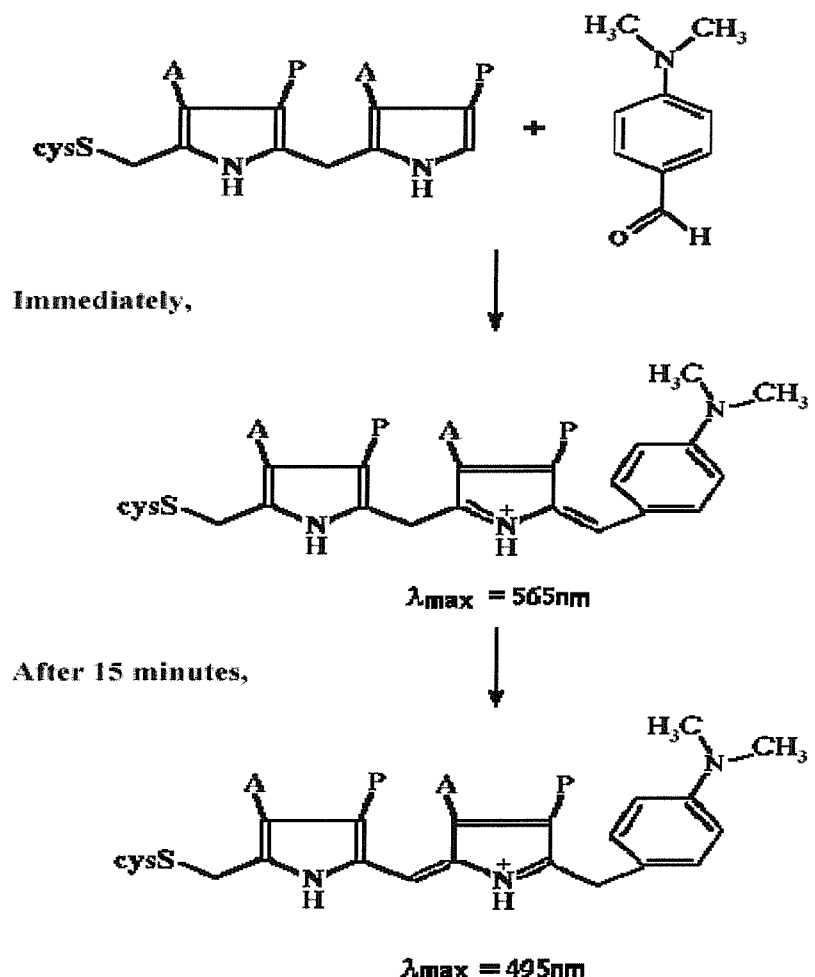


Figure 2.5: Reaction of the dipyrromethane cofactor of the deaminase with Ehrlich's reagent, immediately, and after 15 minutes in the dark.

2.3.10 Attempts to reconstitute human ubiquitous porphobilinogen deaminase holo-enzyme from the apo-enzyme using preuroporphyrinogen

I) Method for reconstitution of bacterial PBGD holo-enzyme with preuroporphyrinogen

In this reconstitution, preuroporphyrinogen was generated by *E. coli* deaminase for reaction with the apo-enzyme, see section 2.3.7 to assembe the dipyromethane co-factor. Preuroporphyrinogen was generated by mixing the *E. coli* holoenzyme (90 μ l of 4mg/ml) with PBG (210 μ l of 2mM) in 20mM Tris/HCl buffer, pH 9.1 in a final volume of 300 μ l at 37°C for 3 minutes (McNeill, 1999). After the incubation, the entire mixture was immediately cooled to 4°C and rapidly filtered through a PM-10 membrane in an Amicon 8003 ultrafiltration cell at 4°C. The filtrate (120 μ l) was added immediately to a solution of apo-enzyme (400 μ g) in 20mM Tris/HCl buffer, pH 9.1, to make a final volume of 220 μ l and the mixture was incubated for 5 minutes at 37°C. A standard deaminase activity assay, as described in section 2.3.1, was carried out to determine the PBGD activity which had been reconstituted. Preuroporphyrinogen forms of a typical *etio*-spectrum, see figure 2.6 (Smith, 1975), if incubated with Ehrlich's reagent in the dark for different times, see figures 2.7 and 2.8, due to the formation of uroporphyrin.

II) Method for the attempted reconstitution of human recombinant ubiquitous Arg 149 Gln and Arg 173 Gln mutant holo-proteins

A similar procedure was followed as above except that human recombinant ubiquitous Arg 149 Gln or Arg 173 Gln mutant apo-proteins (400 μ g) were used in place of the *E. coli* apo-enzyme.

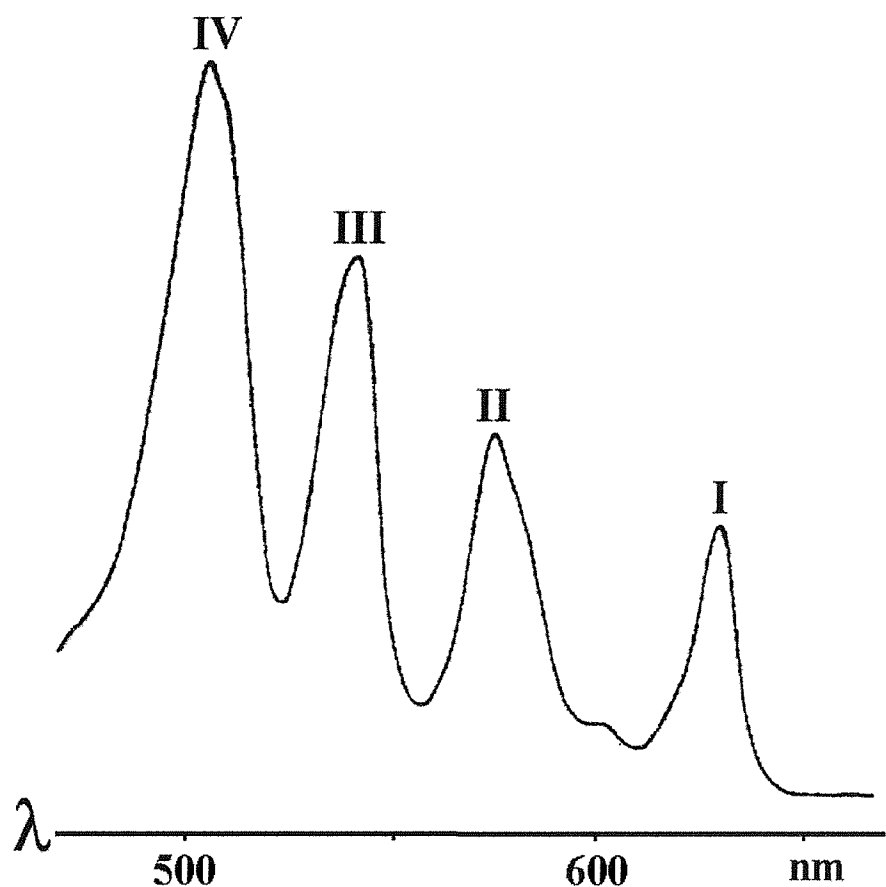


Figure 2.6: Typical visible absorption spectrum (Soret omitted) of porphyrins in chloroform, *etio*-type, (Smith, 1975).

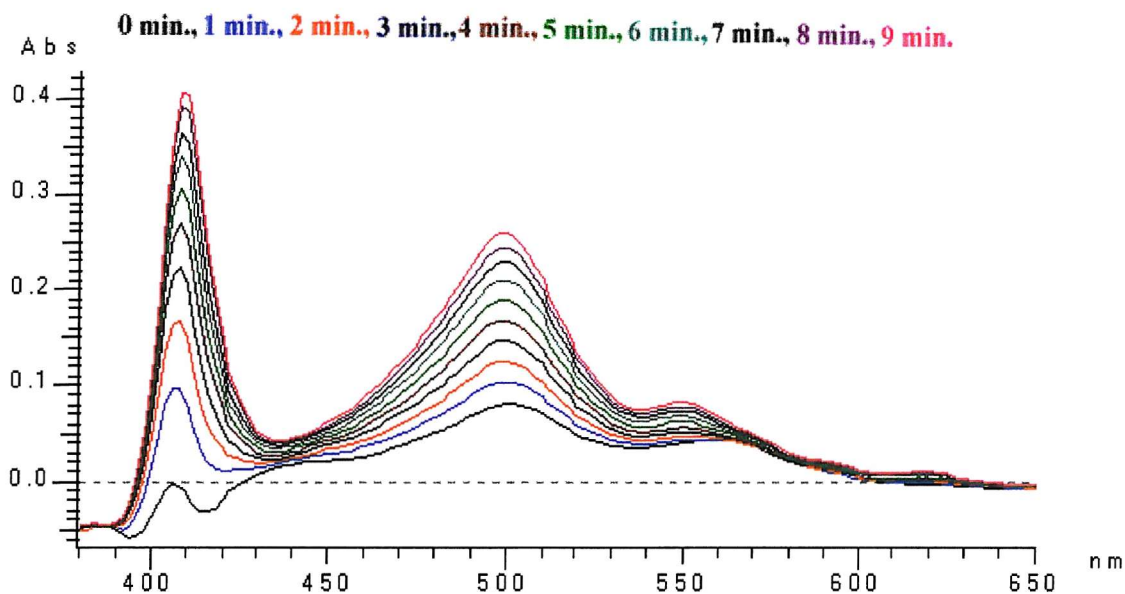


Figure 2.7: **Spectra of preuroporphobilinogen reacted with Ehrlich's reagent.** Spectra were recorded immediately after the reaction was performed using a uv-vis spectrophotometer over a range of 380-650nm. at 1min. intervals for 10min.

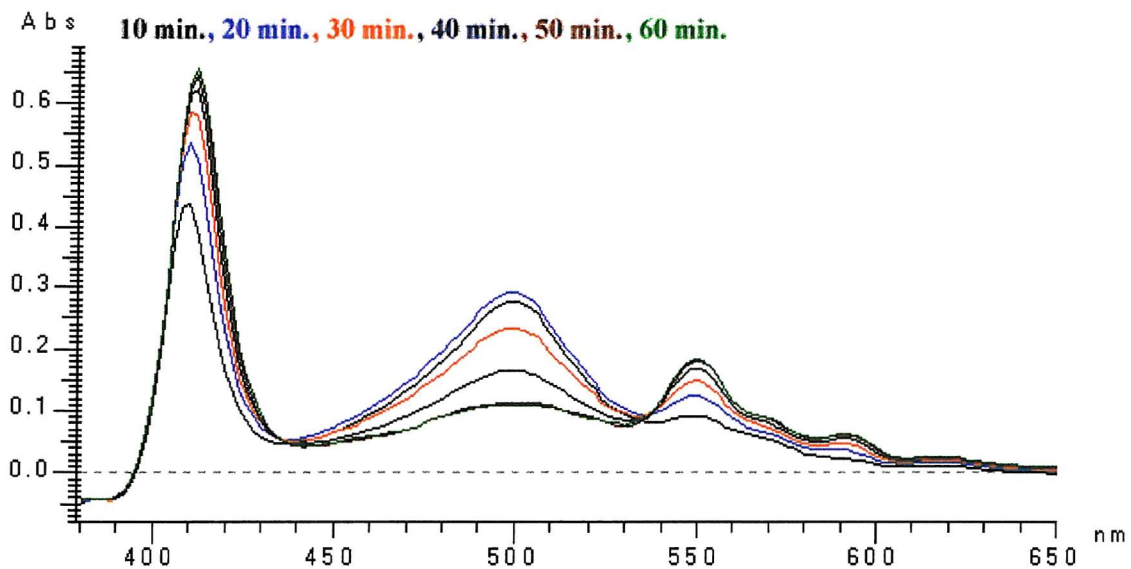


Figure 2.8: **Spectra of preuroporphobilinogen reacted with Ehrlich's reagent.** Spectra were recorded immediately after the reaction was performed using a uv-vis spectrophotometer over a range of 380-650nm. at 10 min. intervals for 60min.

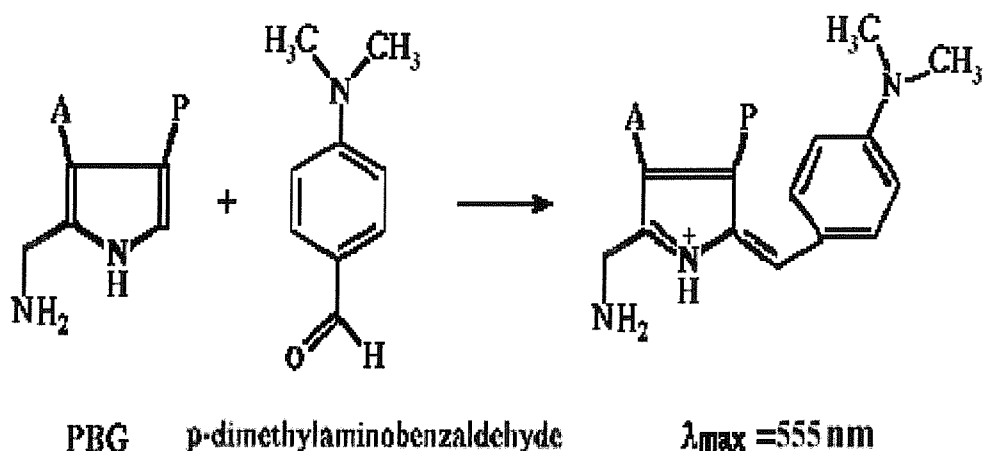


Figure 2.9: Reaction of porphobilinogen with the modified Ehrlich's reagent (*p*-dimethylaminobenzaldehyde), after 20 minutes in the dark.

2.3.11 Quantitative estimation of PBG

The concentration of the PBG in stock solutions used in the above studies and during the synthesis of porphobilinogen (see section 2.3.12) was determined by using modified Ehrlich's reagent. PBG reacts with Ehrlich's reagent to give a purple chromophore, see figure 2.9. In this test, a mixture of 10 μ l of PBG of known dilution, 490 μ l of 20mM Tris/HCl buffer, pH 8.2 and 500 μ l of Modified Ehrlich's reagent was mixed and incubated in the dark for 20min. Then the absorbance of the solution at 555nm was determined. Finally the concentration of PBG was calculated using the molar extinction coefficient of 60200 M⁻¹ cm⁻¹, taking account of the dilutions made.

2.3.12 Porphobilinogen synthesis

Materials

50mM Tris/HCl buffer, pH 7.5
 (4.85gm Trizma base/800ml distilled H₂O adjusted with HCl).
 50μM ZnSO₄ (4ml from 10mM stock of ZnSO₄).
 1mM MgCl₂ (800μl from 1M stock of MgCl₂).
 20mM β -Mercaptoethanol (1.2 ml of the pure reagent).
 5mM ALA (0.67g/800ml in 50mM Tris/HCl buffer, pH 7.5) prepared freshly.
 ca. 30mg (660 units) of purified *E. coli* 5-aminolaevulinic acid dehydratase.

Method

1. The mixture was stirred at room temperature, in the dark, until the PBG concentration, as measured by reaction with modified Ehrlich's reagent, ceased to increase further. This was accomplished by analyzing samples of 10μl by adding 490μl of H₂O and 500μl of modified Ehrlich's reagent, see section 2.3.11.
2. Anion exchange resin (Dowex-1), which had been previously converted from the chloride form to the acetate form by treating it with glacial acetic acid and washing it with distilled water, pH 8.8, was added to the mixture which was stirred at room temperature overnight.
3. PBG was bound to the Dowex-1 acetate at room temperature, the binding being checked using the Ehrlich's test. The resin was washed quickly several times with water and adjusted to pH 8 to remove excess ALA and other water-soluble contaminants.
4. The resin was then placed in a Pharmacia chromatography column (100cm × 2cm) closed only at the lower end and the PBG was eluted with 0.3M acetic acid in the cold room (4°C). Fractions (5ml) were collected in cooled test tubes. PBG elutes soon after the bubbles formed by the released of CO₂.

5. Aliquots ($10\mu\text{l}$) from all the fractions were tested with $500\mu\text{l}$ of modified Ehrlich's reagent in $490\mu\text{l}$ of water and the most concentrated fractions were rapidly freeze-dried to remove the acetic acid.
6. The freeze-dried fractions were resuspended in a minimal volume of 20% (v/v) ammonia (3-4ml) and the solution was cooled to 0-4°C. The PBG was recrystallized at its isoelectric point by the addition of a few drops of cold glacial acetic acid to adjust the pH to 5-5.5.
7. PBG crystals, which formed after 4 hours, were collected by centrifugation in a microfuge, washed with cold methanol and freeze-dried.
8. Finally, the PBG was stored desiccated at -20°C.

Chapter 3

Studies on recombinant human ubiquitous porphobilinogen deaminase arginine mutants Arg 167 Gln and Arg 167 Trp

3.1 Introduction

Nearly 200 mutations affecting the human porphobilinogen deaminase gene are now known, many of which are unpublished. Several have been described in chapter 1 and reviews are available (see Shoolingin-Jordan and Wood, 1998; Deybach and Puy, 1995). Among the most common mutations are those involving bases 499 and 500 in the cDNA encoded by exon 10. The bases 499, 500 and 501 specify the arginine codon CGG. Mutation of the first base of the codon from C→T generates the codon for tryptophan (TCG) and mutation of the second base G→A generates the codon for glutamine (CAG). Arg 167 Trp and Arg 167 Gln mutations

were originally discovered in families from France and England (Delfau *et al.*, 1990; Gu *et al.*, 1992; Lundin, *et al.*, 1997). Compound heterozygotes with these mutations, Arg 167 Trp / Gln, were found in two Dutch siblings, since each of their parents had a different mutation in exon 10 of the PBG deaminase gene, mentioned above (Llewellyn *et al.*, 1992b; Brownlie *et al.*, 1994). For a recent list see "<http://archive.uwcm.ac.uk/uwcm/mg/search/120528.html>".

The Arg 167 Gln mutation has been investigated in two laboratories (Delfau *et al.*, 1990; Llewellyn *et al.*, 1992b; Lundin, *et al.*, 1997). The patient who had this mutation, had decreased erythrocyte porphobilinogen deaminase activities and increased urinary porphobilinogen with normal faecal porphyrin excretion, latent AIP (Llewellyn *et al.*, 1992b).

The Arg 167 Trp mutation has been described by (Gu *et al.*, 1992; Llewellyn *et al.*, 1992b; Andersson *et al.*, 2000). It has been found that the patient, who carried this mutation as a heterozygote, shows the same symptoms generated by the mutation Arg 167 Gln described above (Llewellyn *et al.*, 1992b).

Arg 167 Gln and Arg 167 Trp mutants in human ubiquitous porphobilinogen deaminase cause decreased enzyme activity but have normal, or even increased, CRIM +ve status (Delfau *et al.*, 1990).

The amino acid analogous to arginine 167 in human porphobilinogen deaminase, Arg 149 in *E. coli*, has been the subject of a detailed investigation by site directed mutagenesis to histidine (Jordan and Woodcock, 1991) and leucine (Lander *et al.*, 1991). The bacterial mutants are interesting because they have close parallels to the human mutant proteins in that they are stable, contain the dipyrromethane cofactor and possess low but significant catalytic activity.

The X-ray structure of the Arg 149 His mutant has been determined (Lambert *et al.*, 1994) with the imidazole ring of the histidine residue occupying the space

vacated by the arginine side chain. The enzyme shows an abnormal pH profile and forms stable enzyme intermediate complexes. Arginine 149 forms an ion-pair with the acetate side chain of the cofactor ring C2 close to the substrate binding site. As a result, the mutation of this amino acid effects both substrate binding and chain elongation.

This chapter describes studies on the arginine mutants, Arg 167 Gln and Arg 167 Trp, found in Sweden, by comparing them to the native enzyme. The separation and characterization of the double bands that are observed on native gel electrophoresis of recombinant human ubiquitous PBGD is described. Detailed experiments will be discussed in which the Arg 167 Gln and Arg 167 Trp mutant proteins have been isolated and characterized.

3.2 Results

3.2.1 PCR and cloning of cDNA specifying recombinant human ubiquitous porphobilinogen deaminase native enzyme into the expression vector pT7-7

To generate an amplified fragment of the 1140 base pair sequence encoding human ubiquitous porphobilinogen deaminase, an expression cassette polymerase chain reaction, ECPCR, was carried out by Dr. Sarwar in this laboratory. The PCR product was restricted with the enzymes *Nde*I and *Bam*HI and the DNA fragment was purified using agarose gel electrophoresis and purification using the GenecleanTM protocol, described in section 2.2.2. The modified cDNA was ligated into the expression vector, pT7-7 that had also been restricted with the same enzymes and the resulting recombinant plasmid was transformed into DH5 α and selected on LB agar plates containing ampicillin (100 μ g/ml). After identification of positive clones, checked by restriction

analysis and DNA sequencing, the plasmid harbouring the ubiquitous deaminase sequence was transformed into the expression strain BL-21(DE3). This strain contains a single copy of the gene for T7 RNA polymerase in its chromosome under the control of the inducible lacUV5 promoter. This is essential for high-level expression of the cDNA under the control of the T7 promoter that directs overexpression of the deaminase protein in *E. coli*. On sequencing the human cDNA (obtained from Bernard Grandchamp, Paris) two mutations were found; one comprising a silent mutation Leu 188 (CTA → CTG) and another, Lys 210 Glu (AAA → GAA) as shown in table 3.1. Despite these mutations, this cDNA was used for all the studies described in this chapter and in chapter 4.

3.2.2 Theoretical primer optimisation

A set of primers were required for the amplification of the human ubiquitous porphobilinogen deaminase coding sequence. The 5'-primer was designed with an *Nde*I restriction site at the 5' end. The 3'-primer was designed with a *Bam*HI restriction site at the 3' end, see table 3.1. The incorporation of *Nde*I and *Bam*HI restriction sites into the amplified cDNA facilitates subcloning into the expression vector pT7-7. It is also important that these restriction sites are absent in the human cDNA, so that the DNA remains intact throughout the procedure.

3.2.3 Site directed mutagenesis of cDNA specifying human ubiquitous porphobilinogen deaminase by PCR

The DNA amplification to generate the Arg 167 Gln mutation was carried out in conjunction with Dr. Sarwar (this laboratory) using the polymerase chain reactions (PCR) according to the general method described in section 2.2.3, using the oligonucleotide primers prepared by Oswel (Southampton) see table 3.2.

Arginine 167 was mutated to glutamine by the change of one base, G → A. The agarose gel analysis of products from the first and second PCR mutagenesis reactions used to generate the Arg 167 Gln mutant are shown in figures 3.1 a and b respectively. The required bands were excised from the gel that contain the PCR2 products, to be ready for gene cleaning.

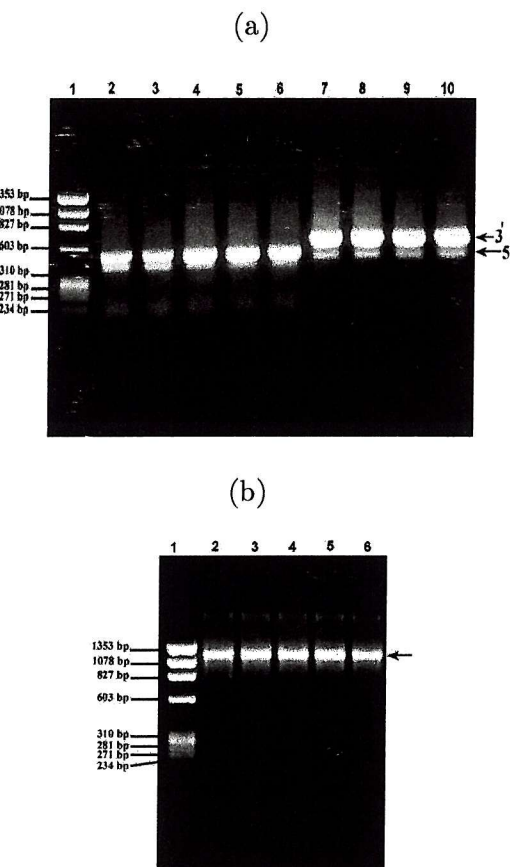


Figure 3.1: Agarose gel analysis of the PCR products formed from cDNA specifying ubiquitous human porphobilinogen deaminase to generate the Arg 167 Gln mutant: a) The first PCR reaction yields two overlapping DNA fragments specifying ubiquitous human porphobilinogen deaminase to generate the Arg 167 Gln mutant. Track 1 represents the DNA marker, ϕ X174, restricted with *Hae*III, tracks 2, 3, 4, 5 and 6 show the 5' end of the cDNA; tracks 7, 8, 9 and 10, represent the 3' end of the cDNA. In gel (b) the second PCR reaction combines the two fragments to yield a DNA fragment (1.14kb) harbouring the desired mutated codon. Track 1 represents the DNA marker, ϕ X174 restricted with *Hae*III; tracks 2, 3, 4, 5 and 6, represent the full cDNA.

The sequence of the native huPBGD native primers

The sense strand (Non coding):

5' GGGATTCC**CATATGT**CTGGTAACGGTAACGCT
NdeI
 GCTGCAACGGCGGAAGAAAAACAGCCAAAG 3'

The antisense strand (coding):

5' GCG**CGGATCC**GATGTAGGC**ACTGG**ACAGCAGC 3'
BamHI

Table 3.1: The oligonucleotide primers employed for PCR of the native human ubiquitous porphobilinogen deaminase gene.

The sequence of the huPBGD Arg 167 Gln mutant primers

The sense strand (non-coding):

5' GTTCAGGAGTATT**CAGGGAAAC**CTCAAC 3'

The antisense strand (coding):

5' GTTGAGGTT**CCCTGA**ATACTCCTGAAC 3'

The sequence of the huPBGD Arg 167 Trp mutant primers

The sense strand (non-coding):

5' GTTCAGGAGTATT**TGGGGAAAC**CTCAAC 3'

The antisense strand (coding):

5' GTTGAGGTT**CCCCAA**ATACTCCTGAAC 3'

Table 3.2: The sequence of the mutagenic oligonucleotide primers of Arg 167 Gln and Arg 167 Trp. The sense primers of the Arg 167 Gln and Arg 167 Trp are generated by the mutation (CGG → CAG) and (CGG → TGG) respectively. The antisense primers for Arg 167 Gln and Arg 167 Trp are generated by the mutation (GCC → GTC) and (CCG → CCA) respectively. All the mutated codons are in bold.

3.2.4 Digestion of cDNA fragments specifying the human ubiquitous porphobilinogen deaminase Arg 167 Gln mutant and ligation into the pT7-7 plasmid

The gene-cleaned cDNA fragment specifying mutated ubiquitous human porphobilinogen deaminase resulting from PCR2 was digested with *Bam*HI and *Nde*I restriction enzymes before ligation into gene-cleaned pT7-7 vector that had been cut with the same enzymes. The protocols of digestion and ligation used in this project are described in sections 2.2.4 and 2.2.5 respectively. After this stage, the plasmid DNA from the ligation was transformed into *E. coli* strain DH5 α as follows. A similar procedure was used for the Arg 167 Trp mutant.

3.2.5 Transformation of cDNA specifying the human ubiquitous porphobilinogen deaminase Arg 167 Gln mutant into *E. coli* strain DH5 α and screening for positive clones

The pT7-7 plasmid containing the mutated ubiquitous human porphobilinogen deaminase cDNA specifying the Arg 167 Gln mutant was transformed into *E. coli* strain, DH5 α , as described in section 2.2.8. The plasmid DNA was isolated from the bacterial strains using the Promega Wizard[®] Plus V Minipreps DNA Purification System and checked by restriction enzyme analysis with *Bam*HI and *Nde*I, as described in sections 2.2.6 and 2.2.4. The plasmid DNA samples, before and after restriction with *Bam*HI and *Nde*I, were analysed on agarose gels, as described in section 2.2.1, to check the presence of the insert, see figures 3.2 and 3.3 respectively. Finally, DNA sequencing was carried out by Oswel (Southampton) to confirm the presence of the desired mutation, see table 3.3, before the expression protocol. A similar procedure was used for the Arg 167 Trp mutant.

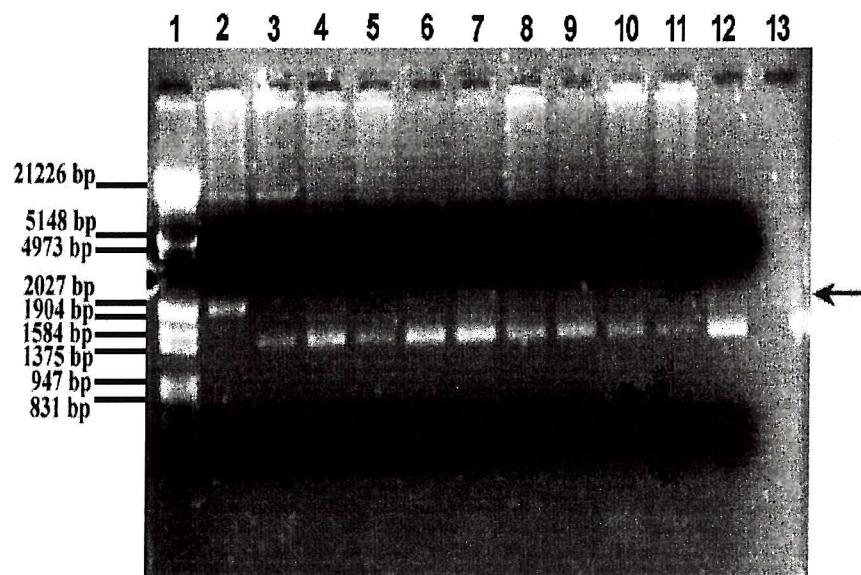


Figure 3.2: Agarose gel analysis of the DNA mini-prep to confirm the presence of the ubiquitous human porphobilinogen deaminase mutated cDNA (1.14kb) harbouring the desired mutated codon of Arg 167 Gln. Track 1, DNA marker, λ DNA/*Eco*RI + *Hind*III; tracks 2-13, plasmid DNA samples isolated from the bacterial strain using the Promega Wizard[®] Plus SV Minipreps DNA Purification System. From the gel we can see clearly that only the sample in track 2 contains the correct DNA size which had the required insert, (1.14 kb), while the other tracks from 3-13 represent the vector pT7-7 only.

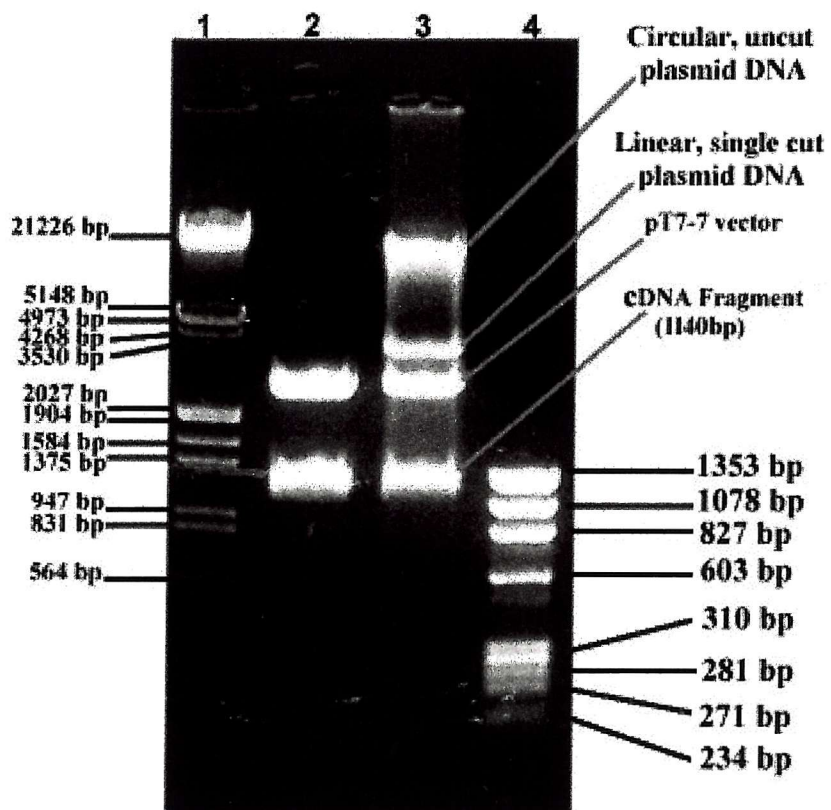


Figure 3.3: Agarose gel analysis to check the presence of ubiquitous human porphobilinogen deaminase cDNA ligated into pT7-7 by restriction enzyme analysis with *Bam*HI and *Nde*I. Track 1, DNA marker, Bacteriophage λ DNA restricted with *Eco*RI + *Hind*III; track 2, plasmid DNA, carrying a 1.14 kb fragment of native ubiquitous human porphobilinogen deaminase cDNA restricted with *Bam*HI and *Nde*I; track 3, plasmid DNA, carrying a fragment of ubiquitous human porphobilinogen deaminase cDNA, 1.14kb, harbouring the desired mutated codon restricted with *Bam*HI and *Nde*I; track 4, DNA marker, ϕ X174 restricted with *Hae*III.

3.2.6 Expression and purification of recombinant human ubiquitous porphobilinogen deaminase Arg 167 Gln and Arg 167 Trp mutants

The ubiquitous human porphobilinogen deaminase Arg 167 Gln and Arg 167 Trp mutant enzymes have been isolated to 90% purity using the same protocol used for the native enzyme that involves a heat treatment step (Mosley Ph.D. thesis, 2001) as described in section 2.3.2. The heat treatment step is a very useful purification stage since it precipitates a large quantity of unwanted protein. Both mutant enzymes were found to be as stable as the native enzyme to the heat-treatment at 60°C for 10min. The ubiquitous human porphobilinogen deaminase native enzyme has also been purified. The crude cell free extract of the native enzyme was loaded onto a DEAE-Sephacel column then eluted isocratically with 20mM Tris/HCl buffer, pH 8.2, containing 5mM DTT, 100μM PMSF and 70mM KCl. The elution profiles are shown in figure 3.4. The active fractions were pooled and concentrated to be loaded onto a Superdex G-75 gel filtration column. The enzyme was eluted with 100mM Tris/HCl buffer, pH 8.2, containing 5mM DTT and 100μM PMSF, as shown in figure 3.5. The results of the purification steps are shown in table 3.4 and the SDS PAGE analysis in figure 3.6. The elution of the Arg 167 Gln mutant from the DEAE-Sephacel column is shown in figure 3.7 and the elution from the Superdex G-75 gel filtration column is shown in figure 3.8. The results from the different steps of the purification are summarized in table 3.5 and figure 3.9. The Arg 167 Trp mutant was also purified using the same protocol as that used for the native enzyme up to and including the stage using DEAE-Sephacel column. The elution profile of the Arg 167 Trp from the DEAE-Sephacel column is shown in figure 3.10 and the summary of the purification steps is shown in table 3.6 and figure 3.11.

During the second isolation of the Arg 167 Gln mutant, it was found from SDS-PAGE analysis that the mutant enzyme eluted from the DEAE-Sephacel column in three peaks, see figure 3.12. The first peak showed a single band on SDS-PAGE, while

Start
→

CACACAGCCT	ACTTTCCAAG	CGGAGCC(ATG) ¹	TCTGGTAACG	GCAATGCCGC	0050
TGCAACGGCG	GAAGAAAACA	GCCC AAAG(AT	G) ² AGAGTGATT	CGCGTGGGTA	0100
CCCGCAAGAG	CCAGCTTGCT	CGCATA CAGA	CGGACAGTGT	GGTGGCAACA	0150
TTGAAAGCCT	CGTACCTGG	CCTGCAGTT	GAAATCATTG	CTATGTCCAC	0200
CACAGGGGAC	AAGATTCTTG	ATACTGCACT	CTCTAAGATT	GGAGAGAAAA	0250
GCCTGTTAC	CAAGGAGCTT	GAACATGCC	TGGAGAAGAA	TGAAGTGGAC	0300
CTGGTTGTT	ACTCCTTGAA	GGACCTGCC	ACTGTGCTTC	CTCCTGGCTT	0350
CACCATCGGA	GCCATCTGCA	AGCGGGAAAA	CCCTCATGAT	GCTGTTGTCT	0400
TTCACCCAAA	ATTTGTTGGG	AAGACCCCTAG	AAACCCCTGCC	AGAGAAAGAGT	0450
GTGGTGGGAA	CCAGCTCCCT	G(CGA) ³ AGAGCAGGCCAGCTGC	AGAGAAAGTT	0500	
CCCGCATCTG	GAGTCAGGA	GTATT(CGG) ⁴ GGAAACCTCAAC	ACC(CGG) ⁵ CTTC	0550	
GGAAGCTGGA	CGAGCAGCAG	GAGTTCACTG	CCATCATC(CT	A) ⁶ GCAACAGCT	0600
GGCCTGCAGC	GCATGGGC(TG G) ⁷ CACAACCGG	GTGGGGCAGA	TCCTGCACCC	0650	
TGAG(AAA) ⁸ TGCATGTATGCTG	TGGGCCAGGG	GGCCTTGGGC	GTGGAAGTGC	0700	
GAGCCAAGGA	CCAGGACATC	TTGGATCTGG	TGGGTGTGCT	GCACGATCCC	0750
GAGACTCTGC	TTCGCTGCAT	CGCTGAAAGG	GCCTTCCTGA	GGCACCTGGA	0800
AGGAGGCTGC	AGTGTGCCAG	TAGCCGTGCA	TACAGCTATG	AAGGATGGGC	0850
AACTGTACCT	GAATGGAGGA	GTCTGGAGTC	TAGACGGCTC	AGATAGCATA	0900
CAAGAGACCA	TGCAGGCTAC	CATCCATGTC	CCTGCCCCAGC	ATGAAGATGG	0950
CCCTGAGGAT	GACCCACAGT	TGGTAGGCAT	CACTGCTCGT	AACATTCAC	1000
GAGGGCCCCA	GTTGGCTGCC	CAGAACTTGG	GCATCAGCCT	GGCCAACTTG	1050
TTGCTGAGCA	AAGGAGCAA	AAACATCCTG	GATGTTGCAC	GGCAGCTTAA	1100
CGATGCCCAT	TAAC TGGTT	GTGGGGCACA	GATGCCTGGG	TTGCTGCTGT	1150
CCAGTGCCTA	CATCCCAGGC	CTCAGTGCC	CATTCTCACT	GCTATCTGGG	1200
GAGTGATTAC	CCCGGGAGAC	TGAAC TGCAG	GGTTCAAGCC	TTCCAGGGAT	1250
TTGCCTCACC	TTGGGGCCTT	GATGACTGCC	TTGCCTCCTC	AGTATGTGGG	1300
GGCTTCATCT	CTTTAGAGAA	GTCCAAGCAA	CAGCCTTGA	ATGTAACCAA	1350
TCCTACTAAT	AAACCAAGTTC	TGAAGGT→poly(A) tail.			1377

Table 3.3: Sequence of human ubiquitous porphobilinogen deaminase cDNA. 1 Hepatic start codon; 2 erythroid start codon; 3, 4 and 5 represent the arginine residues that have been mutated in this thesis to glutamine to generate the mutants Arg 149 Gln, Arg 167 Gln and Arg 173 Gln [3 Arg 149 Gln (CGA → CAG); 4 Arg 167 Gln (CGG → CAG); 5 Arg 173 Gln (CGG → CAG)]; 6 and 8 represent mutations found on sequencing the cDNA, 6 represents a silent mutation Leu 188 Leu (CTA → CTG) and 8 represents the mutation Lys 210 Glu (AAA → GAA); 7 represents the Trp 198 Ter mutation (TGG → TAG). The amino acid specified by codon 4 was studied in this chapter (Arg 167 Trp (CGG → TGG)). The amino acids specified by codons 3, 5 and 7 were studied in chapter 4.

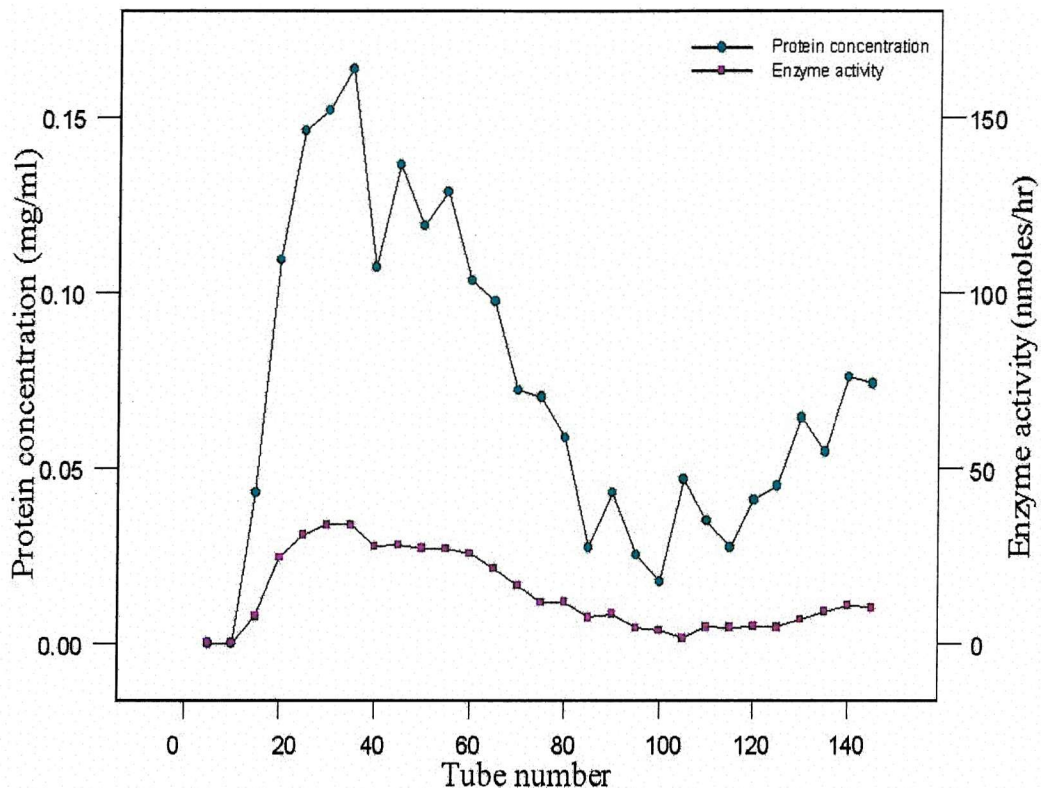


Figure 3.4: The elution profile of native ubiquitous human porphobilinogen deaminase from DEAE-Sephacel ion exchange chromatography. The crude enzyme after ultracentrifugation was loaded onto a pre-equilibrated column using 20mMTris/HCl, buffer pH 8.2, containing 5mM DTT and 100 μ m PMSF then eluted isocratically with the same buffer containing 70mM KCl.

Stage of purification	Total Protein (mg)	Specific activity nmoles/mg/hr	Yield %	Purification fold
Crude cell free-extract	639.6	214	100	1
After heat-treatment and ultracentrifugation	335.2	312	76.3	1.5
After DEAE Sephadex	23.98	404	11.76	1.89
After gel filtration on Superdex G-75	15.75	920	10.6	4.3

Table 3.4: The purification table for native ubiquitous human porphobilinogen deaminase.

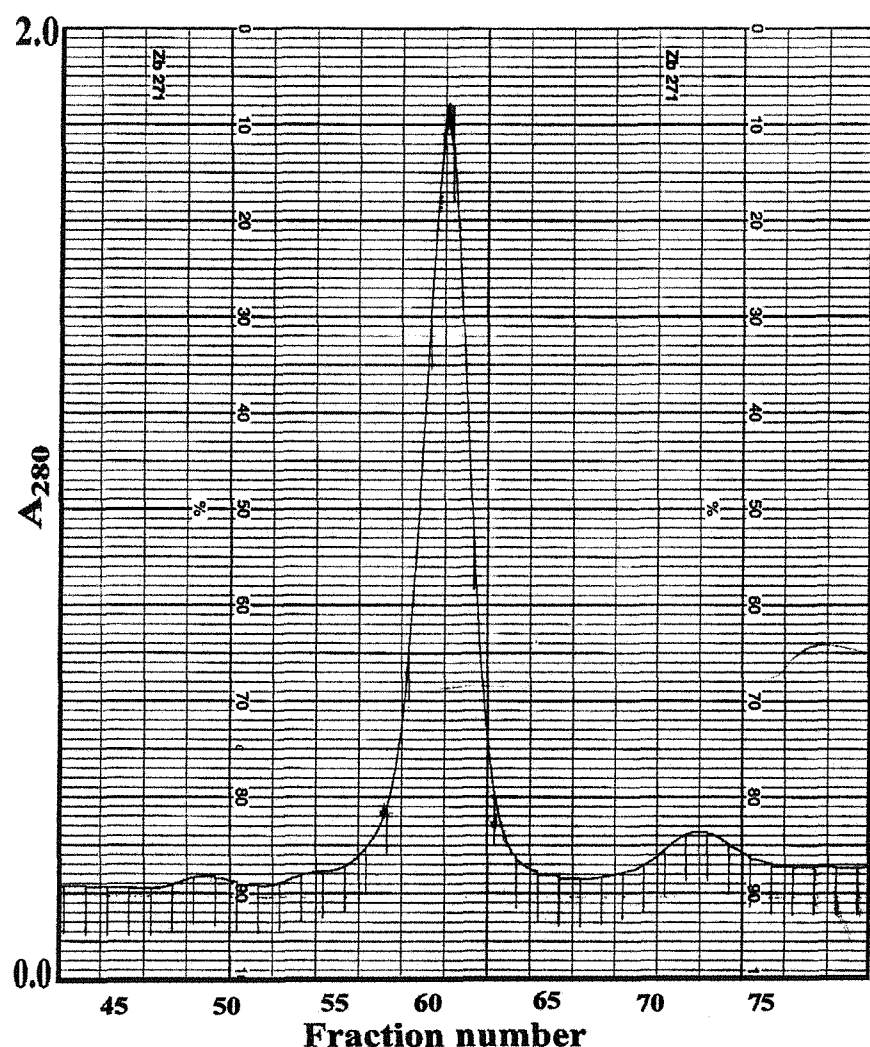


Figure 3.5: Chromatography of native ubiquitous human porphobilinogen deaminase from a Superdex G-75 gel filtration column attached to a f.p.l.c. The symmetrical peak represents the native ubiquitous human porphobilinogen deaminase. Very small peaks before and after this symmetrical peak were noticed.

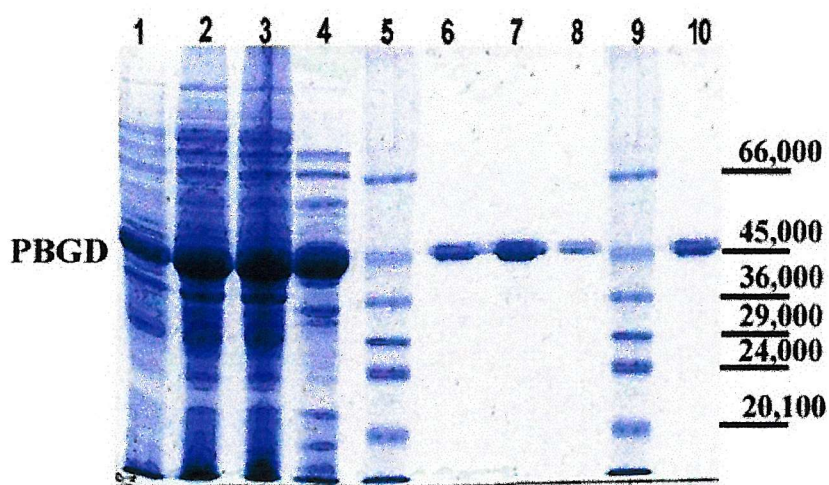


Figure 3.6: SDS-PAGE analysis to show native ubiquitous human porphobilinogen deaminase at different steps of purification. Samples were submitted to 12% PAGE in the presence of SDS. Track 1, complete lysate from *E. coli* cells expressing native ubiquitous porphobilinogen deaminase; track 2, after sonication; track 3, after heat treatment at 60°C; track 4, after ultracentrifugation; track 5, molecular weight marker, Dalton VII; track 6, 7 and 8, after DEAE-Sephadex chromatography; track 9, molecular weight marker, Dalton VII; track 10, after Superdex G-75 chromatography.

Stage of purification	Total Protein (mg)	Specific activity nmoles/mg/hr	Yield %	Purification fold
Crude cell free-extract	1164	11	100	1
After heat-treatment and ultracentrifugation	411.32	20	73.7	2
After DEAE Sephadex	42.4	70	24.7	6.65
After gel filtration on Superdex G-75	13.4	80	8.14	6.9

Table 3.5: The purification table for ubiquitous human porphobilinogen deaminase Arg 167 Gln mutant.

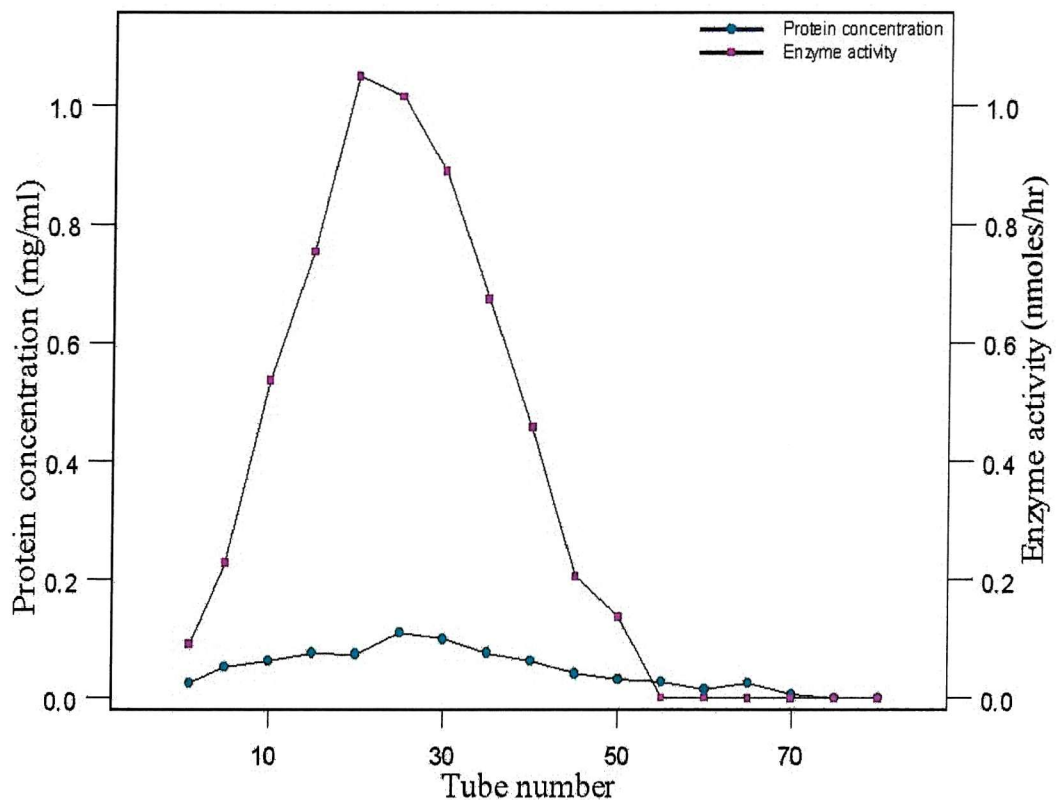


Figure 3.7: The elution profile of ubiquitous human porphobilinogen deaminase Arg 167 Gln mutant from DEAE-Sephadex ion exchange chromatography, first preparation. The crude enzyme after ultracentrifugation was loaded onto a pre-equilibrated column using 20mM Tris/HCl buffer, pH 8.2, containing 5mM DTT and 100 μ M PMSF then eluted isocratically with the same buffer containing 70mM KCl.

Stage of purification	Total Protein (mg)	Specific activity nmoles/mg/hr	Yield %	Purification fold
Crude cell free-extract	1072	19	100	1
After heat-treatment and ultracentrifugation	316.24	50	80.98	2.75
After DEAE Sephadex	16.9	87	7.2	4.58

Table 3.6: The purification table for ubiquitous human porphobilinogen deaminase Arg 167 Trp mutant.

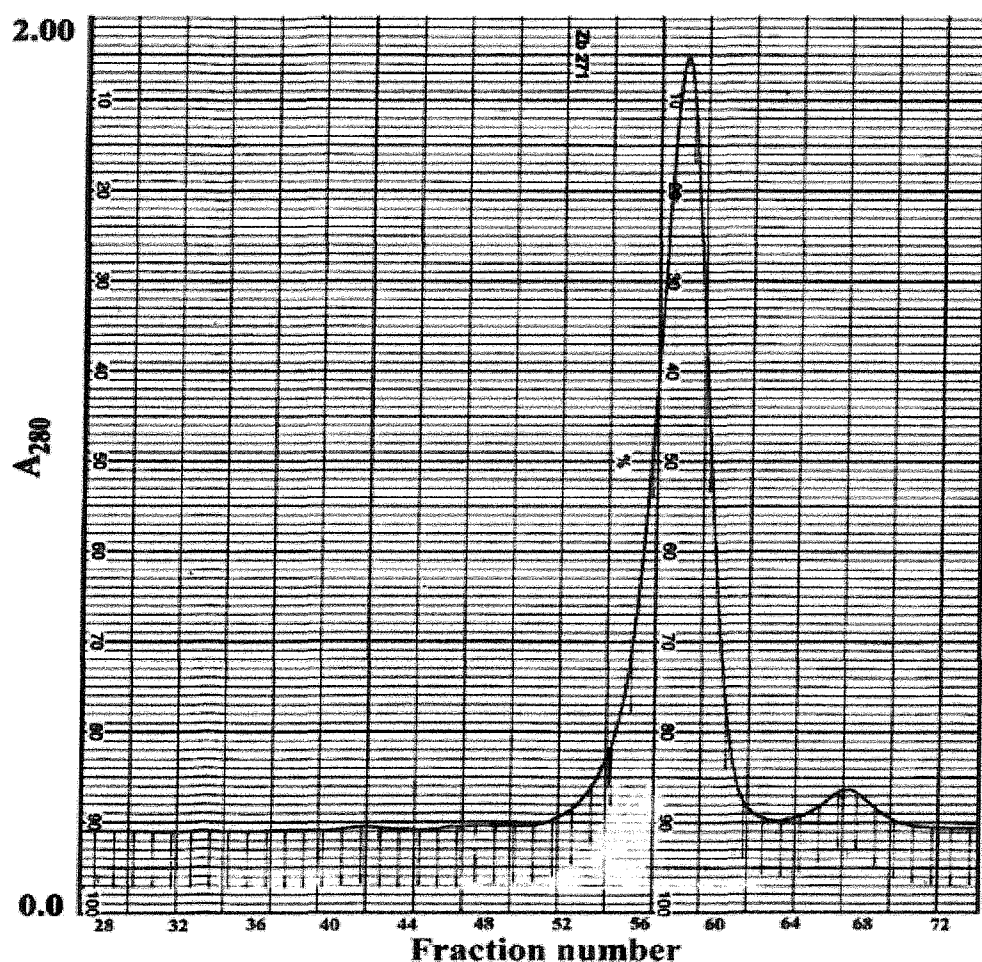


Figure 3.8: Chromatography of ubiquitous human porphobilinogen deaminase Arg 167 Gln mutant from a Superdex G-75 gel filtration column attached to a f.p.l.c. The symmetrical peak represents the mutant ubiquitous human porphobilinogen deaminase Arg 167 Gln mutant. Very small peaks before and after this symmetrical peak were also noticed.

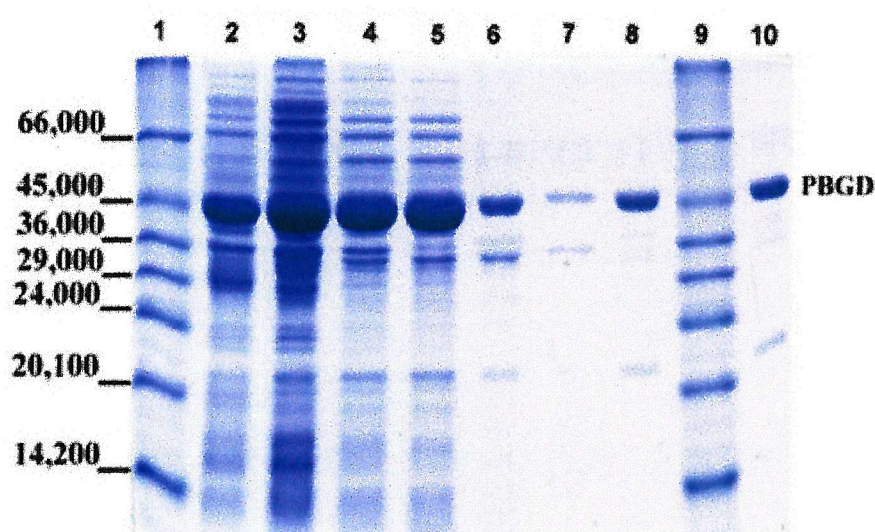


Figure 3.9: SDS-PAGE analysis to show the ubiquitous human porphobilinogen deaminase Arg 167 Gln mutant at different steps of purification. Samples were submitted to 12% PAGE in the presence of SDS. Track 1, molecular weight marker, Dalton VII; track 2, complete lysate from *E. coli* cells expressing the ubiquitous porphobilinogen deaminase Arg 167 Gln mutant; track 3, after sonication; track 4, after heat treatment at 60°C.; track 5, after ultracentrifugation; tracks 6 and 7, after DEAE-Sephadex chromatography; tracks 8 and 10, after Superdex G-75 column chromatography; track 9, molecular weight marker, Dalton VII.

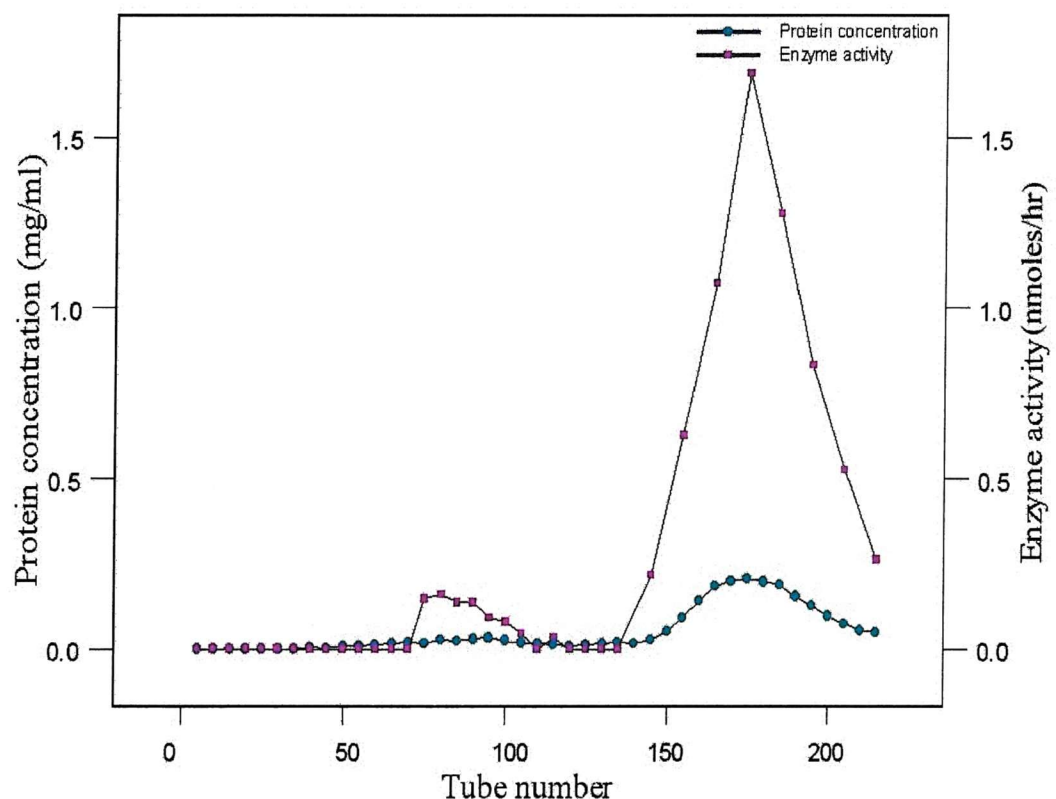


Figure 3.10: The elution profile of ubiquitous human porphobilinogen deaminase Arg 167 Trp mutant from DEAE-Sephadex ion exchange chromatography. The crude enzyme after ultracentrifugation was loaded onto a pre-equilibrated column using 20mM Tris/HCl buffer, pH 8.2, containing 5mM DTT and 100 μ M PMSF then eluted isocratically with the same buffer containing 70mM KCl.

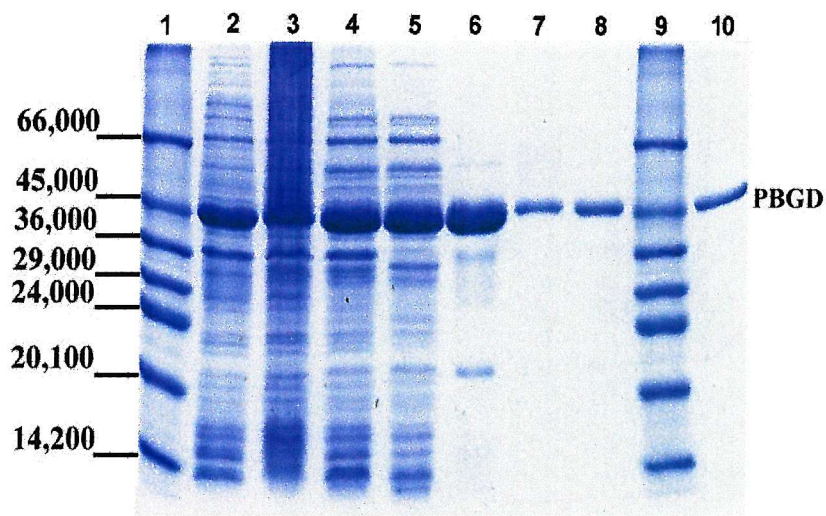


Figure 3.11: SDS-PAGE analysis to show the human ubiquitous porphobilinogen deaminase Arg 167 Trp mutant at different steps of purification. Samples were submitted to 12% PAGE in the presence of SDS. Track 1, molecular weight marker, Dalton VII; track 2, complete lysate from *E. coli* cells expressing the ubiquitous porphobilinogen deaminase Arg 167 Trp mutant; track 3, after sonication; track 4, after heat-treatment; track 5, after ultracentrifugation; track 6, after DEAE-Sephadex chromatography, pooled fraction; track 7, after DEAE-Sephadex chromatography, tube 30; track 8, after DEAE-Sephadex chromatography, tube 40; track 9, molecular weight marker, Dalton VII; track 10, after DEAE-Sephadex chromatography, tube 50.

the second peak had a contaminant of $M_r = 21,000$ and the third peak contained a contaminant of $M_r = 28,000$ see figure 3.14. Attempts to separate the contaminants using Superdex G-75 gel filtration was required if the enzyme was to be crystallised. The first and second peaks from the DEAE Sephacel column, gave the same elution profile on gel filtration, with a symmetrical peak which represented the ubiquitous human porphobilinogen deaminase Arg 167 Gln mutant. Very small peaks before and after this symmetrical peak were also noticed from the most active fractions of Arg 167 Gln mutant, see figure 3.8. The third peak from the DEAE-Sephacel column also gave a symmetrical peak which represented the Arg 167 Gln mutant but, before this peak, there was another contaminating peak about three quarters the size of the deaminase peak, see figure 3.13. This latter peak represented the contaminant of $M_r = 28,000$ mentioned above, see figure 3.14. A second attempt was made to separate the M_r 21,000 contaminant by adding 300mM NaCl in the elution buffer of the Superdex G-75 column and decreasing the flow rate from 0.5ml/min. to 0.3ml/min., but this was not successful.

The elution profile of both mutants following DEAE-Sephacel ion-exchange chromatography shows that the main protein peak coincides with deaminase activity. These fractions showed a protein band on SDS-PAGE of a similar mobility to the M_r 45,000 standard, while the fractions before and after contain the contaminants.

After the final stage of purification, it was found that both the purified native and mutant enzymes, although they displayed a single band of 45,000 when analyzed by SDS-PAGE, showed double bands when analyzed under non-denaturing gel conditions. As a result, the following section describes attempts to separate and characterize the double bands of the native and the Arg 167 Gln mutant enzymes using high-resolution anion-exchange Mono Q chromatography.

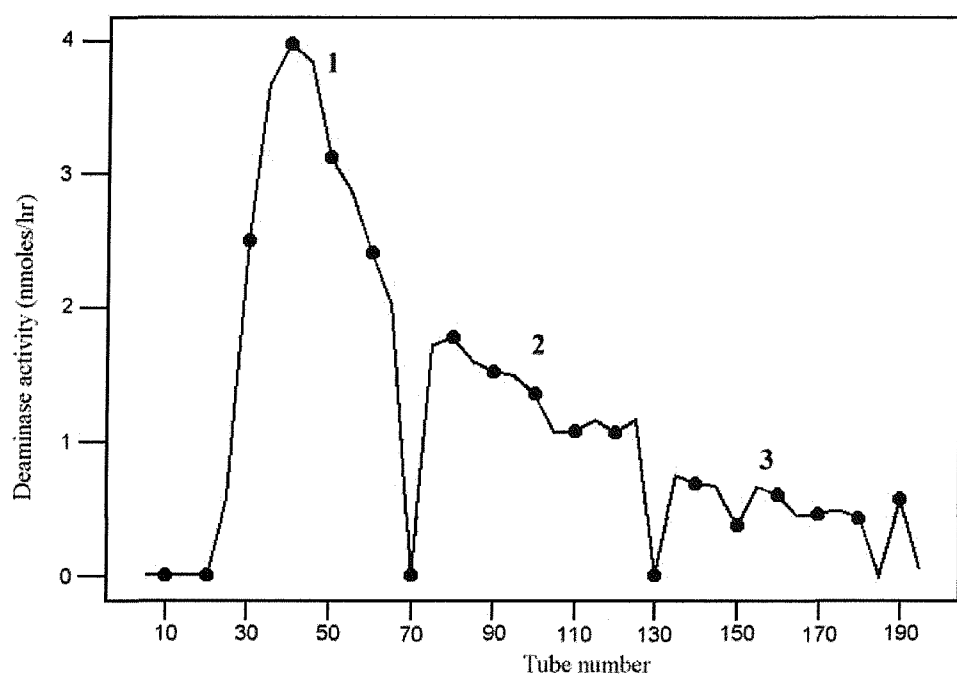


Figure 3.12: The elution profile of the ubiquitous human porphobilinogen deaminase Arg 167 Gln mutant from DEAE Sephacel ion exchange chromatography. The crude enzyme after ultracentrifugation was loaded onto a pre-equilibrated column using 20mM Tris/HCl buffer, pH 8.2, containing 5mM DTT and 100 μ M PMSF then eluted isocratically with the same buffer containing 70mM KCl.

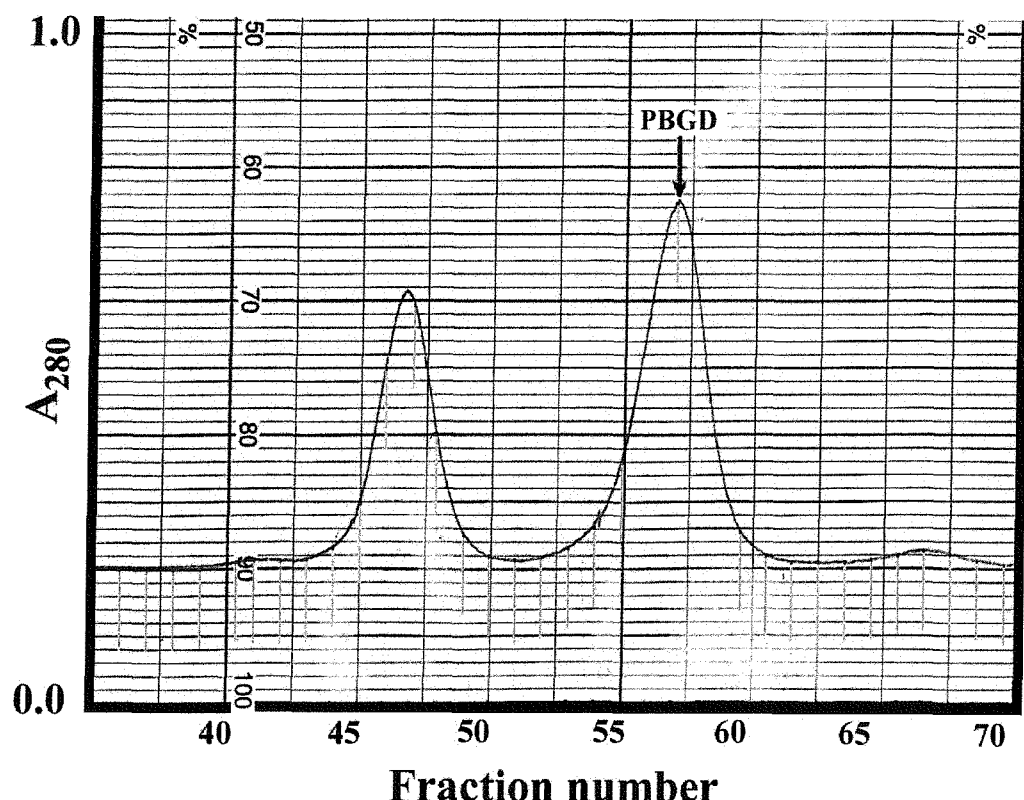


Figure 3.13: Chromatography of ubiquitous human porphobilinogen deaminase Arg 167 Gln mutant from a Superdex G-75 gel filtration column attached to a f.p.l.c. The third peak from the DEAE Sephadex column, see figure 3.12, gave a symmetrical peak that represented the Arg 167 Gln mutant but, before this peak, there was another peak about a three quarters the size of the deaminase peak. A very small peak before and after these peaks were also noticed.

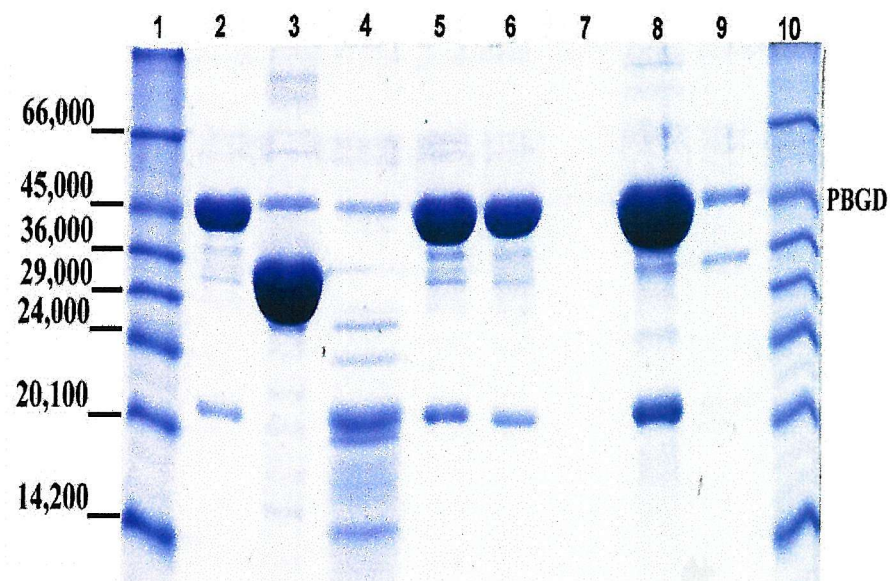


Figure 3.14: SDS-PAGE analysis to check the contaminant that appeared in the Superdex G-75 elution profile of ubiquitous human porphobilinogen deaminase Arg 167 Gln mutant and the stability of this mutant at -20°C. Track 1, molecular weight marker, Dalton VII; track 2, after Superdex G-75 column chromatography; track 3, contaminant of M_r approximately 28,000, (peak 1 from the elution of the third peak from the Superdex G-75 column); track 4, contaminant of M_r approximately 21,000; track 5, as in track 2 but after freezing at -20°C in 20% glycerol; track 6, as in track 2; track 7, blank; track 8, after DEAE-Sephacel chromatography, second peak; track 9, after DEAE-Sephacel chromatography, third peak; track 10, molecular weight marker, Dalton VII.

3.2.7 Attempts to separate and characterize the double bands of the native recombinant human ubiquitous porphobilinogen deaminase observed in native gels

Human ubiquitous porphobilinogen deaminase, purified as described in section 2.3.2, displayed a single band of 45,000 when analyzed by SDS-PAGE. In spite of the apparent homogeneity of the native deaminases (both ubiquitous and erythroid isozymes) and the Arg 167 Gln and Arg 167 Trp mutants, all the enzymes exhibited double bands when analyzed by non-denaturing gel electrophoresis. This phenomenon has been previously observed without a final conclusion (Jordan *et al.*, 1988a; Scott *et al.*, 1989). Previous studies with *E. coli* porphobilinogen deaminase (Jordan *et al.*, 1988a), had eliminated the possibility of proteolytic degradation products since each species displayed a single band in the SDS-PAGE. Since the mobilities of the double bands did not change on treatment with hydroxylamine it seemed unlikely that the *E. coli* enzyme existed in the form of enzyme-intermediate complexes. Moreover in the studies with the *E. coli* enzyme each species exhibited the typical spectral profile of a dipyrromethane cofactor with Ehrlich's reagent and possessed the same specific activity.

In this project, the double bands seen with native ubiquitous deaminase and the Arg 167 Gln mutant enzyme were separated using high-resolution Mono Q anion exchange column chromatography and different experiments were carried out to study their individual properties. Figure 3.15 and figure 3.16 show the elution profile of native enzyme from Mono Q chromatography and non-denaturing PAGE analysis of the separated protein peaks in which the two bands observed in the native gel, after the gel filtration, were separated. The upper band represents the first peak from the Mono Q column and the lower band, the second. M_r determination of the protein from each peak was carried out by using a Micromass LCT nanoflow time of flight mass spectrometer, in an attempt to find any small difference between the two species, see figures 3.17 and 3.18. The spectra show that there was a difference of one atomic

mass unit (amu) between the two native protein species, although it is by no means certain that the instrument is able to resolve such a small difference.

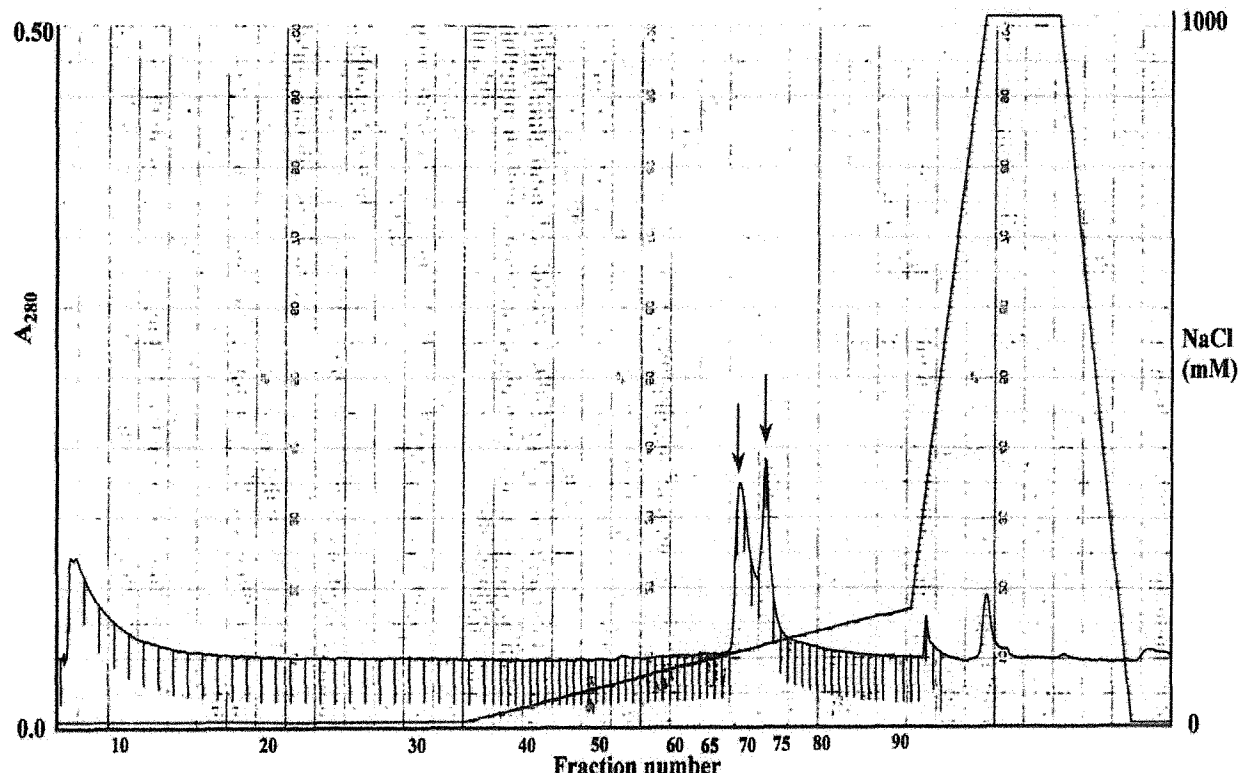


Figure 3.15: The elution profile of native ubiquitous human porphobilinogen deaminase from the high resolution ion exchange chromatography, HR5/5 Mono Q column attached to a f.p.l.c. system, as an attempt to separate the double bands. The enzyme after the gel filtration G-75 Superdex column was loaded onto a pre-equilibrated Mono Q column using 20mMTris/HCl buffer, pH 7.5, then eluted at 110mM NaCl by using a gradient from 0-160mM NaCl (60ml). Two peaks were observed for the native ubiquitous human porphobilinogen deaminase in the fractions between 69-74, where the size of each fraction equal to 0.5ml. The blue line is the absorbance at 280nm, the red line is the salt concentration from 0 to 1000mM NaCl.

In figure 3.19 the ubiquitous and erythroid (from Sweden) human porphobilinogen deaminase isozymes were compared with the two bands of the ubiquitous isozyme that had been separated using Mono Q chromatography. In figure 3.20 and 3.21, the elution

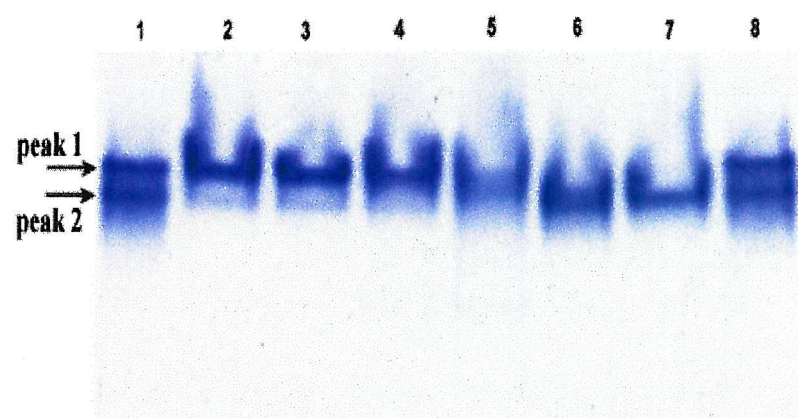


Figure 3.16: Non-denaturing PAGE analysis to show the elution of native ubiquitous porphobilinogen deaminase from a Pharmacia f.p.l.c. HR5/5 Mono-Q chromatography column where the two bands of the enzyme in the native gel after the gel filtration, were separated. Tracks 1 and 8, native enzyme after Superdex G-75 column chromatography; tracks 2, 3, 4, 5, 6 and 7 represent the elution of native enzyme from a Mono-Q chromatography (tubes 69,70,71,72,73 and 74 respectively). It is clearly shown that the two bands were separated where the upper band represents the first peak and the lower band represents the second peak.

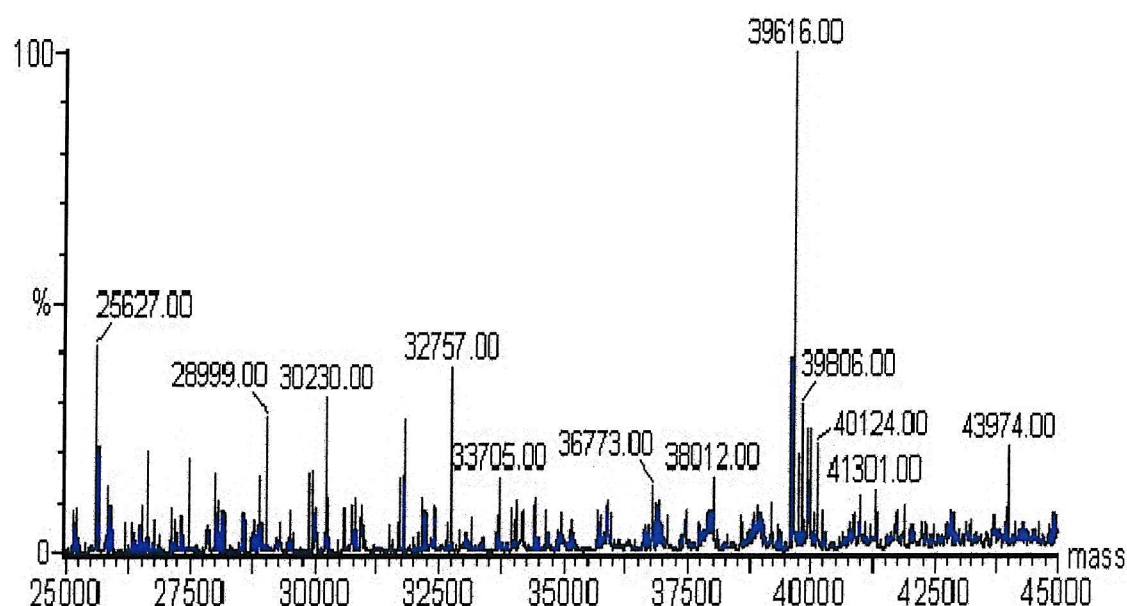


Figure 3.17: Spectrum obtained from a Micromass LcT nanoflow time of flight mass spectrometric analysis of the first peak (the top band in the native gel) of native ubiquitous human porphobilinogen deaminase, after HR5/5 Mono Q chromatography. This peak was shown to have a M_r of 39616.00 (kindly carried out by Paul Skipp).

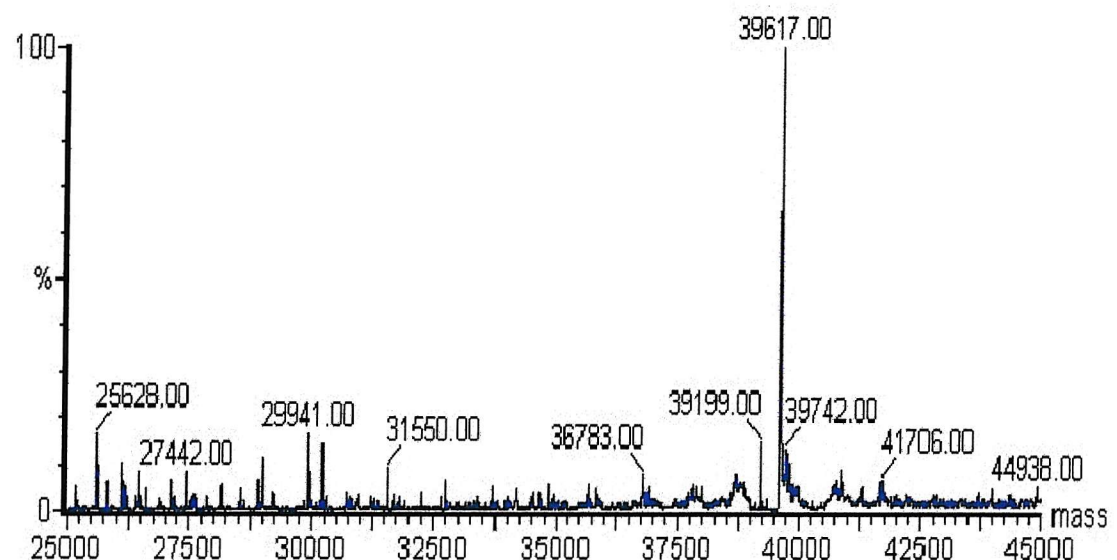


Figure 3.18: Spectrum obtained from a Micromass LcT nanoflow time of flight mass spectrometric analysis of the second peak (the bottom band in the native gel) of native ubiquitous human porphobilinogen deaminase, after HR5/5 Mono Q chromatography. This peak was shown to have a M_r of 39617.00 (kindly carried out by Paul Skipp).

profile shows the elution of the Arg 167 Gln mutant from the Mono Q column and the non-denaturing PAGE analysis, respectively. The two bands of the Arg 167 Gln mutant enzyme seen in the native gel, after gel filtration, were separated. The second peak of the Arg 167 Gln mutant from Mono Q chromatography, which represents the lower band (not shown in this gel) was very small and was not detectable on the gel.

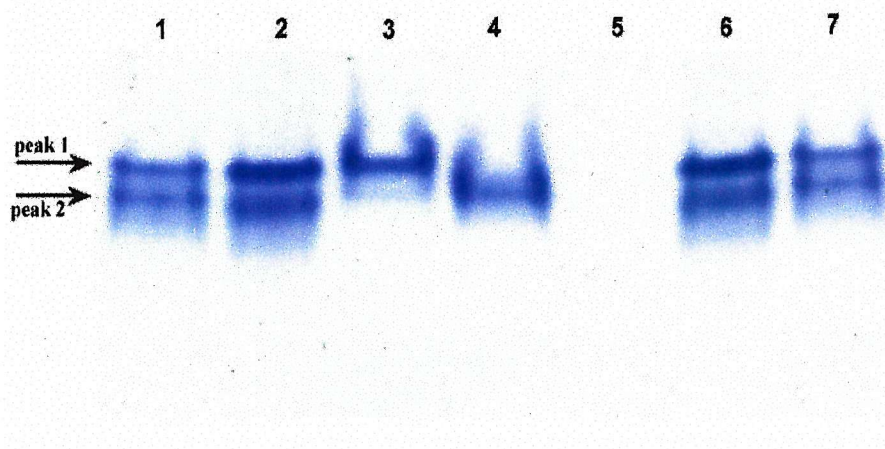


Figure 3.19: Non-denaturing PAGE analysis to compare the two isozymes, ubiquitous and erythroid (Swedish Sample) human porphobilinogen deaminases, with the two bands of ubiquitous isozymes separated using the Pharmacia f.p.l.c. HR5/5 Mono Q chromatography column. Track 1, ubiquitous porphobilinogen deaminase; track 2, erythroid porphobilinogen deaminase (from Sweden); track 3, peak 1 of ubiquitous porphobilinogen deaminase from Mono Q chromatography; track 4, peak 2 of ubiquitous porphobilinogen deaminase after Mono Q chromatography; track 5, blank; tracks 6 and 7 as tracks 2 and 1 respectively.

Experiments were carried out using five non-denaturing gels, to investigate the nature of the two protein bands.

Firstly, experiments were conducted to investigate the possible interconversion of double protein bands by the heat-treatment at 37°C, see figure 3.22, and 70°C, see figures 3.23 and 3.24. From the gels, the stability of the double bands from the native and Arg 167 Gln mutant ubiquitous human porphobilinogen deaminase can be seen. On the other hand the double bands from the erythroid human porphobilinogen deaminase isoenzyme (from Sweden), both protein bands appear to fade

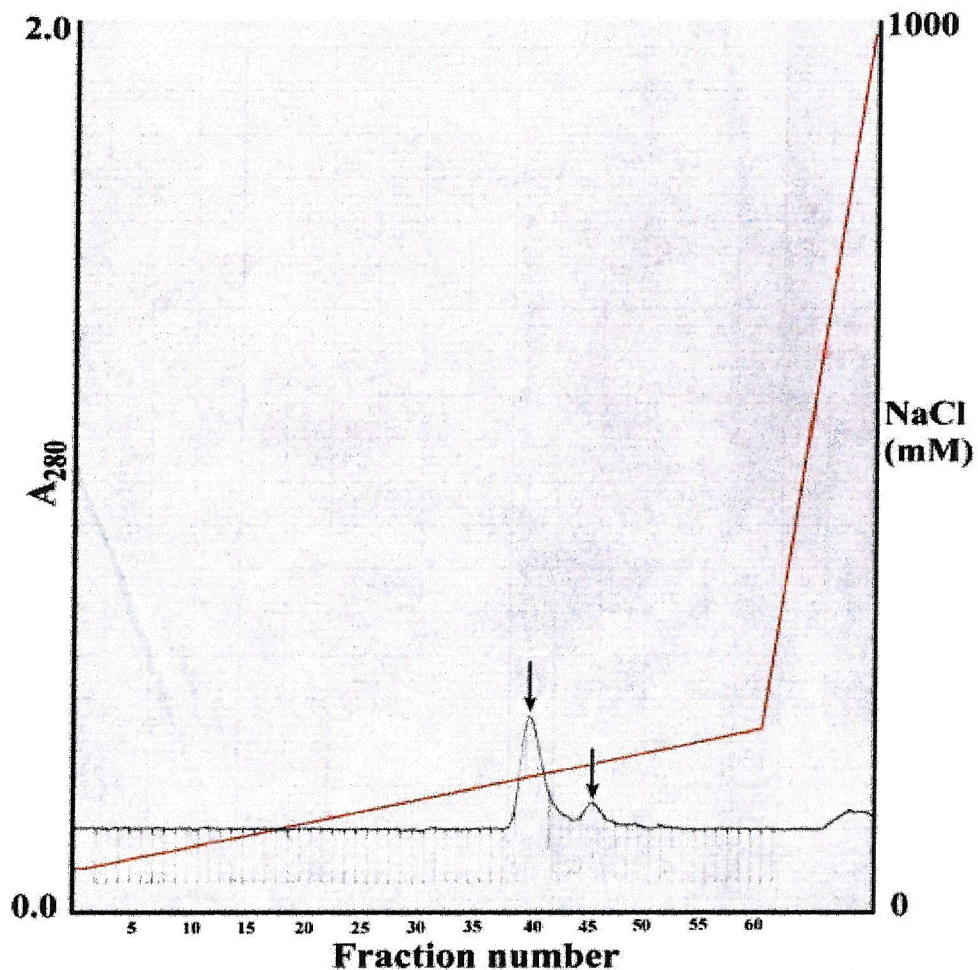


Figure 3.20: The elution profile of ubiquitous human porphobilinogen deaminase Arg 167 Gln mutant from the high resolution ion exchange chromatography, HR5/5 MonoQ column attached to a f.p.l.c. system, in an attempt to separate the double bands. The enzyme after the gel filtration on G-75 Superdex was loaded onto a pre-equilibrated Mono Q column using 20mMTris/HCl buffer, pH 7.5, then eluted at 110mM NaCl by using a gradient from 0-160mM NaCl (30ml). Two peaks were observed for the Arg 167 Gln mutant of ubiquitous human porphobilinogen deaminase in the fractions between 39-46. The blue line is the absorbance at 280nm; the red line is the salt concentration from 0 to 1000mM NaCl.

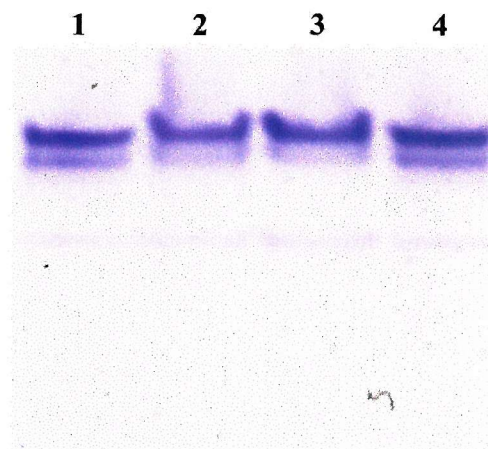


Figure 3.21: **Non-denaturing PAGE analysis showing ubiquitous porphobilinogen deaminase Arg 167 Gln mutant after the separation of the two protein bands using a Pharmacia f.p.l.c. HR5/5 Mono Q chromatography column.** Track 1, Arg 167 Gln mutant after the Superdex G-75 column before the separation of the double bands; track 2, peak one of Arg 167 Gln mutant after Mono Q chromatography; track 3, as in track 2; track 4, Arg 167 Gln mutant after Superdex G-75 column before the separation of the double bands. The second peak of Arg 167 Gln mutant from the Mono Q chromatography, which represents the lower band (not shown in this gel) was very small and was not detectable. Details of experiments are described in the Materials and Methods section.

at approximately the same rate. No interconversion of the double bands to single bands, or *vice versa*, occurred.

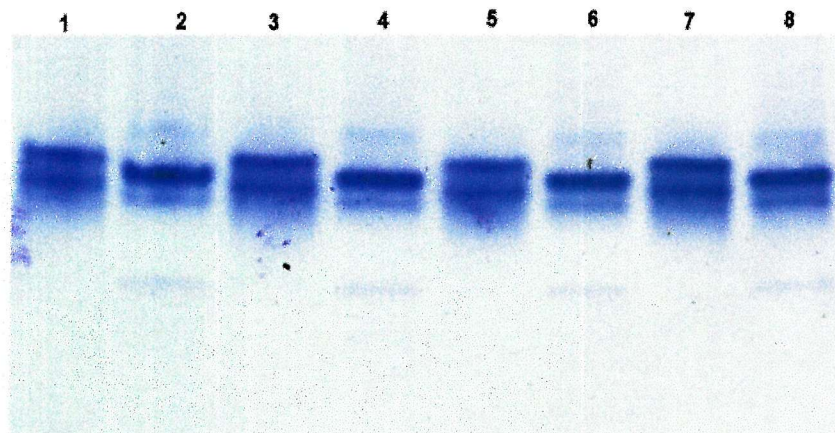


Figure 3.22: Non-denaturing PAGE analysis of ubiquitous porphobilinogen deaminase, native enzyme and Arg 167 Gln mutant to investigate possible interconversion of double protein bands. Heat-treatment at 37°C for three different times was carried out. Track 1, native enzyme as control; track 2, Arg 167 Gln mutant enzyme as control; track 3, native enzyme after heat treatment at 37°C for 30min; track 4, Arg 167 Gln mutant after heat treatment at 37°C for 30min.; track 5, native enzyme after heat treatment at 37°C for 60min; track 6, Arg 167 Gln mutant after heat treatment at 37°C for 60min; track 7, native enzyme after heat treatment at 37°C for 2 hours; track 8, Arg 167 Gln mutant after heat treatment at 37°C for 2 hours. The stability of the double bands and the inability to convert the double bands to single bands, or *vice versa*, is evident.

A second non-denaturing gel was run in duplicate to show the analysis of a crude cell free extract of native ubiquitous human porphobilinogen deaminase, before and after heat treatment, to determine if the double bands have been created as a result of the heat treatment, see figures 3.25 a and b. One of these duplicates, gel (a), was stained with Coomassie blue and the other duplicate, (b), was incubated with porphobilinogen and the fluorescent uroporphyrin was visualised. From gel (a), it is clear that the extract after ultracentrifugation, track 2, has the same major band of the deaminase as the sample after treatment, track 3. In gel (b), a fluorescent double band can be seen before and after heat-treatment, with the upper stronger

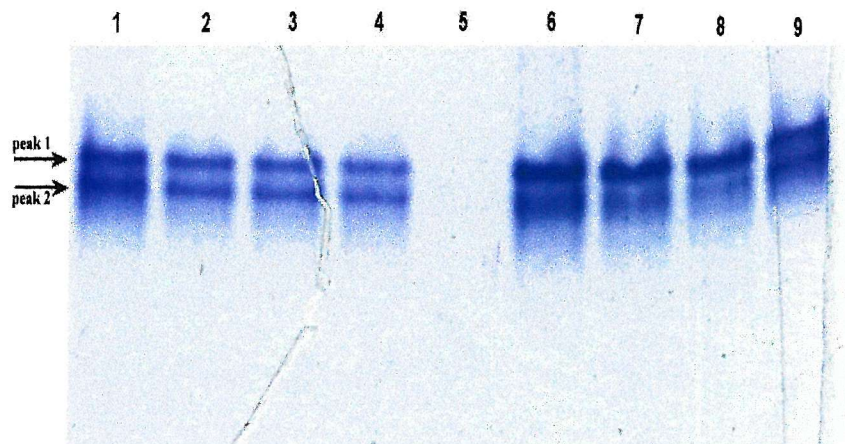


Figure 3.23: **Non-denaturing PAGE analysis to determine if the double bands of the native enzyme of ubiquitous and erythroid (Swedish sample) human porphobilinogen deaminase can be converted to a single band by heat treatment at 70°C for different incubation times.** Track 1, native ubiquitous human porphobilinogen deaminase; track 2, sample as track 1 but heat treated at 70°C for 10min.; track 3, sample as in track 1 but heat treated at 70°C for 20 min.; track 4, sample as in track 1 but heat treated at 70°C for 30min.; track 5, sample as in track 1 but heat treated at 70°C for one hour; track 6, native erythroid human porphobilinogen deaminase (Swedish sample); track 7, sample as in track 6 but heat treated at 70°C for 10min.; track 8, sample as in track 6 but heat treated at 70°C for 20min.; track 9, sample as in track 1. Each sample contained 10 μ g of protein. From the gel it can be seen that the double bands of ubiquitous porphobilinogen deaminase are stable and are not changed by heat-treatment. However the erythroid isozyme (Swedish sample), lower band starts to disappear specifically with heat treatment at 70°C for 20min. or more.

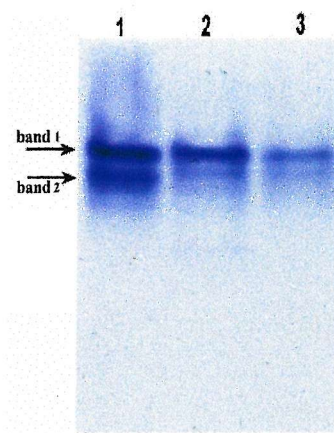


Figure 3.24: Non-denaturing PAGE analysis to determine if the double bands of the erythroid human porphobilinogen deaminase (from Sweden) can be converted to a single band. Track 1, native erythroid porphobilinogen deaminase (from Sweden); track 2, as track 1 but heat treated at 70°C for 30min.; track 3, sample as in track 1 but heat treated at 70°C for 1 hour. Each sample contained 10 μ g of protein. From the gel it can be seen that both protein bands from the erythroid human porphobilinogen deaminase isozyme appear to fade at approximately the same rate.

band coincident with the major staining protein band. There is no indication that heat treatment has caused one band to change into another, confirming that the heat-treatment step was not likely to cause the formation of the double band.

In the third experiment, non-denaturing PAGE analysis was carried out to determine the behavior of the two separated bands of the native human ubiquitous deaminase on treatment with porphobilinogen. Each purified protein sample appears to behave identically, producing ES complexes that appear as four bands E, ES, ES₂ and ES₃. On heat treatment the enzyme, E is regenerated from a proportion of the complexes as shown in figure 3.26.

The above experiments suggest that the double bands of native ubiquitous porphobilinogen deaminase represent two independent species of the deaminase rather than arising as a consequence of the purification. Scrutiny of the DNA sequencing data did not reveal any heterogeneity or known polymorphisms so the route by which

the two enzymic species are formed is as yet unknown. The differences could be as a result of deamidation during the bacterial growth, where an amide group of either glutamine or asparagine has been replaced with a carboxyl group. Alternatively the differences could be due to mistranslation of a glutamate or glutamine codon (or asparagine or aspartate) as a result of expressing a human cDNA in *E. coli*. In this respect, there are several amino acids that have similar M_r values and which have different charges that could lead to the observed bands; asparagine and aspartate - 114.11 and 115.09; glutamine and glutamate - 128.14 and 129.12; and most unlikely glutamine and lysine - 128.14 and 128.18 (values apply to amino acids in protein).

In the following sections, the properties of both ubiquitous human porphobilinogen deaminase mutants, Arg 167 Gln and Arg 167 Trp are studied.

3.2.8 Assay for the determination of K_m and V_{max} for recombinant human ubiquitous porphobilinogen deaminase Arg 167 Gln and Arg 167 Trp mutants

Enzyme activity was determined as μ mole of uroporphyrin formed/h per mg of protein (Jordan *et al.*, 1988a) for both mutants, as described in section 2.3.1. It has been found that the K_m for the Arg 149 His *E. coli* mutant, equivalent to human deaminase Arg 167, was increased due to the disruptive effect on essential interactions at the substrate-binding site, (Lambert *et al.*, 1994). The deaminase assay for the determination of K_m and V_{max} was carried out at different substrate concentrations. The substrate concentrations used for the native human recombinant ubiquitous porphobilinogen deaminase ranged from 1.6 - 53 μ M while the range used for the arginine mutants, Arg 167 Gln and Arg 167 Trp, were from 160 - 480 μ M and 20 - 561 μ M porphobilinogen, respectively. Incubations were carried out for 5min. at 37°C in the case of the native enzyme and for one hour in the case of the less active arginine mutants. The data was plotted as an Eadie-Hofstee plot, see figure 3.27 for the

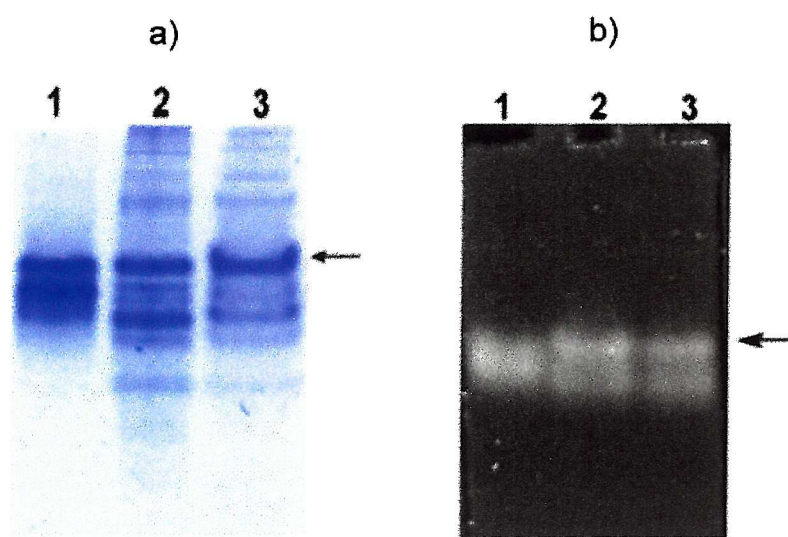


Figure 3.25: **Non-denaturing PAGE analysis of crude extract of native ubiquitous human porphobilinogen deaminase before and after heat treatment to determine if the double bands have been created as a result of the heat treatment.** Track 1, purified deaminase after Superdex G-75 column; track 2, extract after ultracentrifugation; track 3, extract after heat-treatment. Details of experiments are described in the Materials and Methods section. From the gel a), we can see that track 2 has the main band of the deaminase plus a light band in the place of the second band plus other bands, while in track 3 only a major band appeared in the place of the deaminase plus other bands in the bottom away from the deaminase band. In gel b), the fluorescent double bands can be seen in both stages of ubiquitous human porphobilinogen deaminase purification, before heat-treatment and after. This observation confirms that the heat-treatment step does not lead to the double bands.

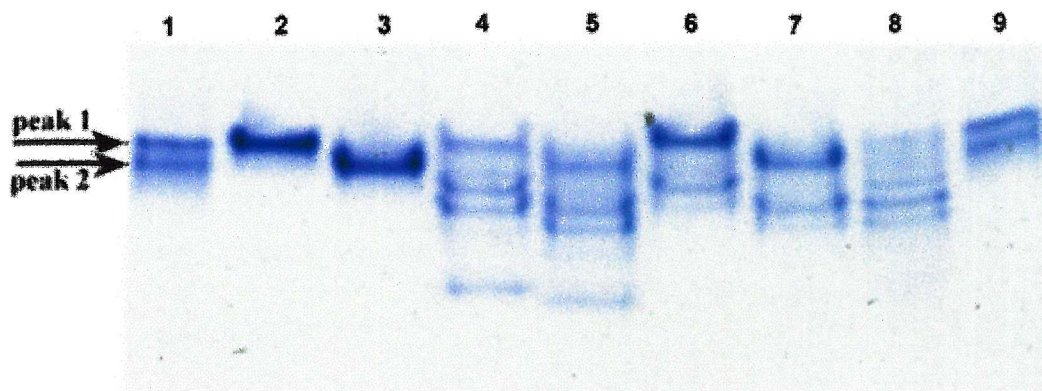


Figure 3.26: Non-denaturing PAGE analysis of native ubiquitous porphobilinogen deaminase to determine the behaviour of the two separated bands; separated by using a Pharmacia f.p.l.c. HR5/5 Mono Q chromatography column, after reacting with 10 mole equivalents of PBG. Incubations were carried out for 5min. at 37°C in 20mM Tris/HCl buffer, pH 8. Track 1, native enzyme after Superdex G-75; track 2, peak 1 of native enzyme from Mono Q chromatography; track 3, peak 2 of native enzyme from Mono Q chromatography; track 4, sample of track 2 (peak 1) + PBG; track 5, sample of track 3 (peak 2) + PBG; tracks 6 and 7 as in tracks 4 and 5 but the reaction mixtures were heat-treated at 60°C for 5min.; track 8, native enzyme after Superdex G-75 + PBG; track 9, native enzyme after Superdex G-75.

native enzyme, figure 3.28 for the Arg 167 Gln mutant and figure 3.29 for the Arg 167 Trp mutant. The K_m and V_{max} for the Arg 167 Gln and Arg 167 Trp mutants enzymes were calculated and were compared to the native enzyme. From the table 3.7, it can be seen that both mutants exhibit K_m values greater than that of the native enzyme with lower V_{max} values. The K_m and the V_{max} for the Arg 167 Trp mutant have been determined at the pH optimum instead of the native enzyme pH optimum, pH 6.8, since the data obtained from the enzyme assays at pH 8.2 using different substrate concentrations showed a positive correlation between the rate of reaction and the rate of reaction/substrate concentration. However, at pH 6.8, all the available data was used to construct the Eadie-Hofstee plot, resulting in a line of a best fit that shows the expected negative correlation between the rate of reaction and the rate of reaction/substrate concentration.

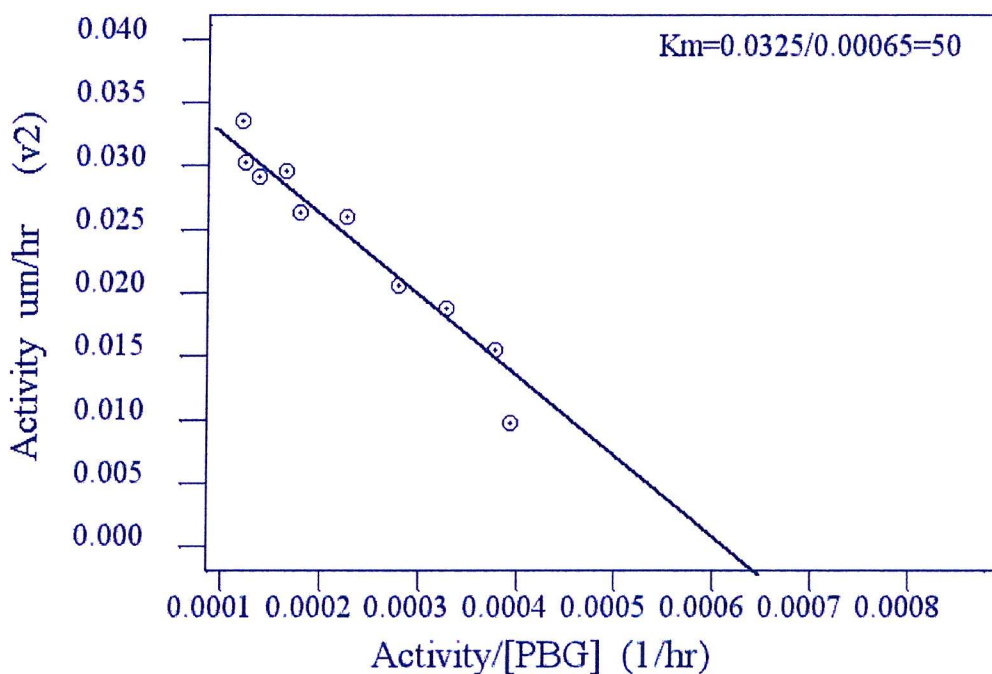


Figure 3.27: **Eadie-Hofstee plot for the pure human ubiquitous porphobilinogen deaminase, native enzyme.** The enzyme was incubated in the presence of 1.6 - 53 μ M porphobilinogen at 37°C for 5min., as described in section 2.3.1. The data are displayed as a plot of v against v/S , where v = activity (μ mole hr^{-1}) and S = substrate concentration, [PBG] (μ M). Values shown are an average of two assays.

Mutant strain	K_m (μ M)	V_{max} (μ mole hr^{-1})
Arg 167 Gln	368	0.015
Arg 167 Trp	333.3	0.017
Native	50	0.033

Table 3.7: **The kinetic parameters of the arginine 167 mutants, Arg 167Gln and Arg 167 Trp compared to native human recombinant ubiquitous porphobilinogen deaminase.**

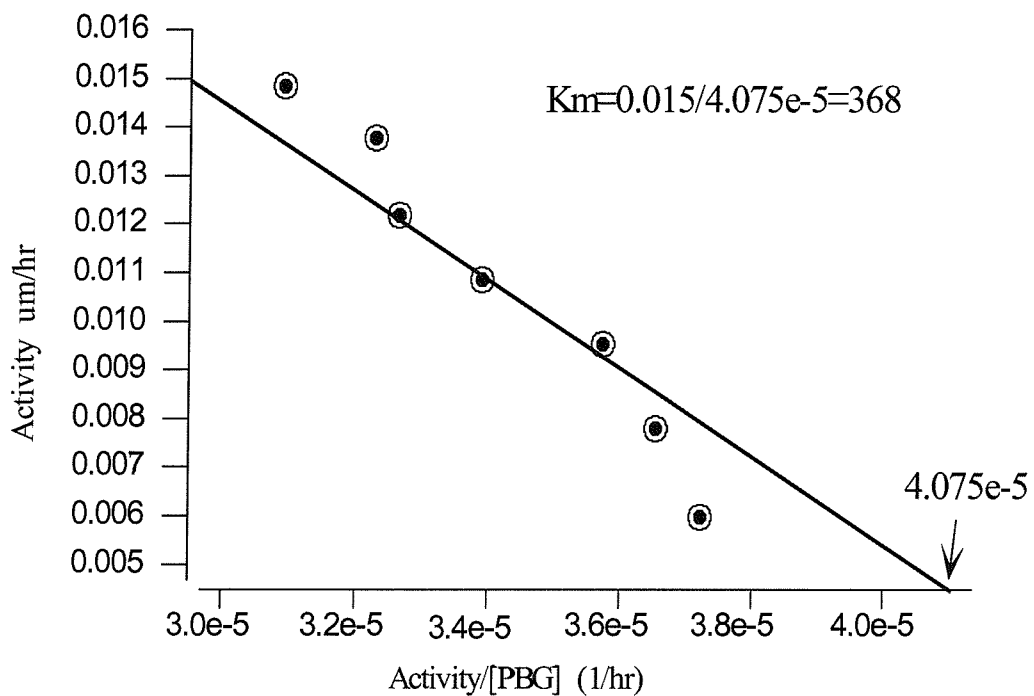


Figure 3.28: **Eadie-Hofstee plot for the pure human ubiquitous porphobilinogen deaminase Arg 167 Gln mutant.** The enzyme was incubated in the presence of 160 - 480 μ M porphobilinogen at 37°C for one hour., as described in section 2.3.1. The data are displayed as a plot of v against v/S , where v = activity (μ mole hr^{-1}) and S = substrate concentration, [PBG] (μ M). Values shown are an average of two assays.

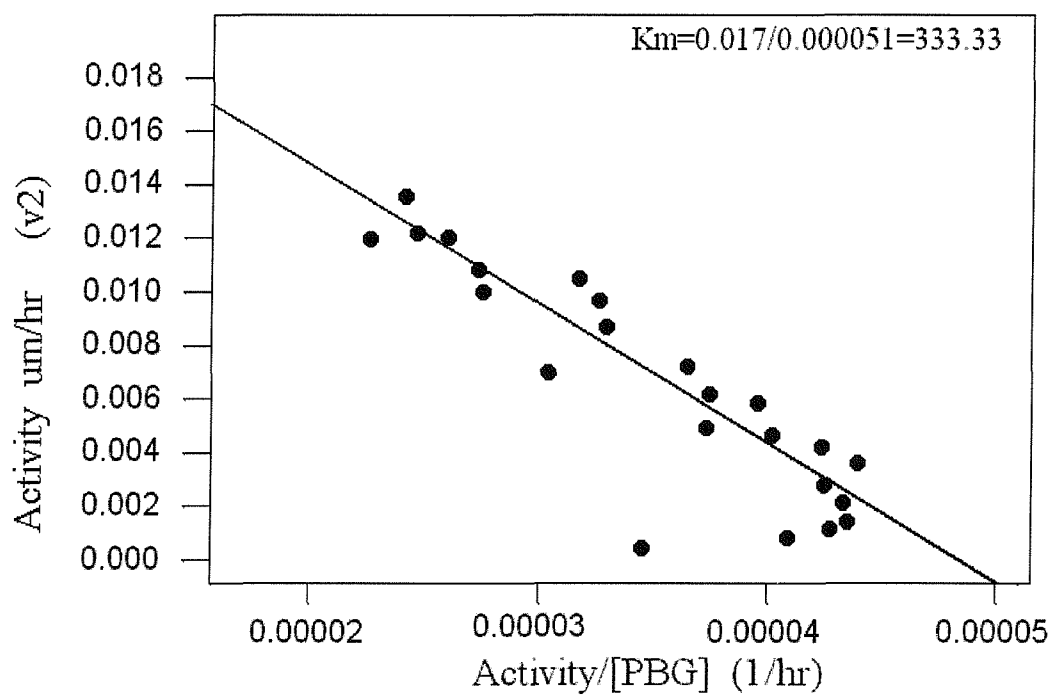


Figure 3.29: Eadie-Hofstee plot for the pure human ubiquitous porphobilinogen deaminase Arg 167 Trp mutant. The enzyme was incubated in the presence of 20 - 561 μ M porphobilinogen at 37°C for one hour, as described in section 2.3.1. The data are displayed as a plot of v against v/S , where v = activity (μ mole hr^{-1}) and S = substrate concentration, [PBG] (μ M). Values shown are an average of two assays.

3.2.9 Electrospray mass spectrometry (ESMS) of recombinant human ubiquitous porphobilinogen deaminase Arg 167 Gln and Arg 167 Trp mutants

M_r determination of the Arg 167 Gln and Arg 167 Trp mutant deaminases were carried out by using electrospray mass spectrometry. Samples of purified proteins were prepared as described in section 2.3.4. The M_r of each mutant enzyme was compared to the predicted value, 39749 of the native ubiquitous porphobilinogen deaminase. The M_r of the Arg 167 Gln mutant 39592, see figure 3.30, is within the range expected (39590) for the substitution of an arginine residue by glutamine, minus the mass of the *N*-terminal methionine residue, as confirmed by the *N*-terminal sequence. The difference between arginine and glutamine is 28.06 amu and the M_r of methionine, when attached to the protein, is 131.21. The Arg 167 Trp mutant was shown to have an M_r of 39652, see figure 3.31, that is within the range expected (39648) for the substitution of an arginine residue by tryptophan, also minus the mass of one methionine residue. The molecular weight difference between tryptophan and arginine is 30.01.

3.2.10 Reaction with modified Ehrlich's reagent to check the presence of the dipyrromethane cofactor and the porphyrin products of the recombinant human ubiquitous porphobilinogen deaminase Arg 167 Gln mutant, compared to the native enzyme

All porphobilinogen deaminases require a resident cofactor, the dipyrromethane cofactor, for activity. The dipyrromethane cofactor was originally detected by reaction of the enzyme with Ehrlich's reagent and shown to be bound to the protein through a cysteine residue, (Warren and Jordan, 1988; Miller *et al.*, 1988) see section

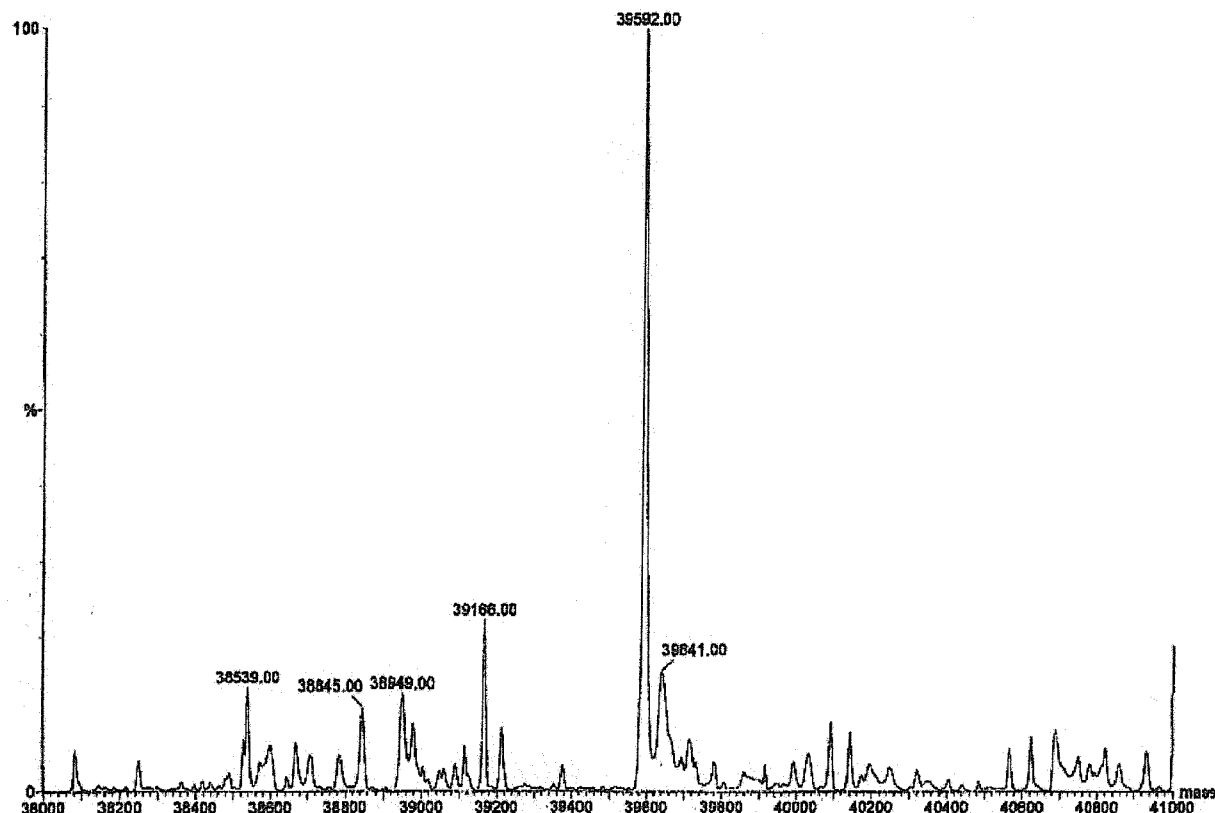


Figure 3.30: Spectrum obtained from electrospray mass spectroscopic (ESMS) analysis of 1000ng/10 μ l ubiquitous human porphobilinogen deaminase mutant, Arg 167 Gln after Superdex G-75 column chromatography. The Arg 167 Gln mutant was shown to have a M_r of 39592 which agrees with that predicted (39590) by the nucleotide sequence and the *N*-terminal sequence.

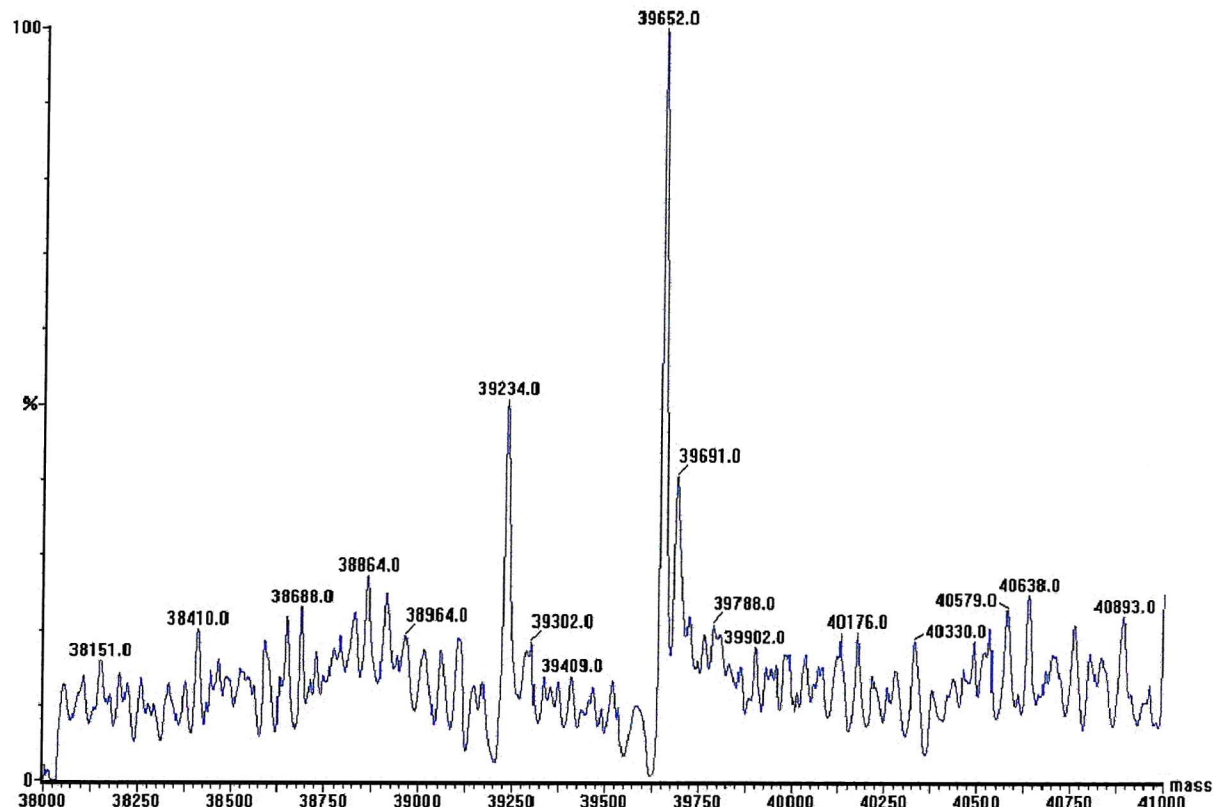


Figure 3.31: Spectrum obtained from electrospray mass spectrometry (ESMS) analysis of 1000ng/10 μ l human ubiquitous porphobilinogen deaminase mutant, Arg 167 Trp after DEAE Sephacel chromatography. The Arg 167 Trp mutant was shown to have a M_r of 39652 which agrees with that predicted (39648) by the nucleotide sequence and the *N*-terminal sequence.

2.3.9. The reaction between the holoenzyme and Ehrlich's reagent initially results in an intense purple colour at $\lambda_{\text{max}} = 565\text{nm}$, typical of a reaction between Ehrlich's reagent and the free α -position of a pyrrole. After approximately 15min., the colour changes to orange with a $\lambda_{\text{max}} = 495\text{nm}$, due to the formation of a conjugated dipyrromethene. It is thought that the change in the spectrum is not only due to oxidation but also to tautomerisation of the Ehrlich's adduct with the pyrromethene, see figure 2.5 (Woodcock's Ph.D. thesis, 1992).

Reactions were observed for both the native enzyme and Arg 167 Gln mutant using a uv-vis spectrophotometer (U-3010 instrument) over a range of 380-650nm. Spectra were recorded immediately after the reaction was performed and within 1min. and 10min. intervals for 10min. and one hour respectively. Spectra of the native enzyme when incubated with Ehrlich's reagent for 1min and 10min. intervals are shown in figures 3.32 and 3.33, respectively. Spectra of the Arg 167 Gln mutant after reaction with Ehrlich's reagent for 1min and 10min. intervals are shown in figures 3.34 and 3.35, respectively. The reaction of the Arg 167 Gln mutant is similar to the reaction of native enzyme with modified Ehrlich's reagent. This indicates that the Arg 167 Gln mutant contains the dipyrromethane cofactor.

The spectra for the reaction of Ehrlich's reagent with the native human ubiquitous porphobilinogen deaminase and the Arg 167 Gln mutant after reaction with porphobilinogen was observed using a manual uv-vis spectrophotometer over a range of 380-650nm. The deaminase samples and porphobilinogen were incubated for 5min at 37°C and filtered through a PD-10 column to remove the unreacted PBG molecules before reaction with Ehrlich's reagent, see section 2.3.9. Spectra for the native human deaminase were recorded immediately and at intervals of 5, 15 and 51min figures 3.36 and 3.37, respectively. The spectra for a similar experiment with the Arg 167 Gln mutant for 0, 5, 15 and 60min are shown in figures 3.38 and 3.39, respectively. Both native and mutant enzymes reacted rapidly with Ehrlich's reagent forming a spectrum indicative of a polypyrrolic enzyme intermediate complexe (ES₂ for exam-

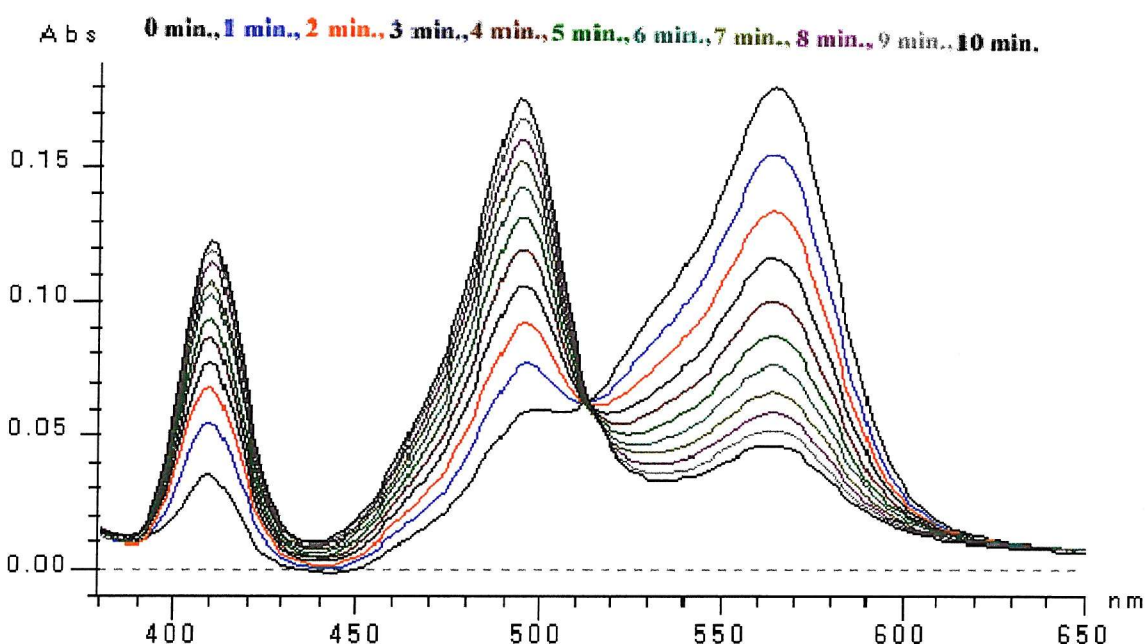


Figure 3.32: Spectra of human ubiquitous porphobilinogen deaminase, native enzyme after reaction with Ehrlich's reagent. Spectra were recorded immediately after the reaction was performed using a uv-vis spectrophotometer over a range of 380-650nm. at 1min. intervals for 10min.

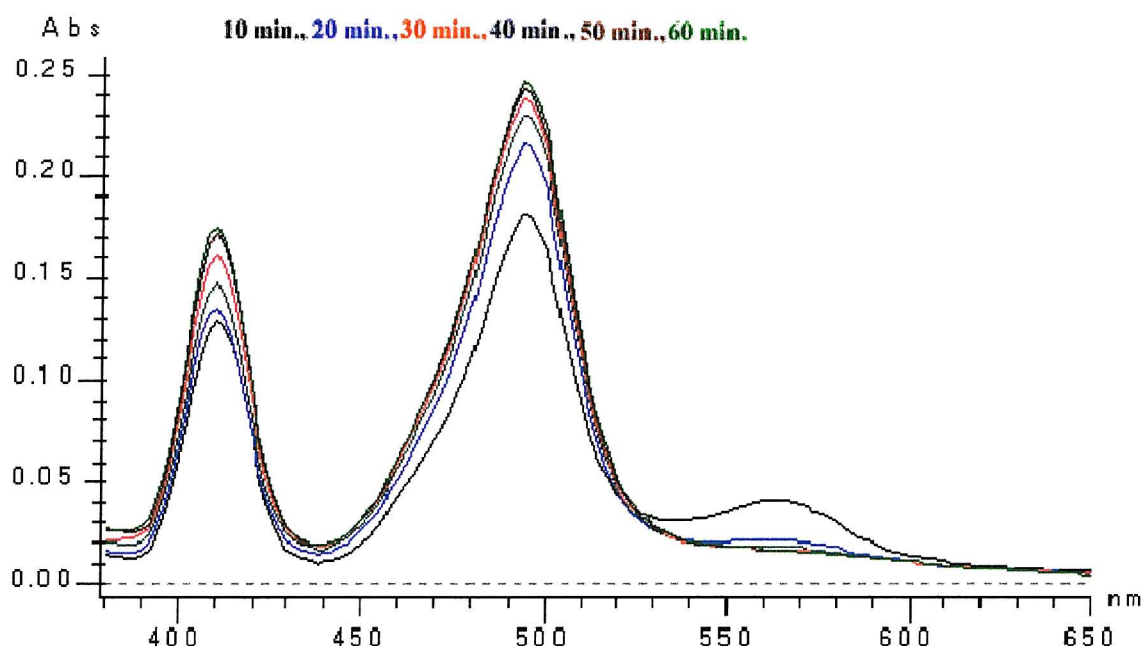


Figure 3.33: Spectra of human ubiquitous porphobilinogen deaminase, native enzyme after reaction with Ehrlich's reagent. Spectra were recorded immediately after the reaction was performed using a uv-vis spectrophotometer over a range of 380-650nm. at 10min. intervals for 60min.

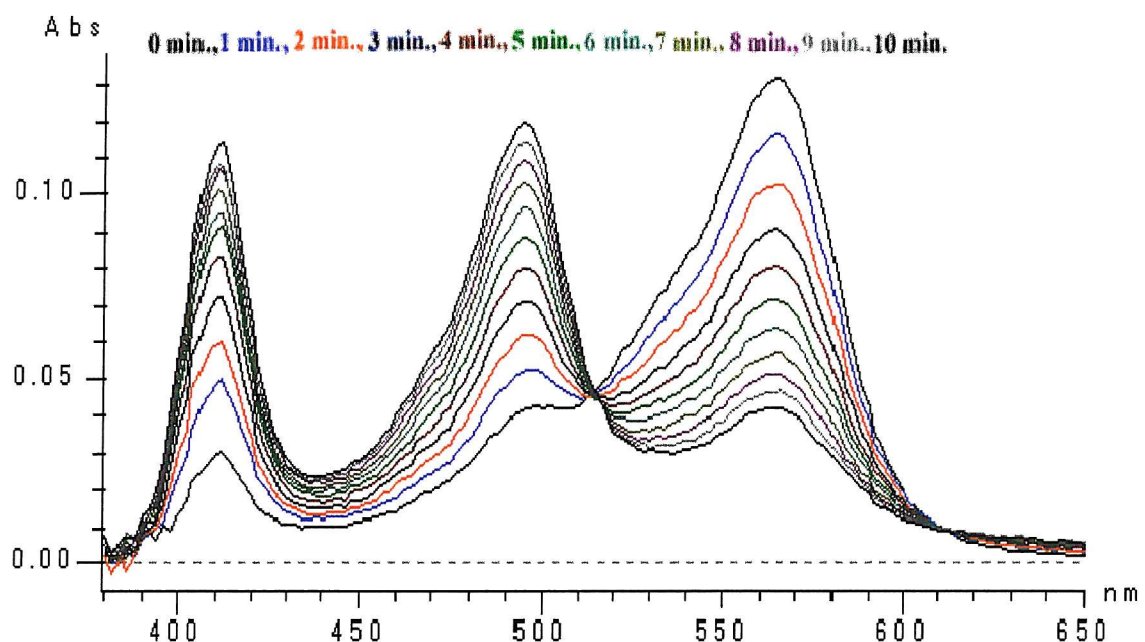


Figure 3.34: Spectra of human ubiquitous porphobilinogen deaminase mutant Arg 167 Gln after reaction with Ehrlich's reagent. Spectra were recorded immediately after the reaction was performed using a uv-vis spectrophotometer over a range of 380-650nm. at 1min. intervals for 10min.

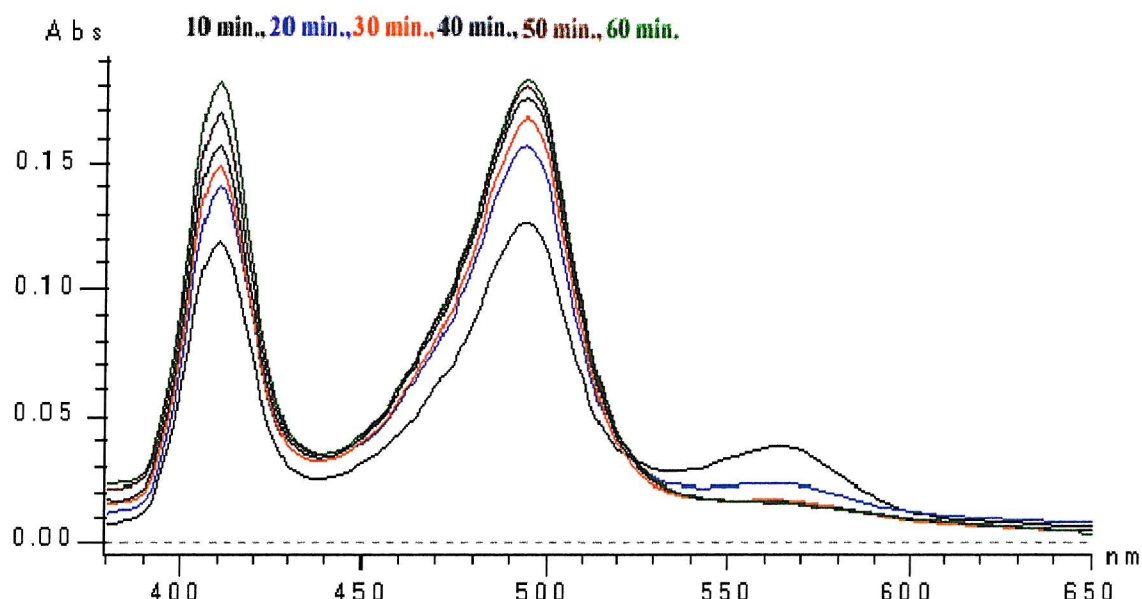


Figure 3.35: **Spectra of human ubiquitous porphobilinogen deaminase mutant Arg 167 Gln after reaction with Ehrlich's reagent.** Spectra were recorded immediately after the reaction was performed using a uv-vis spectrophotometer over a range of 380-650nm. at 10min. intervals for 60min.

ple) that was transformed in to an *etio*-type spectrum characteristic of uroporphyrin I. This was formed, presumably, from the release of enzymically bound polypyrroles that cyclised to uroporphyrinogen I followed by oxidation (by the Ehrlich's reagent) to uroporphyrin I. The formation of the porphyrin spectra confirm that the native and mutant enzymes were able to catalyse the polymerization reaction of porphobilinogen through ES complexes.

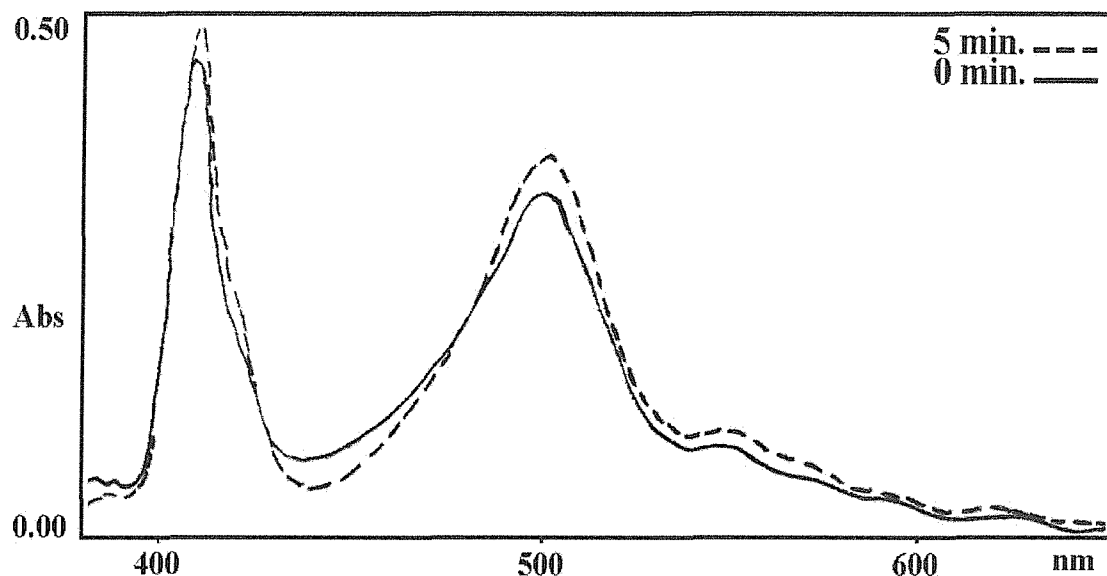


Figure 3.36: Spectra of human ubiquitous porphobilinogen deaminase, native enzyme, with PBG after reaction with Ehrlich's reagent. Spectra were recorded immediately after the reaction was performed using a uv-vis spectrophotometer over a range of 380-650nm. after 0min and 5min.

3.2.11 Determination of the isoelectric point of ubiquitous human porphobilinogen deaminase by isoelectric focusing (IEF)

It has been found that the isoelectric point for *E. coli* porphobilinogen deaminase is between pH 4 and 5 (Shoolingin-Jordan, 1995), but no detailed investigations have

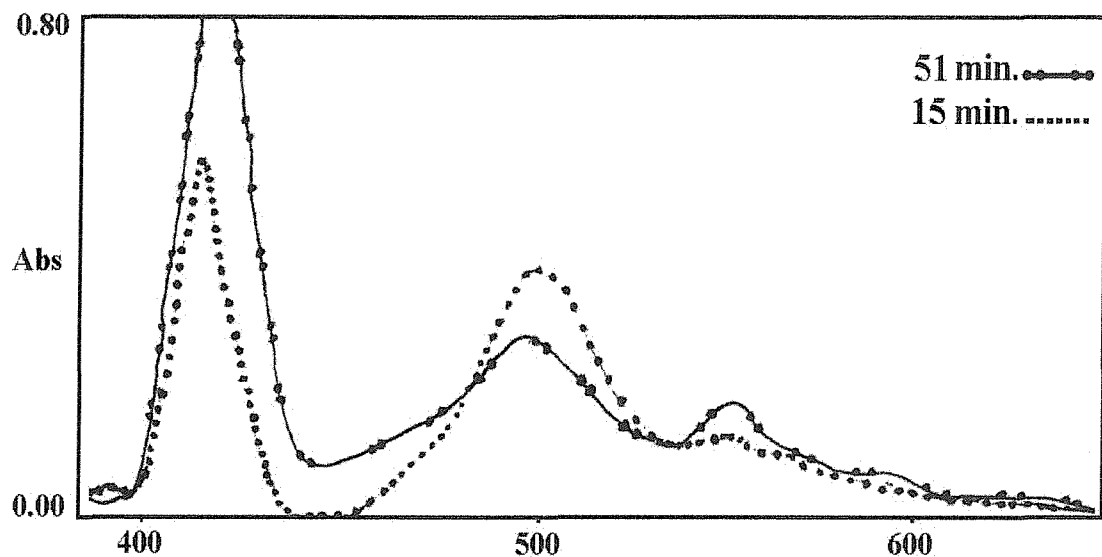


Figure 3.37: Spectra of native human ubiquitous porphobilinogen deaminase reacted with Ehrlich's reagent after incubation with PBG. Spectra were recorded immediately after separation of the enzyme on a PD-10 column using a uv-vis spectrophotometer over a range of 380-650nm. after 15min and 51min.

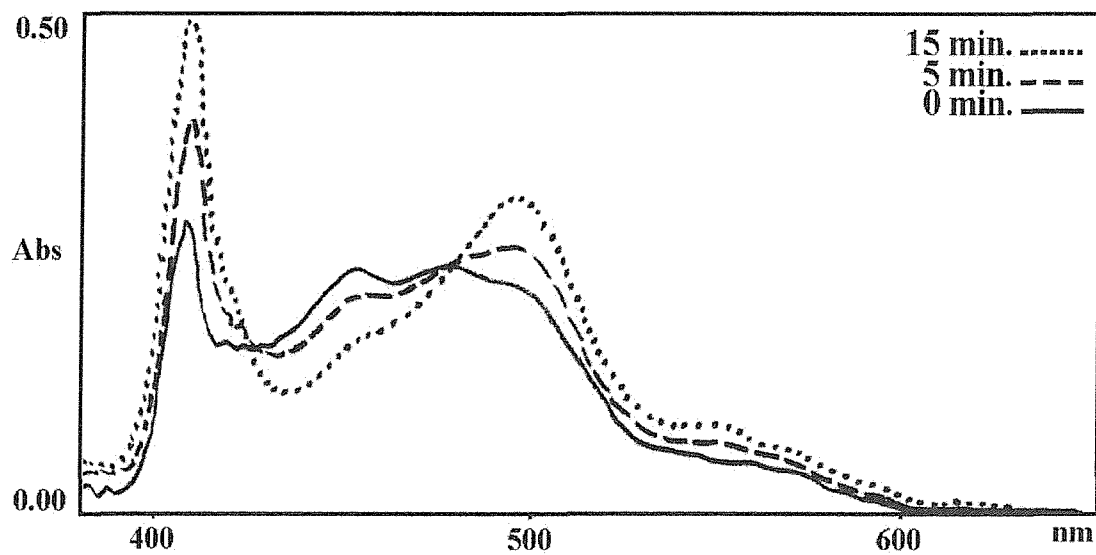


Figure 3.38: Spectra of human ubiquitous porphobilinogen deaminase, Arg 167 Gln mutant, with PBG after reaction with Ehrlich's reagent. Spectra were recorded immediately after the reaction was performed using a uv-vis spectrophotometer over a range of 380-650nm. after 0min., 5min. and 15min.

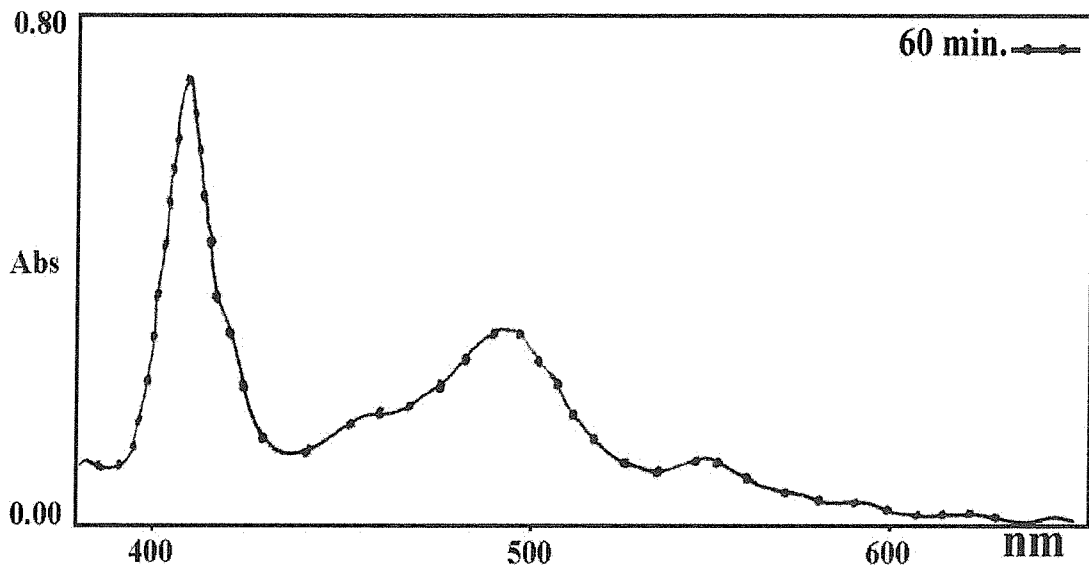


Figure 3.39: **Spectra of human ubiquitous porphobilinogen deaminase mutant Arg 167 Gln reacted with Ehrlich's reagent after incubation with PBG.** Spectra were recorded immediately after separation of the enzyme on a PD-10 column using a uv-vis spectrophotometer over a range of 380-650nm. after 60min.

been carried out on the human enzyme. Isoelectric focusing (IEF) is a highly sensitive analytical technique that has been used to study micro-heterogeneity in a protein where small charge differences between proteins can be detected. IEF analysis was performed using NOVEX IEF precast vertical gels of pH range 3-10, as described in section 2.3.1, to determine possible differences between the two protein bands of the ubiquitous human porphobilinogen deaminase separated by ion exchange Mono Q chromatography and to compare them with native human recombinant erythroid deaminase (from Sweden). The human deaminase samples were investigated together with the IEF marker, pH 3-10, to determine the pI of each deaminase by comparison with the markers (Wilson and Walker, 1994).

Figure 3.40 shows that the first peak from the Mono Q column chromatography showed a pI of 6.1. The second peak from the Mono Q column showed a pI of 5.95. The recombinant erythroid deaminase (from Sweden) showed a major species at pI

6.25 although there were three additional bands, two of which were of identical pI to the two ubiquitous species. The native ubiquitous human porphobilinogen deaminase, has a lower pI than that of the erythroid isozyme due largely to the presence of two additional glutamate residues in the *N*-terminal extension.

The pI values for the arginine mutants, Arg 167 Gln and Arg 167 Trp, Arg 173 Gln and Arg 149 Gln were also determined as shown in figure 3.41. The arginine mutants Arg 167 Gln and Arg 167 Trp have pI values lower than the native enzyme, as expected for proteins with one less positive charge, but the presence of an additional band suggests that some substrate may also be bound. In contrast Arg 173 Gln and Arg 149 Gln mutants migrate between pI 6.5 and 6.8 confirming that they exist largely as unfolded apo-enzymes. In these latter samples there is a trace of a band close to that expected for ES₂ suggesting that a small amount of this mutant has bound the cofactor covalently. (See chapter 4 for a detailed discussion of Arg 173 Gln and Arg 149 Gln mutants).

3.2.12 Determination of pH optimum of human ubiquitous porphobilinogen deaminase Arg 167 Gln and Arg 167 Trp mutants

The optimum pH for native deaminases range from pH 8 - 8.5 (Shoolingin-Jordan, 1995). In this study, the optimum pH for both human ubiquitous porphobilinogen deaminase Arg 167 Gln and Arg 167 Trp mutants have been determined by measuring the deaminase activity at different pH values over the range from pH 6.0-10, see figure 3.42 and 3.43, respectively. The pH optimum for both mutant deaminases decreased from 8.2 to 6.8. This reason for this pH optimum shift may be explained by the loss of the positively charged arginine for the neutral glutamine, or tryptophan, if one considers the possible role of the arginine 167 in substrate binding. From the information arising from X-ray structure analysis, arginine 167 is thought to form

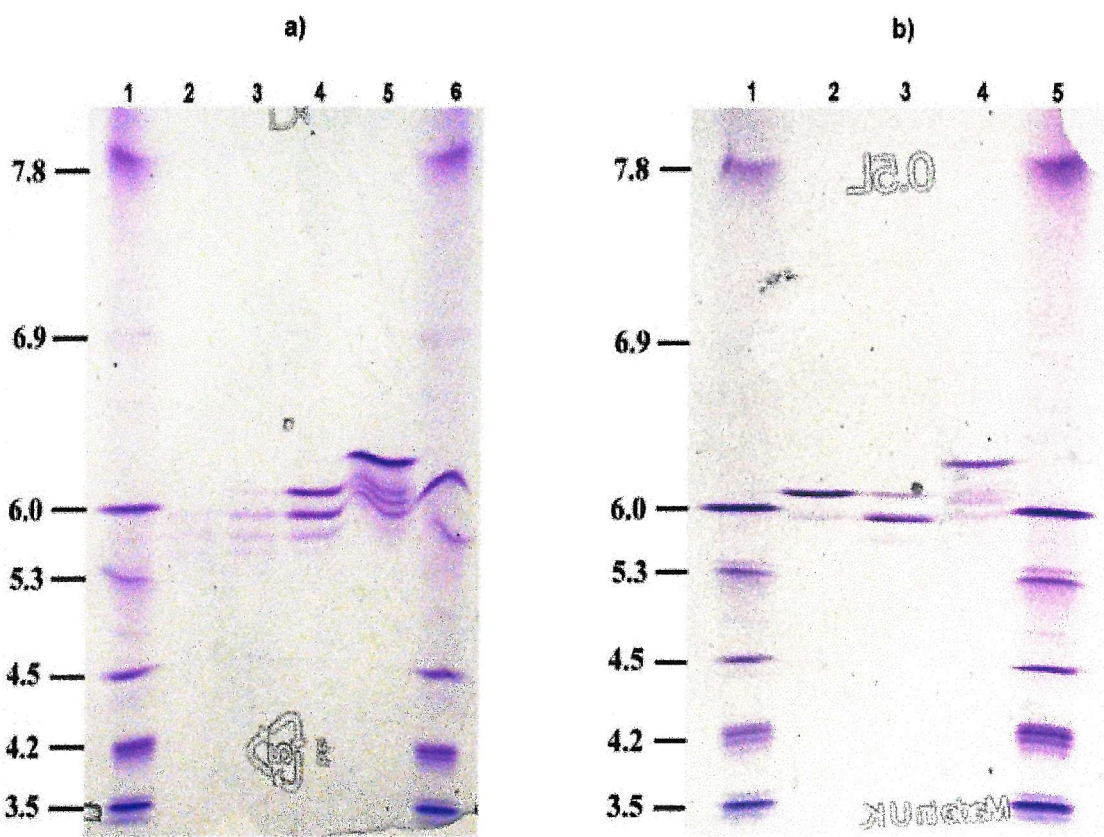


Figure 3.40: Isoelectric focusing (IEF) analysis using NOVEX IEF precast vertical gel of pH 3-10, to determine possible differences between the two protein bands of the ubiquitous human porphobilinogen deaminase which have been separated by Mono Q chromatography and to compare them with the native recombinant human erythroid porphobilinogen deaminase (from Sweden). a) Before chromatography with Mono Q. Track 1, 10 μ l of IEF marker 3-10 (pI from the top = 8.3, 7.8, 7.4, 6.9, 6.0, 5.3, 5.2, 4.5, 4.2 and 3.5); track 2 blank; tracks 3 and 4, ubiquitous human porphobilinogen deaminase; track 5, human erythroid porphobilinogen deaminase (from Sweden); Track 6, as track 1. b) After chromatography with Mono Q. Track 1, 10 μ l of IFE marker 3-10 (pI from the top = 8.3, 7.8, 7.4, 6.9, 6.0, 5.3, 5.2, 4.5, 4.2 and 3.5); track 2, peak 1 of ubiquitous human porphobilinogen deaminase from Mono Q chromatography; track 3, peak 2 of ubiquitous human porphobilinogen deaminase from Mono Q chromatography; track 4, erythroid porphobilinogen deaminase (from Sweden); track 5, 20 μ l of IFE marker 3-10.

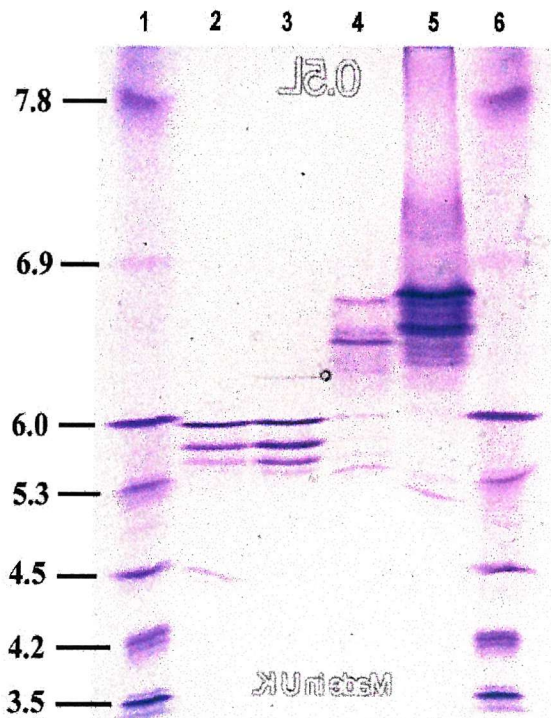


Figure 3.41: Isoelectric focusing (IEF) analysis using NOVEX IEF precast vertical gel of pH 3-10, to determine possible differences between the arginine mutants, Arg 167 Gln Arg 167 Trp, Arg 173 Gln and Arg 149 Gln of the recombinant human ubiquitous porphobilinogen deaminase. Track 1, 10 μ l of IFE marker 3-10 (pI from the top = 8.3, 7.8, 7.4, 6.9, 6.0, 5.3, 5.2, 4.5, 4.2 and 3.5); track 2, Arg 167 Trp mutant; track 3, Arg 167 Gln mutant; track 4, Arg 173 Gln mutant; track 5, Arg 149 Gln mutant; track 6, 20 μ l of IFE marker 3-10.

an ion pair with the acetic acid side chain of the substrate, porphobilinogen. In solution, the acetic acid side chain of porphobilinogen is internally ion paired to the aminomethyl group. As porphobilinogen approaches the active site, arginine 167 is thought to break this ion pair by binding the acetic acid side chain and releasing the aminomethyl group, thus allowing it to deaminate with greater facility. In the absence of arginine 167, however, it would be necessary to protonate the acetic acid side chain from the medium in order to break the internal salt link, hence a more acid pH would be necessary for the enzyme to function (Jordan, 1994a).

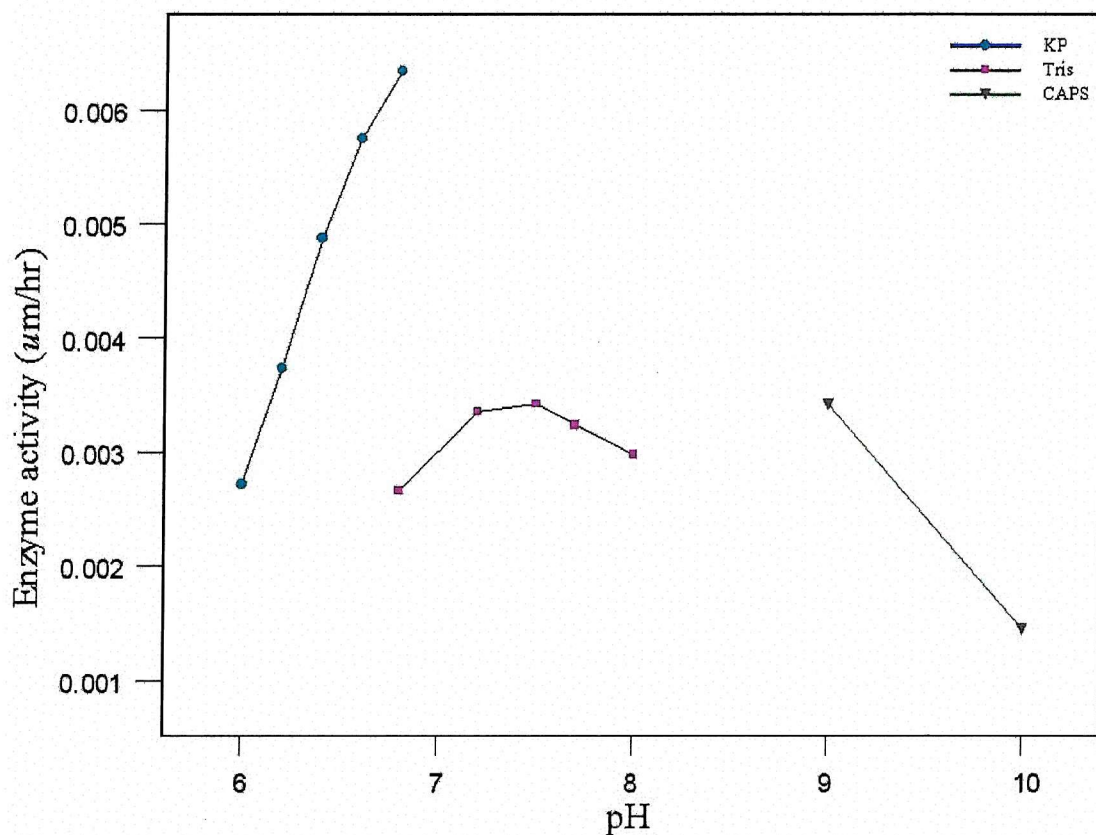


Figure 3.42: **pH dependence of ubiquitous porphobilinogen deaminase Arg 167 Gln mutant.** Buffers used: 20mM potassium-phosphate buffer (KP) from pH 6.0-6.8; 20mM Tris/HCl buffer (Tris) from pH 6.8-8; 20mM CAPS buffer (CAPS) for pH 9 and 10. Activity was determined as described in Materials and Methods, using 1mg/ml stock enzyme solution, 200μM PBG and 60 minutes incubation at 37°C.

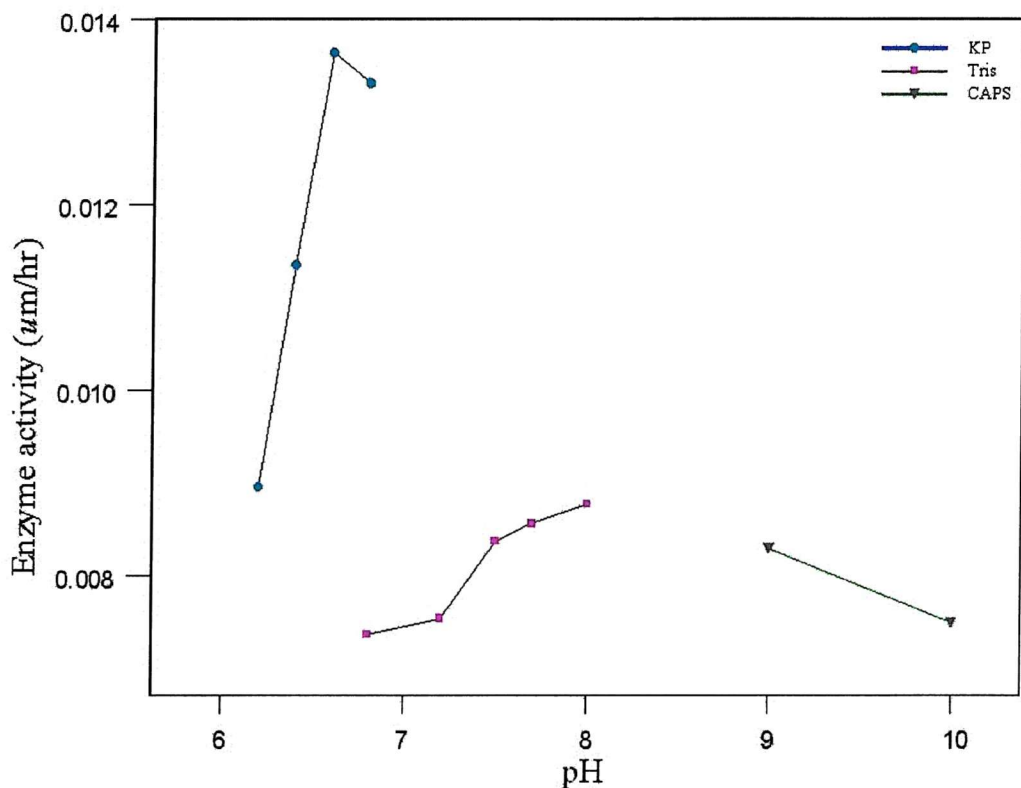


Figure 3.43: **pH dependence of human ubiquitous porphobilinogen deaminase Arg 167 Trp mutant.** Buffers used: 20mM potassium-phosphate buffer (KP) from pH 6.0-6.8; 20mM Tris/HCl buffer (Tris) from pH 6.8-8; 20mM CAPS buffer (CAPS) for pH 9 and 10. Activity was determined as described in Materials and Methods, using 1mg/ml stock enzyme solution, 200μM PBG and 60 minutes incubation at 37°C.

3.2.13 Thermal stability of the recombinant human ubiquitous porphobilinogen deaminase Arg 167 Gln mutant

Porphobilinogen deaminases from all sources investigated exhibit remarkable thermal stability on heating to 60°C and this property has been used successfully as a major step in the purification protocol (Anderson and Desnick, 1980; Mazzetti and Tomio, 1988; Jordan *et al.*, 1988a; Jordan *et al.*, 1988b). At temperatures higher than 80°C, there is a rapid loss in the activity of the deaminase (Jones and Jordan, 1994). The heat-stability of the deaminase is explained by the X-ray structure of the *E. coli* porphobilinogen deaminase (Louie *et al.*, 1992) that shows a large number of protein-cofactor interactions. The apo-deaminase, which lacks the cofactor, is very labile to heat treatment and is rapidly denatured above 40°C, (Scott *et al.*, 1989; Jordan and Woodcock, 1991). In this study, it has been found that the Arg 167 Gln mutant exhibited similar thermal stability to the native enzyme, with activity being lost above 60°C, as shown in figure 3.44 suggesting that the protein is folded normally. This is somewhat expected since this mutant contains the cofactor.

3.2.14 Studies on the stability of ES complexes of recombinant human ubiquitous porphobilinogen deaminase Arg 167 Gln and Arg 167 Trp mutants using non-denaturing PAGE

Porphobilinogen deaminases catalyse the polymerization of four molecules of porphobilinogen (PBG) to give a chain of six pyrrole residues in which the dipyrromethane cofactor is linked to four substrate molecules in the form of a hexapyrrole. The addition of the four porphobilinogen molecules occur in a stepwise mechanism via the enzyme intermediate complexes ES, ES₂, ES₃ and ES₄. Finally, the unstable tetrapyrrole product, preuroporphyrinogen is released from the hexapyrrole by hy-

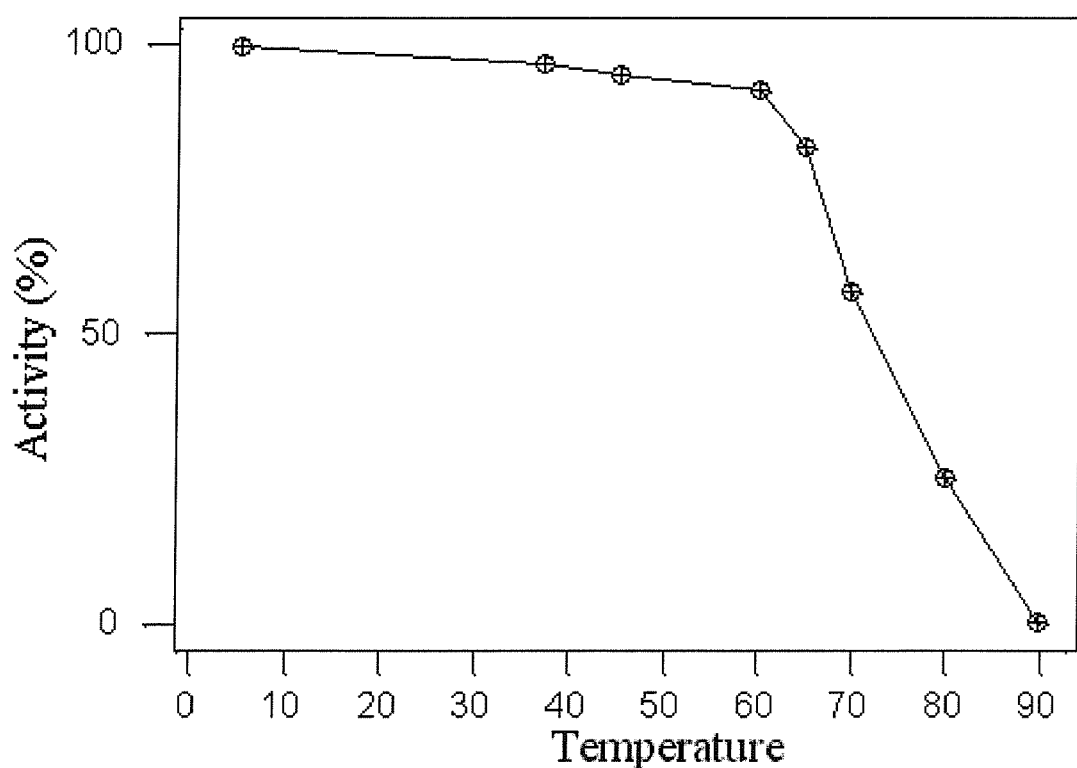


Figure 3.44: **Effect of thermal denaturation on the recombinant human ubiquitous porphobilinogen deaminase Arg 167 Gln mutant activity.** Arg 167 Gln mutant was preincubated for 10min. at a variety of temperatures and the effect on activity determined, as described in section 2.3.1.

drolysis regenerating the dipyrromethane cofactor (Jordan and Warren, 1987; Hart *et al.*, 1987)

ES complexes of the human deaminase Arg 167 Gln and Arg 167 Trp mutants were generated by incubating the enzymes with 10 moles equivalents of porphobilinogen (1:10). The ES complexes thus formed were compared to those from the native enzyme in terms of their stability and other properties. The enzymes and their substrate complexes were detected by separation using non-denaturing gel electrophoresis and the bands were visualized by staining with Coomassie Brilliant Blue. The ES complexes migrate through non-denaturing gels with different mobilities depending on the number of the negative charges which build up. Therefore as additional acetate and propionate groups of the bound substrates are added to the enzyme, intermediates ES, ES₂, ES₃ and ES₄ are formed, each with a higher negative charge and higher mobility on the gel. The formation of ES complexes is accompanied by a decrease in the intensity of the enzyme band.

In this analysis the heat treatment was used to investigate the stability of the ES complexes formed by the Arg 167 Gln and Arg 167 Trp mutants compared to the native enzyme. The enzyme intermediate complexes of the native enzyme are quite stable at 4°C but unstable at 37°C or higher. From figure 3.45 it can be seen that the ES complexes produced by the Arg 167 Gln mutant were very stable, unlike those of the native enzyme shown in figure 3.46. Similarly, the enzyme intermediate complexes formed by Arg 167 Trp are more stable than the native enzyme (figure 3.47) but less stable than those of the Arg 167 Gln mutant, as they disappear when incubated at 37°C for 30min. or more. The bands of the free Arg 167 Trp mutant enzyme, without substrate bound, also disappear with time unlike those of the native enzyme or the Arg 167 Gln mutant suggesting the Arg 167 Trp mutant is less thermally stable than the Arg 167 Gln mutant.

Hydroxylamine (NH₂OH) is an analogue of NH₃ and reacts with ES complexes to release pyrrole units as hydroxylamine-derivatives of porphobilinogen in the reverse of

the forward catalytic reaction. ES complexes of the native deaminase are converted back to free enzyme with hydroxylamine. When ES complexes of the Arg 167 Gln mutant were incubated with hydroxylamine, no release of bound intermediates occurred (figure 3.45 tracks 10 and 11 and figure 3.48) whereas the free native enzyme is regenerated more rapidly (figures 3.49 and 3.48). There was no significant difference between the effects of hydroxylamine treatments at 25°C or at 37°C.

Both Arg 167 Gln and Arg 167 Trp mutants migrated with a slightly higher mobility than the native enzyme, consistent with the replacement of the positively charged arginine 167 with a neutral glutamine or tryptophan amino acids. The experiments with porphobilinogen indicate that the mutant enzymes work at a slower rate than the native enzyme although they both form enzyme intermediate complexes with substrate.

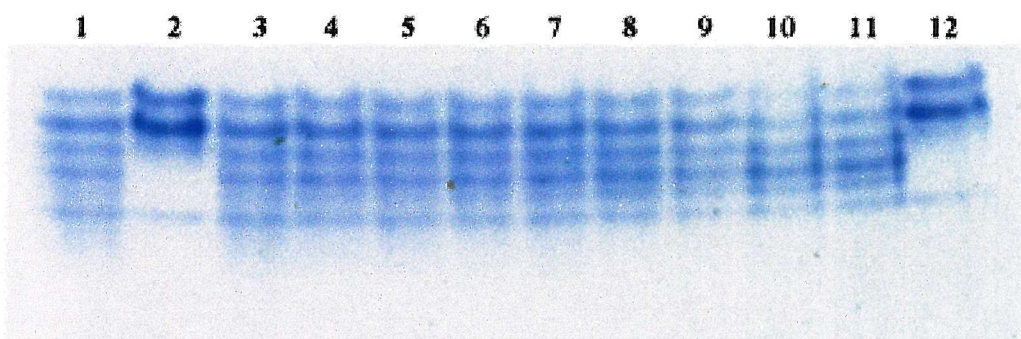


Figure 3.45: Non-denaturing PAGE analysis showing the production of ES complexes by the ubiquitous porphobilinogen deaminase Arg 167 Gln mutant and their stability. Tracks 1 and 3, Arg 167 Gln mutant + 10 mole equivalents of PBG after 60min. at 37°C in 20mM Tris/HCl buffer, pH 8.2; track 2, control, Arg 167 Gln mutant (enzyme only); tracks 4 and 5, Arg 167 Gln mutant + PBG after 30min.; tracks 6 and 7, Arg 167 Gln mutant + PBG after 3min.; tracks 8 and 9, Arg 167 Gln mutant + PBG after 30sec.; track 10, sample from track 4 + 77mM hydroxylamine, incubated for 30min.; track 11, sample from track 5 + 333mM hydroxylamine, incubated for 30min.; track 12, control, Arg 167 Gln mutant.

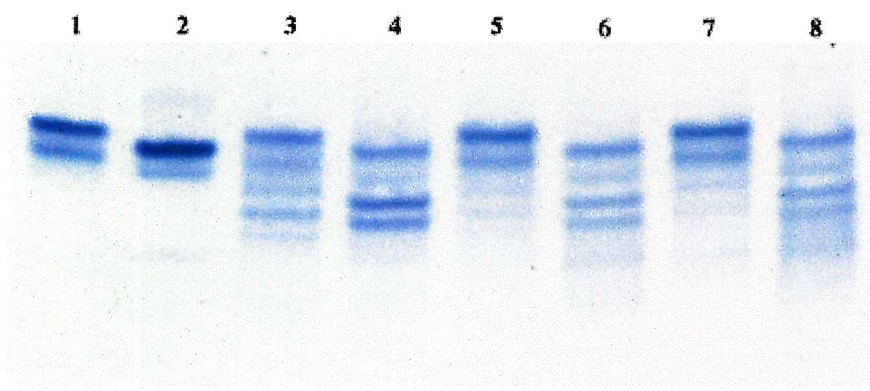


Figure 3.46: Non-denaturing PAGE analysis showing the stability of the ES complexes produced by the ubiquitous porphobilinogen deaminase Arg 167 Gln mutant compared to those produced by the native enzyme when incubated with PBG. Enzyme was incubated with 10mole equivalents of PBG for 5min. at 37°C in 20mM Tris/HCl buffer, pH 8, then heat-treated at 37°C for one hour or two hours. Track 1, native enzyme; track 2, Arg 167 Gln mutant enzyme; track 3, native enzyme + PBG; track 4, Arg 167 Gln mutant + PBG; track 5, sample as in track 3 but heat-treated at 37°C for 1 hour; track 6, sample as in track 4 but heat-treated at 37°C for 1 hour; track 7, sample as in track 3 but heat-treated at 37°C for 2 hours; track 8, sample as in track 4 but heat-treated at 37°C for 2 hours.

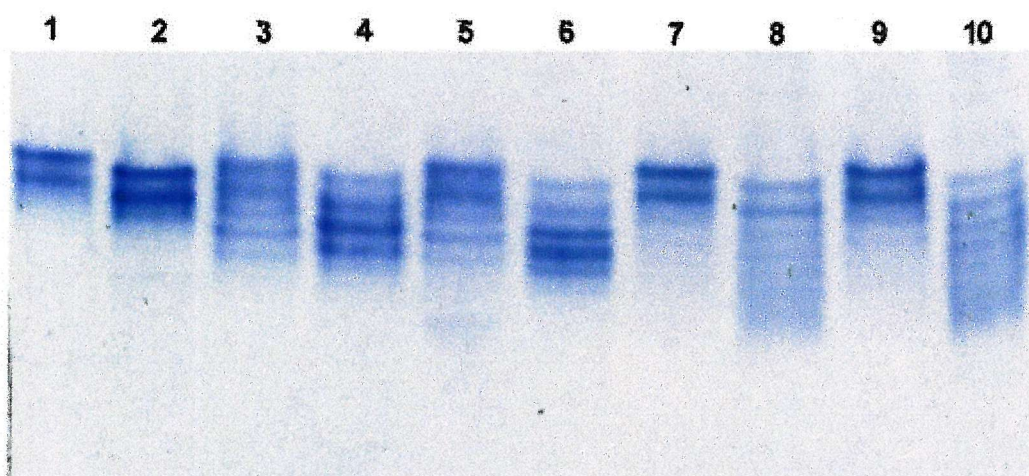


Figure 3.47: Non-denaturing PAGE analysis showing the production of ES complexes by ubiquitous porphobilinogen deaminase native enzyme and Arg 167 Trp mutant and their stability. Track 1, native enzyme as control at 37°C in 20mM Tris/HCl buffer, pH 8.2; track 2, Arg 167 Trp mutant as control; track 3, native enzyme + 10 mole equivalents of PBG after 3sec. ; track 4, Arg 167 Trp mutant + 10 mole equivalents of PBG after 3sec.; track 5, native enzyme + PBG after 3min.; track 6, Arg 167 Trp mutant + PBG after 3min.; track 7 , native enzyme + PBG after 30min.; track 8; Arg 167 Trp mutant + PBG after 30min.; track 9, native enzyme + PBG after 1 hour; track 10, Arg 167 Trp mutant + PBG after one hour.

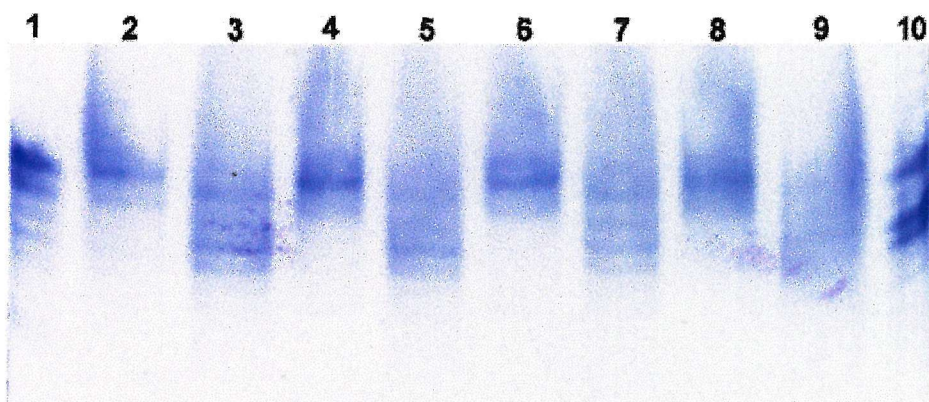


Figure 3.48: **Non-denaturing PAGE analysis showing the effect of hydroxylamine on the ES complexes from both the native enzyme and the ubiquitous porphobilinogen deaminase Arg 167 Gln mutant at two different temperatures.** The native protein and the Arg 167 Gln mutant were incubated with 10 mole equivalents of PBG for 5min. at 37°C in 20mM Tris/HCl buffer, pH 8, then treated with hydroxylamine. Track 1, native enzyme + PBG; track 2, native enzyme + PBG + 2M hydroxylamine, incubated at 25°C for 30min.; track 3, Arg 167 Gln mutant enzyme + PBG + 2M hydroxylamine, incubated at 25°C for 30min.; track 4, native enzyme + PBG + 2M hydroxylamine, incubated at 25°C for 3 hours; track 5, Arg 167 Gln mutant enzyme + PBG + 2M hydroxylamine, incubated at 25°C for 3 hours; tracks 6, 7, 8 and 9, as tracks 2, 3, 4 and 5, respectively, but at 37°C; lane 10, Arg 167 Gln mutant + PBG. There was no difference between the results at the two temperatures.

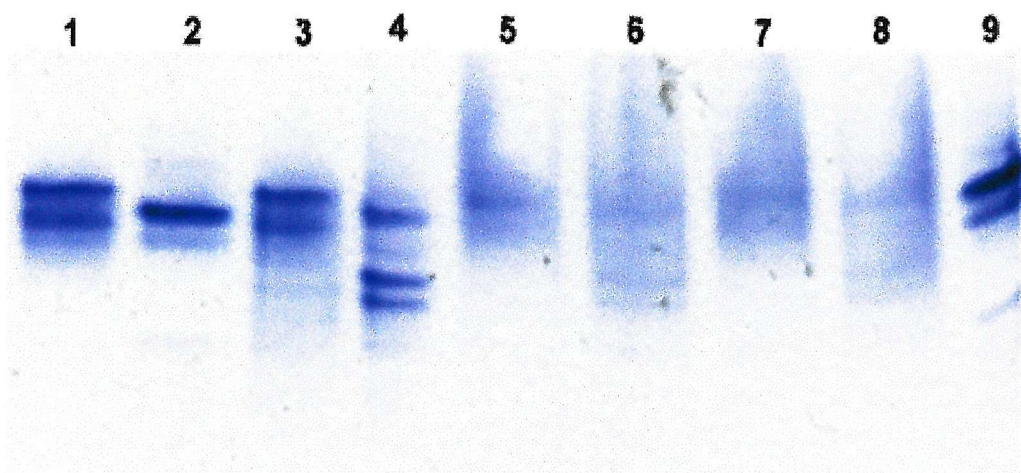


Figure 3.49: Non-denaturing PAGE analysis showing the production of ES complexes by the native ubiquitous porphobilinogen deaminase and Arg 167 Gln mutant and their stability using hydroxylamine. The native protein and the Arg 167 Gln mutant were incubated with 10 mole equivalents of PBG for 5min. at 37°C in 20mM Tris/HCl buffer, pH 8, then treated with hydroxylamine. Track 1, native enzyme; track 2, Arg 167 Gln mutant; track 3, native enzyme + PBG; track 4, Arg 167 Gln mutant + PBG; track 5, sample as in track 3 + 2M hydroxylamine, incubated for 30min. at 37°C; track 6, sample as in track 4 + 2M hydroxylamine, incubated for 30min. at 37°C; track 7, sample as in track 3 + 2M hydroxylamine, incubated for 60min. at 37°C; track 8, sample as in track 4 + 2M hydroxylamine, incubated for 60min. at 37°C; track 9, Arg 167 Gln mutant. Each sample contained 10 μ g of protein.

3.3 Discussion and conclusions

Recombinant native human ubiquitous porphobilinogen deaminase and two mutants that cause acute intermittent porphyria, Arg 167 Gln and Arg 167 Trp, have been expressed in *E. coli*. Assays for enzyme activity in crude extracts indicated that the mutant enzymes had less than 10% of the activity of the native enzyme. The mutant enzymes were purified to at least 90% homogeneity as shown in figures 3.9 and 3.11, using essentially the same protocol as used for the native enzyme. Since the purification method involves heat treatment at 60°C for 10 minutes, it is concluded that the mutant proteins had folded normally and were as stable as the native human ubiquitous deaminase. Detailed studies on the thermostability of the Arg 167 Gln mutant revealed that it has similar thermal properties to the native enzyme, that is stable at 60°C for several minute but is denatured at 80°C or higher, see figure 3.44. During the purification of the Arg 167 Gln mutant, isocratic elution from DEAE Sephacel yielded three protein peaks, as shown in figure 3.12, like the native enzyme. The first protein peak represents the active enzyme and gives a single band on SDS-PAGE. The second protein fraction contained a contaminant of M_r approximately 21,000 and the third fraction contained a contaminant of approximately 28,000, as shown in figure 3.14. Individual fractions from each peak were concentrated and separately passed through a Superdex G-75 gel filtration column using the f.p.l.c. system. The first contaminant of 21,000 cannot be separated from the deaminase while the 28,000 contaminant can be separated partially from the deaminase, as shown in figures 3.13 and 3.14. The two contaminants, especially the one of approximately 21,000, copurified with the Arg 167 Gln mutant and cannot be separated completely from it, even by using 300mM NaCl in 100mM Tris/HCl buffer, pH 7.5.

The other ubiquitous porphobilinogen deaminase mutant, Arg 167 Trp, was also purified by isocratic elution from DEAE-Sephacel. The first protein peak yielded fractions with small amounts of protein and almost no deaminase activity and were discarded. The second peak contained the majority of the Arg 167 Trp mutant with

a maximum protein concentration and maximum activity, see table 3.6. The protein peak coincided with the peak of deaminase activity. All the fractions contained a band at approximately 45,000 on SDS-PAGE, representing the purified Arg 167 Trp mutant. The 21,000 contaminant was also present with the Arg 167 Trp mutant. The ratio between this contaminant and the Arg 167 Trp protein was lower in the middle fractions. As a result the middle fractions were pooled, concentrated and desalted to study the properties.

It has also been shown in this chapter that the pH optimum of Arg 167 Gln and Arg 167 Trp mutants is pH 6.8 using potassium phosphate buffer. In Tris/HCl buffer, at this pH, the activity was reduced dramatically. The activity rises from pH 6.8 using Tris/HCl buffer to peak at approximately pH 7.5 in case of the Arg 167 Gln mutant and at pH 8 in case of Arg 167 Trp mutant. Using CAPS buffer, the activity increases to a peak at pH 9 in the case of the Arg 167 Gln mutant, and decreases in the case of the Arg 167 Trp mutant. As mentioned previously the positive charge of arginine 167 is thought to play an important role in destabilizing the salt bridge between the negatively charged acetate side chain and the protonated aminomethyl side chain of the porphobilinogen molecule (Jordan, 1994a). The lower pH buffers could substitute for the positive charge of the mutated arginine in the destabilization mechanism. The lower pH optimum for the Arg 167 mutant has been noted previously (Delfau *et al.*, 1990) and is also evident in the analogous mutation Arg 149 His in the *E. coli* enzyme (Jordan and Woodcock, 1991).

The purified Arg 167 Gln and Arg 167 Trp mutants exhibited 8.6% and 8.9% of the specific activity of the native enzyme at pH 8.2, respectively. The K_m value of the Arg 167 Gln mutant, measured at the pH optimum of the native enzyme, was found to be $368\mu M$, using an Eadie-Hofstee plot, however, the K_m value for the Arg 167 Trp mutant was measured at pH 6.8, as $333\mu M$, instead of at the pH optimum of the native enzyme. As mentioned in section 3.2.8, the kinetic data obtained for the Arg 167 Trp mutant at pH 8.2 led to a positive correlation for the rate divided by

rate/substrate concentration. On the other hand, the data obtained from the enzyme assays at pH 6.8 gave a negative correlation for the rate divided by rate/substrate concentration. Possibly, the reason for this is due to the instability of the Arg 167 Trp mutant enzyme compared to the native human deaminase. It was noted that the Arg 167 Trp mutant enzyme is inactivated slowly at 37°C (figure 3.47) and may be increasingly stabilised by the increasing porphobilinogen concentrations used in the assays for the kinetic determinations.

Mass spectrometry was used to determine the M_r values for the Arg 167 Gln and Arg 167 Trp mutants. The predicted value for the native ubiquitous enzyme is 39,749. The M_r of the Arg 167 Gln mutant was 39,592, as shown in figure 3.30 within the range expected (39,590) for the substitution of an arginine residue by glutamine and minus the mass of the *N*-terminal methionine residue as confirmed by *N*-terminal sequencing. The difference between arginine and glutamine is 28 and the molecular weight of methionine when attached to the protein is 131.21. The M_r of the Arg 167 Trp mutant was 39,652, as shown in figure 3.31, within the range expected (39,648) for the substitution of an arginine residue by tryptophan and minus the mass of one methionine residue. The difference between tryptophan and arginine is 30.

Although the purified native human ubiquitous and erythroid porphobilinogen deaminases and the Arg 167 Gln and Arg 167 Trp mutants all displayed a single band around 45,000 when analyzed by SDS-PAGE, they all showed double bands when analyzed by non-denaturing gel electrophoresis. The double bands of the native and Arg 167 Gln human ubiquitous porphobilinogen deaminases were separated by Mono Q anion exchange chromatography and studied individually in an attempt to ascertain their nature and origin. Heat treatment of crude extracts had no effect on the ratio of the two bands and heat treatment of either purified band at 37°C did not generate the other band. Both bands behaved in the same way when they were treated with PBG, both forming a similar set of ES complexes, as shown in figure 3.26. These results suggest that the two deaminase species are generated early

in the expression of the enzyme, possibly due to the deamidation of an asparagine residue to aspartate or the deamidation of a glutamine to glutamate. Alternatively the double bands could arise from mistranslation of the human cDNA by the *E. coli* ribosome. This would result in the gain of a net negative charge as suggested by the band separation on the non-denaturing gels. The mass difference between the two species, as shown by LCT nanoflow time of flight mass spectrometric analysis are essentially identical within the error of the instrument suggesting they may represent amidated and deamidated species. The double bands from the native enzyme have the same intensity while the less negative band of the Arg 167 Gln mutant has more intensity than the more negative band. The reason for this difference in the intensity is not clear. The Arg 167 Gln and Arg 167 Trp mutant bands migrate further than the native enzyme bands, as expected due to the conversion of a positively charged residue to the neutral residues glutamine and tryptophan.

Using vertical isoelectric focussing (IEF) analysis, the small charge difference between the two human ubiquitous protein species and their isoelectric points have also been detected (figure 3.40). The first deaminase peak to elute from the Mono Q ion exchange column had a pI around 6.1 and a faint band at 5.95, while the second protein peak showed a major band at a pI of 5.95 with a faint band at 6.1 suggesting that each species was slightly contaminated with the other. Comparison of the ubiquitous porphobilinogen deaminases with the erythroid enzyme (from Sweden) showed an interesting difference, the erythroid enzyme showing four bands, the major species having a pI of around 6.25, substantially higher than the two bands of the ubiquitous enzyme. The other bands from the erythroid enzyme had lower pIs, two of which coincided surprisingly with the two bands of the ubiquitous enzyme. The difference in pI between the two human isozymes is due to the extra 17 amino acid residues in *N*-terminal extension of the ubiquitous enzyme. Within these 17 amino acids there are three charged amino acids, two glutamates and one lysine. The additional negatively charged glutamates must play a major role in the pI difference between the human ubiquitous and erythroid enzymes.

IEF studies with human ubiquitous porphobilinogen deaminase Arg 167 Gln and Arg 167 Trp mutants revealed important information about the molecular consequences of the human mutations (figure 3.41). Both mutants exhibit four main bands where the pI values range from 5.4-6.0, lower than the native human deaminase because of the loss of the arginine 167 positive charge. The most negative band is probably due to an ES complex. The Arg 167 Trp mutant forms four bands with those of higher pI being similar to those for Arg 167 Gln with pI values ranging from 5.6-6.0, two of which are strong bands. The fourth band at pI 4.5 could be a contaminant. The small difference between the Arg 167 Gln and Arg 167 Trp mutants may be due to small differences in conformation caused by the mutation.

The Arg 149 Gln and Arg 173 Gln mutants (see chapter 4) were also analysed at the same time as the Arg 167 mutants, migrating between pI 6.5 and 6.8 confirming that they both exist as apo-enzymes. There is a trace of a band close to that expected for ES_2 suggesting that a small amount of this mutant may have bound a small amount of the cofactor covalently. A detailed discussion of Arg 173 Gln and Arg 149 Gln mutants is presented in chapter 4.

Because of the stepwise addition of negatively charged porphobilinogen molecules to the deaminase during the catalytic cycle, a great deal of information about the function of the enzyme can be obtained from investigations with non-denaturing gel electrophoresis. The native ubiquitous deaminase, as discussed above exhibits two protein bands but, on addition of porphobilinogen, five bands are evident due to the formation of ES, ES_2 and ES_3 by each species. The additional bands form rapidly after the incubation with porphobilinogen for 3sec. Within 3min. or more, the two bands of the free enzyme reappear, indicating that the majority of the substrate has been used up and very few molecules of the enzyme still carry the substrate. In contrast, the two bands of the Arg 167 Gln mutant are transformed into up to six bands in the presence of porphobilinogen, with the third and fourth bands being the most intense. These represent ES_2 for each of the two protein species. This is evident

since the ES complexes formed by the Arg 167 Gln mutant have the same distribution as the ES complexes formed by the double bands, after separation from each other and reaction with porphobilinogen separately. What is particularly notable is that the bands that represent the ES complexes of Arg 167 Gln are very stable and remain largely unchanged even after incubation for two hours at 37°C. Furthermore, the ES complexes from this mutant are largely resistant to incubation with hydroxylamine (NH₂OH), an ammonia analogue that releases pyrrole units from the ES complexes of the native enzyme. The Arg 167 Gln mutant thus represents a good model for investigating the polymerisation mechanism by X-ray crystallography, since each stage of the catalytic cycle is slowed down and it may therefore be possible to isolate the individual ES complexes for detailed crystallographic study.

Like the Arg 167 Gln mutant, the purified Arg 167 Trp mutant also exists as two protein bands on non-denaturing gel electrophoresis. On addition of porphobilinogen, up to seven bands appear, the darkest being the third fourth and fifth bands, suggesting that both ES₂, ES₃ and possibly ES₄ intermediates are stabilised by this mutation. Although the ES complexes of the Arg 167 Trp mutant are as stable as the equivalent complexes for the Arg 167 Gln mutant, prolonged incubation led to the disappearance of all the bands indicating that the Arg 167 Trp mutant was less thermally stable than the Arg 167 Gln mutant.

In addition the Arg 167 Trp mutant is slightly less thermostable than the Arg 167 Gln mutant. The accumulation of ES complexes was observed previously and has been used to explain the raised CRIM +ve found in patients with this mutation. Presumably the conformational changes that accompany the formation of ES complexes lead to molecular species with higher affinity for the deaminase antibodies used for the analysis.

The enzyme resulting from the Arg 167 Trp mutation is partially active *in vitro* although the *in vivo* activity still remains to be determined. The fact that some activity is present in both Arg 167 mutant enzymes presumably allows pairing with

more severe deaminase mutations in the form of compound heterozygote patients (Elder, 1997; Llewellyn *et al.*, 1992) indicating that sufficient deaminase activity must be present *in vivo* to fulfill the background requirements for haem biosynthesis.

Chapter 4

Studies on the recombinant human ubiquitous porphobilinogen deaminase Arg 173 Gln, Arg 149 Gln and Trp 198 Ter mutants

4.1 Introduction

The previous chapter discusses the mutations Arg 167 Gln and Arg 167 Trp that affect an essential active site arginine residue involved in substrate and cofactor binding. Close examination of the three-dimensional structure of the *E. coli* porphobilinogen deaminase model shows, however, that there are five other highly conserved active site arginine residues, at positions 26, 149, 150, 173 and 195. These are equivalent to arginines at positions 11, 131, 132, 155 and 176 in *E. coli* deaminase, respectively. Of these, human mutations affecting Arg 26, Arg 149 and Arg 173 are known.

Arg 26 His was first described in a case of acute intermittent porphyria by the

Elder group (Llewellyn *et al.*, 1993). From studies with the *E. coli* deaminase mutants (Jordan and Woodcock, 1991; Lander *et al.*, 1991) this arginine residue (position 11 in *E. coli* deaminase) is located in the active site and is essential for substrate binding. Its mutation to any other amino acid would result in a completely inactive enzyme. This mutation is particularly interesting since it has been found in a rare compound heterozygote form (Elder, 1997). Compatibility with life depends on a leaky mutation in the other allele that can contribute a low level of deaminase activity. Patients with both alleles affected in this way are severely affected with diminished stature and severely impaired development of the central nervous system.

Arginine 149, encoded within exon 9, is also located within the active site cavity. The side chain of this arginine interacts with the C1 ring of the dipyrromethane cofactor (Louie *et al.*, 1992; Wood *et al.*, 1995). Two mutations involving arginine 149 have been described. These include Arg 149 Gln (Delfau *et al.*, 1991) caused by the mutation of 446 G → A and 447 A → G and Arg 149 Leu caused by the mutation of 446 G → T (Gu *et al.*, 1994). Both of these arginine 149 mutations appear to be severe with a CRIM-ve profile (Wood *et al.*, 1995). Patients were diagnosed on the basis of typical clinical symptoms accompanied by an increased urinary excretion of porphobilinogen and 5-aminolaevulinic acid but normal faecal porphyrin excretion. Diminished levels of porphobilinogen deaminase activity was observed in the erythrocytes of all patients (Delfau *et al.*, 1991). Mutations at the equivalent position, Arg 131, in the *E. coli* deaminase, either to histidine or leucine, lead to completely inactive and unstable apo-enzymes (Jordan and Woodcock, 1991; Lander *et al.*, 1991).

Mutations of arginine 173, encoded in exon 10, have been described by several laboratories and include Arg 173 Gln and Arg 173 Trp. Arg 173 Gln is caused by the mutation of 518 G → A (Delfau *et al.*, 1990; Ong *et al.*, 1997) and Arg 173 Trp by the mutation of 517 C → T (Lee and Anvret, 1991; Andersson *et al.*, 2000). Arginine 173 is also located in the active site cavity with its side chain interacting with the

propionic acid side chain of the C1 cofactor ring and with the acetic acid side chain of the substrate, porphobilinogen. The Arg 173 Trp mutation is found in two Swedish CRIM-ve families whereas the mutation Arg 173 Gln has been reported in French and Finnish CRIM+ve patients (Lundin *et al.*, 1997). Mutations at the equivalent position, Arg 155, in the *E. coli* deaminase, either to histidine or leucine, lead to enzymes with extremely low activity in which substrate binding is severely affected (Lander *et al.*, 1991; Jordan and Woodcock, 1991).

One other human porphobilinogen deaminase mutation investigated in this chapter is Trp 198 Ter. This is the most common mutation in Sweden, accounting for more than half of the cases in that country. It involves the change of 593 G → A leading to the formation of a stop codon (Lee and Anvret, 1991). The mutation has been traced to a founder effect in the north part of the country. This mutation results in a deaminase protein that is lacking part of domain 1 and all of domain 3, including the cofactor attachment site. Patients carrying this defect had the CRIM-ve phenotype (Lee and Anvret, 1991).

In this chapter the mutations Arg 173 Gln, Arg 149 Gln and Trp 198 Ter have been constructed from the cDNA specifying the ubiquitous human porphobilinogen deaminase. The proteins have been purified and their properties have been investigated, particularly with respect to enzyme activity, temperature stability and ability to assemble the dipyrromethane cofactor.

4.2 Results

4.2.1 Site directed mutagenesis of cDNA specifying human ubiquitous porphobilinogen deaminase by PCR

The generation of the Arg 173 Gln and Arg 149 Gln mutations in human ubiquitous porphobilinogen deaminase was carried out in conjunction with Dr. Sarwar (this laboratory) using native cDNA kindly provided by Bernard Grandchamp, Paris. Both mutants were generated by PCR according to the general method described in section 2.2.3 using oligonucleotide primers prepared by Oswel (Southampton), see table 4.1. Arginine 173 (arginine 155 in *E. coli*) was mutated to glutamine by the change of one base in the arginine codon CGG → CAG. Arginine 149 (arginine 131 in *E. coli*) was mutated to glutamine by the change of two base in the arginine codon, CGA → CAG. Agarose gel analysis of products from the first and second PCR mutagenesis reactions used to generate the Arg 173 Gln and Arg 149 Gln mutations are shown in figures 4.1 a and b and 4.2 a and b, respectively. The required bands were excised from the gels that contain the PCR2 products for treatment with Geneclean, as described in section 2.2.2. A similar procedure was used to generate the Trp 198 Ter mutant (TGG → TAG) by Dr. Sarwar, in this laboratory.

4.2.2 Digestion of the mutagenic DNA fragments and ligation into the pT7-7 plasmid

The mutated ubiquitous human porphobilinogen deaminase cDNAs resulting from PCR2 were digested with *Bam*HI and *Nde*I restriction enzymes before ligation into the pT7-7 vector that had been digested with the same enzymes and treated with Geneclean. The protocols of digestion and ligation that are used in this project are described in sections 2.2.4 and 2.2.5, respectively. A similar procedure was used for

The sequence of Arg 173 Gln primers:

The sense strand (non-coding):

5' GAAACCTAACACCC**A**GCTTCGGAAGCTG 3'

The antisense strand (coding):

5' CAGCTTCCGAAG**C**TGGGTGTTGAGGTTTC 3'

The sequence of Arg 149 Gln mutant primers:

The sense strand (non-coding):

5' CCAGCTCC**C**TGC**A**GAGAGCAGCCCAGC 3'

The antisense strand (coding):

5' GCTGGG**C**TGCT**C**TGCAGGGAGCTGG 3'

The sequence of Trp 198 Ter mutant primers:

The sense strand (non-coding):

5' GCAGCG**C**ATGGG**C**TAGCACAACCGGGTG 3'

The antisense strand (coding):

5' CACCCGGTT**T**G**C**TAGGCCATGCGCTGC 3'

Table 4.1: **The sequence of the mutagenic oligonucleotide primers of Arg 173 Gln, Arg 149 Gln and Trp 198 Ter.** The sense primers of the Arg 173 Gln, Arg 149 Gln and Trp 198 Ter are generated by the mutation (CGG → CAG), (CGA → CAG) and (TGG → TAG) respectively. The antisense primers for Arg 173 Gln, Arg 149 Gln and Trp 198 Ter are generated by the mutation (GCC → GTC), (GCT → GTC) and (ACC → ATC) respectively. All the mutated codons are in bold.

the Trp 198 Ter mutant. After this stage, the plasmid DNA from the ligation was transformed into *E. coli* strain DH5 α as follows.

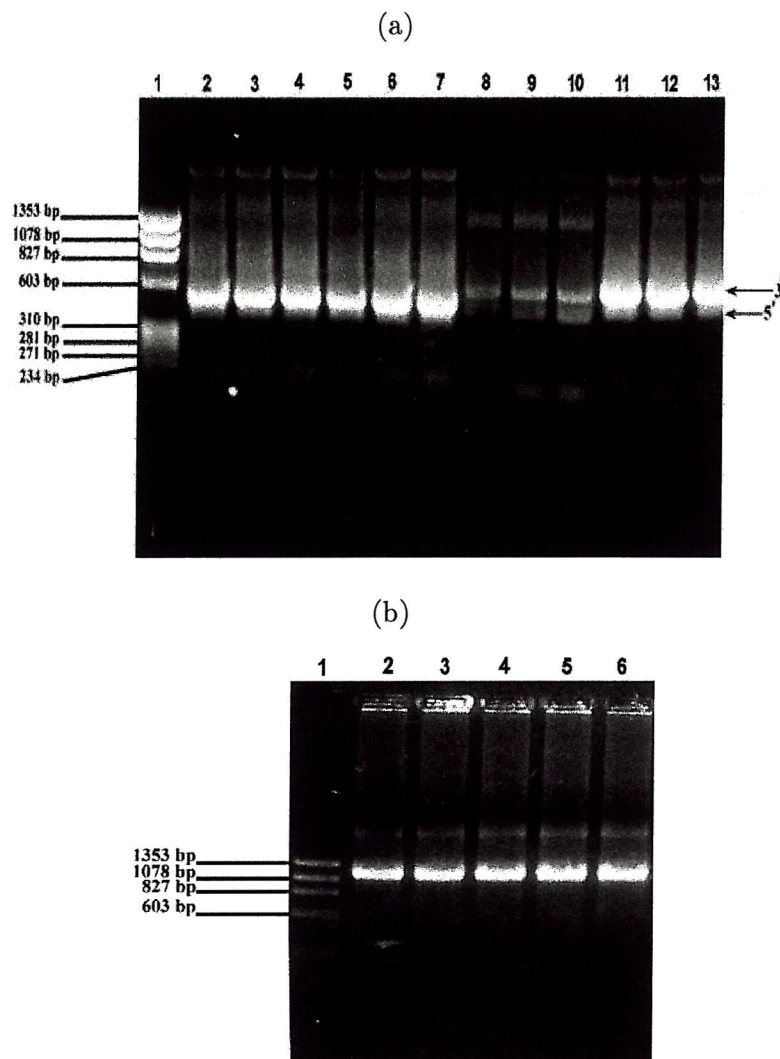


Figure 4.1: Agarose gel analysis of the PCR products formed from cDNA specifying ubiquitous human porphobilinogen deaminase to generate the Arg 173 Gln mutant: a) The first PCR reaction yields two overlapping DNA fragments specifying ubiquitous human porphobilinogen deaminase to generate the Arg 173 Gln mutant. Track 1 represents the DNA marker, ϕ X174, restricted with *Hae*III, tracks 2, 3, 4, 5, 6 and 7 show the 5' end of the cDNA; tracks 8, 9, 10, 11, 12 and 13, represent the 3' end of the cDNA. In gel (b) the second PCR reaction combines the two fragments to yield a DNA fragment (1.14kb) harbouring the desired mutated codon. Track 1 represents the DNA marker, ϕ X174 restricted with *Hae*III; tracks 2, 3, 4, 5 and 6, represent the the full cDNA.

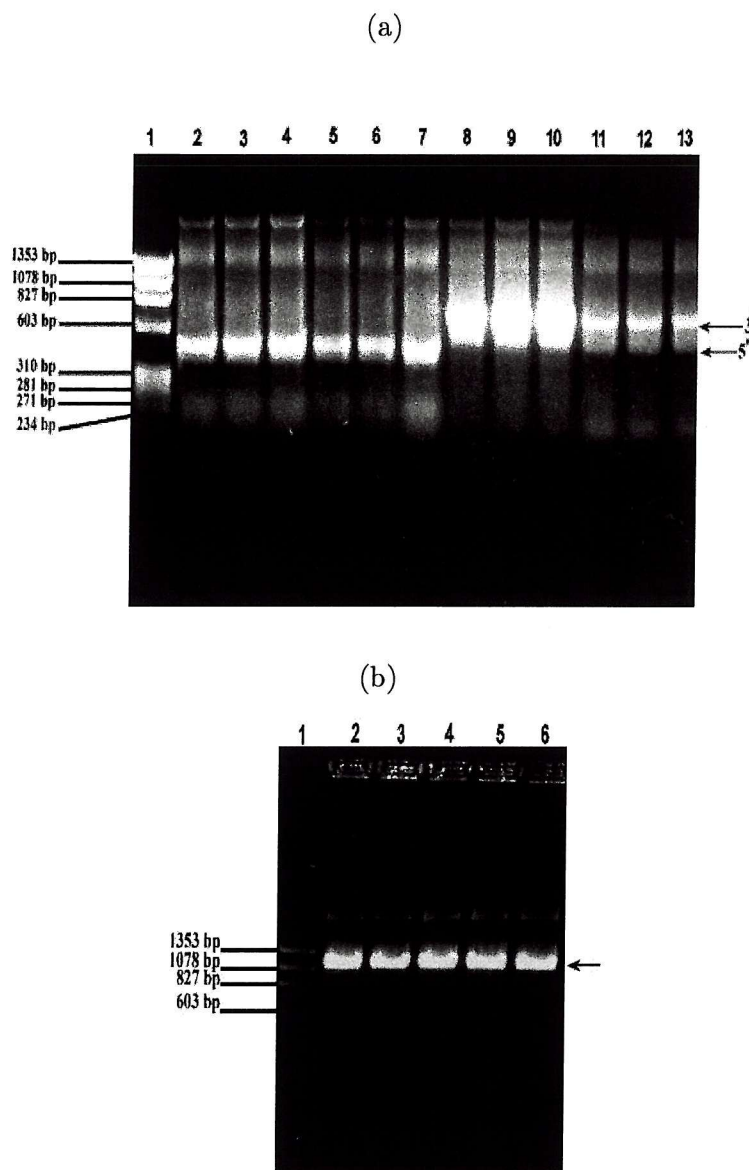


Figure 4.2: Agarose gel analysis of the PCR products formed from cDNA specifying ubiquitous human porphobilinogen deaminase to generate the Arg 149 Gln mutant: a) The first PCR reaction yields two overlapping DNA fragments specifying ubiquitous human porphobilinogen deaminase to generate the Arg 149 Gln mutant. Track 1 represents the DNA marker, ϕ X174, restricted with *Hae*III; tracks 2, 3, 4, 5, 6 and 7 show the 5'-end of the cDNA; tracks 8, 9, 10, 11, 12 and 13 show the 3'-end of the cDNA. In gel (b) the second PCR reaction combines the two fragments to yield a DNA fragment (1.14kb) harbouring the desired mutated codon. Track 1 represents the DNA marker, ϕ X174 restricted with *Hae*III; tracks 2, 3, 4, 5 and 6, represent the full cDNA.

4.2.3 Transformation of cDNA specifying human ubiquitous porphobilinogen deaminase Arg 173 Gln and Arg 149 Gln mutants into *Escherichia coli* strain DH5 α and screening for positive mutants

The pT7-7 plasmid containing the mutated cDNAs encoding the ubiquitous human porphobilinogen deaminase, Arg 173 Gln and Arg 149 Gln mutants were all transformed into *E. coli* strain DH5 α as described in section 2.2.8. The plasmid DNAs were isolated from the bacterial strains using the Promega Wizard[®] Plus SV Minipreps DNA Purification System as described in sections 2.2.6. The plasmid DNA samples were analyzed using agarose gels, as described in section 2.2.1, to check the presence of the insert see figures 4.3 and 4.4. Finally DNA sequencing by the Oswel (Southampton) was carried out to confirm the presence of the desired mutations (see table 3.3). A similar procedure was used for the Trp 198 Ter mutant.

4.2.4 Expression and purification of recombinant human ubiquitous porphobilinogen deaminase Arg 173 Gln mutant

The ubiquitous human porphobilinogen deaminase Arg 173 Gln mutant enzyme was purified by the method described for the native and Arg 167 mutants as described in section 2.3.2 except that the heat treatment and final Superdex G-75 gel filtration steps were omitted. At each stage of the purification a sample was analysed by SDS PAGE, as shown in figure 4.5. Assay of the mutant with porphobilinogen showed a complete absence of enzyme activity. Therefore it was necessary to follow the purification by SDS PAGE.

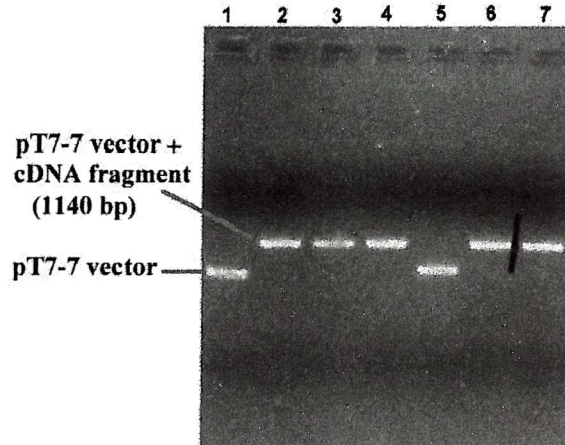


Figure 4.3: Agarose gel analysis of the DNA mini-prep to confirm the presence of the ubiquitous human porphobilinogen deaminase mutated cDNA (1.14kb) harbouring the desired mutated codon of Arg 173 Gln. Tracks 1 - 7, plasmid DNA samples isolated from the bacterial strain using the Promega Wizard[®] Plus SV Minipreps DNA Purification System. From the gel we can see clearly that the samples in tracks 2, 3, 4, 6 and 7 contain the correct DNA size which had the required insert (1.14 kb), while tracks 1 and 5 represent the vector pT7-7 only.

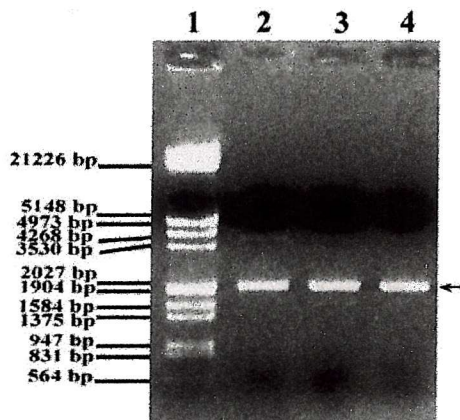


Figure 4.4: Agarose gel analysis of the DNA mini-prep to confirm the presence of the ubiquitous human porphobilinogen deaminase mutated cDNA (1.14kb) harbouring the desired mutated codon of Arg 149 Gln. Track 1, DNA marker, λDNA/EcoRI + HindIII; tracks 2, 3 and 4, plasmid DNA samples isolated from the bacterial strain using the Promega Wizard[®] Plus SV Minipreps DNA Purification System. From the gel we can see clearly that the samples in tracks 2, 3 and 4 contain the correct DNA size which had the required insert (1.14 kb).

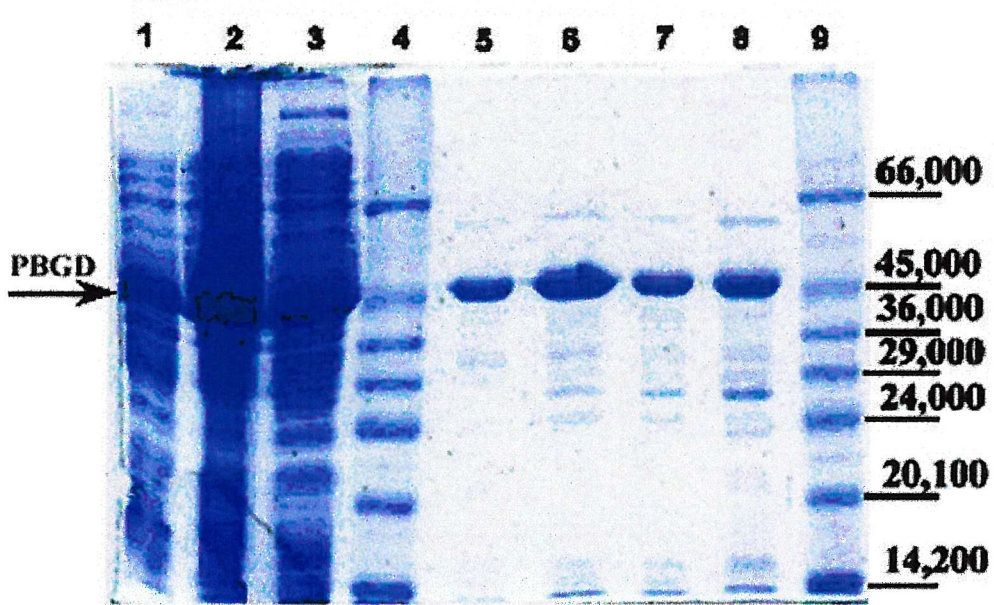


Figure 4.5: SDS-PAGE analysis to show ubiquitous human porphobilinogen deaminase Arg 173 Gln mutant at different steps of purification. Samples were submitted to 12% PAGE under denaturing conditions. Track 1, lysate from *Escherichia coli* cells expressing ubiquitous porphobilinogen deaminase Arg 173 Gln mutant; track 2, after sonication; track 3, after ultracentrifugation; track 4; molecular weight marker, Dalton VII; track 5, after DEAE Sephadex chromatography (pooled fractions from tubes 115-119); track 6, after DEAE Sephadex chromatography (pooled tubes 120 and 121); track 7, after DEAE Sephadex chromatography (pooled fractions from tubes 122-124); track 8, after DEAE Sephadex chromatography (pooled fractions from tubes 125-215); track 9, molecular weight marker, Dalton VII.

4.2.5 Expression and purification of recombinant human ubiquitous porphobilinogen deaminase Arg 149 Gln mutant

The ubiquitous human porphobilinogen deaminase Arg 149 Gln mutant enzyme, was purified as an apoenzyme to 90% purity using Mimetic Orange 1 affinity column chromatography and Superdex G-75 gel-filtration chromatography, as described in section 2.3.7. Unlike Arg 167 Gln and Arg 167 Trp mutant deaminases, the Arg 149 Gln mutant is unstable when heat-treated at 60°C, since it appears to exist as an apoenzyme, lacking the cofactor necessary to stabilize the enzyme structure. Deaminase apo-enzymes can be isolated using Mimetic Orange 1 affinity chromatography since the affinity ligand is able to bind to the dipyrromethane cofactor pocket at the active site (Shoolingin-Jordan *et al.*, 1996). Purification is accomplished by loading the Arg 149 Gln mutant cell free extract onto the Mimetic Orange 1 column immediately after centrifugation. The apo-deaminase protein was then eluted by a gradient of NaCl from 100mM - 1M in 20mM Tris/HCl, pH 7.5, containing 5mM DTT. Since the Arg 149 Gln protein was inactive, fractions from the column were examined immediately by SDS-PAGE in 12% acrylamide to detect the presence of the apoenzyme, see section 2.3.1. The pooled fractions from the affinity column were then concentrated and loaded onto a Superdex G-75 gel filtration column and eluted with 100mM Tris/HCl buffer, pH 8.2, containing 5mM DTT and 100μM PMSF. The protein profile from this chromatography is shown in figure 4.6. The results of the purification steps are shown in figure 4.7.

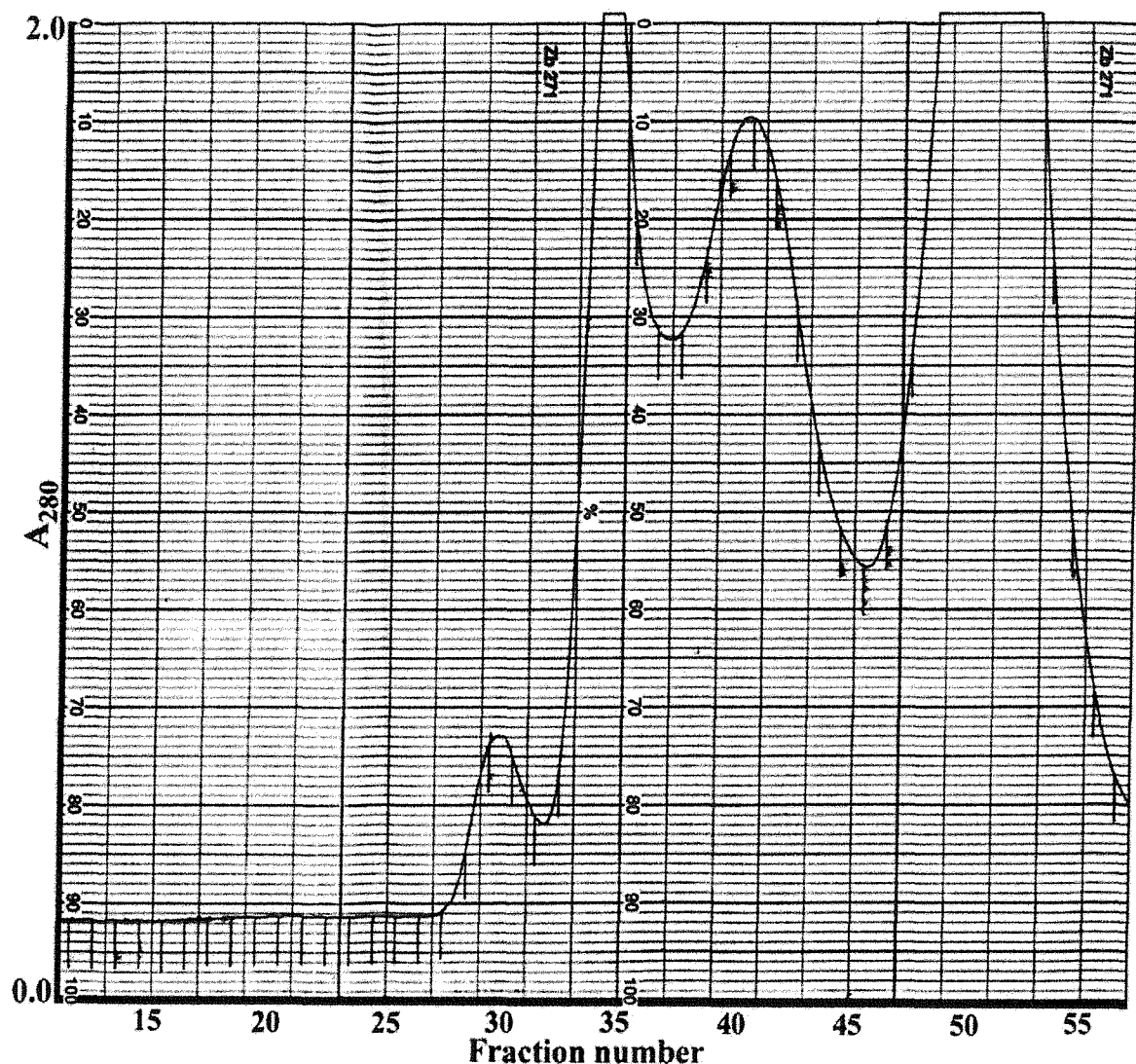


Figure 4.6: Chromatography of recombinant ubiquitous human porphobilinogen deaminase Arg 149 Gln mutant from a Superdex G-75 gel filtration column attached to a f.p.l.c. By loading the most pure fraction from the Mimetic Orange 1 column onto Superdex G-75, four peaks were eluted. The fourth peak represents the most pure fractions of the ubiquitous human porphobilinogen deaminase Arg 149 Gln mutant as proved by SDS PAGE.

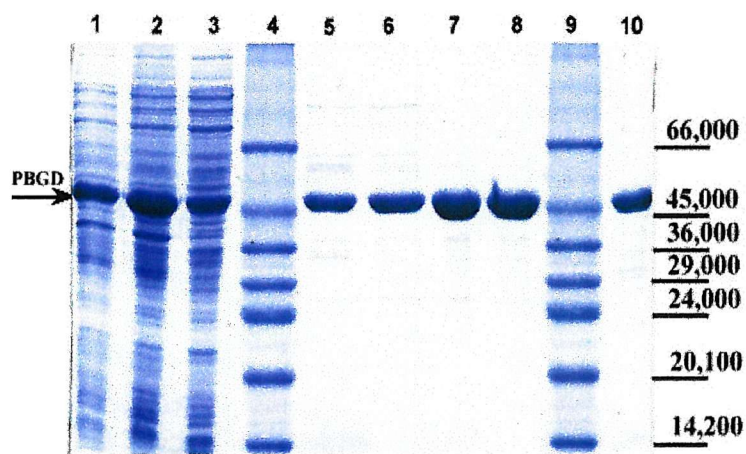


Figure 4.7: SDS-PAGE analysis to show the ubiquitous human porphobilinogen deaminase Arg 149 Gln mutant at different stages of purification. Samples were submitted to 12% PAGE under denaturing conditions. Track 1, lysate from *Escherichia coli* cells expressing ubiquitous porphobilinogen deaminase Arg 149 Gln mutant; track 2, after sonication; track 3, after ultracentrifugation; track 4, molecular weight markers, Dalton VII; track 5, after Mimetic Orange 1 affinity chromatography, tube 32; track 6, after Mimetic Orange 1 affinity chromatography, tube 34; track 7, after Superdex G-75 chromatography, tube 51; track 8, after Superdex G-75 chromatography, tube 53; track 9, molecular weight markers, Dalton VII; track 10, after Superdex G-75 chromatography, tube 55.

4.2.6 Reaction of recombinant human ubiquitous porphobilinogen deaminase Arg 173 Gln and Arg 149 Gln mutants with modified Ehrlich's reagent to check the presence of the dipyrromethane cofactor

The recombinant human ubiquitous porphobilinogen deaminase mutants were reacted with Ehrlich's reagent, as described in section 2.3.9, to investigate the presence or absence of the dipyrromethane cofactor or bound polypyrroles. Reaction of native deaminase with Ehrlich's reagent results in an initial spectral peak at 556nm that, over a period of 15 min., transforms into a new maximum at 495nm indicative of a reaction with a dipyrromethane. Tripyrroles and tetrapyrroles react so rapidly with the reagent that the spectrum seen initially has a maximum at 495nm or lower. Reactions for both Arg 173 Gln and Arg 149 Gln mutants were followed using a manual uv-vis spectrophotometer over a range of 380-650nm. Spectra were recorded immediately after the addition of Ehrlich's reagent and after reaction for 15min.

Reaction of the Arg 173 Gln mutant deaminase in cell-free extracts showed an anomalous reaction with Ehrlich's reagent, figure 4.8. This may be due to unbound polypyrrole, possibly a tetrapyrrole that forms uroporphyrin I under the acid condition of Ehrlich's reagent. However, after purification with DEAE-Sephacel, the mutant showed only a slight reaction with Ehrlich's reagent with a marginal rise in the spectrum at 490nm indicating that this mutant was largely in the form of an apo-enzyme, as shown in figures 4.9 and 4.10. The small peak at 490 is suggestive of a trace of covalently bond tetrapyrrole that survives the DEAE Sephadex chromatography. These results suggest that a small amount of abnormal holo-enzyme is formed. Interestingly, this mutant was unable to bind to Mimetic Orange 1, typical of deaminase holo-enzymes. It was possible therefore that if cofactor, or tetrapyrrole, was bound to a proportion of this mutant it was either non-covalently bound or in an abnormal or oxidised form.

Similarly, the Arg 149 Gln mutant gave no characteristic reaction with modified Ehrlich's reagent, see figure 4.11. This observation also agreed with the observation that the Arg 149 Gln mutant is able to bind to Mimetic Orange 1 consistent with the absence of the dipyrromethane cofactor and the existence of this mutant as an apo-enzyme.

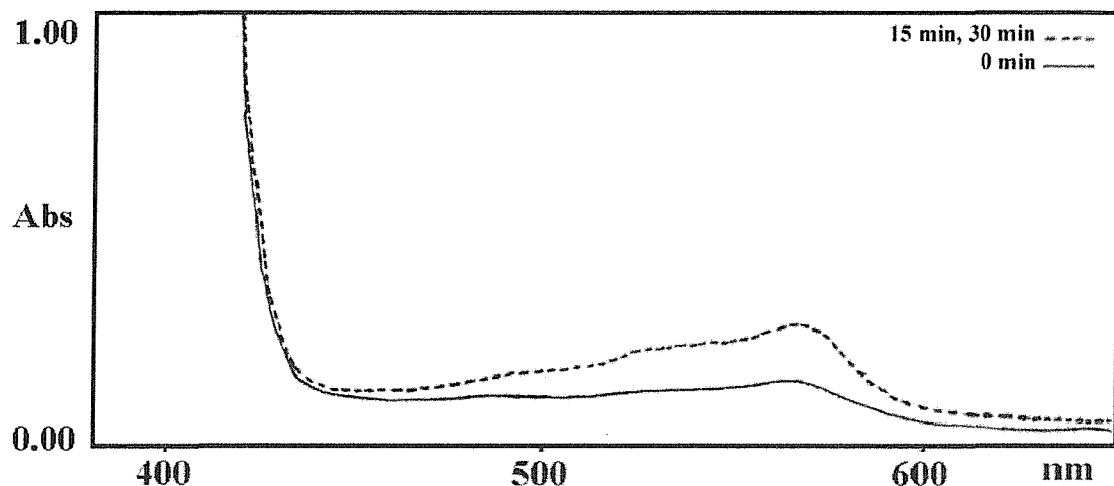


Figure 4.8: Spectra of recombinant human ubiquitous porphobilinogen deaminase Arg 173 Gln mutant after reaction with Ehrlich's reagent. The protein samples from the supernatant of the cell free crude extract after the PD-10 column. Spectra were recorded immediately after the reaction was performed using a manual uv-vis spectrophotometer over a range of 380-650nm. after 0min and 15min.

4.2.7 Attempts to reconstitute recombinant human ubiquitous porphobilinogen deaminase Arg 173 Gln and Arg 149 Gln mutant holo-enzymes from the apo-enzymes, using preuroporphyrinogen

In the above section, it was shown that the Arg 173 Gln and Arg 149 Gln mutant human ubiquitous porphobilinogen deaminases exist as apo-enzymes. It was important to establish whether the dipyrromethane cofactor had been lost from the

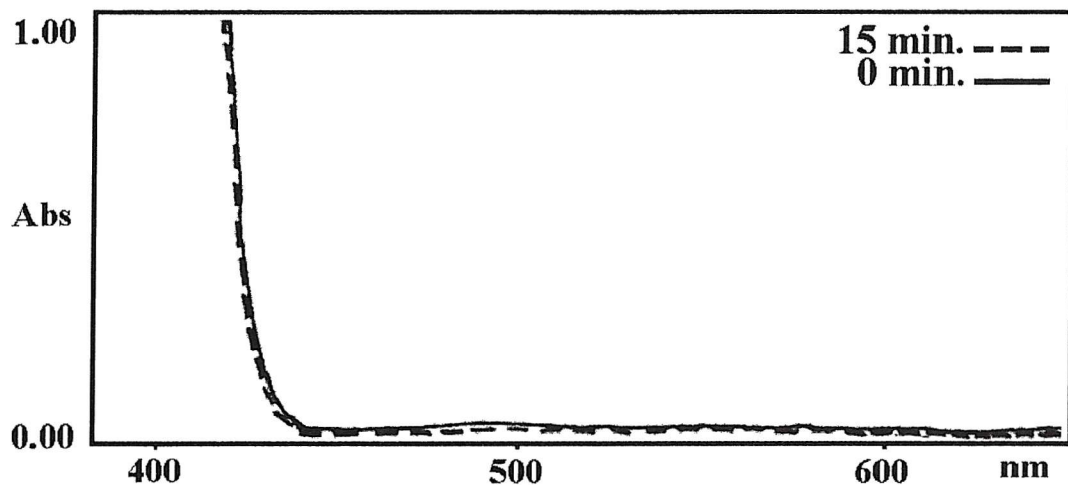


Figure 4.9: Spectra of recombinant human ubiquitous porphobilinogen deaminase Arg 173 Gln mutant after reaction with Ehrlich's reagent. Spectra were recorded immediately after the reaction was performed using a manual uv-vis spectrophotometer over a range of 380-650nm. after 0 min and 15 min.

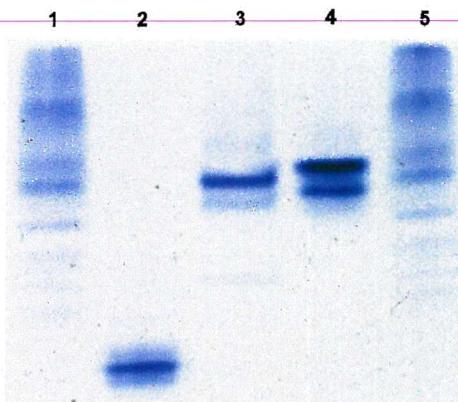


Figure 4.10: Non-denaturing PAGE analysis to compare Arg 173 Gln mutant with the *E. coli* porphobilinogen deaminase holo-enzyme, native enzyme of human ubiquitous porphobilinogen deaminase and Arg 167 Gln mutant. Track 1, Arg 173 Gln mutant after DEAE Sephadex chromatography; track 2, *E. coli* porphobilinogen deaminase holo-enzyme after Mono Q chromatography; track 3, Arg 167 Gln mutant after Superdex G-75 gel filtration column; track 4, native enzyme after Superdex G-75 gel filtration column; track 5, Arg 173 Gln mutant after DEAE Sephadex chromatography. The native gel shows that the Arg 173 Gln mutant migrates as three bands plus a smear showing it is an apo-enzyme.

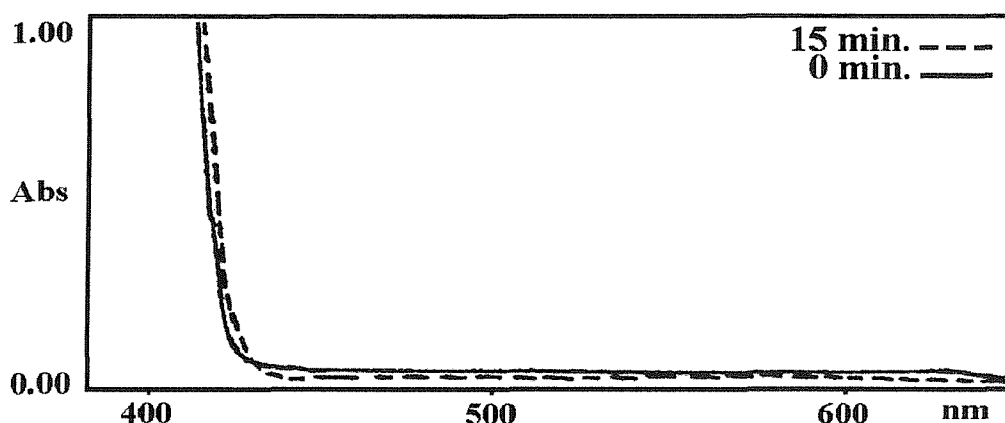


Figure 4.11: **Spectra of recombinant human ubiquitous porphobilinogen deaminase Arg 149 Gln mutant after reaction with Ehrlich's reagent.** Spectra were recorded immediately after the reaction was performed using a manual uv-vis spectrophotometer over a range of 380-650nm. after 0 min and 15 min.

mutant enzymes during purification or whether the mutations prevented the reaction of preuroporphyrinogen with the mutant apo-enzyme in the first place. To investigate this it was necessary to incubate the purified mutant apo-deaminases with preuroporphyrinogen and to determine whether the holo-protein could be reconstituted.

It has been demonstrated, using the *E. coli* porphobilinogen deaminase, that the apo-enzyme form can be rapidly reconstituted into the holo-enzyme by incubation with preuroporphyrinogen (Shoolingin-Jordan *et al.*, 1996). Preuroporphyrinogen is exceptionally unstable with a half-life of $4\frac{1}{2}$ min. at 37°C and is generated by rapidly incubating an excess of active *E. coli* porphobilinogen deaminase with porphobilinogen followed by pressure dialysis at 4°C to remove the unwanted deaminase. Thus isolated, preuroporphyrinogen is stable enough to carry out reconstitution experiments for 30 minutes. After attempted reconstitution, the mutant deaminase is separated from any small molecules by gel-filtration using a PD-10 column and reacted with Ehrlich's reagent to determine if any holoenzyme has been reconstituted. The reconstitution assay was carried out as described in section 2.3.10.

The reaction of Ehrlich's reagent with the reconstituted Arg 173 Gln mutant was observed using a uv-vis U-3010 spectrometer over a range of 380-650nm and spectra were recorded immediately after the reaction was performed and at intervals up to one hour. Ehrlich's reagent gave a positive reaction with the Arg173 Gln mutant, however, the spectral profile was more indicative of a reaction of a tetrapyrrole rather than a dipyrromethane, as judged by the immediate appearance of a maximum at 495nm and the growth of a Soret peak at 405nm (figure 4.12). Continued reaction (figure 4.13) confirmed this, with a Soret peak developing further together with additional peaks in the visible region indicative of an *etio*-type spectrum characteristic of uroporphyrin (Smith, 1975). It thus appears that the Arg 173 Gln mutant can bind preuroporphyrinogen but that this may not be through a covalent link, allowing the Ehrlich's reagent to release it from the enzyme followed by cyclisation to uroporphyrinogen I. In the presence of perchloric acid and oxygen this is oxidised to uroporphyrin I. Despite being able to react with preuroporphyrinogen, the reconstituted Arg 173 Gln mutant was enzymically inactive.

Several attempts were made to reconstitute the Arg 149 Gln mutant to the holo-enzyme, however, assays showed that no enzyme activity was restored by the treatment with preuroporphyrinogen. Furthermore, when the Arg 149 Gln mutant was analysed by non-denaturing gel electrophoresis, before and after attempted reconstitution, both samples formed a slow migrating smear, see figure 4.14, indicative of the apo-enzyme (Shoolingin-Jordan *et al.*, 1996). Holo-enzymes migrate faster as clear double bands, as shown in the previous chapter for Arg 167 Gln. Thus if any holo-enzyme had been formed it was not sufficiently stable to withstand the electrophoretic separation.

The reaction of Ehrlich's reagent with the reconstituted Arg 149 Gln mutant was also observed using a uv-vis spectrophotometer. The results were similar to those found for Arg 173 Gln (figures 4.15 and 4.16), suggesting that this mutant also can bind preuroporphyrinogen but that it is easily released and can cyclise to uropor-

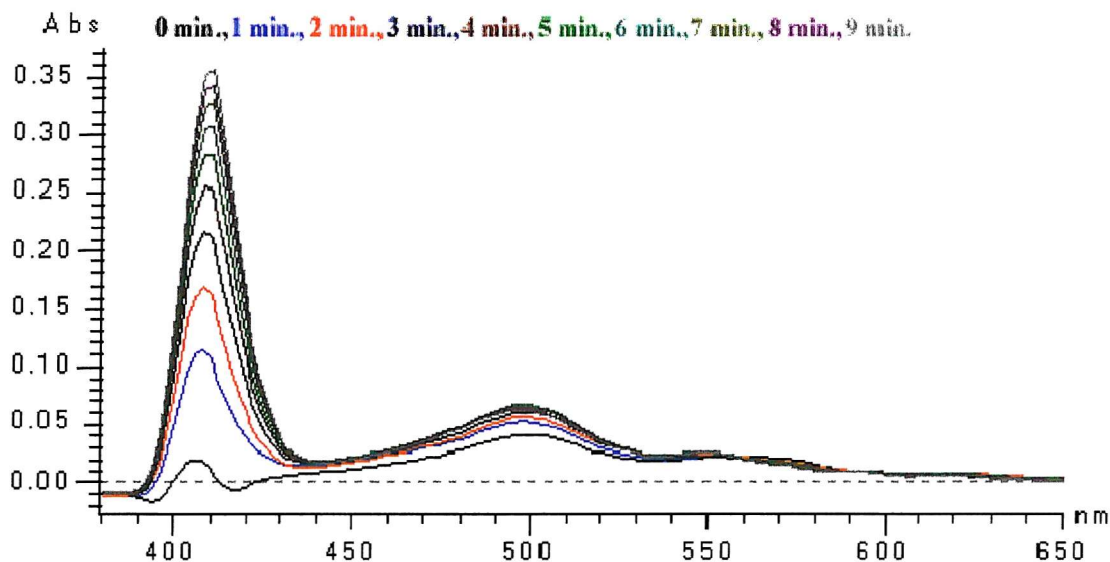


Figure 4.12: **Spectra of human ubiquitous porphobilinogen deaminase Arg 173 Gln mutant reacted with Ehrlich's reagent after reconstitution.** Spectra were recorded immediately after the reaction was performed using a uv-vis spectrophotometer over a range of 380-650nm. at 1min. intervals for 10min.

phyrinogen I and finally oxidise to uroporphyrin I. It is likely that the mutations of both arginine 173 and 149 impair the binding of preuroporphyrinogen to the active site cleft so that cysteine 261 is unable to form a covalent link to generate the ES_2 complex that ultimately transforms into the dipyrromethane cofactor.

4.2.8 Electrospray mass spectrometry (ESMS) of recombinant human ubiquitous porphobilinogen deaminase Arg 173 Gln and Arg 149 Gln mutants

M_r determinations of the mutant deaminases were carried out by using electrospray mass spectrometry. Samples of the purified proteins were prepared as described in section 2.3.4. The M_r of the Arg 173 Gln and Arg 149 Gln mutants were compared to the native ubiquitous porphobilinogen deaminase apo-enzyme ($M_r = 39,330$). The

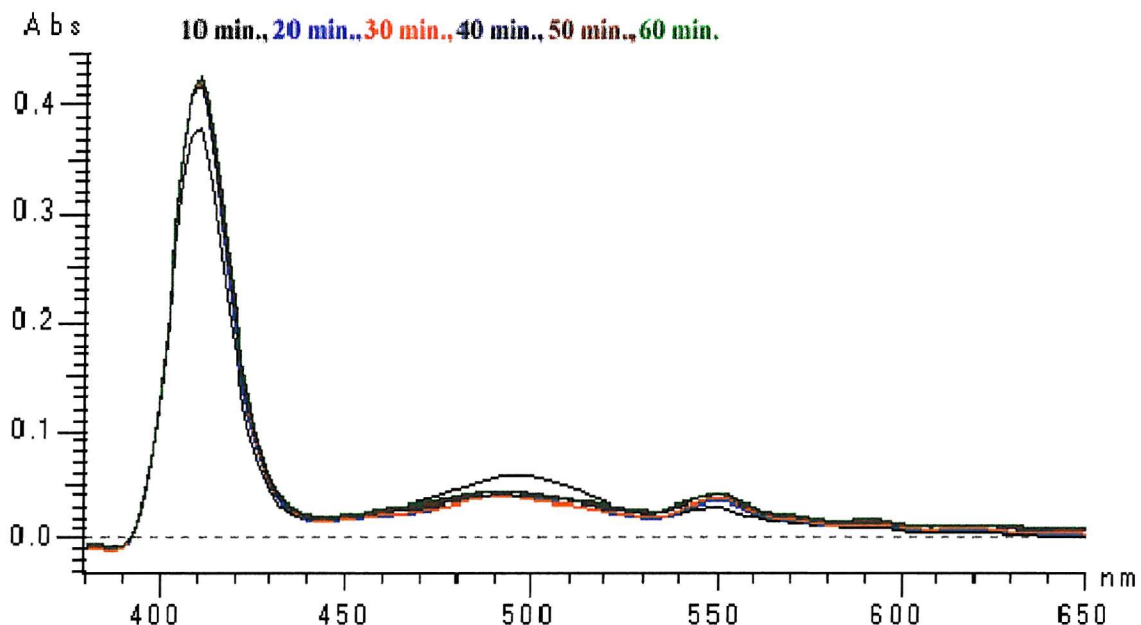


Figure 4.13: **Spectra of human ubiquitous porphobilinogen deaminase Arg 173 Gln mutant reacted with Ehrlich's reagent after reconstitution.** Spectra were recorded immediately after the reaction was performed using a uv-vis spectrophotometer over a range of 380-650nm. at 10 min. intervals for 60min.

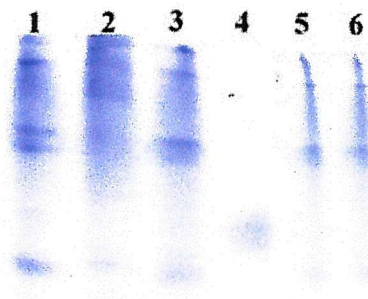


Figure 4.14: **Non-denaturing PAGE analysis showing the negative response by the ubiquitous human porphobilinogen deaminase Arg 149 Gln mutant to attempts at holo-enzyme reconstitution.** Track 1, Arg 149 Gln mutant after Mimetic Orange 1 chromatography eluted with 250mM NaCl; track 2, Arg 149 Gln mutant after Mimetic Orange 1 chromatography eluted with 500mM NaCl; track 3, Arg 149 Gln mutant after Mimetic Orange 1 chromatography eluted with 250mM NaCl after freeze drying and dissolved with 20mM Tris/HCl buffer, pH 9.1; track 4, purified Arg 167 Gln mutant; tracks 5 and 6, Arg 149 Gln mutant after attempted reconstitution.

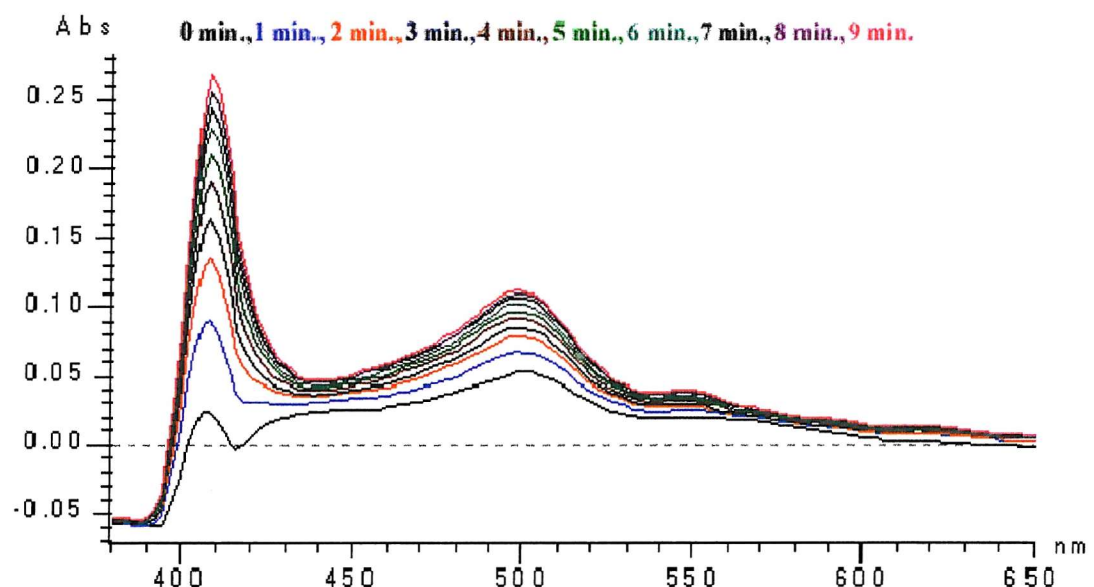


Figure 4.15: Spectra of human ubiquitous porphobilinogen deaminase **Arg 149 Gln** mutant reacted with Ehrlich's reagent after reconstitution. Spectra were recorded immediately after the reaction was performed using a uv-vis spectrophotometer over a range of 380-650nm. at 1min. intervals for 10min.

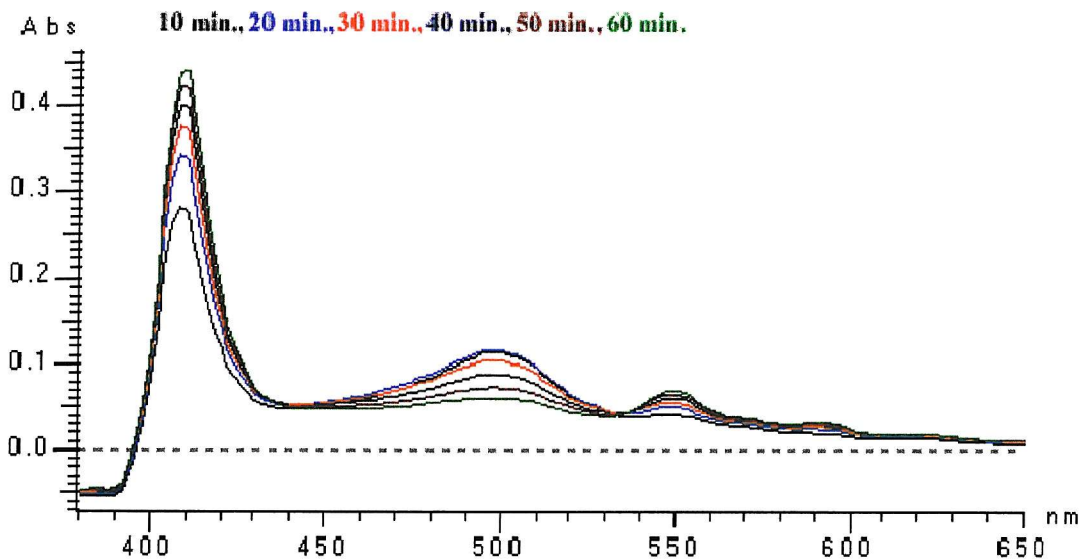


Figure 4.16: **Spectra of human ubiquitous porphobilinogen deaminase Arg 149 Gln mutant reacted with Ehrlich's reagent after reconstitution.** Spectra were recorded immediately after the reaction was performed using a uv-vis spectrophotometer over a range of 380-650nm. at 10 min. intervals for 60min.

M_r of Arg 173 Gln mutant was 39,175.35, see figure 4.17, close to the predicted value of 39,175.65 for the mutant apo-enzyme lacking the *N*-terminal methionine, as shown by protein sequencing. The M_r of the Arg 149 Gln mutant was 39,173.42, see figure 4.18, close to the predicted value of 39,175.65 for the mutant lacking the *N*-terminal methionine. As a result of M_r determinations it is concluded that both the Arg 173 Gln and Arg 149 Gln mutants exist as apo-enzymes.

4.2.9 Expression and purification of recombinant human ubiquitous porphobilinogen deaminase Trp 198 Ter mutant

The recombinant human ubiquitous porphobilinogen deaminase Trp 198 Ter mutant was also expressed in the bacterial strain BL21(DE3), see section 2.3.2 and was compared to the expression of the recombinant human ubiquitous porphobilinogen deaminase Arg 167 Trp mutant by SDS PAGE using complete bacterial lysates. Fig-

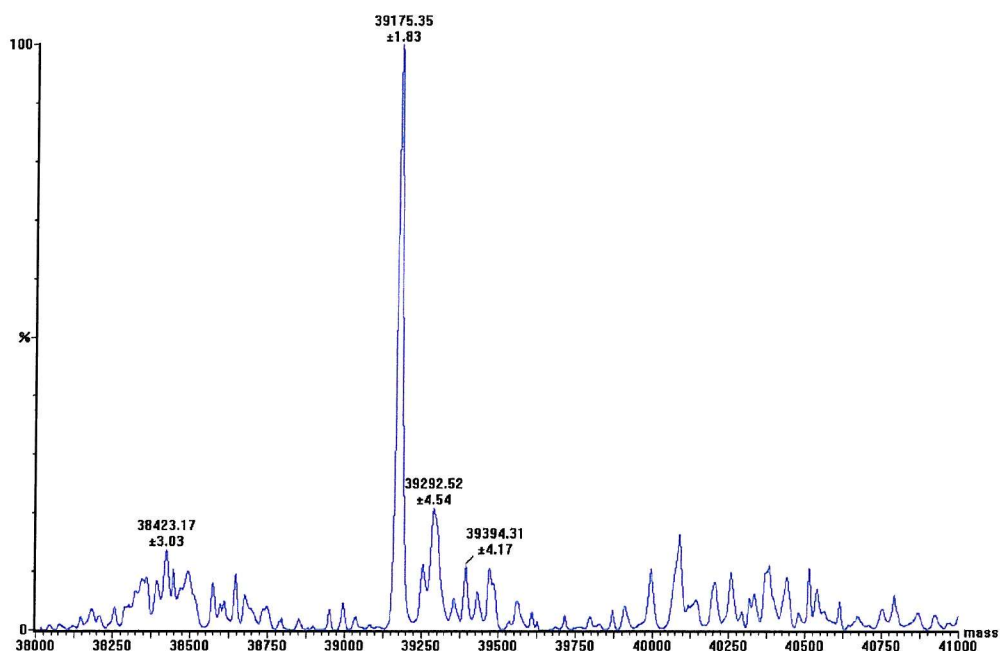


Figure 4.17: Spectrum obtained from electrospray mass spectroscopic (ESMS) analysis of 1000ng/10 μ l ubiquitous human porphobilinogen deaminase mutants, Arg 173 Gln mutant after Superdex G-75 column. The Arg 173 Gln mutant was shown to have a M_r of 39175.35 \pm 1.83 which agrees with that predicted by the nucleotide sequence and the *N*-terminal sequence.

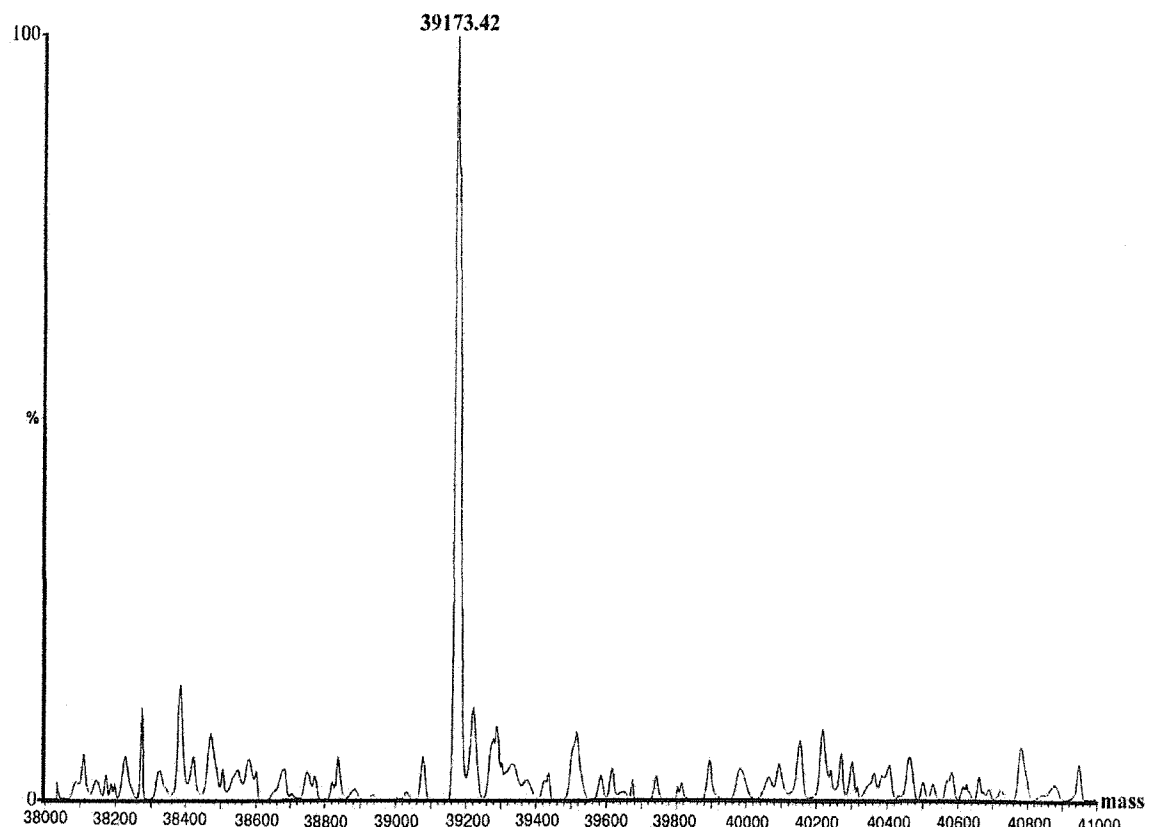


Figure 4.18: Spectrum obtained from electrospray mass spectrometric (ESMS) analysis of 1000ng/10 μ l ubiquitous human porphobilinogen deaminase mutants, Arg 149 Gln mutant after Superdex G-75 chromatography. The Arg 149 Gln mutant was shown to have a M_r of 39173.42 which agrees with that predicted by the nucleotide sequence and the *N*-terminal sequence.

ure 4.19 shows that the Trp 198 Ter mutant has been expressed as well as the Arg 167 Trp mutant. The Arg 167 Trp protein can clearly be seen as a thick band approximately level with the 45,000 marker whereas the Trp 198 Ter truncated protein shows as a clear band, between the 20,100 and 24,000 markers, as predicted. In the partial purification of the Trp 198 Ter mutant, the crude extract was analysed by Bio-rad protein and deaminase assays. It was found that the Trp 198 Ter mutant had no detectable deaminase activity.

To obtain further information about the Trp 198 Ter mutant a sample of the supernatant from a cell free extract was analysed using SDS PAGE to show the protein content. Although the Trp 198 Ter protein appeared to have been expressed well from the analysis of the bacterial lysate following induction with IPTG, (figure 4.19, tracks 6, 7 and 8), the supernatant from the cell free extract showed a complete lack of the mutant protein (figure 4.20) suggesting that the protein was insoluble and was likely to be in the pellet from the centrifugation in the form of bacterial membrane coaggregates or inclusion bodies.

An alternative approach was therefore necessary to isolate the apparently insoluble Trp 198 Ter truncated mutant. Two procedures have been used, as described in section 2.3.8, either by preventing the formation of the coaggregates or by disrupting them after they have formed. In both procedures, different concentrations of the detergent Sarkosyl have been used. The protein thus obtained in the cell free extract was then analysed by SDS PAGE, as shown in figure 4.21. It was found that by using 0.2% Sarkosyl detergent before sonication, a small amount of Trp 198 Ter protein could be separated from the coaggregate, as seen by the faint band in figure 4.21, track 3. When the Sarkosyl was increased to 1%, more Trp 198 Ter protein was solubilized, as seen in figure 4.21, track 4. Using the second procedure, large protein bands of Trp 198 Ter were observed in tracks 7 and 8, using 0.5% and 1.5% Sarkosyl detergent in the buffer used to resuspend the pellets from the centrifugation of the crude extract.

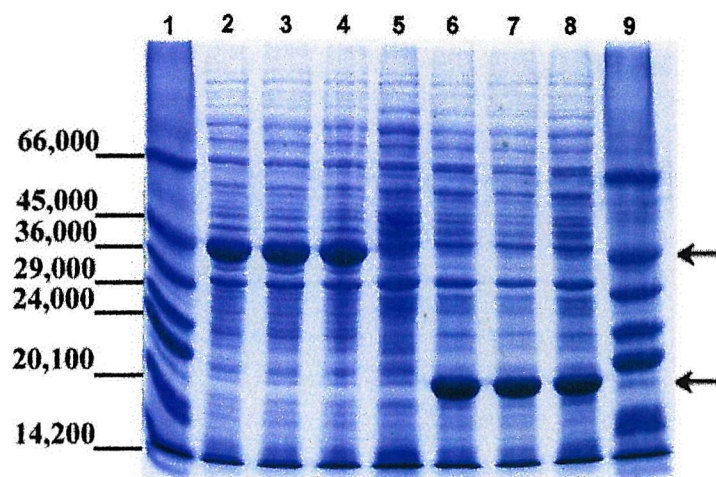


Figure 4.19: SDS-PAGE analysis to show the expression of recombinant human ubiquitous porphobilinogen deaminase mutants Arg 167 Trp and Trp 198 Ter, in complete lysates of recombinant *Escherichia coli* BL21 cells. Bacterial samples were prepared by taking 1ml of bacterial culture, centrifuging and resuspending the pellet in 50 μ l of 50mM Tris/HCl buffer, pH 8.2, followed by 50 μ l of disruption buffer as described in section 2.3.1. Track 1, molecular weight markers, Dalton VII; tracks 2, 3 and 4, lysate of Arg 167 Trp mutant; tracks 5, lysate from *E. coli* BL21 cells; tracks 6, 7 and 8, lysate of Trp 198 Ter mutant; track 9, molecular weight markers, Dalton VII.

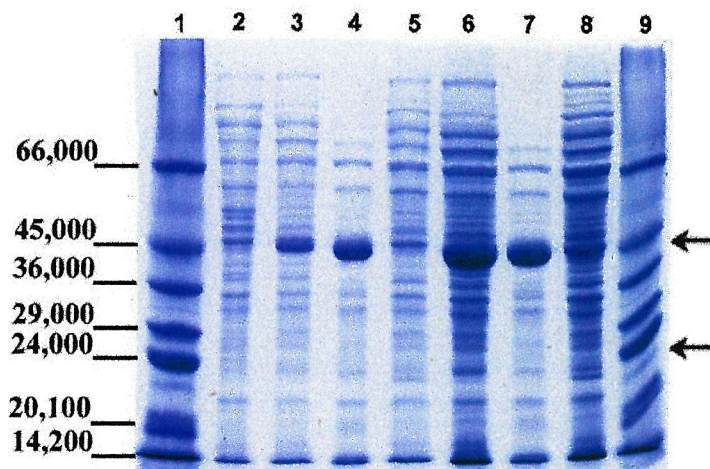


Figure 4.20: SDS-PAGE analysis to show expression of ubiquitous porphobilinogen deaminase mutants Arg 167 Trp and Trp 198 Ter in *Escherichia coli* sonicated extracts. All samples are supernatants from cell free extracts after sonication and centrifugation. Track 1, molecular weight markers, Dalton VII; track 2, crude extract of cell free *E. coli* BL21 cells, 10 μ g of protein; track 3, crude extract of cell free extract from Arg 167 Trp mutant, 10 μ g of protein; track 4, crude extract of cell free of Arg 167 Trp mutant heat-treated at 60°C for 10min., 10 μ g of protein; track 5, crude extract of Trp 198 Ter mutant after ultracentrifugation, 10 μ g of protein; track 6, sample as in track 3, approximately 50 μ g; track 7, sample as in track 4, approximately 50 μ g; track 8, sample as in track 5, approximately 50 μ g; track 9, molecular weight markers, Dalton VII.

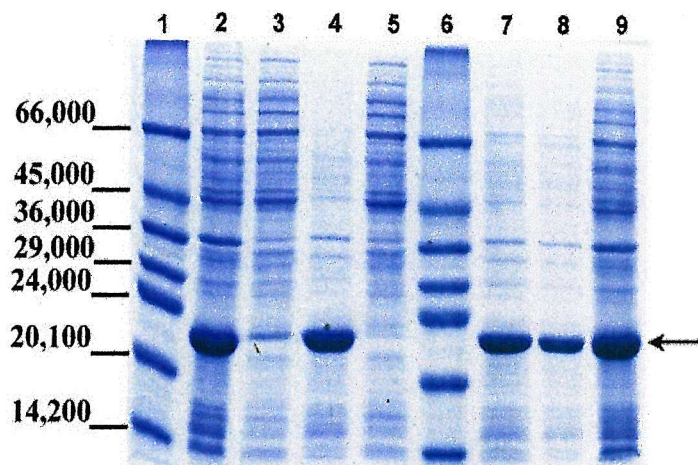


Figure 4.21: SDS-PAGE analysis to show the solublisation of the insoluble, recombinant human ubiquitous porphobilinogen deaminase Trp 198 Ter mutant by using the detergent Sarkosyl. Track 1, molecular weight markers, Dalton VII; track 2, lysate from *E. coli* cells expressing Trp 198 Ter mutant as in figure 4.20, tracks 6, 7 and 8; track 3, supernatant from cell free extract of Trp 198 Ter mutant after sonication in the presence of 0.2% Sarkosyl; track 4, supernatant from the resuspended pellet from the previous experiment resonicated in 20mM Tris/HCl buffer, pH 8.2, containing 1% Sarkosyl; track 5, crude extract of Trp 198 Ter mutant supernatant after sonication without Sarkosyl; track 6, molecular weight markers, Dalton VII; track 7, pellet resulting from centrifugation of the total crude extract of Trp 198 Ter mutant after sonication without Sarkosyl, resuspended and resonicated in 20mM Tris/HCl buffer, pH 8.2, containing 0.5% Sarkosyl; track 8, pellet resulting from sonicated total crude extract of Trp 198 Ter mutant without detergent, resuspended and resonicated in 20mM Tris/HCl buffer, pH 8.2, containing 1.5% Sarkosyl.

4.2.10 Discussion and conclusions

Arg 173 Gln, Arg 149 Gln and Trp 198 Ter mutants of recombinant human ubiquitous porphobilinogen deaminases have been purified and their properties investigated by a combination of techniques. Important information about the effects of the mutations on the structures of both mutants was obtained as a result of the purifications.

The Arg 173 Gln mutant was isolated by a protocol similar to that for the native holo-enzyme, yielding a protein with only a few impurities, figure 4.5. The Arg 173 Gln mutant deaminase exhibited interesting properties suggesting that a proportion of the protein in crude extracts contained bound “tetrapyrrole”. Arginine 173 occupies a central position in the active site being involved in both cofactor and substrate binding (Louie *et al.*, 1996; Wood *et al.*, 1995). Studies on the equivalent arginine-155 in the *E. coli* deaminase (Jordan and Woodcock, 1991; Lander *et al.*, 1991) indicates that the enzyme reacts with Ehrlich’s reagent to give an anomalous cofactor reaction. The bacterial mutant exhibits only a trace of activity and is unable to bind substrate unless very high concentrations are used. There is some evidence to suggest that the Arg 155 Leu mutant may be deficient in product release (Lander *et al.*, 1991) and can accumulate the enzyme intermediate complex ES₄. Cell-free extracts of the human ubiquitous porphobilinogen deaminases Arg 173 Gln mutant also showed an anomalous reaction with Ehrlich’s reagent, however after DEAE Sephadex chromatography, the mutant appeared to exist as an apo-enzyme with only a trace of Ehrlich’s positive reaction (figure 4.9). Non-denaturing gel electrophoresis, figure 4.10, revealed a ladder of bands indicative of an apo-enzyme (Shoolingin-Jordan *et al.*, 1996). Electrospray mass spectrometry (ESMS) confirmed the presence of apo-enzyme, see figure 4.17. ESMS also indicated that the mutant had no *N*-terminal methionine, consistent with results from *N*-terminal sequencing. When attempts were made to reconstitute the holo-enzyme from the mutant apo-deaminase a holo-enzyme variant was formed in which the tetrapyrrole system appeared to become non-covalently bound to the mutant protein. Treatment of the “reconstituted” mu-

tant with Ehrlich's reagent resulted in the formation of uroporphyrin I (figures 4.12 and 4.13).

In contrast, the Arg 149 Gln mutant was purified by the method normally used only for apo-deaminases, using Mimetic Orange 1 affinity column chromatography. During the affinity purification, only one third of the protein bound to the column. This proportion was expected to be correctly folded mutant apo-protein. One third of the Arg 149 Gln mutant appeared to be weakly bound to the affinity column and eluted with other protein impurities at the beginning of the gradient. One third of the mutant did not bind to the column and was recovered in the wash using 100mM NaCl. These observations contrast to those seen for the native *E. coli* apo-enzyme that binds strongly to the Mimetic Orange 1 column (Shoolingin-Jordan *et al.*, 1996). The tightly bound protein eluting between the fractions (5-25) gave 10mg/ml protein from two liters of culture with 70% purity. Native gel electrophoresis showed a ladder of bands (figure 4.14) consisting of different folded forms of the apo-enzyme.

The Arg 149 Gln mutant deaminase was very different from the native human enzyme since it is unstable when heat-treated at 60°C, as expected for an apo-deaminase. It is suggested that the Arg 149 Gln mutant fraction that does not bind to the column, or which is weakly bound, is likely to be poorly folded or denatured as a result of the mutation. It has been suggested that arginine 149 is essential for cofactor assembly and for correct folding of the enzyme (Wood *et al.*, 1995; Llewellyn *et al.*, 1993). Arginine 149 forms salt bridge interactions with the cofactor ring C1 acetate so that substitution of a positively charged side chain by a neutral side chain would be expected to cause severe disruption to the hydrogen bonding network involved in cofactor binding. It is hardly surprising therefore that the Arg 149 Gln mutant has no cofactor, exhibits no enzyme activity and gives a negative reaction with Ehrlich's reagent. Electrospray mass spectrometry (ESMS) confirmed that this mutant exists as an apo-enzyme. ESMS also indicated that the mutant has lost the *N*-terminus methionine in agreement with *N*-terminal sequencing. The mutant apo-enzyme Arg

149 Gln is unable to regenerate to the holo-enzyme in the reconstitution reaction with preuroporphyrinogen, since the cofactor binding site was disrupted as a result of losing the important positive charge from arginine 149. The apoenzyme appears as a broad smudge migrating at lower mobility, unlike the holoenzyme which migrates as a doublet with higher mobility. As with Arg 173 Gln, there is evidence that preuroporphyrinogen can interact weakly with the Arg 149 Gln apo-enzyme to generate a holo-enzyme variant in which the tetrapyrrole system is non-covalently bound. Treatment of the "reconstituted" mutant with Ehrlich's reagent also resulted in the formation of uroporphyrin I (figures 4.15 and 4.16). *In vivo* where the level of preuroporphyrinogen is very low, the Arg 149 Gln mutant would exist as an unstable apo-protein consistent with its CRIM-ve profile.

The final study in this chapter centered on the severe mutation Trp 198 Ter, a common mutation found in the north of Sweden. The residue tryptophan 198 is located on one of the two amino acid strands that link domain 1 and 2 of the deaminase to form the deep cleft where the dipyrromethane cofactor lies (Louie *et al.*, 1992). Mutation of the codon specifying this tryptophan to a termination codon will therefore generate a protein without a small part of domain 1 and without the entire domain 3. Since the dipyrromethane cofactor is bound covalently to cysteine 261 in domain 3 it is unlikely that the enzyme would show any enzymic activity or have any dipyrromethane cofactor bound. In addition to its catalytic role as a primer for the polymerization process (Jordan and Warren, 1987; Warren and Jordan, 1988; Shoolingin-Jordan *et al.*, 1997) the dipyrromethane cofactor also plays an important role in stabilising the tertiary structure of the holoenzyme. This is achieved by forming an extensive network of hydrogen bonds and salt bridges between the three domains and partially neutralizing the electropositivity in the active-site cleft (Louie *et al.*, 1992).

The naturally occurring Trp 198 Ter human mutant causing acute intermittent porphyria results in a CRIM-ve phenotype since the *C*-terminal part of the protein

is missing and could be important for antigenicity (Lee and Anvret, 1991). It is also possible that, *in vivo*, the truncated protein is so unstable that it is rapidly digested by intracellular proteinases. It is expected that the absence of domain 3 would expose hydrophobic faces of domains 1 and 2 to the medium, lowering the solubility of the mutant substantially and encouraging the formation of membrane coaggregates. In the studies described in this chapter, the Trp 198 Ter mutant, is expressed, predictably, as a truncated protein that is inactive and insoluble. The extreme insolubility probably results from the coaggregation of the mutant deaminase with bacterial outer membrane components in the bacterial lysate in a way reported for the actin protein (Frankel *et al.*, 1990; 1991). It has been found previously that the outer membrane is resistant to solubilisation by different concentrations of Sarkosyl, ranging from 0.25 to 2% (Filip *et al.*, 1973). The strong band of the Trp 198 Ter human mutant obtained from the partial purification using 0.5% Sarkosyl detergent demonstrates that this concentration of the detergent is sufficient to disrupt the interactions maintaining protein coaggregates with bacterial outer membrane components. Despite being solubilised there was no indication that this mutant was any more than completely inactive.

Without doubt, the Trp 198 Ter mutation is severe and disabling for the human enzyme. It would be interesting if such a severe mutation resulted in a higher incidence of acute attacks of AIP and greater penetrance compared with individuals that carry a milder mutation such as Arg 167 Gln. Currently there is no evidence to suggest this, except in the case of compound heterozygotes where a severe mutation such as Trp 198 Ter would have to be paired with a less severe mutation to be compatible with life.

Chapter 5

Crystallization and X-ray structure of the recombinant ubiquitous human porphobilinogen deaminase Arg 167 Gln mutant

5.1 Introduction

The X-ray structure of *E. coli* porphobilinogen deaminase was first determined in 1992 (Louie *et al.*, 1992) and subsequently refined to a resolution of 1.76Å (Louie *et al.*, 1996). The structure has also been solved independently (Hädener *et al.*, 1993; 1999). The structure shows the protein to consist of three domains, each of about 100 aminoacids. Domains 1 and 2 provide a flexible structure between which the active site is located with domain 3, providing the attachment point for the dipyrromethane cofactor. This three-dimensional structure has greatly increased our understanding of how the enzyme accommodates the dipyrromethane cofactor. In

addition the structure has provided insight into how the enzyme recognises the substrate porphobilinogen and catalyses the polymerisation reaction. Interpretation of the structural and functional properties of several *E. coli* deaminase mutants (Jordan and Woodcock, 1991; Lander *et al.*, 1991; Woodcock and Jordan, 1994) has been made possible using this structure.

A comparison of the primary sequences of several porphobilinogen deaminase enzymes reveals that there is a remarkable homology indicating that its structure has been strongly conserved during evolutions. For example, there is a 60% sequence homology between the deaminases from *E. coli* and human sources, indicating that the structural similarity extends to secondary and tertiary structure. With this similarity in mind, the X-ray structure of the *E. coli* enzyme has been used to map the position of several human mutations (Wood *et al.*, 1995). Coupled with *in vitro* experiments involving the expression and characterisation of human mutant deaminases, a clearer picture is being built up of structure functional relationships in the human enzyme, particularly with respect to the CRIM status of the mutation.

Despite the similarity between the *E. coli* and human deaminases, there are still substantial differences in the sequence of amino acids, particularly in domain 3 where there is an insertion of 29 amino acids. In addition the ubiquitous human enzyme possesses an *N*-terminal extension of 15 amino acids compared to the *E. coli* enzyme. It was therefore important to determine the structure of the human deaminase independently so the precise effects of human mutations that lead to acute intermittent porphyria (AIP) could be evaluated. The previous chapters in this thesis have described the expression and characterisation of several human mutant ubiquitous porphobilinogen deaminases, including Arg 167 Gln, Arg 167 Trp, Arg 173 Gln, Arg 149 Gln and Trp 198 Ter. This final chapter describes the crystallisation of one of these mutants, Arg 167 Gln, and the initial stages in the determination of its X-ray structure at 2.65Å resolution. Arg 167 Gln causes acute intermittent porphyria and has been studied in several families (Delfau *et al* 1990; Llewellyn *et al.*, 1990).

5.2 Preparation of Arg 167 Gln for crystallization

The purification of human recombinant porphobilinogen deaminase mutant Arg 167 Gln has already been described in section 2.3.2, however, the enzyme samples used for crystallization needed to be purified further to increase the likelihood of obtaining high quality crystals. To achieve this, after the DEAE-Sephadex column chromatography stage, the enzyme (1ml of 10mg/ml in 20mM Tris/HCl buffer, pH 8.2, containing 5mM DTT, 100 μ M PMSF and 70mM KCl) was applied to a Superdex G-75 gel filtration column previously equilibrated in 100mM Tris/HCl buffer, pH 8.2, containing 5mM DTT and 100 μ M PMSF. Elution was carried out at a flow rate of 0.5ml/min. and the enzyme collected in 1ml fractions. The active fractions from the column were pooled and concentrated to a volume of 2.5ml and desalting into 20mM Tris/HCl buffer, pH 8.2 containing 5mM DTT using a PD-10 column. The concentrations of the enzyme used for crystallization were 5mg/ml and 2.13mg/ml.

5.3 Crystallisation of Arg 167 Gln by the vapour diffusion method

Crystallisation trials of the recombinant human ubiquitous porphobilinogen deaminase were initially carried out with the native enzyme using Hampton Screens I and II by the vapour diffusion technique, as described in section 2.3.3. Cover slips used to form the hanging drops were coated in silane and oven dried. Crystallization solution (1ml) was added to each of the 24 wells of Linbro tissue culture plates. The hanging drop was formed by mixing 4 μ l of crystallization solution from the appropriate well with 4 μ l protein solution on the middle of the cover-slip before the cover slip was inverted over the well. The edges of each well had been previously coated with high vacuum grease before the cover-slips were pressed into place. Finally, the tray was wrapped in foil and placed in a dark cupboard at room temperature to al-

low the crystals to form. Two "hits" were obtained: tube 35 in screen I containing 0.1M Na Hepes, pH 7.5, with 0.8M Na phosphate/0.8M K phosphate as precipitant and tube 15 in screen II containing 0.1M tri-sodium citrate dihydrate, pH 5.6, with 0.5M ammonium sulphate as the salt and 1M lithium sulphate monohydrate as the precipitant. These initial screens were carried out in collaboration with Julie Mosley.

Having obtained this preliminary success, attempts to crystallize the Arg 167 Gln mutant were made using variations to the tube 15 conditions of Hampton Screen II that contained 0.1M tri-sodium citrate dihydrate, pH 5.6, with 0.5M ammonium sulphate as the salt and 1M lithium sulphate monohydrate as the precipitant, see figure , see figure 5.1. The buffer was prepared using AnalaR water, filtered and sparged with helium just before use. Crystallisation was carried out under N₂ gas in the dark at room temperature. A range of different protein concentrations and buffer conditions were used to obtain the best crystals. Small crystals were obtained with several different conditions around this hit, see figure 5.2. The best crystals formed in a group of three approximately 42 μ m x 15 μ m, on equilibration against reservoir containing 0.6M ammonium sulphate, 1.2M lithium sulphate monohydrate, 5% ethylene glycol, 50mM tri-sodium citrate dihydrate buffer, pH 5.6, and 50mM dithiothreitol (DTT), see table 5.1. Under these conditions, recombinant human ubiquitous porphobilinogen deaminase Arg 167 Gln mutant crystallizes in the orthorhombic class. It was significant that the best crystals appeared during the Christmas holiday (1998) when the temperature in the laboratory was below 10°G and there was minimal disturbance.

5.4 X-Ray crystallography

Protein crystals diffract an X-ray beam into many discrete beams, each of which produces a distinct spot (reflection) on a film positioned to collect the data. The in-

Reagent Formulation

Tube Number	Salt	Tube Number	Buffer [†]	Tube Number	Precipitant
1.	2.0 M Sodium chloride	1.	None	1.	10% w/v PEG 6000
2.	0.01 M Hexadecyltrimethylammonium Bromide	2.	None	2.	0.5 M Sodium Chloride, 0.01 M Magnesium Chloride hexahydrate
3.	None	3.	None	3.	25% v/v Ethylene Glycol
4.	None	4.	None	4.	35% v/v Dioxane
5.	2.0 M Ammonium Sulfate	5.	None	5.	5% v/v iso-Propanol
6.	None	6.	None	6.	1.0 M Imidazole pH 7.0
7.	None	7.	None	7.	10% w/v Polyethylene Glycol 1000 10% w/v Polyethylene Glycol 8000
8.	1.5 M Sodium Chloride	8.	None	8.	10% v/v Ethanol
9.	None	9.	0.1 M Sodium Acetate trihydrate pH 4.6	9.	2.0 M Sodium Chloride
10.	0.2 M Sodium Chloride	10.	0.1 M Sodium Acetate trihydrate pH 4.6	10.	30% w/v MPD
11.	0.01 M Cobaltous Chloride hexahydrate	11.	0.1 M Sodium Acetate trihydrate pH 4.6	11.	1.0 M 1,6 Hexanediol
12.	0.1 M Cadmium Chloride dihydrate	12.	0.1 M Sodium Acetate trihydrate pH 4.6	12.	30% v/v Polyethylene Glycol 400
13.	0.2 M Ammonium Sulfate	13.	0.1 M Sodium Acetate trihydrate pH 4.6	13.	30% w/v Polyethylene Glycol Monomethyl Ether 2000
14.	0.2 M Potassium Sodium Tartrate tetrahydrate	14.	0.1 M tri-Sodium Citrate dihydrate pH 5.6	14.	2.0 M Ammonium Sulfate
15.	0.5 M Ammonium Sulfate	15.	0.1 M tri-Sodium Citrate dihydrate pH 5.6	15.	1.0 M Lithium Sulfate monohydrate
16.	0.5 M Sodium Chloride	16.	0.1 M tri-Sodium Citrate dihydrate pH 5.6	16.	2% w/v Ethylene Imine Polymer
17.	None	17.	0.1 M tri-Sodium Citrate dihydrate pH 5.6	17.	35% v/v tert-Butanol
18.	0.01 M Ferric Chloride hexahydrate	18.	0.1 M tri-Sodium Citrate dihydrate pH 5.6	18.	10% v/v Jeffamine M-600 [*]
19.	None	19.	0.1 M tri-Sodium Citrate dihydrate pH 5.6	19.	2.5 M 1,6 Hexanediol
20.	None	20.	0.1 M MES pH 6.5	20.	1.6 M Magnesium Sulfate heptahydrate
21.	0.1 M Sodium dihydrogen phosphate mono 0.1 M mono-Potassium dihydrogen Phosphate	21.	0.1 M MES pH 6.5	21.	2.0 M Sodium Chloride
22.	None	22.	0.1 M MES pH 6.5	22.	12% w/v Polyethylene Glycol 20,000
23.	1.6 M Ammonium Sulfate	23.	0.1 M MES pH 6.5	23.	10% v/v Dioxane
24.	0.05 M Cesium Chloride	24.	0.1 M MES pH 6.5	24.	30% v/v Jeffamine M-600 [*]
25.	0.01 M Cobaltous Chloride hexahydrate	25.	0.1 M MES pH 6.5	25.	1.8 M Ammonium Sulfate
26.	0.2 M Ammonium Sulfate	26.	0.1 M MES pH 6.5	26.	30% w/v Polyethylene Glycol Monomethyl Ether 5000
27.	0.01 M Zinc Sulfate heptahydrate	27.	0.1 M MES pH 6.5	27.	25% v/v Polyethylene Glycol Monomethyl Ether 550
28.	None	28.	None	28.	1.6 M tri-Sodium Citrate dihydrate pH 6.5
29.	0.5 M Ammonium Sulfate	29.	0.1 M HEPES pH 7.5	29.	30% v/v MPD
30.	None	30.	0.1 M HEPES pH 7.5	30.	10% w/v Polyethylene Glycol 6000, 5% v/v MPD
31.	None	31.	0.1 M HEPES pH 7.5	31.	20% v/v Jeffamine M-600 [*]
32.	0.1 M Sodium Chloride	32.	0.1 M HEPES pH 7.5	32.	1.6 M Ammonium Sulfate
33.	None	33.	0.1 M HEPES pH 7.5	33.	2.0 M Ammonium Formate
34.	0.05 M Cadmium Sulfate hydrate	34.	0.1 M HEPES pH 7.5	34.	1.0 M Sodium Acetate
35.	None	35.	0.1 M HEPES pH 7.5	35.	70% v/v MPD
36.	None	36.	0.1 M HEPES pH 7.5	36.	4.3 M Sodium Chloride
37.	None	37.	0.1 M HEPES pH 7.5	37.	10% w/v Polyethylene Glycol 8000, 8% v/v Ethylene Glycol
38.	None	38.	0.1 M HEPES pH 7.5	38.	20% w/v Polyethylene Glycol 10,000
39.	0.2 M Magnesium Chloride hexahydrate	39.	0.1 M TRIS pH 8.5	39.	3.4 M 1,6 Hexanediol
40.	None	40.	0.1 M TRIS pH 8.5	40.	25% v/v tert-Butanol
41.	0.01 M Nickel(II) Chloride hexahydrate	41.	0.1 M TRIS pH 8.5	41.	1.0 M Lithium Sulfate monohydrate
42.	1.5 M Ammonium Sulfate	42.	0.1 M TRIS pH 8.5	42.	12% v/v Glycerol anhydrous
43.	0.2 M mono Ammonium dihydrogen Phosphate	43.	0.1 M TRIS pH 8.5	43.	50% v/v MPD
44.	None	44.	0.1 M TRIS pH 8.5	44.	20% v/v Ethanol
45.	0.01 M Nickel(II) Chloride hexahydrate	45.	0.1 M TRIS pH 8.5	45.	20% w/v Polyethylene Glycol Monomethyl Ether 2000
46.	0.1 M Sodium Chloride	46.	0.1 M Bicine pH 9.0	46.	20% w/v Polyethylene Glycol Monomethyl Ether 550
47.	None	47.	0.1 M Bicine pH 9.0	47.	2.0 M Magnesium Chloride hexahydrate
48.	2% v/v Dioxane	48.	0.1 M Bicine pH 9.0	48.	10% w/v Polyethylene Glycol 20,000

[†] Buffer pH is that of a 1.0 M stock (0.5 M for MES) prior to dilution with other reagent components. pH with HCl or NaOH.

Figure 5.1: Hampton screen II reagent formulation, from Hampton research.



Figure 5.2: Human ubiquitous porphobilinogen deaminase Arg 167 Gln mutant crystals.

	AS (M)	LS (M)				EG (%)
		1.2	1.4	1.5	1.6	
0.6	A ₁	B ₁	C ₁	D ₁	2.5	
0.7	A ₂	B ₂	C ₂	D ₂	2.5	
0.8	A ₃	B ₃	C ₃	D ₃	2.5	EG
0.6	A ₄	B ₄	C ₄	D ₄	5.0	(%)
0.7	A ₅	B ₅	C ₅	D ₅	5.0	
0.8	A ₆	B ₆	C ₆	D ₆	5.0	

Table 5.1: **Schematic of crystal tray containing the conditions that formed the best crystals.** All of the wells contain 50mM tri-sodium citrate dihydrate buffer, pH 5.6, and 50mM dithiothreitol (DTT). The best crystals used for X-ray analysis formed in well A₄. Other small single crystals formed in well B₄. (LS = lithium sulphate; As = ammonium sulphate; EG = ethylene glycol; M = molar (concentration).

tensities and phases of these reflections contain the information needed to reconstruct the electron density in the crystal (figure 5.3).

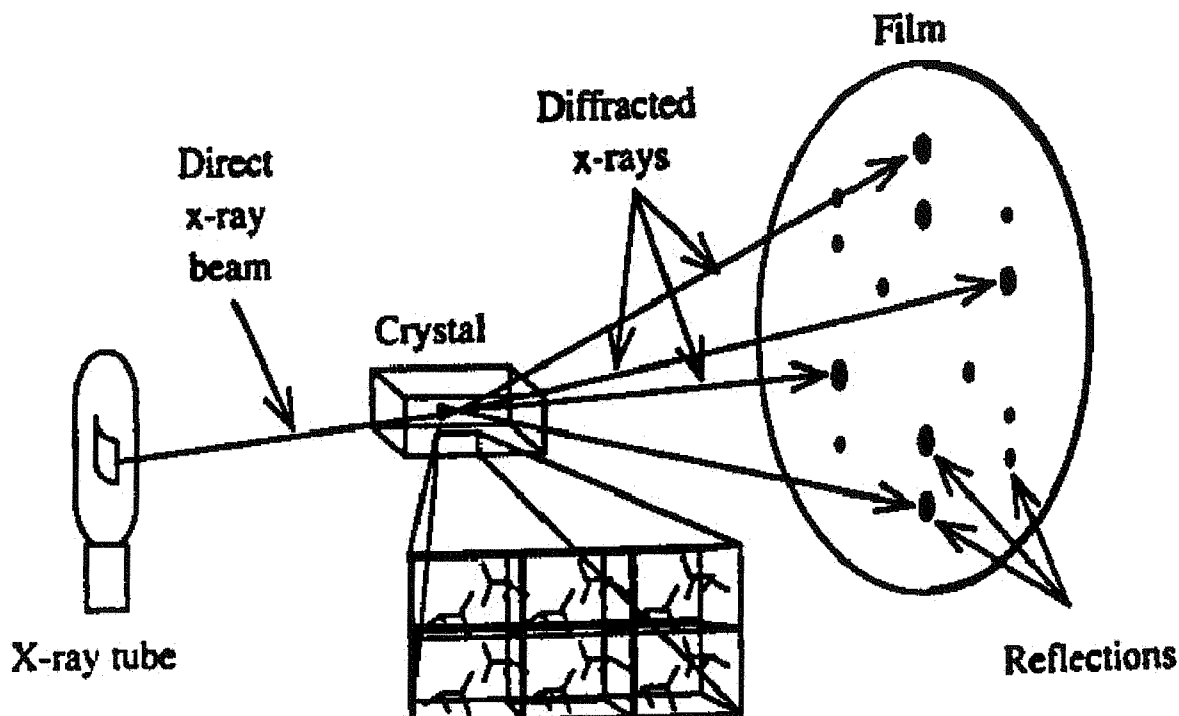


Figure 5.3: **Crysallographic data collection.** The crystal diffracts the source beam into many discrete beams, each of which produces a distinct spot (reflection) on the film. The intensities and phases of these reflections contain the information needed to determine molecular structures (Rhodes, 1993).

Synchrotron diffraction data from a single crystal of recombinant human ubiquitous porphobilinogen deaminase mutant Arg 167 Gln were collected with a MAR CCD detector at the European Synchrotron Radiation Facility (ESRF) at Grenoble station BM14 ($\lambda = 1.00 \text{ \AA}$). Low temperature data (100 K) were collected using an Oxford Cryostream cooler. Prior to flash freezing the crystal was transferred to a reservoir containing the crystallization cocktail including 30% (v/v) glycerol. Successful flash freezing was accomplished when the crystal was transferred from 0 % to 30 % glycerol in steps of 7.5 %.

X-ray data were collected to 2.65 Å, (figure 5.4) although towards the end of the collection the resolution deteriorated due to radiation damage. A total of 180 0.5°-oscillation frames were measured with an exposure time of 120sec. per frame and a crystal to detector distance of 145.5mm. The data collection from these reflections and the processing of the data to determine the structure are beyond the scope of this thesis, (Mohammed, 2001) and will only be outlined briefly.

The raw data were processed using the program MOSFLM and scaled and merged using programs from the CCP4 suite. The merged intensities were subsequently converted to structure factor amplitudes using ROTVATA, AGROVATA and TRUNCATE (CCP4, 1994). The unit cell dimensions for the human recombinant ubiquitous porphobilinogen deaminase Arg 167 Gln mutant were determined using the REFIX algorithm within MOSFLM ($a=81.1\text{ \AA}$, $b=105.2\text{ \AA}$, $c=109.6\text{ \AA}$; $\alpha=\beta=\gamma=90^\circ$). This indicated that the crystal belonged to the orthorhombic space group either $P222_1$, $P2_12_12_1$ or $P2_12_12$.

The structure was solved by molecular replacement assuming that two molecules were present in the asymmetric unit, using the coordinates of PBGD from *E. coli*. The rotational and translational searches were performed with the program MOLREP (Vagin and Teplyakov, 1997) and the crystal packing was visualized with MOLPACK. The structure was refined with the program CNS and converted into the X-PLOR format using MAPMAN. Map inspections and model manipulations were performed with QUANTA and a model was obtained that showed the dipyrromethane cofactor and most of the amino acid side chains. Further cycles of refinement were performed and the large insert in domain 3 was built into the structure as the electron density improved. No electron density could be detected for the *N*-terminal region (residues 1-18), for a mobile loop in domain 1 (residues 57-78), a small section of the insert in domain 3 (residues 307-312) and the *C*-terminus (residues 359-361).

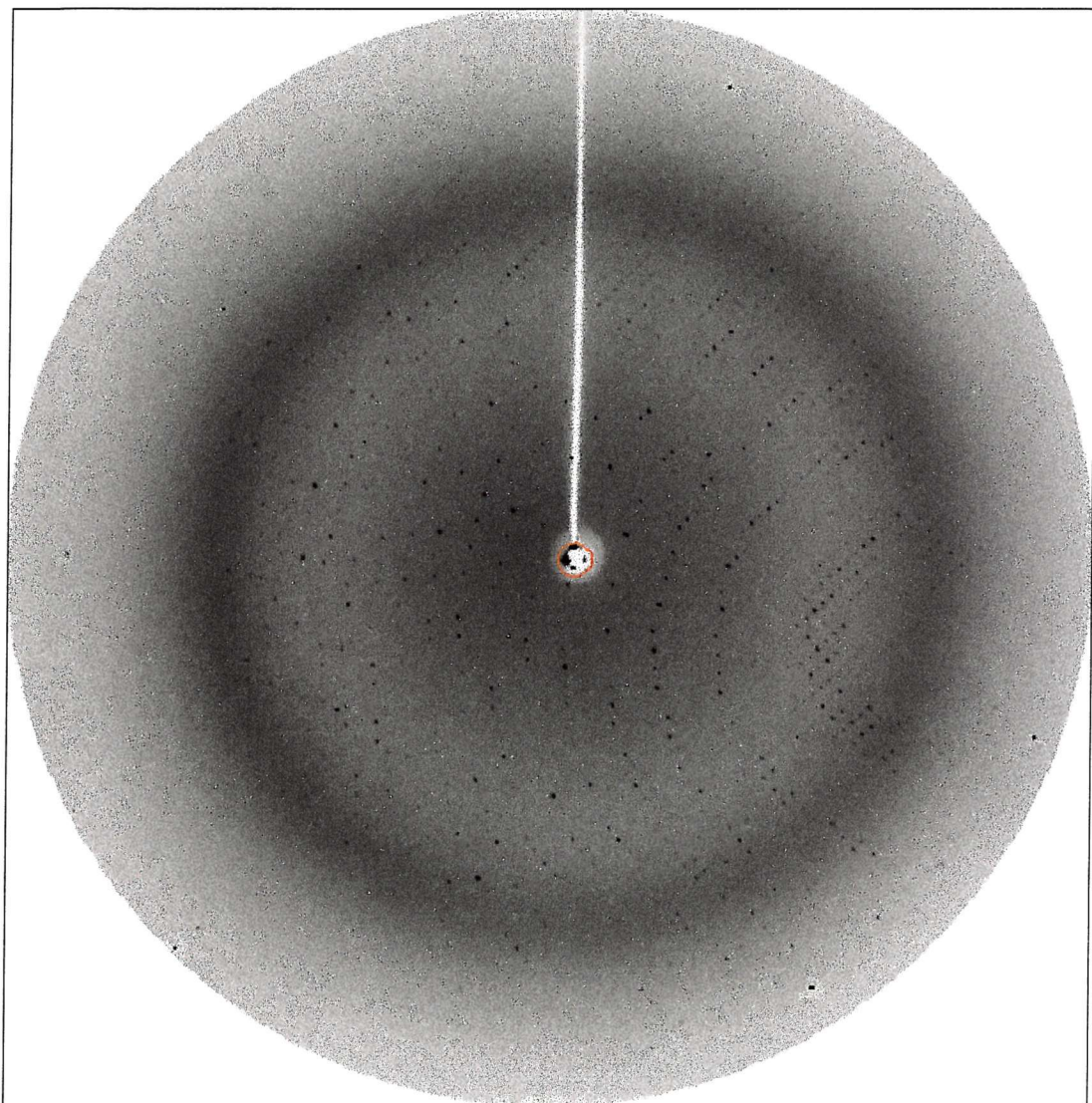


Figure 5.4: An oscillation image (0.5 degree) from the human porphobilinogen deaminase Arg 167 Gln mutant crystal collected on a MAR CCD detector at Grenoble, France. The crystal was flash cooled at 100 K and diffracted X-rays to a resolution of 2.65 Å. The exposure time was 120 s with a crystal-to detector distance of 145.5 mm (Mohammed, 2001).

5.5 The X-ray structure of the recombinant human ubiquitous porphobilinogen deaminase Arg 167 Gln mutant

As expected; overall structure of the recombinant human ubiquitous porphobilinogen deaminase Arg 167 Gln mutant is made up of three domains, similar to the *E. coli* enzyme, but with dimensions of 57 x 47 x 55 Å. The topologies of domains 1 and 2 are similar to each other, consisting of five β -sheets and α -helical segments pack against each face of the β -sheet. Domain 3 consists of a three stranded β -sheet and three α -helical segments. Domains 1 and 2 are linked together by two hinge segments whereas domain 3 is linked to domain 1 by a single strand (residues 237-240). The structure of the human deaminase Arg 167 Gln mutant is depicted in figure 5.5.

5.6 The structure of the active site and the dipyrromethane cofactor and implications for the properties of Arg 149, Arg 167 and Arg 173 mutations

The dipyrromethane cofactor is bound to Cys 261 in domain 3 and is present in the reduced state with the C2 ring towards the back of the active site cavity (figures 5.6 and 5.7). Arginines 149, 150 and 173, two of which are the subject of this thesis, make salt bridges with the carboxylate groups from cofactor ring C1. Serine residues 146 and 147 also make interactions with the carboxylates of the C1 ring of the cofactor. The human mutations affecting Arg 149 and Arg 173 can readily be explained because, during the reaction of preuroporphyrinogen with the apo-enzyme, these arginines must play a vital role in positioning the terminal ring of preuro-

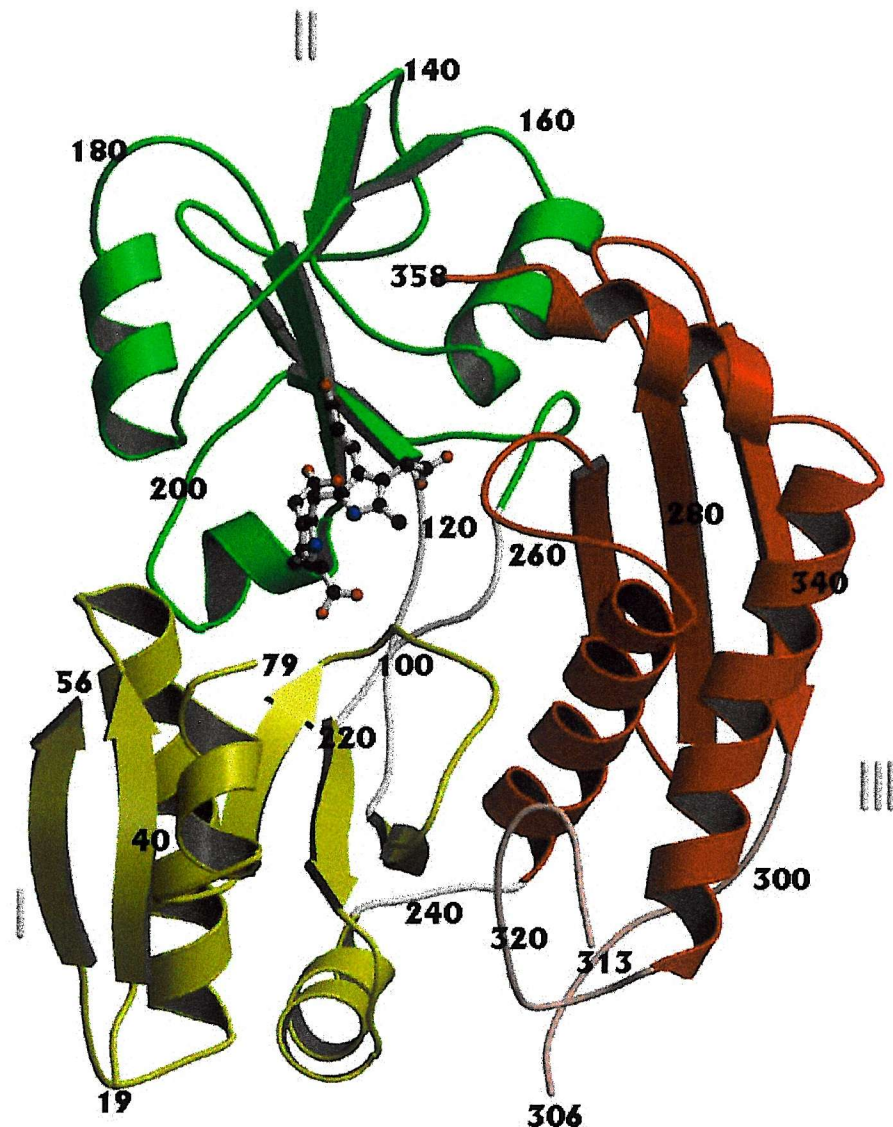


Figure 5.5: The X-ray structure of human recombinant ubiquitous porphobilinogen deaminase Arg 167 Gln mutant. The structure is made up of three domains (domain 1 in yellow; domain 2 in green and domain 3 in red). The connecting polypeptide segments are shown in white. The topologies of domain 1 (residues 18-114 and 219-236) and domain 2 (residues 120-212) are similar, each domain, comprising a doubly wound, mainly parallel β -sheet of five strands with α -helical segments packing against each face of the sheet. The dipyrromethane cofactor is located in the deep cleft between domains 1 and 2. Domain 3 (residues 241-357) is an open faced, three stranded antiparallel β -sheet with three α -helical segments on one face and a large insertion loop of 29 residues from 298-327 (coloured pink) that follows the third β -strand. This loop interacts with domain 1 and is not found in the *E. coli* enzyme. The dipyrromethane cofactor is also displayed in CPK representation (Mohammed, 2001).

porphyrinogen with its hydroxymethyl group adjacent to Cys 261 to facilitate the formation of the thioether bond. Without these essential interactions, the covalent attachment of the preuroporphyrinogen to the deaminase is prevented and the enzymes remain largely as apo-proteins. The stability afforded by the dipyrromethane in the holo-enzyme explains why these mutations are CRIM-ve.

The carboxylate groups of the C2 cofactor ring also form salt links with the protein principally through Arg 150 and Arg 195. No human mutations are known at these positions. Lysine 98 also makes interactions with the carboxylates from the C2 ring. Mutations of the equivalent residue lysine 83 in the *E. coli* deaminase to any of several residues leads to a highly unstable protein that is rapidly degraded in vivo. No human mutations at this position have been reported. Mutations of aspartate 99, a key catalytic group, have been identified in Sweden (unpublished). One of the carboxyl oxygen atoms of the aspartate side chains interacts with both NH atoms from the pyrrole rings of the dipyrromethane cofactor.

The crystal structure of the human Arg 167 Gln mutant shows the glutamine side chain to be disordered and its precise location cannot be determined. It is clear, however that the arginine side chain is not present since this would have been resolved clearly, as judged by the structure of the *E. coli* enzyme. It is of particular interest that the active site cavity contains electron density that is closely associated, but not covalently linked, with the cofactor C2 ring. It is possible that this represents a disordered substrate molecule. The orientation observed suggests that the carboxylate groups may interact with Arg 26, Arg 173 and Ser 28 and that the NH of the pyrrole ring can hydrogen bond with Asp 99 as shown in figure 5.8.

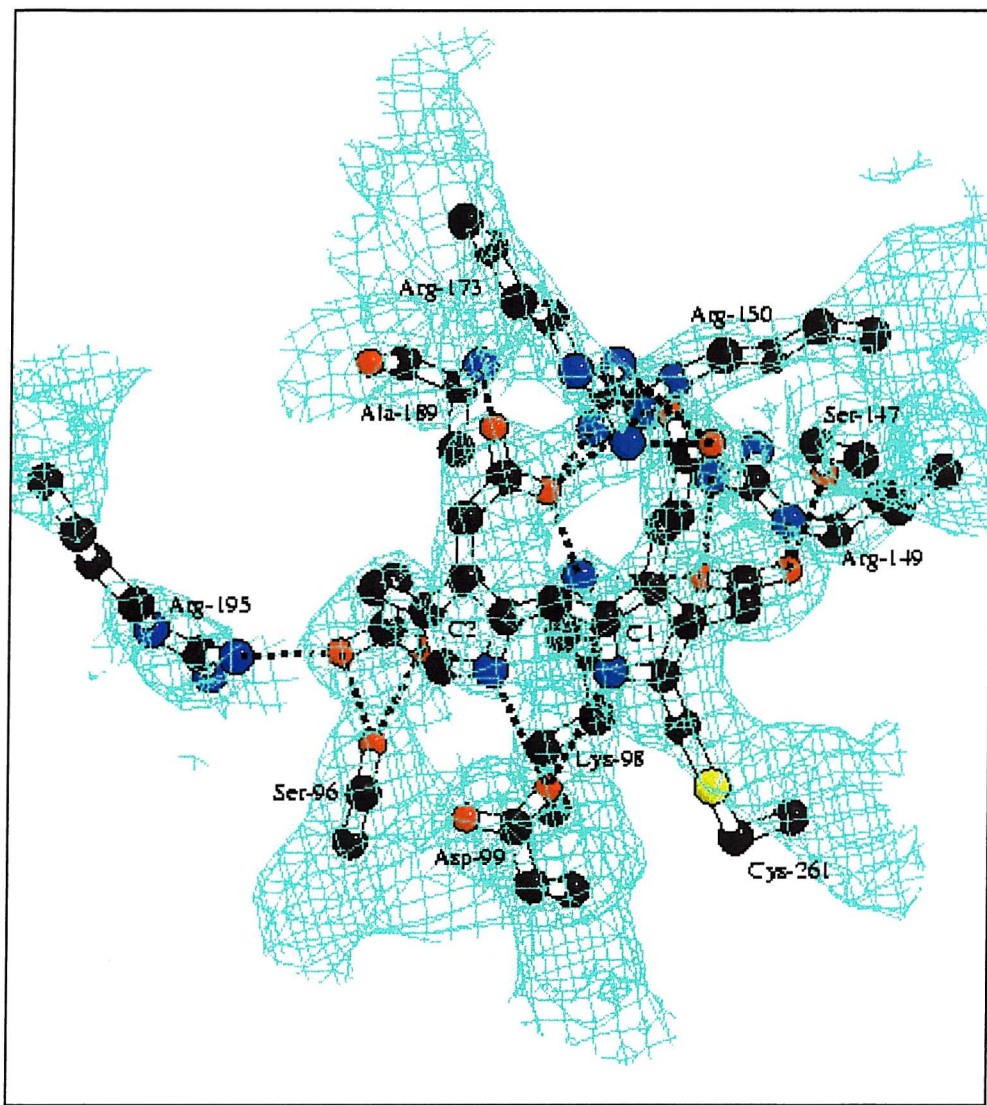


Figure 5.6: The interactions (shown in black) between the dipyrromethane (DPM) cofactor and protein side chains in the active site cleft of the recombinant human ubiquitous porphobilinogen deaminase. The DPM cofactor is covalently attached to Cys 261 and adopts the reduced conformation with ring C2 occupying a position at the rear of the cleft. The electron density map is depicted in sky-blue (Mohammed, 2001).

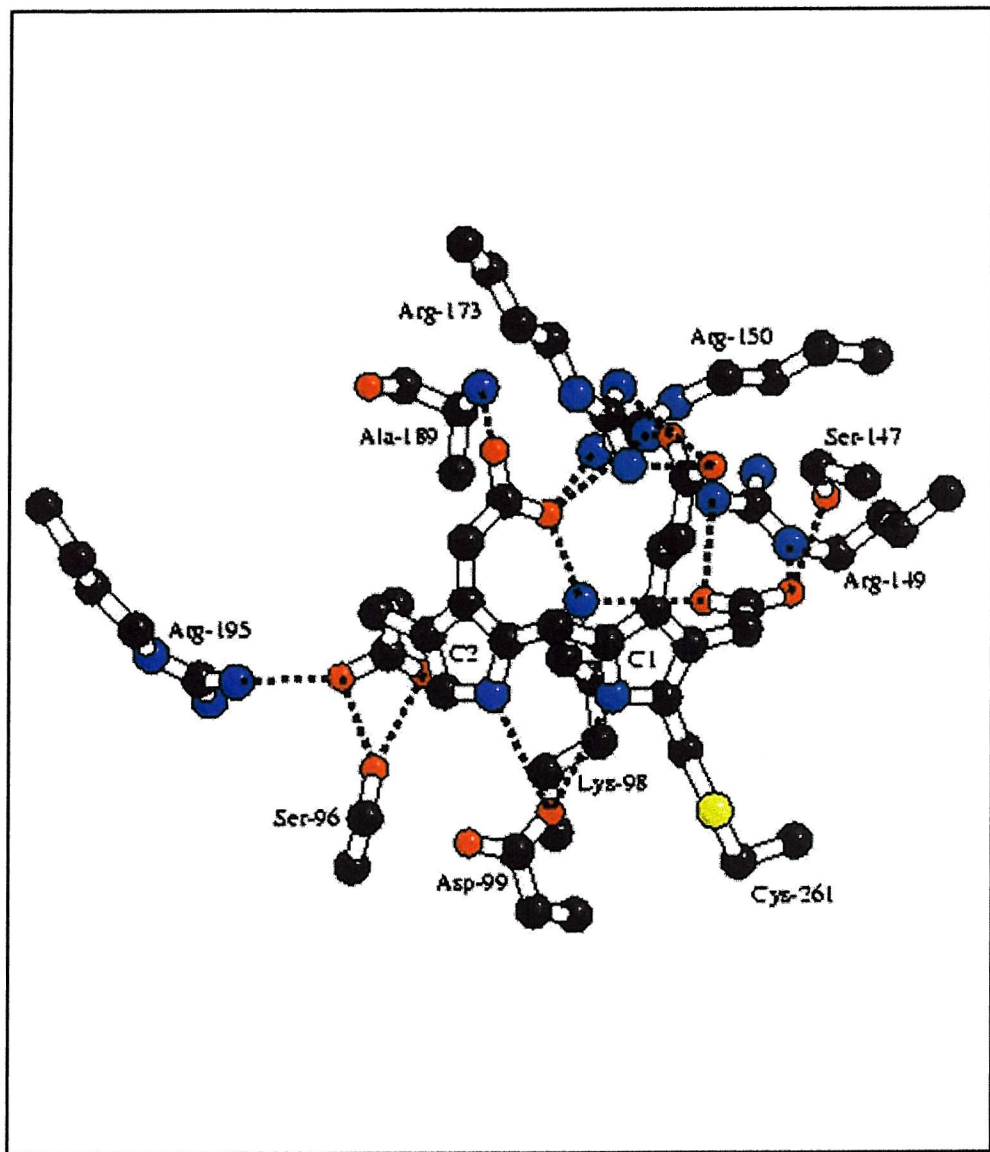


Figure 5.7: The interactions between the dipyrrromethane (DPM) cofactor and protein side chains in the active site cleft of the recombinant human ubiquitous porphobilinogen deaminase, without the electron density.

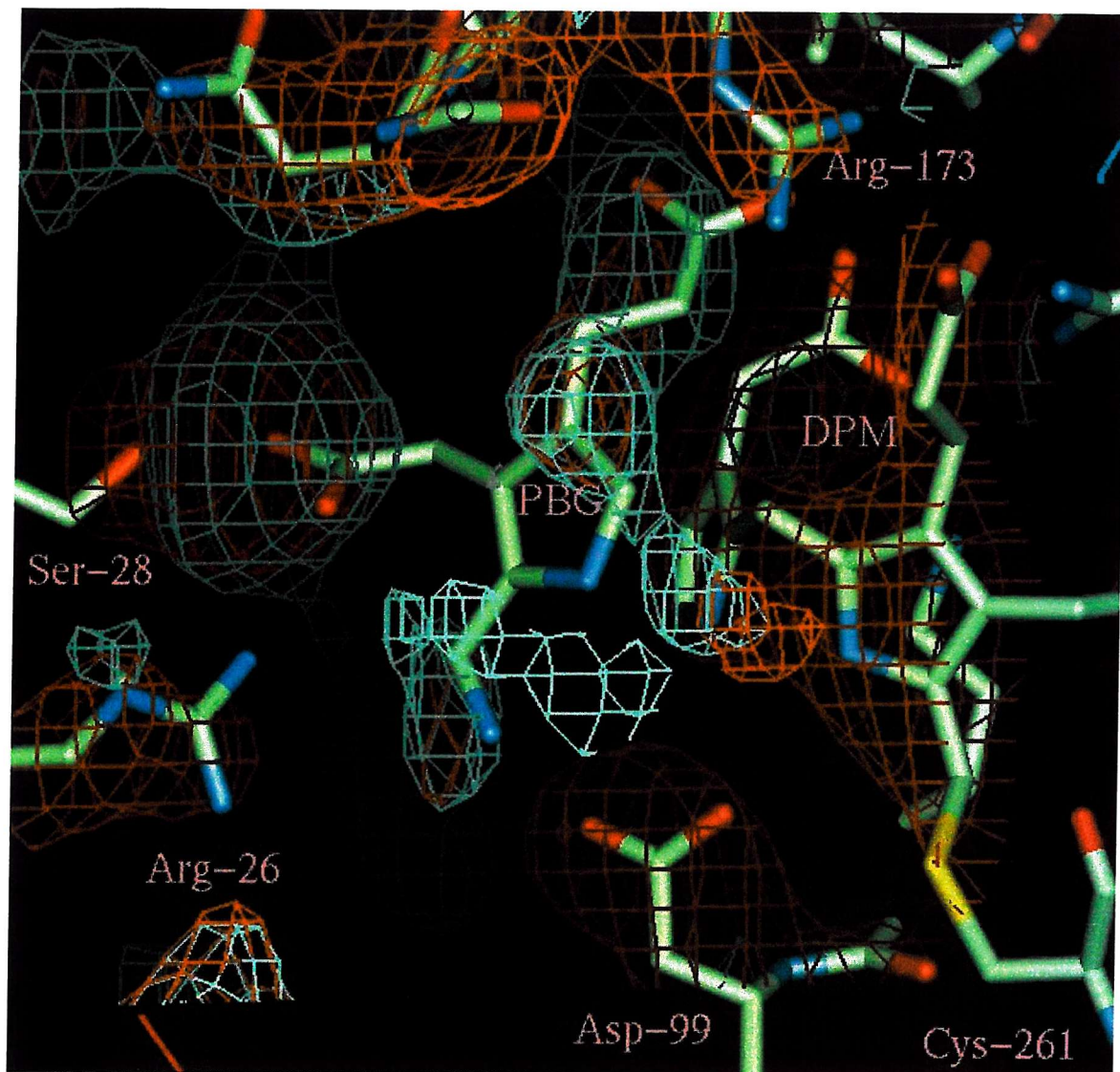


Figure 5.8: The active site cleft of human deaminase Arg 167 Gln mutant demonstrating the presence of a molecule of porphobilinogen (PBG) proximal to the dipyrromethane (DPM) cofactor and the importance of Arg 173 and Arg 26 in substrate binding.

5.7 Comparison between the human ubiquitous deaminase and the *E. coli* enzyme

Comparisons between the human recombinant deaminase and the enzyme from *E. coli* reveal that the two enzymes are very similar in their tertiary structure, as expected for proteins with 60% amino acid similarity and 49% sequence identity. Superposition of the two structures shows that the core and active site regions are very similar with the main differences occurring at the extremities of the molecules and at the large insert in domain 3, found only in eukaryote deaminases (figure 5.9).

Interestingly, the human deaminase crystallizes as a dimer. As each monomer within the dimer is related by a 2-fold rotation, all interactions at the interface occur twice, with contacts principally between domain 1 of one monomer and domain 2 of the other, see figure 5.10. The area of the dimer interface, 1631 Å² per subunit, is quite extensive and is made up of a large number of hydrophobic contacts. In addition, there are several hydrogen bonds and salt bridges with Arg 32, Asp 36, Asp 178 and Glu 179 playing a role in the latter. There is some evidence that the human deaminase exists as a dimer in solution since SDS-PAGE electrophoresis consistently displays a weak protein band with M_r value around 90,000 (Mosley, personal communication).

The structure of the human recombinant ubiquitous Arg 167 Gln mutant is an important step towards a full understanding of the functional consequences of inherited human mutations. However, further work is necessary to improve the resolution of the structure and to investigate other mutations in this highly sensitive and important region of the enzyme. Further studies should also focus on determining the structure of the ES complexes. To this end the Arg 167 Gln mutant has many useful properties that can be exploited for the isolation of ES, ES₂, ES₃ and possibly ES₄ for individual characterization.

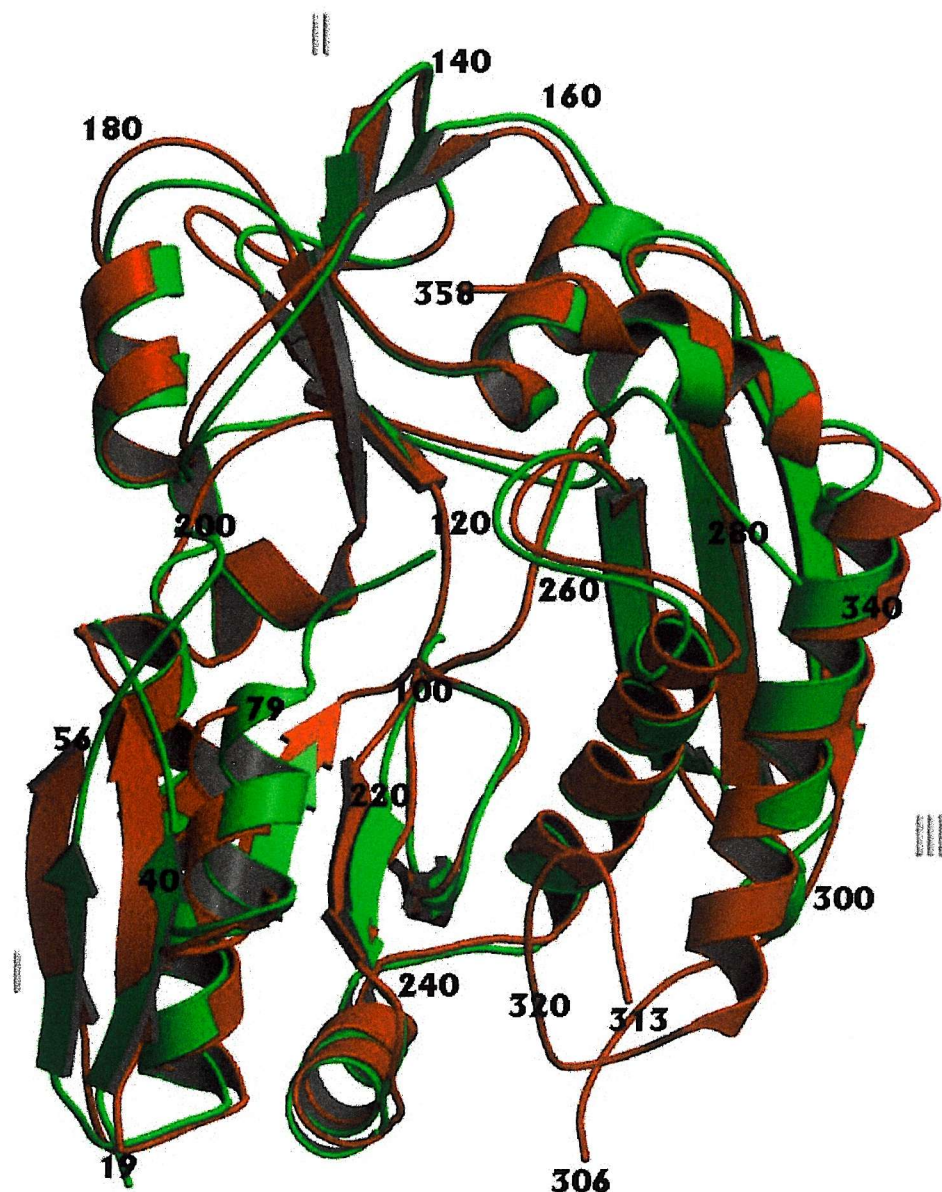


Figure 5.9: The superposition of human ubiquitous porphobilinogen deaminase mutant Arg 167 Gln (coloured in red) and *E. coli* porphobilinogen deaminase (oxidized form coloured in green). The overall structure of the human Arg 167 Gln mutant deaminase is very similar to that of the *E. coli* deaminase, with the main structural differences occurring at several solvent exposed loop regions and at the large insertion (residues 297-324 in domain 3) (Mohammed, 2001).

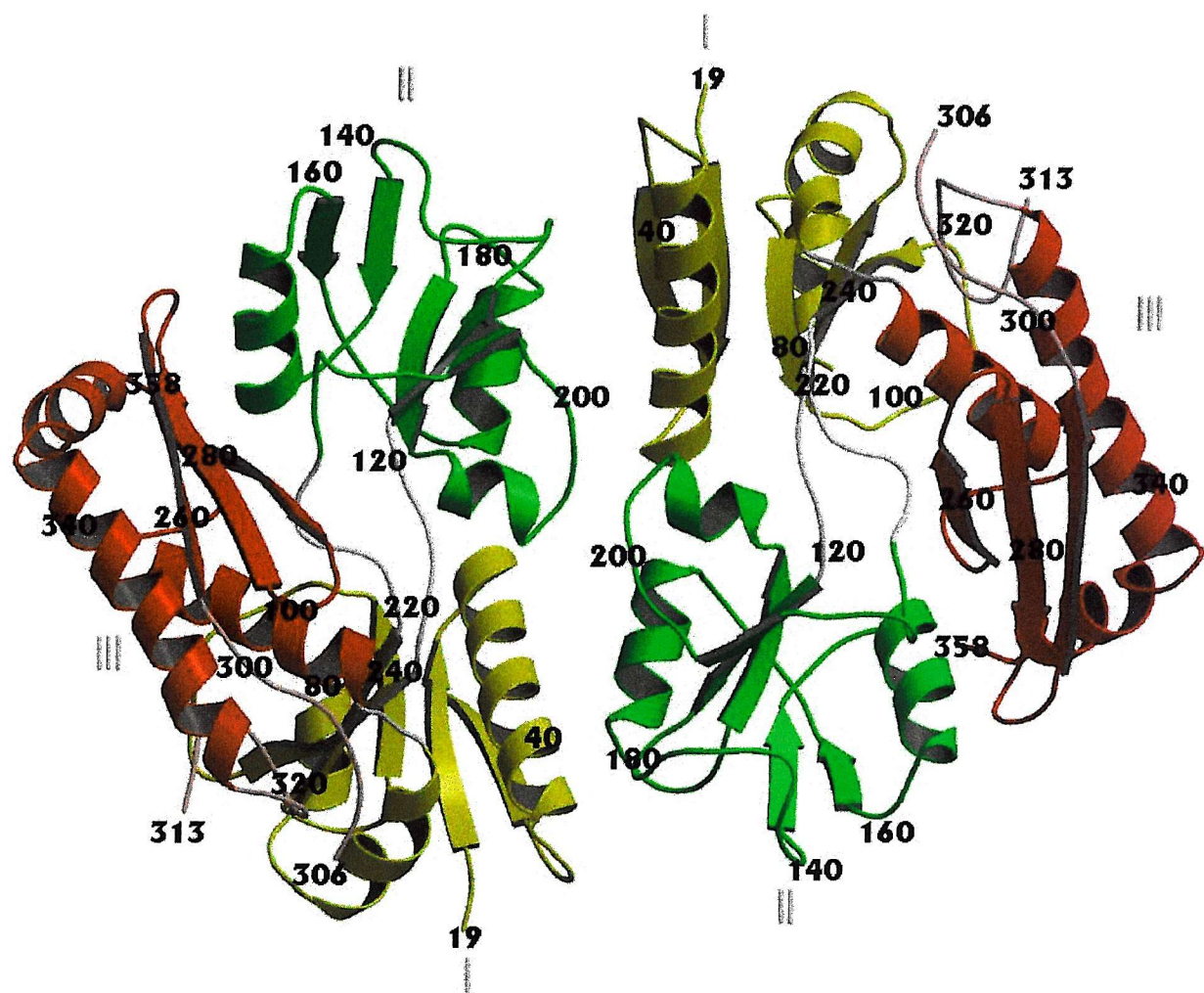


Figure 5.10: **The human ubiquitous porphobilinogen deaminase Arg 167 Gln mutant dimer.** The dimer is stabilised by a series of hydrogen bonds and hydrophobic interactions. All the interactions at the interface are duplicated since each monomer within the dimer is related by a 2-fold rotation (Mohammed, 2001).

References

- Al-Karadaghi S, Hansson M, Nikonorov S, Jonsson B, Hederstedt L. (1997). *Structure*. **5(11)**, 1501-1510.
- Andersson, P. M. and Desnick, R. J. (1980). *J. Biol. Chem.* **255**, 1993-1999.
- Andersson, C., Floderus, Y., Wikberg, A. and Lithner, F. (2000). *Scand. J. Clin. Lab. Invest.* **60**, 643-648.
- Attwood, T. K., Payne, A. W. R., Michie, A. D. and Parry-Smith, D. J. (1997). *EMBnet news*, **3(3)**.
- Battersby, A. R., Fookes, C. J. R., Matcham, G. W. J. and McDonald, E. (1980). *Nature*. **285**, 17-21.
- Bottomley, S., S., May, B., K., Cox, T., C., Cotter, P., D. and Bishop, D., F. (1995). *Journal of bioenergetics and biomembranes*. **27(2)**, 161-168.
- Brownlie, P. D., Lambert, R., Louie, G. V., Jordan, P. M., Blundell, T. L., Warren, M. J., Cooper, J. B. and Wood, S. P. (1994). *Protein Science*. **3**, 1644-1650.
- CCP4 Collaborative Computational Project, Number 4. (1994). *Acta. Cryst.* D50. 760.
- Chen, C. H., Warner, C. A. and Desnick, R. J. (1992). *Am. J. Hum. Genet*, **51**(Suppl): A45.

- Cotter, P. D., Drabkin, H. A., Varkony, T., Smith, D. I. and Bishop, D. F. (1995). *Cytogenet. Cell Genet.* **69**, 207-208.
- Delfau, M. H., Picat, C., de Rooij, F. W. M., Hamer, K. Bogard, M., Wilson, J. H. P., Deybach, J. C., Nordmann, Y. and Grandchamp, B. (1990). *J. Clin. Invest.* **86**, 1511-1516.
- Delfau, M. H., Picat, C., de Rooij, F., Voortman, G., Deybach, C., Nordmann, Y. and Grandchamp, B. (1991). *Am. J. Hum. Genet.* **49**, 412-428.
- Desnick, R. J., Ostasiewicz, L. T., Tishler, P. A. and Mustajoki, P. (1985). *J. Clin. Invest.* **76**, 865-874.
- Deybach, Jean-Charles and Puy, H. (1995). *Journal of Bioenergetics and Biomembranes.* **27(2)**, 197-205.
- Elder, G. H. (1997). *Journal of Inherited Metabolic Disease.* **20**, 237-246.
- Elder, G. H., Hift, R. J. and Meissner (1997). *Lancet.* **349**, 1613-1617.
- Elder, G. H. and Roberts, A. G. (1995). *Journal of Bioenergetics and Biomembranes.* **27 (12)**, 207-214.
- Erskine, P. T., Senior, N., Awan, S., Lambert, R., Lewis, G., Tickle, I. J., Sarwar, M., Spencer, P., Thomas, P., Warren, M. J., Shoolingin-Jordan, P. M. and Cooper, J. B. (1997). *Nature St. Biol.* **4**, 1025-1031.
- Ferreira, G. C. (1995). *Journal of Bioenergetics and Biomembranes.* **27 (2)**, 147-150.
- Ferreira, G. C. and Gong, J. (1995). *Journal of Bioenergetics and Biomembranes.* **27 (2)**, 151-159.
- Filip, C., Fletcher, G., Wulff, J. L. and Earhart, C. F. (1973). *American Society for Microbiology.* **115 (3)**, 717-722.

- Frankel, S., Condeelis, J. and Leinwand, L. (1990). *J. Biol. Chem.* **265**, 17980-17987.
- Frankel, S., Sohn, R. and Leinwand, L., 1991, *Proc. Natl. Acad. Sci. USA*. **88**, 1192-1169.
- Fritsch, E. F. and Maniatis, T. (1989). *Molecular cloning A Laboratory Manual*. Sambrook, J. (ed), Cold Spring Harbor Laboratory Press: New York.
- Gorchein, A. (1997). *Br. J. Clin. Pharmacol.* **44**, 427-434.
- Grandchamp, B.(1998). *Seminars in liver diseasee*. **18(1)**, 17- 24.
- Grandchamp, B., Picat, C., de Rooj, F., Beaumont C., Deybach, J. C.and Nordmann, Y. (1989a). *Nucleic Acids Res.*, **17**, 6637-6649.
- Grandchamp, B., de Verneuil, H., Beaumont, C., Chretien, S., Walter, O. and Nordmann, Y. (1987). *Eur. J. Biochem.* **162**, 105-110.
- Grandchamp, B., Picat, C., Kauppinen, R., Mignotte, V., Peltonen, L., Mustajoki, P., Romeo, P. H., Goossens, M. and Nordmann, Y. (1989b). *Eur. J. Clin. Invest.* **19**, 415-418.
- Grandchamp, B., Picat, C., Mignotte, V., Wilson, J. H. P., Te Velde, K., Sandkuyl, L., Roméo, P. H., Goossens, M. and Nordmann, Y. (1989c). *Proc. Natl. Acad. Sci. USA*. **86**, 661-664.
- Gu, X. K., de Rooij, F., Voortman, G., Te Velde, K., Deybach, J. C., Nordmann, Y. and Grandchamp, B. (1994). *Hum. Genet.* **93**, 47-52.
- Gu, X., de Rooij, F., Voortman, G., Te Velde, K., Nordmann, Y. and Grandchamp, B. (1992). *Am. J. Hum. Genet.* **51**, 660-665.
- Hädener, A., Matzinger, P. K., Battersby, A. R., McSweeney, S., Thompson, A. W., Hammersley, A. P., Harrop, S. J., Cassetta, A., Deacon, A., Hunter, W.

N., Nieh, Y. P., Raftery, J., Hunter, N. and Helliwell, J. R. (1999). *Acta Cryst.* D55, 631-643.

- Hädener, A., Matzinger, P. K., Malashkevich, V. N., Louie, G. V., Wood, S. P., Oliver, P., Alefounder, P. R., Pitt, A. R., Abell, C. and Battersby, A. R. (1993). *Eur. J. Biochem.* 211, 615-624.
- Hart, G. J., Leeper, F. J. and Battersby, A. R. (1984). *Biochem. J.* **222**, 93-102.
- Hart, G. J., Miller, A. D. and Battersby, A. R. (1988). *Biochem. J.* **252**, 909-912.
- Hart, G. J., Miller, A. D., Beifuss, U., Leeper, F. J. and Battersby, A. R. (1990). *J. Chem. Soc. Perkin Trans. I.*, 1979-1993.
- Hart, G. J., Miller, A. D., Leeper, F. J. and Battersby, A. R. (1987). *J. Chem. Soc. Chem. Commun.* 1762-1765.
- Innis, M. A., Gelfand, D. H., Sninsky, J. J. and White T. J. (1990). *PCR protocols, A guide to methods and applications.* Academic press, INC: New York, 178.
- Johnson, M. S., 1990, Modelling and Biocomputing group, Center for Biotechnology, P. O., Box 123, FIN-20521 Turku, Finland. MALIGN: ©1990 Kramsku, Finland.
- Jones, R. M. and Jordan, P. M. (1994). *Biochemical Journal.* **299**, 895-902.
- Jordan, P. M. (1994a). *The Biosynthesis of The Tetrapyrrole Pigments.* Chadwick, D. J. and Ackrill, K.(ed), Ciba Foundation Symposium, **180**, Wiley: Chichester, 70-96.
- Jordan, P. M. (1994b). *Current Opinion in Structural Biology.* **4**, 902-911.
- Jordan, P. M. (1991). *New Comprehensive Biochemistry.* **19**, Series edited by A. Neuberger and L. L. M., Van Deenen. Elsevier: Amsterdam.

- Jordan, P. M., Thomas, S. D. and Warren, M. J. (1988a). *Biochem. J.* **254**, 427-435.
- Jordan, P. M. and Seehra, J. S. (1979). *FEBS Lett.* **104**, 364-366.
- Jordan, P. M. and Warren, M. J. (1987). *FEBS Lett.* **225**, 87-92.
- Jordan, P. M., Warren, M. J., Williams, H. J., Stolowich, N. J., Roessner, C. A., Grant, S. K. and Scott, A. I. (1988b). *FEBS Lett.* **235**, 189-193.
- Jordan, P.M. and Woodcock, S. C. (1991). *Biochem. J.* **280**, 445-449.
- Kappas, A. , Sassa, S., Galbraith, R. A. and Nordmann, Y. (1989). *The porphyria*. 6th ed, (Scriven, C. R., Beaudet, A. L., Sly, W. S. and Valle, D.,eds), McGraw-Hill: New York, 1305-1365.
- Lambert, R., Brownlie, P. D., Woodcock, S. C., Louie, G. V., Cooper, J. C., Warren, M. J., Jordan, P. M., Blundell, T. L. and Wood, S. P. (1994). *The Biosynthesis of Tetrapyrrole Pigments*. Chadwick, D. J. and Ackrill, K. (eds.), Ciba Foundation Symposium, **180**, Wiley: Chichester, 97-110.
- Lander, M., Pitt, A. R., Alefounder, P. R., Bardy, D., Abell, C. and Battersby, A. R. (1991). *Biochem. J.* **275**, 447-452.
- Lee, J., Anvert, M. (1991). *Proc. Natl. Acad. Sci. USA.* **88**, 10912-10915.
- Lee, J. S., Grandchamp, B. and Anvret, M. (1990). *Am. J. Hum. Genet.*, **47**(Suppl): A162.
- Lindberg, R. L. P., Martini, R., Baumgartner, M., Erne, B., Borg, J., Zielasek, J., Ricker, K., Steck, A., Toyka, K. V. and Meyer U. A. (1999). *J.clin. Invest.* **103**(8), 1127-1134.
- Llewellyn, D. H., Scobie, G. A., Urqhart, A. J., Harrison P. R. and Elder, G. H. (1992a). *Neth. J. Med.* **24**, A28.

- Llewellyn, D. H., Smyth, S. J., Elder, G. H., Huchesson, A. C., Rattenbury, J. M. and Smith, M. F. (1992). *Hum. Genet.* **89**, 97-98.
- Llewellyn, D. H., Whatley, S. and Elder, G. H. (1993). *Human Molecular Genetics*. **2 (8)**, 1315-1316.
- Louie, G. V., Brownlie, P. D., Lambert, R., Cooper, J. B., Blundell, T. L., Wood, S. P., Malashkevich, V. N., Hädener, A., Warren, M. J. and Shoolingin-Jordan, P. M. (1996). *PROTEINS : Structure, Function and Genetics*. **25**, 48-78.
- Louie, G. V., Brownlie, P. D. Lambert, R., Cooper, J. B., Blundell, T. L., Wood, S. P., Warren, M. J., Woodcock, S. C. and Jordan, P. M. (1992) *Nature (London)*. **359**, 33-39.
- Lundin, G., Lee, J. S., Persson, B. and Anvert, M. (1993). *Neth. J. Med.* **42**, A28.
- Lundin, G., Lee, J. S., Thunell, S. and Anvert, M. (1997). *Hum. Genet.* **100**, 63-66.
- May, B. K., Dogra, S. C., Sadlon, T. J., Bhasker, C. R., Cox, T. C. and Bottomley, S. S. (1995). *Prog Nucleic Acid Res Mol Biol.* **51**, 1-51.
- Mazzetti, M. B. and Tomio, J. M. (1988). *Biochimica et Biophysica Acta*. **957**, 97-104.
- McNeill, L. A. (1999). Ph. D. Thesis. University of Southampton.
- Mgone, C. S., Lanyon, W. G., Moore M. R. and Connor, J. M. (1992). *Hum. Genet.* **90**, 12-16.
- Mgone, C. S., Lanyon, W. G., Moore M. R., Louie, G. V., and Connor, J. M. (1994). *Hum. Mol. Genet.* **3**, 809-811.

- Mgone, C. S., Lanyon, W. G., Moore M. R., Louie, G. V., and Connor, J. M. (1993). *Hum. Genet.* **92**, 619-622.
- Miller, A. D., Hart, G. J., Packman, L. C. and Battersby, A. R. (1988). *Biochem. J.* **254**, 915-918.
- Mohammed, F. (2001). Ph. D. Thesis. University of Southampton.
- Moore, M. R. (1993). *Int. J. Biochem.* **25**, 1353-1368.
- Mosley, J. (2001) Ph. D. Thesis. University of Southampton.
- Mustajoki, P. and Nordmann, Y. (1993). *Arch. Int. Med.* **153**, 2004-2008.
- Ong, P. M. L., Lanyon, W. G., Graham, G., Hift, R. J., Halkett, J., Moore, M. R. and Connor, J. M. (1997). *Molecular and Cellular Probes.* **11**, 293-296.
- Rhodes, G. (1993). *Crystallography Made Crystal Clear.* Academic Press.
- Sassa, S. and Kappas, A. (2000). *Journal of Internal Medicine.* **247**, 169-178.
- Scobie, G. A., Llewellyn, D. H., Urquhart, A. J., Smyth, S. J., Kalsheker, N. A., Harrison, P. R. and Elder, G. H. (1990). *Hum. Genet.* **87**, 631-634.
- Scott, A., I., Clemens, K., R., Stolowich, N., J., Santander, P., J., Gonzalez, M., D. and Roessner, C., A. (1989). *FEBS.* **242(2)**, 319-324.
- Scott, A. I., Roessner, C. A., Stolowich, N. J., Karuso, P., Williams, H. J., Grant, S. K., Gonzalez, M. D. and Hoshino, T. (1988). *Biochemistry.* **27**, 7984-7990.
- Seehra, J. S. and Jordan, P. M. (1980). *J. Amer. Chem. Soc.* **102**, 6841-6846.
- Shoolingin-Jordan, P. M. (1998). *Biochemical Society Transactions.* **27**, 326-336.
- Shoolingin-Jordan, P. M. (1995). *Journal of Bioenergetics and Biomembranes.* **27(2)**, 181-195.

- Shoolingin-Jordan, P. M. and Cheung, K. (1999). Biosynthesis of heme. In *Comprehensive Natural Products Chemistry*. Kelly, J. W., ed, **4**, Series edited by Barton, S. D., Nakanishi, K. and Meth-Cohn, O., Elsevier Science Ltd., Oxford: England, 61-108.
- Shoolingin-Jordan, P. M., Warren, M. J. and Awan, S. J. (1996). *Biochem.J.* **316**, 373-376.
- Shoolingin-Jordan, P. M., Warren, M., J. and Awan, S. J. (1997). *Methods Enzymol.* **281**, 317-327.
- Shoolingin-Jordan, P. M. and Wood, S. P. (1998). *Genetics and Psychiatric Disorders*. Wahlstrom, J.(ed), Pergamon Press, 81-102.
- Smith, K. M. (1975). *Porphyrins And Metalloporphyrins*. Falk, J. E. (ed), Elsevier Scientific Publishing Company: Amsterdam, 1-28.
- Strand, L. J., Felsher, B. F., Redeker, A. G. and Marver, H. S. (1970). *Proc. Natl. Acad. Sci. USA.* **67**, 1315-1320.
- Tabor, S. (1990). Current Protocols in Molecular Biology (Ausubel, F. A., Brent, R., Kingston, R. E., Moore, D. D., Seidman, J. G., Smith, J. A. and struhl, K., eds), Greene Publishing and Wiley-Interscience, New York, 16.2.1-16.2.11.
- Thadani, H., Deacon, A. and Peters, T. (2000). *British medical Journal*. **320**, 1647-1651.
- Thunell, S., Harper, P., Brock, A. and Petersen, N. E., 2000, *Scand. J. Clin. Lab. Invest.* **60**, 541-560.
- Vagin, A. and Teplyakov, A. (1997). *J. Appl. Cryst.* **30**, 1022-1025.
- Warren, M. J., Gul, S., Aplin, R. T., Scott, A. I., Roessner, C. A., O'Grady, P. and Shoolingin-Jordan, P. M. (1995). *Biochemistry*. **34**, 11288-11295.

- Warren, M. J., Jay, M., Hunt, D. M., Elder, G. H., Rohl, J. C. (1996). *Trends Biochem Sci.* **21(6)**, 229-234.
- Warren, M. J., and Jordan, P. M. (1988). *Biochemistry*. **27**, 9020-9030.
- Whatley, S. D., Roberts, A. G and Elder, G. H. (1995). *Lancet*. **346**, 1007-1008.
- Whitby, F. G., Phillips, J. D. Kushner, J. P. and Hill, C. P. (1998). *EMBO Journal*. **17(9)**, 2463-2471.
- Wilson, K. and Walker, J. M. (1994). *Principles and techniques of Practical Biochemistry*. 4th ed., Cambridge University Press: UK, 438-441.
- Wood, S., Lambert, R. and Jordan, P. M. (1995). *Molecular Medicine Today*. **1**, 232-239.
- Woodcock, S., C. (1992). Ph. D. Thesis. University of Southampton.
- Woodcock, S. C. and Jordan, P. M. (1994). *Biochemistry*. **33**, 2688-2695.

Appendix



The Human Gene Mutation Database
Cardiff

**Hydroxymethylbilane
synthase (porphobilinogen
deaminase)**

Gene symbol : HMBS

Location : 11q23.3

In association with



Mutations in this gene were first reported in 1989

Grandchamp (1989) *Nucleic Acids Res* 17, 6637
Grandchamp (1989) *Eur J Clin Invest* 19, 415

Number of entries by mutation type

Click on the respective mutation type to view detailed information about the mutations as logged in HGMD.

Mutation type	Total number of mutations
Nucleotide substitutions (missense / nonsense)	81
Nucleotide substitutions (splicing)	36
Nucleotide substitutions (regulatory)	0
Small deletions	32
Small insertions	19
Small indels	1
Gross deletions	1
Gross insertions & duplications	2
Complex rearrangements (including inversions)	0
Repeat variations	0
TOTAL	172

Number of entries by phenotype

Phenotype	Nucleotide substitutions	Micro-lesions	Gross lesions
Porphyria, acute intermittent	117	52	3

Clicking on the respective phenotype will start a search for that item at the OMIM web site. As HGMD only records the first literature report of a mutation, the possibility that reported mutations may be responsible for more than one disease state cannot be ruled out.

Associated data -	HGMD options -	External sites -
Mutation map	HGMD search	OMIM entry for HMBS
cDNA sequence	HGMD help	GDB entry for HMBS

[Splice junctions](#)[HGMD home](#)[GenAtlas entry for HMBS](#)[Nomenclature entry for HMBS](#)

Accession Number	Codon	Nucleotide	Amino acid	Phenotype	Reference
CM940933	18	ATG a -ATA	Met-Ile	Porphyria, acute intermittent	1
CM960837	22	tCGC-TGC	Arg-Cys	Porphyria, acute intermittent	2
CM970727	24	gGGT-AGT	Gly-Ser	Porphyria, acute intermittent	3
CM950636	26	cCGC-TGC	Arg-Cys	Porphyria, acute intermittent	4
CM930401	26	CGC-CAC	Arg-His	Porphyria, acute intermittent	5
CM970728	28	AGC-AAC	Ser-Asn	Porphyria, acute intermittent	3
CM990732	31	tGCT-CCT	Ala-Pro	Porphyria, acute intermittent	6
CM940934	31	tGCT-ACT	Ala-Thr	Porphyria, acute intermittent	7
CM920342	34	aCAG-AAG	Gln-Lys	Porphyria, acute intermittent	8
CM992340	34	CAG-CCG	Gln-Pro	Porphyria, acute intermittent	9
CM950637	34	aCAG-TAG	Gln-Term	Porphyria, acute intermittent	4
CM002609	35	ACG-ATG	Thr-Met	Porphyria, acute intermittent	10
CM990733	42	TTG-TCG	Leu-Ser	Porphyria, acute intermittent	6
CM960838	42	TTG-TAG	Leu-Term	Porphyria, acute intermittent	11
CM001191	45	TCG-TAG	Ser-Term	Porphyria, acute intermittent	12
CM940935	55	tGCT-TCT	Ala-Ser	Porphyria, acute intermittent	7
CM990734	61	gGAC-AAC	Asp-Asn	Porphyria, acute intermittent	6
CM990735	85	CTG-CGG	Leu-Arg	Porphyria, acute intermittent	6
CM990736	90	GTG-GGG	Val-Gly	Porphyria, acute intermittent	6
CM940936	93	gGTT-TTT	Val-Phe	Porphyria, acute intermittent	1
CM950638	98	AAG-AGG	Lys-Arg	Porphyria, acute intermittent	4
CM930402	111	cGGA-AGA	Gly-Arg	Porphyria, acute intermittent	13
CM970729	114	TG C a-TGA	Cys-Term	Porphyria, acute intermittent	3
CM940937	116	CGG-CAG	Arg-Gln	Porphyria, acute intermittent	14
CM930403	116	gCGG-TGG	Arg-Trp	Porphyria, acute intermittent	15

CM950639	119	CCT-CTT	Pro-Leu	Porphyria, acute intermittent	<u>16</u>
CM970730	124	GTC-GAC	Val-Asp	Porphyria, acute intermittent	<u>3</u>
CM910223	149	CGA-CAA	Arg-Gln	Porphyria, acute intermittent	<u>17</u>
CM940938	149	CGA-CTA	Arg-Leu	Porphyria, acute intermittent	<u>7</u>
CM950640	149	gCGA-TGA	Arg-Term	Porphyria, acute intermittent	<u>4</u>
CM900129	155	gCAG-TAG	Gln-Term	Porphyria, acute intermittent	<u>18</u>
CM900130	167	CGG-CAG	Arg-Gln	Porphyria, acute intermittent	<u>19</u>
CM920343	167	tCGG-TGG	Arg-Trp	Porphyria, acute intermittent	<u>20</u>
CM900131	173	CGG-CAG	Arg-Gln	Porphyria, acute intermittent	<u>19</u>
CM920344	173	cCGG-TGG	Arg-Trp	Porphyria, acute intermittent	<u>21</u>
CM920345	177	CTG-CGG	Leu-Arg	Porphyria, acute intermittent	<u>8</u>
CM970731	178	gGAC-AAC	Asp-Asn	Porphyria, acute intermittent	<u>3</u>
CM990737	181	gCAG-TAG	Gln-Term	Porphyria, acute intermittent	<u>6</u>
CM950641	195	gCGC-TGC	Arg-Cys	Porphyria, acute intermittent	<u>4</u>
CM910224	198	TGG-TAG	Trp-Term	Porphyria, acute intermittent	<u>22</u>
CM940939	201	cCGG-TGG	Arg-Trp	Porphyria, acute intermittent	<u>1</u>
CM993452	202	gGTG-TTG	Val-Leu	Porphyria, acute intermittent	<u>23</u>
CM940940	204	gCAG-TAG	Gln-Term	Porphyria, acute intermittent	<u>14</u>
CM890062	209	tGAG-AAG	Glu-Lys	Porphyria, acute intermittent	<u>24</u>
CM993731	212	cATG-GTG	Met-Val	Porphyria, acute intermittent	<u>25</u>
CM970732	213	TATg-TAG	Tyr-Term	Porphyria, acute intermittent	<u>3</u>
CM970733	216	GGC-GAC	Gly-Asp	Porphyria, acute intermittent	<u>26</u>
CM970734	217	CAGg-CAT	Gln-His	Porphyria, acute intermittent	<u>3</u>
CM000718	217	CAG-CTG	Gln-Leu	Porphyria, acute intermittent	<u>27</u>
CM990738	219	GCC-GAC	Ala-Asp	Porphyria, acute intermittent	<u>6</u>
CM980985	222	cGTG-ATG	Val-Met	Porphyria, acute intermittent	<u>28</u>
CM940941	223	gGAA-AAA	Glu-Lys	Porphyria, acute intermittent	<u>7</u>
CM950642	225	gCGA-GGA	Arg-Gly	Porphyria, acute intermittent	<u>4</u>
CM950643	225	gCGA-TGA	Arg-Term	Porphyria, acute intermittent	<u>29</u>
CM950644	238	CTG-CGG	Leu-Arg	Porphyria, acute intermittent	<u>4</u>
CM910225	245	CTT-CGT	Leu-Arg	Porphyria, acute intermittent	<u>30</u>
CM930404	247	cTGC-CGC	Cys-Arg	Porphyria, acute intermittent	<u>31</u>

CM940942	247	TGC-TTC	Cys-Phe	Porphyria, acute intermittent	<u>1</u>
CM950645	250	tGAA-CAA	Glu-Gln	Porphyria, acute intermittent	<u>16</u>
CM940943	250	tGAA-AAA	Glu-Lys	Porphyria, acute intermittent	<u>7</u>
CM970735	250	GAA-GTA	Glu-Val	Porphyria, acute intermittent	<u>3</u>
CM930406	252	gGCC-ACC	Ala-Thr	Porphyria, acute intermittent	<u>31</u>
CM930405	252	GCC-GTC	Ala-Val	Porphyria, acute intermittent	<u>31</u>
CM920346	256	gCAC-AAC	His-Asn	Porphyria, acute intermittent	<u>8</u>
CM970736	256	gCAC-TAC	His-Tyr	Porphyria, acute intermittent	<u>3</u>
CM970737	267	cGTG-ATG	Val-Met	Porphyria, acute intermittent	<u>3</u>
CM940944	269	ACA-ATA	Thr-Ile	Porphyria, acute intermittent	<u>14</u>
CM970738	270	GCT-GAT	Ala-Asp	Porphyria, acute intermittent	<u>3</u>
CM002280	270	GCT-GGT	Ala-Gly	Porphyria, acute intermittent	<u>32</u>
CM940945	274	tGGG-AGG	Gly-Arg	Porphyria, acute intermittent	<u>14</u>
CM970739	275	gCAA-TAA	Gln-Term	Porphyria, acute intermittent	<u>3</u>
CM980986	278	CTG-CCG	Leu-Pro	Porphyria, acute intermittent	<u>28</u>
CM950646	280	tGGA-AGA	Gly-Arg	Porphyria, acute intermittent	<u>4</u>
CM940947	283	TGGa-TGA	Trp-Term	Porphyria, acute intermittent	<u>1</u>
CM940946	283	TGG-TAG	Trp-Term	Porphyria, acute intermittent	<u>14</u>
CM970740	288	TCA-TAA	Ser-Term	Porphyria, acute intermittent	<u>3</u>
CM000719	292	aCAA-TAA	Gln-Term	Porphyria, acute intermittent	<u>27</u>
CM950647	296	gCAG-TAG	Gln-Term	Porphyria, acute intermittent	<u>4</u>
CM960839	325	aCGA-TGA	Arg-Term	Porphyria, acute intermittent	<u>33</u>
CM970741	335	GGC-GAC	Gly-Asp	Porphyria, acute intermittent	<u>3</u>
CM992341	335	gGGC-AGC	Gly-Ser	Porphyria, acute intermittent	<u>9</u>

References

1 - Chen (1994) *J Clin Invest* **94**, 1927

2 - Ong (1996) *Mol Cell Probes* **10**, 57

3 - Puy (1997) *Am J Hum Genet* **60**, 1373

4 - Kauppinen (1995) *Hum Mol Genet* **4**, 215

5 - Llewellyn (1993) *Hum Mol Genet* **2**, 1315

6 - Whatley (1999) *Hum Genet* **104**, 505

7 - Gu (1994) *Hum Genet* **93**, 47

8 - Mgone (1992) *Hum Genet* **90**, 12

9 - De Siervi (1999) *Am J Med Genet* **86**, 366

10 - De Siervi (2000) *Hum Mutat Online*, #370

11 - Puy (1996) *Hum Hered* **46**, 177

12 - Martinez (2000) *Hum Mutat Online*, #319

13 - Gu (1993) *Hum Mol Genet* **2**, 1735

14 - Mgone (1994) *Hum Mol Genet* **3**, 809

15 - Gu (1993) *Hum Genet* **91**, 128

16 - Lundin (1995) *J Med Genet* **32**, 979

17 - Delfau (1991) *Hum Genet* **49**, 421

18 - Scobie (1990) *Hum Genet* **85**, 631

19 - Delfau (1990) *J Clin Invest* **86**, 1511

20 - Llewellyn (1992) *Hum Genet* **89**, 97

21 - Kauppinen (1992) *Hum Mutat* **1**, 392

22 - Lee (1991) *Proc Natl Acad Sci U S A* **88**, 10912

23 - Gross (1999) *Mol Cell Probes* **13**, 443

24 - Grandchamp (1989) *Nucleic Acids Res* **17**, 6637

25 - Solis (1999) *Mol Med* **5**, 664

26 - Lundin (1997) *Hum Genet* **100**, 63

27 - Schneider-Yin (2000) *Hum Hered* **50**, 247

28 - Mustajoki (1998) *Hum Genet* **102**, 541

29 - Lee (1995) *Am J Med Genet* **58**, 155

30 - Delfau (1991) *Am J Hum Genet* **49**, 421

31 - Mgone (1993) *Hum Genet* **92**, 619

32 - Robreau-Fraolini (2000) *Hum Genet* **107**, 150

33 - Petersen (1996) *Clin Chem* **42**, 106